

Doctoral degree dissertation

**Strategies for enrichment of manganese-oxidizing
bacteria to enhance removal of azo dye through
biological Mn-redox processes**

(Mn 酸化還元を利用したアゾ染料排水の脱色促進のための
マンガン酸化細菌の集積戦略)

by

AHMAD SHOIFUL

in partial fulfilment of the requirements for the degree of Doctor of Engineering
in Civil and Environmental Engineering

**Department of Civil and Environmental Engineering,
Graduate School of Engineering,
Hiroshima University, Japan**

January 2020

Strategies for enrichment of manganese-oxidizing bacteria to enhance removal of azo dye through biological Mn-redox processes

Doctoral degree dissertation

Ahmad Shoiful, January 2020

Advisor: Professor Akiyoshi Ohashi

Department of Civil and Environmental Engineering,

Graduate School of Engineering,

Hiroshima University, Japan

Acknowledgements

In the name of Allah, the Most Gracious and the Most Merciful

Alhamdulillahirabbil'alamin...

"All the praises and thanks be to God who is the Lord of the universe".

First of all, I would like to thank to the almighty, Allah SWT, for giving me the opportunity, determination and strength to carry on my PhD.

I wish to express my gratitude to my supervisor, Prof. Akiyoshi Ohashi, who gave me support all the way through this research work. I wish to thank Associate Prof. Noriatsu Ozaki, Assistant Prof. Tomonori Kindaichi and Associate Prof. Yoshiteru Aoi for their advices and valuable comments. I thank to all member of Environmental Preservation Laboratory, giving me inspirations and providing a strongly supportive group.

I would like to thank Ministry of Research, Technology and Higher Education of the Republic of Indonesia through Riset-Pro for PhD scholarship. I would like to thank Dr. Rudi Nugroho, Dr. Muhammad Hanif, and all the staff at Center of Technology for the Environment (PTL), BPPT, for their support.

I give thanks to PhD survivors group for giving me time to be liberated from research, and other Indonesia students for their kindness and moral support during my study. Thanks for the friendship and memories. I would especially like to thank my parents and parents-in-law for their support and unconditional love to our family. My sister and brother for their support and motivation. Finally, a big thank you to my wife, Ajeng Arum Sari, for her greatest support and encouragement, and my son, Agha Rayhan Pradita, the strongest driving force of my life.

Abstract

Manganese-oxidizing bacteria (MnOB) that are capable of oxidizing Mn(II) to biogenic manganese oxides (bio-MnO_x), are ubiquitous in nature and have attracted attention in water and wastewater treatment due to their biotechnological potential of microorganisms for removal organic contaminant, and the high adsorption and oxidation ability of the generated bio-MnO_x towards inorganic and organic pollutants. In this study, several strategies to obtain favorable conditions for MnOB enrichment in a continuous down-flow hanging sponge (DHS) reactor were studied, including the preferred organic substrates for supporting MnOB growth and the effect of residual Mn(II) on the Mn(II) oxidation performance. The potential of the enriched MnOB and bio-MnO_x for the removal of recalcitrant azo dye compounds were also investigated.

Three different organic substrates; K-medium, methanol, and sterilized activated sludge (SAS), can be used to support MnOB enrichment in a continuous DHS reactor. Methanol-fed reactor exhibited the highest Mn(II) oxidation performance of 0.49 kg Mn·m⁻³·d⁻¹. The microbial community of the reactor was strongly governed by organic substrate, and *Comamonas*, *Pseudomonas*, *Mycobacterium*, *Nocardia*, and *Hyphomicrobium* were found to play an important role in Mn(II) oxidation in the reactors. MnOB enrichment can be accelerated by employing abiotic-MnO₂ in the sponge media. The higher residual Mn(II) in the reactor was found to inhibit the Mn(II) oxidation performance. The relative abundance of putative MnOB, *Hyphomicrobium*, was inhibited by the higher residual Mn(II). Maintaining residual Mn(II) at low level is a key factor to achieve sustainable high Mn(II) oxidation performance of the reactor.

The potential of enriched MnOB and bio-MnO_x for the removal of azo dye Acid Orange 7 (AO7) was evaluated. Even though the reactor achieved high Mn(II) oxidation rate, it was unable to remove AO7. The bacterial isolates from the reactor were found to possess Mn(II) oxidation ability but not AO7 removal. There was no catalytic effect of Mn(II) oxidation on the decolorization of AO7. In addition, sodium acetate, in term of COD, could be effectively removed in the Mn(II)-oxidizing reactor. A sulfonated azo dye compound, Bordeaux S (BS), was also resistant to biological Mn(II) oxidation process under aerobic conditions, but it was easily decolorized under anaerobic conditions. Anaerobic decolorization of azo dye was strongly dependent on the co-substrate addition that acts as the electron donor for reductively cleavage of azo bond. Interestingly, this study showed that the abiotic-MnO₂-containing reactor achieved higher decolorization efficiency than the reactor devoid of abiotic-MnO₂ at a low K-medium addition. The presence of abiotic-MnO₂ was beneficial not only to decompose

extracellular polymeric substances (EPS) to more utilizable substrates, which can serve as an electron donor at organic source deficient, but also as a conductive material that promotes electron transfer. Unfortunately, anaerobic decolorization was unable to completely degrade azo dye, and its intermediate products remained in the effluent as indicated by a high COD concentration.

An integrated anaerobic-aerobic DHS reactor under manganese redox conditions was applied to further degrade azo dye wastewater. The results showed that only small portions of COD (< 30%) can be removed in the aerobic reactor, and the residual COD corresponded to the initial BS concentration, which suggested that intermediate products of BS were resistant to both anaerobic and aerobic treatment. Interestingly, nitrogen loss was found to occur in both reactors. In the anaerobic reactor, ammonium, a transformation product of co-substrate K-medium, was oxidized to nitrogen gas by manganese oxides. In addition, sulfate reduction may also contribute to the anaerobic ammonium oxidation. In the aerobic reactor, nitrification occurred on the sponge surfaces, and denitrification was possible to occur inside the sponges by coupled with manganese oxides reduction, as indicated by the higher Mn(II) in the effluent. Thus, the Mn oxides-containing reactor would be a promising method for the treatment of high nitrogen-containing wastewater.

This current study extends our knowledge on the enrichment strategies of MnOB and their potential for removal of organic pollutants. The abiotic MnO₂-containing reactor has potential applications in the treatment of high Mn-containing wastewater from various industries, such as mine drainage, hydrometallurgical processing, steel and alloy industry. In addition, the Mn oxides-containing reactor would be a promising method for the treatment of high organic nitrogen-containing wastewaters, such as municipal wastewater, food industries, etc. Further studies are required to clarify the role of manganese oxide in regulating ammonium removal.

Keywords: manganese-oxidizing bacteria, azo dye decolorization, Mn redox, manganese oxide, nitrogen removal

Summary

Manganese-oxidizing bacteria (MnOB) that are able to oxidize Mn(II) to biogenic manganese oxides (bio-MnO_x) have a great potential for the removal of inorganic and organic pollutants. One of the challenges in the practical application of MnOB is the enrichment of MnOB for promoting sustainable high generation of bio-MnO_x. In this study, the preferred organic substrates to support MnOB enrichment and the effects of residual Mn(II) on the Mn(II) oxidation performance of the reactor were investigated. The potential of the enriched MnOB and bio-MnO_x for the removal of recalcitrant azo dye compounds were studied.

In Chapter 3, three different organic substrates; K-medium, methanol, and sterilized activated sludge (SAS), can be used as the sole carbon source for the enrichment of MnOB in a DHS reactor. Methanol-fed reactor achieved the highest Mn(II) oxidation rate of 0.49 kg Mn·m⁻³·d⁻¹, followed by SAS and K-medium as of 0.41 and 0.26 kg Mn·m⁻³·d⁻¹, respectively. SAS was the promising and cost-effective substrate for MnOB enrichment; regardless, its unstable performance. *Comamonas*, *Pseudomonas*, *Mycobacterium*, *Nocardia* and *Hyphomicrobium* were suggested to play an important role in Mn(II) oxidation in the reactors. The installed abiotic-MnO₂ in the reactors could accelerate the MnOB enrichment. In Chapter 4, the reactor with low residual Mn(II) achieved higher Mn(II) oxidation rate (0.91 kg m⁻³ d⁻¹) than the reactor with high level of residual Mn(II) (0.61 kg m⁻³ d⁻¹). The predominant of putative MnOB, *Hyphomicrobium*, was inhibited by high residual Mn(II). Thus, maintaining residual Mn(II) at low-level would be a key factor for sustainable high performance on Mn(II) oxidation.

In Chapter 5, even though the reactor achieved high Mn(II) oxidation, no Acid Orange 7 (AO7) removal was observed. The bacterial isolates of the reactor were found to possess Mn(II) oxidation ability but not AO7 removal ability. Although Mn(II) oxidation had less effect on decolorization of AO7, sodium acetate can be effectively decomposed. A sulfonated azo dye Bordeaux S (BS) was also persistent under aerobic conditions, but it was easily decolorized under anaerobic (Chapter 6). Anaerobic decolorization of BS was strongly dependent on the availability of organic substrate as the electron donor for reductively cleavage of azo bond. Interestingly, at a low organic co-substrate addition, decolorization efficiency in the abiotic-MnO₂-containing reactor was higher than that of the reactor devoid of abiotic-MnO₂. The presence of abiotic-MnO₂ may decompose extracellular polymeric substances (EPS) to more utilizable substrates that can be used as an electron donor for decolorization of BS.

Unfortunately, anaerobic decolorization was unable to effectively degrade azo dye. Therefore, post treatment process is required for further decomposition of anaerobic effluent.

In Chapter 7, an integrated anaerobic-aerobic reactor under manganese redox process was applied for further degradation of azo dye wastewater. Unfortunately, the aerobic reactor was less effective in removing COD (<30%), and the remaining COD corresponded to the initial BS, suggesting that intermediate products of BS were resistant to biological processes. Remarkably, ammonium oxidation coupled with manganese oxides reduction and sulfate reduction were likely to occur in the anaerobic reactor. Simultaneous nitrification-denitrification was observed in the aerobic reactor. A combination of anaerobic-aerobic reactor with the presence of abiotic-MnO₂ would be an attractive method for the treatment of high organic nitrogen-containing wastewater.

This page is intentionally left blank

Table of Contents

Acknowledgements	i
Abstract	ii
Summary	iv
Table of Contents	vii
List of Tables	xi
List of Figures	xii
Abbreviations	xv
Chapter 1: General Introduction	1
1. 1. Background	2
1. 2. Objectives	4
1. 3. Outline of dissertation	4
Chapter 2: Literature Review	7
2. 1 Manganese element and its natural abundance	8
2. 2 The manganese redox cycling in the environment.....	12
2.2.1 Biological Mn(II) oxidation	13
2.2.2 Biological manganese oxides-reduction.....	20
2. 3 Environmental impacts of azo dyes and their biological treatment methods.....	21
Chapter 3: Multiple organic substrates support Mn(II) removal with enrichment of Mn(II)-oxidizing bacteria	39
3. 1 Introduction	40
3. 2 Materials and methods.....	42
3.2.1 Reactor configurations, inoculation, and operational conditions	42
3.2.2 Analytical methods	44
3.2.3 Microbial community analysis	44
3.2.4 Data analysis.....	44
3. 3 Results	44
3.3.1 Reactor performances.....	44
3.3.2 Microbial community	47
3. 4 Discussion	50
3. 5 Conclusions	53

Chapter 4: Residual Mn(II) concentrations affect the Mn(II) oxidation performance of the reactor	59
4.1 Introduction	60
4.2 Materials and methods.....	61
4.2.1 Reactor configurations, inoculation, and operational conditions	61
4.2.2 Analytical methods.....	63
4.2.3 Microbial community analysis	64
4.2.4 Data analysis.....	64
4.3 Results	65
4.3.1 Reactor performances.....	65
4.3.2 Microbial community	66
4.4 Discussion	70
4.5 Conclusions	72
Chapter 5: Aerobic decolorization of Acid Orange 7 (AO7) dye coupled with Mn(II) oxidation	75
5.1 Introduction	76
5.2 Materials and methods.....	77
5.2.1 Chemicals and reagents	77
5.2.2 Batch decolorization of AO7 by abiotic-MnO ₂	78
5.2.3 Synthetic dye-containing wastewater	78
5.2.4 Reactor configurations and operational conditions	78
5.2.5 Analytical methods.....	83
5.2.6 Isolation, screening and identification of microorganism	83
5.2.7 Dye decolorization and manganese oxidation ability of the isolates	84
5.2.8 Molecular characterization of isolates.....	84
5.2.9 Microbial community analysis	84
5.3 Results	85
5.3.1 Batch decolorization of AO7 by abiotic-MnO ₂	85
5.3.2 Reactor performances.....	86
5.3.3 Microbial community of the reactors	90
5.3.4 Isolation, screening and identification of microorganisms.....	93
5.4 Discussion	96
5.4.1 Reactor performances.....	96
5.4.2 Microbial community and isolates	99

5.5	Conclusions	99
Chapter 6: Decolorization of an azo dye Bordeaux S under manganese-oxidizing and manganese-oxides-reducing conditions		
105		
6.1	Introduction	106
6.2	Materials and methods.....	108
6.2.1	Azo dye.....	108
6.2.2	Batch experiments	109
6.2.3	Continuous azo dye treatment	110
6.2.4	Analytical methods.....	112
6.2.5	Microbial community analysis	112
6.2.6	Statistical analysis	113
6.3	Results	113
6.3.1	Batch experiments	113
6.3.2	Reactor performance	117
6.3.3	Microbial community	122
6.4	Discussion	129
6.5	Conclusions	134
Chapter 7: Integrated anaerobic-aerobic reactor under manganese redox cycling for degradation of azo dye-containing wastewater.....		
143		
7.1	Introduction	144
7.2	Materials and methods.....	145
7.2.1	Synthetic dye wastewater	145
7.2.2	Bioreactor set-up and operational conditions	146
7.2.3	Chemical oxidation of ammonium with abiotic-MnO ₂	147
7.2.4	Analytical methods.....	149
7.3	Results	149
7.3.1	Reactor performances.....	149
7.3.2	Batch experiment with abiotic-MnO ₂	154
7.4	Discussion	156
7.5	Conclusions	159
Chapter 8: General conclusions, perspectives and recommendations		
163		
8.1	Main results of this study	164
8.1.1	Enrichment of manganese-oxidizing bacteria in a continuous DHS reactor using different organic substrates.....	164

8.1.2	Residual Mn(II) concentrations affect the Mn(II) oxidation performance of the reactor	165
8.1.3	Aerobic decolorization of Acid Orange 7 (AO7) dye coupled with Mn(II) oxidation	166
8.1.4	Decolorization of an azo dye Bordeaux S (BS) under manganese-oxidizing and manganese-oxide reducing conditions	166
8.1.5	Integrated anaerobic-aerobic reactor under manganese redox cycling for degradation of azo dye-containing wastewater	167
8.2	Perspectives	167
8.3	Recommendations	169
Appendix A. Publications arising from this thesis		173

List of Tables

Table 2.1:	The basic physico-chemical properties of manganese element
Table 2.2:	Manganese oxides form frequently found in the environment
Table 2.3:	The world production of manganese ore in 2015
Table 2.4:	Some MnOB communities detected in natural and engineered ecosystem
Table 2.5:	Physical and chemical properties of biogenic manganese oxides by different bacteria
Tabel 2.6:	Decolorization of dye compounds by microbial strains in pure culture
Table 2.7:	Bacterial consortiums capable of decolorization of dye
Table 2.8:	Removal of dye in various bioreactors
Table 3.1:	Operational conditions of the three DHS reactors
Table 3.2:	Sequence reads, total number of OTU and diversity of each reactor
Table 4.1:	Operational conditions of the DHS reactors.
Table 4.2:	Sequence reads, total number of OTU and diversity of each sample
Table 5.1:	Physico-chemical properties of Acid Orange 7 (AO7)
Table 5.2:	Reactor operational conditions
Table 5.3:	Sequence reads, total numbers of OTUs and diversities of the reactors
Table 5.4:	Characterization of identified bacterial isolates
Table 6.1:	Chemical structure and properties of Bordeaux S.
Table 6.2:	Operational conditions of the DHS reactors.
Table 6.3:	Abundance of genera related to their functions in the DHS reactors.
Table 6.4:	Sequence reads, total numbers of OTUs and diversities of both reactors under aerobic and anaerobic conditions
Table 6.5:	A comparison of the reactor performances between this study and previous studies
Table 7.1:	Operational conditions of the integrated DHS reactors
Table 7.2:	Column experiment conditions and feed solution
Table 7.3:	The result of batch experiment with abiotic-MnO ₂
Table 7.4:	The results of 1 st experiment of column reactor
Table 7.5:	The results of 2 nd experiment of column reactor
Table 7.6:	The results of 3 rd experiment of column reactor
Table 7.7:	The results of 4 th , 5 th , and 6 th experiment of column reactor

List of Figures

- Figure 1.1: Research design of this dissertation
- Figure 2.1: Manganese ore mine in the Kalahari District of South Africa (adapted from <https://geology.com/usgs/manganese/>)
- Figure 2.2: Application of manganese in various industries (Adapted from Clarke and Upson, 2017)
- Figure 2.3: Ferromanganese nodule from (a) the Clarion Clipperton Zone, Pacific Ocean (adapted from Blöthe et al., 2015), and (b) the Central Indian Ocean Basin (adapted from Randhawa et al., 2016)
- Figure 2.4: Manganese redox cycling in a water-sediment environment mediated by microorganisms (adapted from De Schamphelaire et al., 2007 with modification)
- Figure 3.1: Reactor configuration
- Figure 3.2: The performance of R-1, R-2, and R-3. The arrows indicate biofilm sampling on day-60 and day-131.
- Figure 3.3: Mn(II) removal rates of each reactor during Phase 2 and 3.
- Figure 3.4: Relationship between Mn(II) loading and removal rate.
- Figure 3.5: Microbial community at the phyla level. Phyla with relative abundance <1% were classified as “Others”.
- Figure 3.6: Most dominant genera in the reactors with relative abundance >3% of the total sequence reads in each sample.
- Figure 3.7: Relative abundance of putative manganese-oxidizing bacteria.
- Figure 4.1: Configuration of the DHS reactors.
- Figure 4.2: The performance of R-1 and R-2.
- Figure 4.3: Microbial community at the phyla level. Phyla with relative abundance <1% were classified as “Others”.
- Figure 4.4: Most dominant genera in the reactors with relative abundance >1% of the total sequence reads in each sample.
- Figure 4.5: Relative abundance of putative manganese-oxidizing bacteria with relative abundance greater than 1%.
- Figure 4.6: Relationship between Mn(II) oxidation performance and residual Mn(II) concentration at each phase.

- Figure 5.1: DHS reactor configurations.
- Figure 5.2: Capacity of abiotic-MnO₂ for removal of AO7 in batch experiments.
- Figure 5.3: DHS reactor performances.
- Figure 5.4: Microbial community at the phylum level, the phylum with relative abundance below 1% were grouped in “others”.
- Figure 5.5: Microbial community at the genus level with relative abundances >1%.
- Figure 5.6: Putative MnOB community with relative abundance >1%.
- Figure 5.7: Decolorization ability of isolates and their growth
- Figure 5.8: Mn-oxidizing ability test of isolates using LBB-1, the left-most tube of each photo is using abiotic-MnO₂ as control.
- Figure 5.9: TOC concentration during Stage 1 and Stage 2. Mn-oxidation reactor (R-4) is more effectively decompose organic substances than without Mn-oxidation (R-3).
- Figure 6.1: DHS reactor configurations.
- Figure 6.2: Batch decolorization experiments for BS (10 mg L⁻¹) by abiotic-MnO₂ (0.5 g).
- Figure 6.3: Appearance of abiotic anaerobic BS decolorization experiment with different substrates at 0 h (a-c), and after 48 h incubation (d-f).
- Figure 6.4: Batch decolorization of BS under abiotic anaerobic conditions with different substrate compositions.
- Figure 6.5: Appearance of chemical BS decolorization using 0.01M Na₂S.9H₂O with three different substrate compositions; (1): BS + Na₂S, (2): BS + K-medium (100 mg COD/l) + Na₂S, and (3): BS + K-medium + 0.1 g MnO₂ + Na₂S, at the conditions of before Na₂S.9H₂O addition (1a, 2a, 3a), immediately after addition (1b, 2b, 3b), after 48h incubation (1c, 2c, 3c), and UV-Vis spectrophotometer analysis of each condition (1d, 2d, 3d).
- Figure 6.6: Decolorization of BS using 0.01M Na₂S.9H₂O with different substrate compositions.
- Figure 6.7: The performance of the two DHS reactors. The black arrows indicate the days when biofilm samples were taken from the reactors (day 116, 166, and 534).
- Figure 6.8: Relationships between COD removal rates and BS removal rates at different BS loading rates: (a) 2.8 kg BS m⁻³ d⁻¹, and (b) 5.6 kg BS m⁻³ d⁻¹.
- Figure 6.9: Relationships between COD loading rates and COD removal rates
- Figure 6.10: Illumina 16S rRNA gene amplicon sequencing results

- Figure 6.11: Microbial communities at the phylum level. “Others” represents all phyla that have relative abundances of less than 1%.
- Figure 6.12: Microbial communities at the genus level with relative abundances >1%.
- Figure 6.13: Archaeal community compositions at the genus level.
- Figure 6.14: The effect of the added K-medium on the decolorization of BS under anaerobic conditions at different concentrations, (a) 7.5 mg L⁻¹, (b) 60 mg L⁻¹, (c) 120 mg L⁻¹, and (d) 240 mg L⁻¹.
- Figure 6.15: HPLC traces of (a) a standard solution of Bordeaux S (RT = 2.395) and 4-amino-1-naphthalenesulfonic acid (4-ANS) (RT = 2.911), (b) the influent, the effluent from R-1, and the effluent from R-2 on day 501.
- Figure 6.16: Proposed decolorization mechanism at low K-medium loading rate in (a) R-1, and (b) R-2.
- Figure 6.17: Evaluating the amounts of bio-MnO_x produced under aerobic conditions and reduced MnO_x produced under anaerobic conditions based on the Mn(II) removal-rate performance.
- Figure 7.1: Integrated anaerobic-aerobic DHS reactor configurations.
- Figure 7.2: Column experiment design and photo of the column reactor.
- Figure 7.3: The performance of the integrated anaerobic-aerobic reactor.
- Figure 7.4: Nitrogen mass balance in the anaerobic reactor
- Figure 7.5: Nitrogen mass balance in the aerobic reactor
- Figure 7.6: Ammonium oxidation coupled with manganese reduction mediated by a microbial strain *Shewanella algae* C6G3 (Adapted from Aigle, A. et al. 2017)
- Figure 8.1: The scheme summarizing the main results of this study

Abbreviations

4-ANS	4-amino-1-naphthalenesulfonic acid
AO7	Acid orange 7
ART	Air retention time
BAPs	Biomass-associated products
BS	Bordeaux S
COD	Chemical oxygen demand
DHS	Down-flow hanging sponge reactor
DO	Dissolved oxygen
EAB	Electroactive bacteria
EPS	Extracellular polymeric substance
FAD	Flavin adenine dinucleotide
HPLC	High performance liquid chromatography
HRT	Hydraulic retention time
MCOs	Multicopper oxidases
MnOB	Manganese-oxidizing bacteria
MnRB	Manganese-reducing bacteria
NADPH	Nicotinamide adenine dinucleotide phosphate
NPOC	Non-purgeable organic carbon
OD	Optical density
OTU	Operational taxonomic unit
ROS	Reactive oxygen species
SAS	Sterilized activated sludge
TOC	Total organic carbon
UAPs	Utilization-associated products
UASB	Up-flow anaerobic sludge blanket
USGS	United States geological survey

This page is intentionally left blank

Chapter 1: General Introduction

1. 1. Background

The increase in world population has led to the remarkable increase in textile demand. Recently, textile industries are mostly located in developing countries due to their labor-intensive nature and the lower minimum salary in developing countries. Development of textile industry sector could stimulate and give positive effects to the economic development of developing country; however, textile industries can be harmful to the environment due to their large amount consumption of energy and water, and huge volume of wastewater. Textile industry wastewater is considered to be one of the major contributors to the river water pollution in developing countries (De oliviera Neto et al., 2019; Hossain et al., 2018). Textile wastewater contains toxic substances, such as dyes, heavy metals, ammonia, and alkali salts, which can be dangerous to human health and environment (Yaseen and Scholz, 2019). Among of synthetic dyes, azo dye is the most widely used in textile industries; however, its degradation products constitute a major health issue due to mutagenic and carcinogenic potential (Imran et al., 2015; Brüscheiler and Merlot, 2017). Some aromatic amines are detected in wastewater effluents and sludge (Muz et al., 2017; Ning et al., 2015), indicating that aromatic amines could not be completely treated in wastewater treatment processes. Improvement of environmentally friendly and cost-effective technologies to treat azo dye-containing wastewater without generating harmful products is therefore essential.

Biological methods using microbial system have been extensively studied for the treatment of azo dye-containing wastewater under aerobic and anaerobic conditions (Kolekar et al., 2012; Spagni et al., 2012). Various bacterial strains in pure culture, consortium and mixed culture have been reported to capable of decolorizing azo dye (Karim et al., 2018; Saratale et al., 2011). To the author knowledge, the ability of manganese-oxidizing bacteria (MnOB) to decolorize azo dyes have never been investigated. Manganese-oxidizing bacteria are capable of oxidizing Mn(II) to manganese oxides (Mn(III/IV)), or widely known as biogenic manganese oxides (bio-MnO_x), under aerobic conditions (Tebo et al., 2004). The mechanism of Mn(II) oxidation by MnOB is through directly catalysis by multicopper oxidases (MCOs) (Tebo et al., 2005), or indirectly oxidation by reactive oxygen species (ROS) that generated by MnOB (Learman et al., 2011). MnOB are ubiquitous in the environment and have been found in different ecological conditions, especially oligotrophic environments such as caves (Cloutier et al., 2017), deep oceanic sediments (Blothe et al., 2015), hot spring area (Shiraishi et al., 2019), and river estuaries (Anderson et al., 2011).

In the natural environment, biological redox cycling of manganese play an important role in the biogeochemical cycles of organic carbon, nitrogen, sulfur and many elements (Tebo et al., 2005; Borch et al., 2010; Hyun et al., 2017). Under aerobic conditions, MnOB oxidize Mn(II) to insoluble bio-MnO_x by MnOB, while under anaerobic conditions, bio-MnO_x would be reductively dissolved to Mn(II) by manganese-reducing bacteria (MnRB). Due to their physico-chemical properties, bio-MnO_x have been reported capable of removing organic and inorganic pollutants through redox reaction and adsorption, including heavy metals, methylene blue, steroid hormones, biocides and pharmaceutical compounds (Zhou et al., 2015; Zhou et al., 2016; Forrez et al., 2010). However, it should be noted that these studies employ bio-MnO_x in pure form, which are purified from impurities. Removal of heavy metals by enriched MnOB in a continuous reactor have been previously reported (Cao et al., 2015; Matsushita et al., 2018). Furgal et al. (2014) found that steroid hormones, biocides and pharmaceutical compounds could be removed by using *in situ* generated bio-MnO_x. Degradation of 17- α ethinylestradiol by bio-MnO_x could be enhanced in the presence of MnOB indicating that continuous regeneration of bio-MnO_x by MnOB may occur (Tran et al., 2018). The author therefore expected that biological Mn(II) oxidation possesses potential application for removal of azo dye through biodegradation by MnOB metabolisms, being decomposed by attacking-generated ROS, and chemical oxidation and/or adsorption by generated bio-MnO_x.

However, enrichment of MnOB generating high amounts of bio-MnO_x in a continuous bioreactor is challenging. Limited information on a favorable organic substrate for the enrichment of MnOB. Enrichment of MnOB coupled with nitrification in a continuous down-flow hanging sponge (DHS) reactor has been previously reported (Cao et al., 2015). In early studies, MnOB can be enriched by coupling with methane oxidation under freshwater and sea marine conditions (Matsushita et al., 2018; Kato et al., 2017). However, these techniques require a long time to attain high Mn(II) oxidation, and MnOB growth seems to be highly dependent on soluble microbial products that generated by other heterotrophic bacteria. Enrichment of MnOB in pure culture using different organic substrate compositions has been previously investigated. Queiroz et al. (2018) found that compared with nutrient-poor medium (K-medium), nutrient-rich medium (NB medium) not only enhances the growth of MnOB, *Serratia marcescens*, but also improves Mn(II) oxidation resulting in the increase in bio-MnO_x formation. Considering that MnOB inhabit in a wide variety of habitats, the author expected that MnOB could be enriched with different kind of organic substrates. If MnOB could be enriched in the reactor with preferred substrate in a short period of acclimation achieving high

Mn-oxidation and continuous bio-MnO_x generation, it would be a promising technology option for environmental bioremediation.

In addition to biological Mn(II) oxidation under aerobic conditions producing useful materials bio-MnO_x, manganese oxides could act as an electron acceptor for degradation of organic compounds by dissimilatory metal-reducing bacteria under anaerobic conditions (Ghattas et al., 2017; Liu et al., 2018a). Thus, the author expected that manganese oxides, which would undergo reduction to Mn(II), could also enhance degradation of azo dye under anaerobic conditions. Furthermore, the combination of anaerobic and aerobic process with recirculation system would be more favorable, not only to allow manganese recovery but also more complete degradation of organic pollutants.

1. 2. Objectives

The main objective of this research was to investigate whether enrichment of MnOB in a continuous reactor could enhance removal of a recalcitrant azo dye compound. The more specific objectives of this research were:

- a. To investigate the preferred nutrient to support MnOB enrichment achieving high Mn(II) oxidation performance and sustainable high generation of bio-MnO_x.
- b. To investigate the effect of residual Mn(II) on the Mn(II) oxidation performance of the reactors
- c. To investigate decolorization of an azo dye Acid Orange 7 (AO7) coupled with biological Mn(II) oxidation under aerobic conditions.
- d. To investigate decolorization of a sulfonated azo dye Bordeaux (BS) under Mn(II) oxidation (aerobic conditions) and Mn-oxides reduction (anaerobic conditions).
- e. To investigate the effectiveness of the integrated anaerobic-aerobic reactor under Mn reduction-oxidation for further degradation of azo dye and its intermediate products.

1. 3. Outline of dissertation

This dissertation mainly consists of three parts (Figure 1.1) and can be outlined in detail as follows:

Chapter 1 presents the general background of this study, including problem statement, research purpose and the outline of this dissertation.

Chapter 2 covers a literature review of related topics including manganese and its abundance in the nature, biological Mn(II) oxidation and manganese oxides reduction and their potential application for removal of environmental pollutants, the environmental impacts of azo dye and its biological treatment methods.

In **Chapter 3**, three different organic substrates; K-medium, sterilized activated sludge and methanol, were applied as the sole carbon source for MnOB enrichment in a continuous reactor. The ability of organic substrate to provide suitable nutrients for MnOB growth resulting in high Mn(II) oxidation performance was evaluated. The effect of organic loading rate on the enhancement of Mn(II) oxidation performance was investigated. Microbial analysis community was analyzed to characterize microbial profile of the reactors.

The result obtained in Chapter 3 demonstrated that residual Mn(II), due to uncomplete oxidation, may cause toxic effects led to unstable Mn(II) oxidation performance of the reactor, therefore, in **Chapter 4**, the effect of residual Mn(II) on the Mn(II) oxidation performance of the reactors was investigated by comparing two reactors; the first is no residual Mn(II) or very low Mn(II) is detected, and another reactor is configured with high residual Mn(II) in the effluent. Microbial analysis community is assessed to analyze impact of residual Mn(II) on the microbial profile of the reactors.

In **Chapter 5**, the performance of enriched MnOB reactor for removal of an azo dye Acid Orange 7 (AO7) under aerobic conditions was investigated. Isolation and characterization of microbial strains were conducted to investigate whether microbial strains which capable of decolorizing azo dye and oxidizing Mn(II) present in the reactor. In addition, microbial community was analyzed to characterize the microbial profile of the reactors.

Chapter 6 addresses the decolorization of a sulfonated azo dye Bordeaux S under aerobic and anaerobic conditions in two reactors; the first reactor devoid abiotic-MnO₂, and the second reactor contains abiotic-MnO₂. The effect of Mn(II) oxidation and Mn(IV)-oxide reduction on the decolorization of Bordeaux S was investigated. Degradation products of Bordeaux S was investigated by using HPLC. Methane gas, an anaerobic decomposition product of organic substances, was measured. Microbial community analysis was also performed to characterize the microbial profile of the reactors.

Based on the results of Chapter 6, the effluent of anaerobic reactor still contains high organic matters as represented by a high COD value. **Chapter 7** addresses degradation of organic substances by integrated anaerobic-aerobic reactor. This system, which is not only combine anaerobic and aerobic process, but also to allow manganese redox cycling recovery, was evaluated for effective decomposition of organic substances.

Chapter 8 presents the main findings and conclusions of overall this study, after which recommendations for future research are also proposed in this chapter.

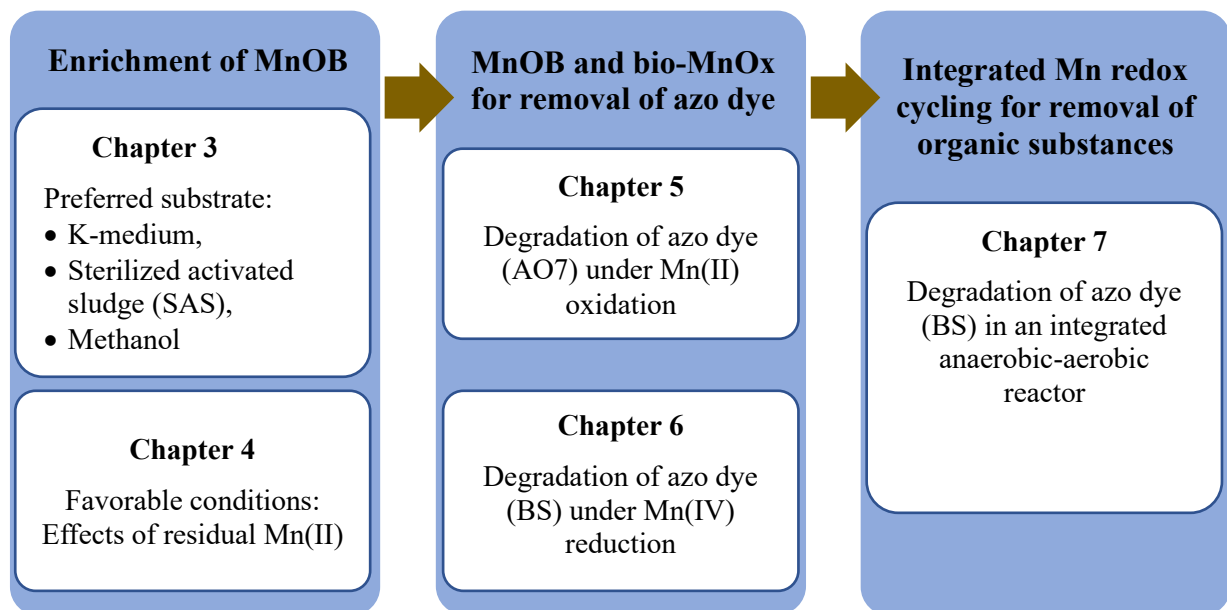


Figure 1.1 Research design of this dissertation

Chapter 2: Literature Review

2.1 Manganese element and its natural abundance

Manganese element, with the symbol Mn and atomic number 25, is one of the transition metal series in the Periodic Table located at group 7 and period 4. In the pure form, the appearance of manganese element (Mn) is a silvery or gray white, very brittle and dense metal. The basic physico-chemical properties of manganese element are given in Table 2.1.

Table 2.1 The basic physico-chemical properties of manganese element

Property	Value
Symbol:	Mn
Atomic Number:	25
Mass Number:	54.93805 amu
Electron Configuration:	[Ar]3d ⁵ 4s ²
Ionization Energy: Mn 3d ⁵ 4s ² → Mn ⁺ 3d ⁵ 4s ¹	7.434 eV
Crystal structure	Complex lattice structure, 54 atom per unit cell
Standard state	Solid at 298 K
Melting Point:	ca. 1,245 °C
Boiling Point	ca. 1,962 °C
Density	7.43 g cm ⁻³ at 293 K
Color	Gray-white or silvery
CAS Registry ID	7439-96-5

Source: Nguyen et al., 2011

Manganese (Mn) is the twelfth abundant elements that are found in nature after oxygen (O), silicon (Si), aluminum (Al), iron (Fe), calcium (Ca), magnesium (Mg), sodium (Na), potassium (K), titanium (Ti), hydrogen (H), and phosphorus (P) (Chang, 2010). Manganese does not occur in nature as free element, but exist in minerals, such as oxides, silicates and carbonates. Manganese oxides form commonly found in the natural environment is given in Table 2.2. They have open crystal structures, large surface areas and high negative charges (Tebo et al., 2004). Among them, birnessite and vernadite are frequently identified in ocean nodules, soils, and Mn-rich ore deposits. Lithiophorite contains Li, and some transition metals, such as Ni, Co, and Cu, commonly substitute in the structure. Todorokite is also one of the major Mn oxides in ocean nodules. Among other polymorphs of MnO₂ (ramsdellite and nsutite), pyrolusite is the most abundant and stable in the environment. However, nsutite is often used as cathode material in dry-cell batteries. Hollandite has been demonstrated for their potential application as ionic conductors and for immobilizing several radioactive cations (Post, 1999).

Table 2.2 Manganese oxides form frequently found in the environment

Mineral name	Formula	Structural type
Birnessite	(Na,Ca,K)Mn ₇ O ₄ ·2.8H ₂ O	Layer structure
Vernadite (δ-MnO ₂)	MnO ₂ ·nH ₂ O	Layer structure
Lithiophorite	LiAl ₂ (Mn ⁴⁺ , Mn ³⁺)O ₆ ·(OH) ₆	Layer structure
Chalcophanite	ZnMn ₃ O ₇ ·3H ₂ O	Layer structure
Pyrolusite (β-MnO ₂)	MnO ₂	Tunnel structure
Ramsdellite	MnO ₂	Tunnel structure
Nsutite (γ-MnO ₂)	Mn(O,OH) ₂	Tunnel structure
Hollandite	Ba _x (Mn ⁴⁺ , Mn ³⁺) ₈ O ₁₆	Tunnel structure
Cryptomelane	K _x (Mn ⁴⁺ , Mn ³⁺) ₈ O ₁₆	Tunnel structure
Manjiroite	Na _x (Mn ⁴⁺ , Mn ³⁺) ₈ O ₁₆	Tunnel structure
Coronadite	Pb _x (Mn ⁴⁺ , Mn ³⁺) ₈ O ₁₆	Tunnel structure
Romanechite	Ba _{0.66} (Mn ⁴⁺ , Mn ³⁺) ₅ O ₁₀ ·1.34H ₂ O	Tunnel structure
Todorokite	(Ca, Na, K) _x (Mn ⁴⁺ , Mn ³⁺) ₆ O ₁₂ ·3.5H ₂ O	Tunnel structure
Manganite (γ-MnOOH)	MnOOH	Tunnel structure
Groutite (α-MnOOH)	MnOOH	Tunnel structure
Feiknechite (β-MnOOH)	MnOOH	Tunnel structure
Hausmannite	Mn ²⁺ Mn ³⁺ ₂ O ₄	Inverse spinel
Bixbyite	Mn ₂ O ₃	Face-centered cubic
Pyrochroite	Mn(OH) ₂	Cubic
Manganosite	MnO	Cubic

Source: Post, 1999

Manganese ores are widespread in all over the world and mined from the open pit mine (Fig. 2.1). However, only high-grade ores, having Mn content of 40%, are feasible to be economically exploitable, and mainly distributed in South Africa, China, Australia, Gabon and Brazil, which are producing approximately 80% of the total global demand (Nguyen et al., 2011). According to USGS report, world production of Mn ores in 2015 was 51,800 thousand metric tons with Mn content was about 17,000 thousand metric tons (Table 2.3). Manganese has been widely used in various applications, such as metallurgical industries (steelmaking industries, including ferrous and non-ferrous metallurgy), and non-metallurgical industries (batteries, electronics, healthcare, agriculture, slag & cements, chemicals, and others) (Clarke and Upson, 2017). Manganese oxides have been used by paleolithic people as pigment of cave painting in Gargas, France (Chalmin et al., 2006). Manganese is a vital element in steel making to improve the strength, toughness, hardenability, and corrosion resistance of steel, and therefore, approximately 80-90% of the total world production of Mn ore is consumed by steel industries (Post, 1999). The wide range application of manganese in various industries is shown in Figure 2.2.



Figure 2.1 Manganese ore mine in the Kalahari District of South Africa (adapted from <https://geology.com/usgs/manganese/>).

Table 2.3 The world production of manganese ore in 2015

Country	Production (thousand metric tons)	
	Gross weight	Mn content
Australia	7,500	2,883
Brazil	2,816	1,226
Burma	70	28
China	13,024	2,084
Gabon	4,112	1,929
Georgia	334	97
Ghana	1,478	416
India	2,117	810
Kazakhstan	615	222
Malaysia	480	187
Mexico	600	217
South Africa	15,952	5,900
Ukraine	1,203	410
Other ¹⁾	1,470	582
Total	51,800	17,000

¹⁾ Other includes Bulgaria, Côte d'Ivoire, Egypt, Hungary, Indonesia, Iran, Morocco, Namibia, Nigeria, Oman, Philippines, Romania, Russia (concentrate), Sudan, Thailand, Turkey, Vietnam, and Zambia.

Source: USGS, accessed on 17 May 2019

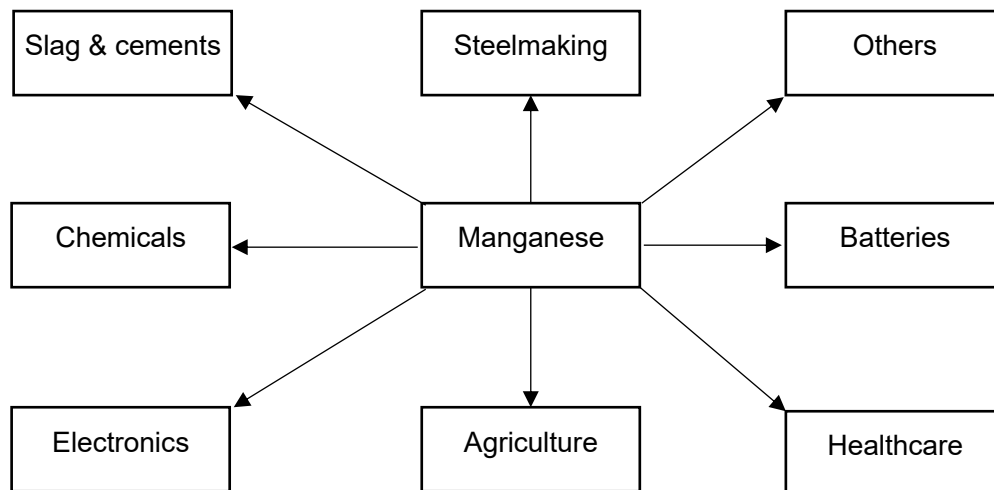


Figure 2.2 Application of manganese in various industries (Adapted from Clarke and Upson, 2017).

In addition to the manganese-ore mining, the manganese nodules deposited at deep ocean floors are being explored as the manganese element and other useful metals source. The manganese nodules not only contain manganese (23.25%), but also iron (6.72%), copper (1.05%), nickel (1.22%), and cobalt (0.073%) (Mishra et al., 2011). The occurrence of manganese and iron in the manganese nodules are in the form of torodokite, busserite, birnessite, vernadite and goethite (Boughriet et al., 1996; Randhawa et al., 2016). The large deposit of manganese nodules have been found in the Pacific Ocean, especially in the Clarion-Clipperton-Zone (CCZ) between the Clarion and Clipperton Fracture Zones, the Peru Basin, near the Cook Islands, and in the Central Indian Ocean Basin (Sprenberg, 2019). Many researchers reported that the formation of manganese nodules in the deep ocean have been associated with microbial activity. Blöthe et al. (2015) shows that microbial Mn(II) oxidation and Mn(IV) reduction are dominant inside the nodule and their composition is different with the microbial community of the sediment near the nodule, indicating that biologically manganese redox cycling may contribute to the nodule formation. Manganese nodules have been reported to grow at slow rate, from a millimeter to centimeter per million years, and located on the seabed sediment, and their sizes vary from micro-sizes (<1 cm in diameter) to macro-sizes (>15 cm in diameter) (Randhawa et al., 2016). Since the demand of manganese and other elements tend to increase while manganese ore mines are depleted, manganese nodules would be a promising element sources in the near future.

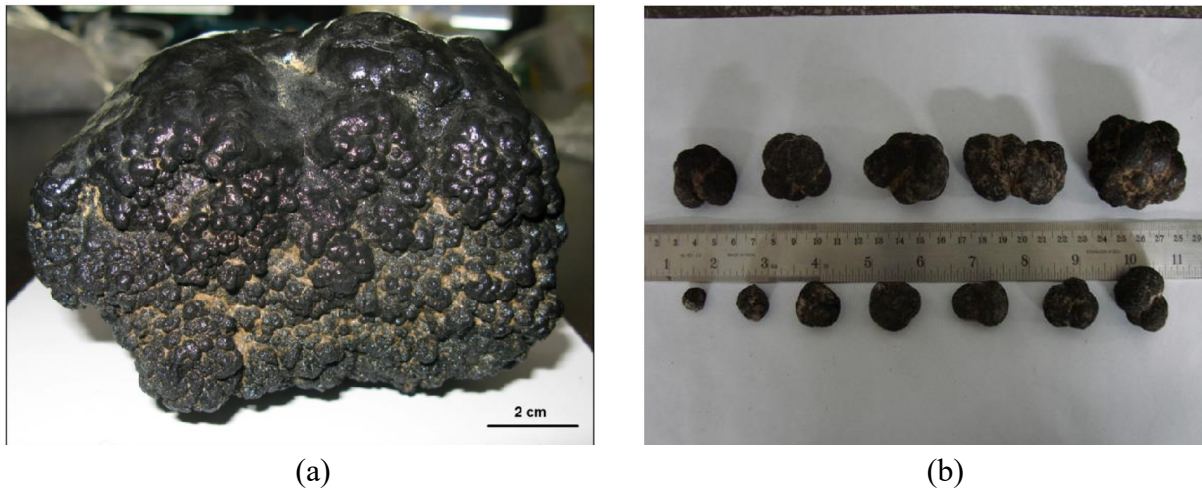


Figure 2.3 Ferromanganese nodule from (a) the Clarion Clipperton Zone, Pacific Ocean (adapted from Blöthe et al., 2015), and (b) the Central Indian Ocean Basin (adapted from Randhawa et al., 2016).

2.2 The manganese redox cycling in the environment

The redox cycling between Mn(II) and MnO_x is an important process for biogeochemical cycle of elements on Earth and microbial metabolism plays a crucial role to control redox chemistry processes. In the water-sediment system, under aerobic conditions or in the presence of oxygen, manganese-oxidizing bacteria (MnOB) facilitate oxidation of Mn(II) to MnO₂, that subsequently precipitate to the sediment due to their nature as insoluble materials. Anaerobic conditions at the sediment and the presence of high organic matters, the deposited MnO₂ would be reduced by manganese-reducing bacteria (MnRB) releasing Mn(II). Disturbance of sediments by organisms or physical factors, such as wave or turbulence, cause the diffusion of Mn(II) to water stream and contact with oxygen, and it will be re-oxidized again by MnOB. This Mn redox cycle usually occurs at the oxic-anoxic boundary, such as the sediment-water interfaces in freshwater environment (Jones et al., 2018), and marine environment (Sulu-Gambari et al. et al., 2016). Therefore, MnO_x are found on the lake sediment layers (Palermo and Dittrich, 2015), surface marine sediment (Sulu-Gambari et al., 2016), or ocean bottom in the form of nodules (Blothe et al., 2018). The microbial manganese redox cycle occurring in a sediment-water system is depicted in Figure 2.4.

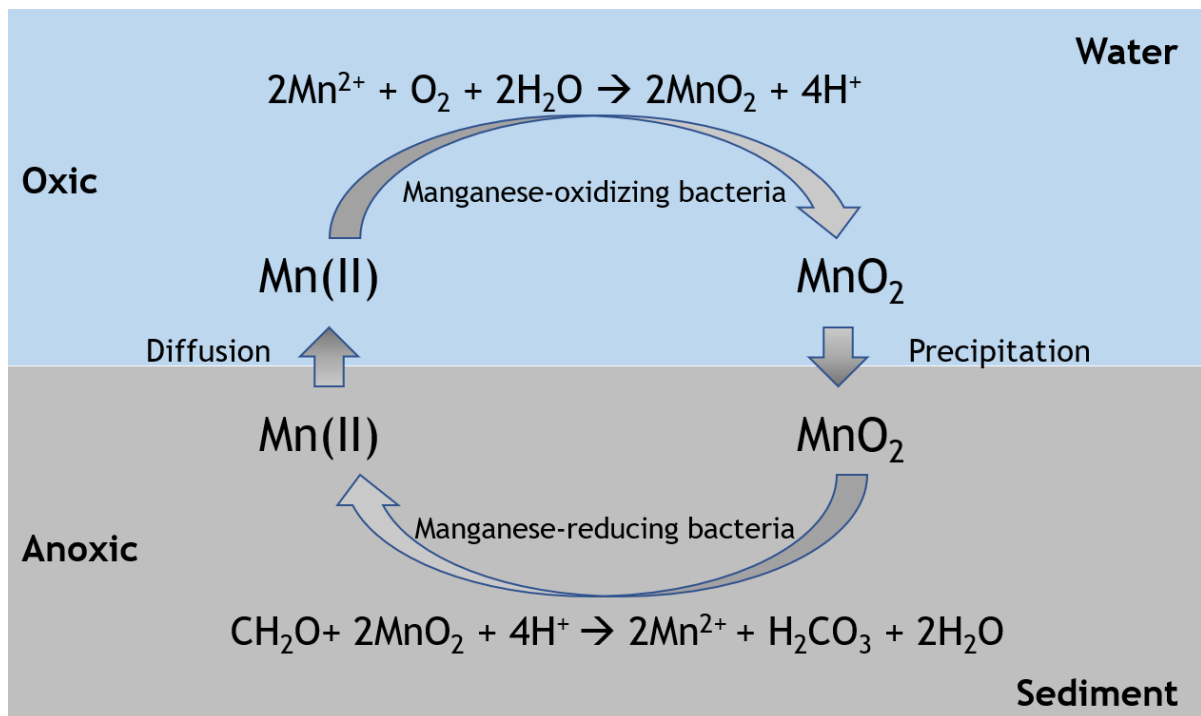


Figure 2.4 Manganese redox cycling in a water-sediment environment mediated by microorganisms (adapted from De Schampelaire et al., 2007 with modification).

2.2.1 Biological Mn(II) oxidation

Biological Mn(II) oxidation mediated by manganese-oxidizing bacteria (MnOB) generates insoluble manganese oxides Mn(III/IV), which is also widely known as biogenic manganese oxides (bio-MnO_x). MnOB are ubiquitous and widespread in nature having high level of manganese, such as freshwater and marine environment, soil, and sediment. They have been detected in oligotrophic environments such as caves and deep oceanic sediments (Carmichael et al., 2015; Cloutier et al., 2017; Blothe et al., 2015), as well as copiotrophic environments, such as river estuary (Anderson et al., 2011). MnOB play an important role in the biogeochemical cycle of elements in nature, such as manganese, carbon, nitrogen, and sulfur (Tebo et al., 2005; Geszvain et al., 2012). They have also been found to facilitate manganese removal in drinking water treatment system (Cerrato et al., 2010). Barboza et al. (2017) isolated a high manganese tolerance and manganese oxidation ability of *Serratia marcescens* from Mn mine in the Iron Quadrangle region, Minas Gerais, Brazil. A diverse MnOB community exists in coal mine drainage treatment system from Pennsylvania, USA (Santelli et al., 2010), the former uranium mining (Akob et al., 2014), and also hot spring area in Japan (Shiraishi et al., 2019). Some MnOB communities detected in natural and engineered ecosystem are given in Table 2.4.

Table 2.4 Some MnOB communities detected in natural and engineered ecosystem.

Habitat	Genus/Species	Phylum	References
Caves in the upper Tennessee River Basin	<i>Arthrobacter</i> sp.	Actinobacteria	Carmichael et al., 2013
	<i>Pseudomonas</i> sp.	Proteobacteria	
	<i>Flavobacterium</i> sp.	Bacteroidetes	
	<i>Janthinobacterium</i> sp.	Proteobacteria	
	<i>Leptothrix</i> sp.	Proteobacteria	
Deep ocean nodules from the northeastern equatorial Pacific	<i>Acinetobacter</i> sp.	Proteobacteria	Blothe et al., 2015
	<i>Shewanella</i>	Proteobacteria	
	<i>Colwellia</i>	Proteobacteria	
The Columbia River Estuary	<i>Pseudomonas</i>	Proteobacteria	Anderson et al., 2011
	<i>Shewanella</i>	Proteobacteria	
	<i>Bacillus</i>	Firmicutes	
	<i>Aurantimonas</i>	Proteobacteria	
The former uranium mining district Ronneburg, Thuringia, Germany	<i>Rhodobacter</i>	Proteobacteria	Akob et al., 2014
	<i>Fulvimarina</i>	Proteobacteria	
	<i>Duganella zoogloeoides</i>	Proteobacteria	
	<i>Janthinobacterium lividum</i>	Proteobacteria	
	<i>Flavobacterium aquidurense</i>	Bacteroidetes	
	<i>Pseudomonas putida</i>	Proteobacteria	
	<i>Burkholderia sordidicola</i>	Proteobacteria	
<i>Arthrobacter stackebrandtii</i>	Actinobacteria		
Mn deposit from Ytterby, Sweden	<i>Frigoribacterium</i> sp.	Actinobacteria	Sjöberg et al., 2018
	<i>Albidiferax ferrireducens</i>	Proteobacteria	
	<i>Pedomicrobium</i> sp.	Proteobacteria	
	<i>Hyphomicrobium</i> sp.	Proteobacteria	
	<i>Terrimonas</i> sp.	Bacteroidetes	
Manganese deposits from Sambe hot spring, Japan	<i>Microbacterium</i> sp.	Actinobacteria	Shiraishi et al., 2019
	<i>Psychrobacillus</i> sp.	Firmicutes	
	<i>Alteromonas</i>	Proteobacteria	
	<i>Arthrobacter</i>	Actinobacteria	
	<i>Hyphomicrobium</i>	Proteobacteria	
Coal Mine Drainage (CMD) treatment system	<i>Mycobacterium</i>	Actinobacteria	Santelli et al., 2010
	<i>Pedomicrobium</i>	Proteobacteria	
	<i>Pseudomonas</i>	Proteobacteria	
	<i>Agrobacterium</i> sp.	Proteobacteria	
Coal Mine Drainage (CMD) treatment system	<i>Bacillus</i> sp.	Firmicutes	Santelli et al., 2010
	<i>Flavobacterium</i> sp.	Bacteroidetes	
	<i>Pseudomonas</i> sp.	Proteobacteria	

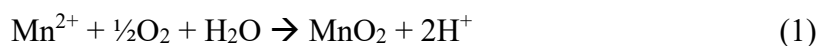
Table 2.4 (continued)

Habitat	Genus/Species	Phylum	References
Drinking water systems in Honduras and USA	<i>L. fusiformis</i>	Firmicutes	Cerrato et al., 2010
	<i>B. pumilus</i>	Firmicutes	
	<i>B. cereus</i>	Firmicutes	
	<i>B. sphaericus</i>	Firmicutes	
	<i>P. aeruginosa</i>	Proteobacteria	
	<i>P. saccharophila</i>	Proteobacteria	
	<i>B. nasdae</i>	Proteobacteria	
	<i>B. simplex</i>	Firmicutes	
	<i>B. brevis</i>	Firmicutes	

MnOB are phylogenetically diverse and belong to several phyla including Firmicutes, Actinobacteria, Bacteroidetes, and Proteobacteria (Tebo et al., 2004). Several MnOB strains in pure culture have been extensively studied and explored as Mn oxidizers and/or catalyst for removal pollutants, such as *Pseudomonas putida* MnB1 (Tran et al., 2018), *Bacillus* sp. (Francis and Tebo, 2002), *Leptothrix discophora* SP6 (Saratovsky et al., 2006), *Roseobacter* sp. AzwK-3b, (Li et al., 2014), *Brevibacillus panacihumi* MK-8 (Zeng et al., 2018), *Acinetobacter* sp. (Hosseinkhani and Emtiazi, 2011), *Shewanella* sp. (Wright et al., 2016), *Aeromonas hydrophila* strain DS02 (Zhang et al., 2019), *Brevibacillus brevis* MO1 and *Brevibacillus parabrevis* MO2 (Zhao et al., 2018), and *Serratia marcescens* (Queiroz et al., 2018).

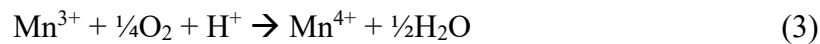
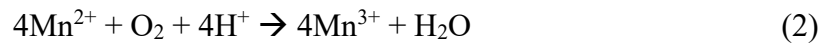
Mechanism of formation of bio-MnO_x

The oxidation of Mn(II) to Mn(III/IV) is thermodynamically favorable at a neutral to high pH and under aerobic conditions according to the equation (1), however, the kinetic of this reaction is very slow with a half-life in the order of hundreds of years (Tebo et al., 2005).

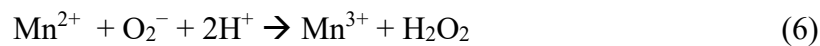


It has been reported that MnOB oxidize manganese as a defense mechanism to protect themselves from toxic environments, such as UV radiation, predation, viral attack, or heavy metals toxicity (Tebo et al., 2005). MnOB oxidize Mn(II) to Mn(III/IV) through direct and indirect process. Multicopper oxidases (MCOs) have been identified in MnOB strains as responsible for direct catalysis of Mn(II) oxidation to Mn(III/IV) (Tebo et al., 2004). MCOs are a group of enzymes that capable of oxidizing various substrates by using copper ions as co-factors. Several MCOs such as MnxG, MofA, MoxA, CotA, CueO, and CopA have identified

as putative Mn(II) oxidases (Tebo et al., 2004; Su et al., 2013; Su et al., 2014; Zeng et al., 2018). Oxidation of Mn(II) to Mn(IV) requires two-electron transfer, however, MCOs oxidize their substrates via one-electron transfer. Therefore, MCOs first catalyze Mn(II) oxidation to Mn(III) and then followed by further oxidation of Mn(III) to Mn(IV) or by disproportionation of complexed Mn(III) (Eq. 2 to 5) (Soldatova et al., 2012). In addition, Soldatova et al. (2012) also shows that Mn(III) is formed during Mn(II) oxidation by MCOs.



Indirect Mn(II) oxidation occurs when organisms release metabolic end products, such as reactive oxygen species (ROS) that can subsequently chemically oxidize Mn(II) to Mn(III/IV) (Eq. 6) (Learman et al., 2011). Learman et al. (2013) demonstrated that oxidation of Mn(II) by abiotically generated superoxide can occur and lead to formation of Mn oxides, which their characteristics are poorly crystalline phyllosilicate with hexagonal symmetry and low Mn(III) content, and structurally similar to those produced biotically by fungi or bacteria.



Potential application of MnOB and bio-MnOx for environmental remediation

Removal of Mn in drinking water system

Soluble Mn(II) in freshwater sources, including river water and groundwater, can cause aesthetic problems and adverse human health effects. As noted above, because the kinetic oxidation of Mn(II) by oxygen is very slow, the stronger chemical oxidants, such as chlorine dioxide (ClO_2), permanganate (MnO_4^-), or ozone (O_3), are required to remove Mn in water (Tobiason et al., 2016). The highly abundant of MnOB in drinking water systems, especially the biological filtration process, has the benefit of not only effective in removing Mn, but also reduce the consumption of chemical oxidants that could generate harmful by-products during catalytic oxidation of Mn (Cerrato et al., 2010; Tobiason et al., 2016).

Several studies demonstrated that manganese from water have been successfully removed through biological process. Abu Hassan et al. (2012) exhibits that ammonium and

manganese could be simultaneously oxidized in biological aerated filter that inoculated with sewage activated sludge, and *Bacillus cereus* is the dominant species in the mixed culture of sewage and the most effective microbe for the removal of ammonium ($\text{NH}_4^+\text{-N}$) and manganese (Mn^{2+}). Groundwater containing Mn(II), Fe(II), As(III), and Sb(III), can be treated by quartz-sand filter bioaugmented with a manganese-oxidizing bacterium (*Pseudomonas* sp. QJX-1) (Bai et al., 2016). The results show that bioaugmentation of MnOB could accelerate the generation of Fe-Mn oxide particles from oxidation Fe(II) and Mn(II), lead to the increase in As(III) and Sb(III) removal through oxidation to As(V) and Sb(V), respectively, followed by adsorption on to the Fe-Mn oxide surfaces. However, contamination or outcompeted by indigenous microbes are the constraints to use pure culture for bioaugmentation in full-scale reactor.

Removal of Mn in acid mine drainage treatment system

Acid mine drainage (AMD) is a contaminated water generated due to the water flows over or through the mining area, and characterized by having low pH and high levels of various heavy metals, such as Fe, Mn, Cd, Cu, Co, Zn, and radionuclides (Tutu et al., 2008). MnOB have been applied in a pilot scale fixed bed bioreactor for removal of manganese from acid mine drainage of the former Wheal Jane tin mine in Cornwall, UK, in which the reactor is initially inoculated with ferromanganese nodules (about 2 cm in diameter), collected from an abandoned mine in north Wales (Hallberg and Johnson, 2005). A treatment system consisting of wetland and limestone bed, is highly effective in removing Mn(II) from acid mine drainage of Pennsylvania, USA, and a diverse MnOB community is present in the system, suggesting that MnOB play a major role in the Mn removal in the treatment system (Santelli et al., 2010). In more recent study, Crafton et al. (2019) reported that a combination of aerobic wetland and limestone bed has shown to be a successful treatment for AMD at the Huff Run watershed of eastern Ohio, USA, for long-term operation (over 13 years), achieving sustainable removal of Fe, Mn, and Al. Fe and Al are primary removed in the aerobic wetland, while high concentration of Mn is only partially removed in the aerobic wetland and further removal takes place in the limestone bed. The high Mn removal in the limestone bed is attributable to the high abundance of MnOB, as revealed by microbial community analysis.

Removal of inorganic pollutants

As mentioned above, MnOB are able to oxidize Mn(II) to bio-MnO_x in the form of Mn(III) or Mn(IV). The physical and chemical characteristics of biogenic manganese oxides are shown in Table 2.5. Due to having high specific surface area, poorly crystalline structure, high number of vacancy sites, and strong oxidant nature, bio-MnO_x possess ability to adsorb and/or oxidize heavy metals. Ba, Ni, Co, Cd, Zn, Ce, Pb and Sb can be adsorbed by bio-MnO_x (Mayanna et al., 2015; Zhou et al., 2015; Wang et al., 2019). Bio-MnO_x have also been shown to oxidize heavy metals, such as Cr(III), Sb(III) and As(III). Cr(III), Sb(III) and As(III) are initially adsorbed on the bio-MnO_x surface and then oxidized to Cr(VI), Sb(V) and As(V), respectively (Murray and Tebo, 2007; Bai et al., 2017; Liang et al., 2017). Oxidation rate of Cr(III) by bio-MnO_x generated from *Bacillus* sp. strain SG-1 is faster than synthetic δ -MnO₂ (Murray and Tebo, 2007). In more recent study, simultaneous removal of Co and Ni through adsorption mechanism using *in situ* generated bio-MnO_x in down-flow hanging sponge (DHS) reactor has been reported by Cao et al. (2015) and Matsushita et al. (2018). More recently, He et al. (2019a) demonstrates that high removal of As(III) can be achieved by manganese-oxidizing aerobic granule sludge (Mn-AGS) in sequencing batch reactor (SBR) through oxidation of As(III) to As(V) by generated bio-MnO_x, H₂O₂, and microbes. In another study, He et al. (2019b) reported that As(III) and Sb(III) can be successfully oxidized to less toxic As(V) and Sb(V), while Cr(III) was not oxidized to Cr(VI) and Cr(VI) can be reduced to Cr(III) in the Mn-AGS reactor. Murray and Tebo (2007) investigated the ability of manganese-oxidizing bacterium *Bacillus* sp. Strain SG-1 to oxidize Cr(III). The results demonstrated that the presence of bacterial strain *Bacillus* sp. Strain SG-1 can accelerate Cr(III) oxidation compared to both abiotic and biogenic Mn oxides. The oxidation of Cr(III) to Cr(VI) in natural systems has been observed by Fandeur et al. (2009) in ultramafic rocks of New Caledonia. The results show that the largest amounts of Cr(VI) is found in the transition laterite, where Mn concentrations are the highest and where this element occurs as Mn(IV). These results indicate that Mn(IV) reduction plays an important role in the oxidation Cr(III) to Cr(VI).

Table 2.5 Physical and chemical properties of biogenic manganese oxides by different bacteria.

Parameter	Nealson et al., 1999	Meng et al., 2009	Su et al., 2014	Zhang et al., 2019
MnOB	<i>Leptothrix discophora</i> SS-1	<i>Bacillus</i> sp. WH4	<i>E. coli</i> strains K-12 substr. MG1655 and BL21	<i>Aeromonas hydrophila</i> strain DS02
Particle diameters	n.a.	Nano size	150–350 nm	n.a.
Structure	poorly crystalline	irregular geometric shape, poor crystallinity	no specific shape, and weak crystalline nature	flake-shaped and porous structure
BET specific surface area	224 m ² g ⁻¹	30.6 m ² g ⁻¹ ¹⁾	n.a.	n.a.

Remark:

n.a. = not available

¹⁾ A mixture of biogenic Mn oxide particulates and spores

Degradation of organic pollutants

Bio-MnO_x are strong oxidant and their abundance in the natural environment have been reported to play an important role in the biogeochemical cycles of organic carbon, nitrogen, sulfur and phosphorus (Tebo et al., 2005; Geszvain et al., 2012). The presence of bio-MnO_x in nature would be beneficial because some microorganisms are known to utilize Mn oxides as electron acceptor for the oxidation of organic compounds. Mn oxides reduction contributes to the organic carbon oxidation in offshore sediments of the deep Ulleung Basin, East Sea (Hyun et al., 2017). Jones et al. (2018) demonstrated that biotic Mn(II) oxidation formed bio-MnO_x, contributes to carbon oxidation along oxic-anoxic interfaces in soils and sediments. The presence of Mn oxides in suboxic sediment of the Clarion-Clipperton fracture zone mediates nitrogen cycling, in which ammonium generated from organic matter decomposition is oxidized by manganese oxides under the oxic zone (Mogollón et al., 2016).

MnOB and bio-MnO_x, as the strong oxidant agent, have gained much attention from many researchers to degrade organic pollutants. Bio-MnO_x have been shown to degrade several organic compounds, such as estrone, 17- α ethinylestradiol, diclofenac, carbofuran, ciprofloxacin (Tu et al., 2014; Furgal et al., 2014; Liu et al., 2016). In recent study, synergistic between MnOB and bio-MnO_x could enhance degradation of 17- α ethinylestradiol, in which its degradation mechanism involves biological degradation by MnOB and chemical reaction with bio-MnO_x (Tran et al., 2018). In another study, degradation of sulfamethoxazole by manganese-oxidizing bacteria has been shown in sequence batch reactor with the removal

efficiency ranging from 40% to 98% and its performance is dependent on the feeding concentrations and hydraulic retention time (Zhang et al., 2017). MnO_x ore filled biological aerated filter (BAF) which is initially inoculated with MnOB consortium (*Leptothrix* sp. and *Pseudomonas* sp.) have been shown capable of removing pharmaceutical compounds, including carbamazepine, diclofenac, and sulfamethoxazole (Zhang et al., 2015). The removal efficiency of diclofenac and sulfamethoxazole are in the range of 80-90%, while carbamazepine is less than 20%. In more recent study, continuous degradation of 1,2,4-triazole, an intermediate product of medicine and widely used in pesticides, coupled with manganese oxidation in biological aerated filter (BAF) inoculated with MnOB consortium achieves 50% removal efficiency, and *Pseudomonas* and *Bacillus* are the most predominant MnOB in the reactor (Wu et al., 2017).

2.2.2 Biological manganese oxides-reduction

Under anaerobic condition, manganese oxides undergo reduction to Mn(II). Manganese oxides reduction is therefore important to provide Mn(II) for metabolism of organisms. Many studies reported that microbial MnO_x reduction in marine sediments affect the biogeochemical cycles of elements, such as carbon, sulfur, nitrogen and many trace metals (Burdige, 1993; Hulth et al., 1999; Hyun et al., 2017). The mechanism of MnO_x reduction can be through direct enzymatic reduction by manganese-reducing bacteria (MnRB) or indirect reduction by dissimilatory manganese oxide-reducing bacteria through coupling with oxidation of organic compounds (Gounot et al., 1994). MnO_x have been reported to catalyze anaerobic ammonium (NH₄⁺) oxidation to nitrite (NO₂⁻) or nitrate (NO₃⁻) in marine sediments, and the ratio of N to Mn is the important factor governing this process (Lin and Taillefert, 2014). Elemental sulfur coupling with MnO_x reduction, is biologically catalyzed to sulfate and sulfide (Thamdrup et al., 1993). Dissimilatory manganese oxide-reducing bacteria utilize manganese oxides as an electron acceptor for their metabolism, which usually occurs under anaerobic conditions (Lovley, 1991).

Shewanella and *Geobacter* are two microbial strain that have been extensively studied for their ability to reduce MnO_x (Shi et al., 2007; Richter et al., 2012). Numerous bacteria which capable of reducing MnO_x have also been isolated and identified by many studies. Manganese-reducing bacteria were isolated from Black Sea, including *Shewanella*, *Pseudomonas* spp., *Bacillus* spp. (Nealson et al., 1991). *Clostridium* sp., a widely known N-fixing bacterium, has been reported to facilitate the reductive dissolution of manganese oxides

(Francis and Dodge, 1988). *Alteromonas putrefaciens* (strain MR-1) isolated from Oneida lake, NY, USA, is not only capable of rapid Mn(IV) reduction under conditions of neutral pH, but also reduces Fe^{3+} to Fe^{2+} , and disproportionates thiosulfate to sulfide and sulfite (Myers and Nealson, 1988). *Arcobacter*, *Colwellia*, *Shewanella*, and *Alteromonadales* found in manganese oxide-rich sediments from Gullmar Fjord (Sweden), Skagerrak (Norway) and Ulleung Basin (Korea), can reduce MnO_x coupled with acetate oxidation (Vandieken et al., 2017). In a more recent study, Henkel et al. (2019) isolates the genus *Sulfurimonas* from the Black Sea, which capable to oxidize H_2S or thiosulfate ($\text{S}_2\text{O}_3^{2-}$) by using Mn-oxides as electron acceptor.

MnO_x reduction would be beneficial for biodegradation of organic pollutants (Ghattas et al., 2017). MnO_x can act as an electron acceptor during the degradation of organic compounds such as BTEX (benzene, toluene, ethylbenzene, and xylenes) and naphthalene (Langenhoff et al., 1996; Villatoro-Monzón et al., 2003; Dorer et al., 2016). Degradation of naproxen, an analgesic micropollutant, can be achieved under anaerobic conditions with Mn(IV) as electron acceptor (Schmidt et al., 2017). Liu et al. (2018a) reported that anaerobic biodegradation of pharmaceutical compounds, such as caffeine and naproxen, can be attained using chemically synthesized Mn(IV) and biogenic Mn(IV) generated from drinking water treatment plants, but no removal is found for ibuprofen and metoprolol. Swathi et al. (2017) reported that microbially mediated anoxic nitrification-denitrification in the presence of nanoscale manganese oxides could remove ammonium, and this method is feasible for application, in term of less energy consumption for aeration and reduce COD requirement compared to conventional method. In addition to MnO_x reduction, *Shewanella xiamenensis*, a widely known dissimilatory manganese-reducing bacterium, is able to decolorize azo dye, and Mn(II) addition improves its performance (Ng et al., 2014).

2.3 Environmental impacts of azo dyes and their biological treatment methods

Azo dye compounds are characterized by the presence of the azo function ($-\text{N}=\text{N}-$). Azo dyes are commonly used in textile industries due to their nature such as easy to use, relatively cheap, high photolytic stability, a wide range of color availability, and strongly attached to the fabric. Due to their variations in chemical structure, azo dyes can be applied in different applications, such as dyeing of natural products (cotton, paper, silk, leather, wool), synthetics products (polyamides, polyesters, acrylics, polyolefins, viscose rayon, and cellulose acetate), coloring

of paints, varnishes, plastics, printing inks, rubber, foods, drugs, and cosmetics (Chudgar, 2000). In general textile manufacturing, approximately 90% of the textile dyes bind to woven fabrics, with 10% discharged to effluent (Nimkar, 2018).

Azo dye-containing wastewaters are of major concern, because of not only their aesthetic problem related to the color appearance, but also many their degradation products are toxic, potentially mutagenic, carcinogenic or causing adverse health (Brüschweiler and Merlot, 2017). Azo dyes and their metabolites persist in the environment and are not completely degraded in the conventional aerobic wastewater treatment, such as activated sludge (Shaul et al., 1991; Ekici et al., 2001); therefore untreated azo dyes and their metabolites are still detected in the river water and sludge (Vacchi et al., 2016; Ning et al., 2015). Aniline, an aromatic amine, affect reproductive functions of fish (Bhunja et al., 2003). Exposure to aromatic amines may increase the risk of cancer in humans. Skipper et al. (2010) reported that alkylaniline, a monocyclic aromatic amine compound, possess carcinogenic effect that may induce bladder cancer in human.

Biological treatment method is a cost-effective and eco-friendly process without generating harmful products for azo dye degradation compared to physical chemical method. Azo dyes are generally resistant to biological activity under aerobic conditions; however, degradation of azo dyes by microbial communities under aerobic conditions have been reported by many studies (Buitron et al., 2002; Kolekar et al., 2012; Tan et al., 2013; Krishnan et al., 2017; Sarvajith et al., 2018). Some strains in pure culture have been shown to decolorize azo dye under aerobic conditions, such as *Klebsiella oxytoca*, *Comamonas* sp., *Bacillus* sp., *Aeromonas* sp., *Pseudomonas* (Yu et al., 2014; Jadhav et al., 2008; Telke et al., 2009; Du et al., 2015; Meerbergen et al., 2018). Microbial strains which capable of decolorizing dye were summarized in Table 2.6. Decolorization of azo dye using microbial consortium under aerobic conditions can be achieved if additional co-substrate is supplemented, and without any extra supplementary carbon source, decolorization of azo dye is found to be difficult (Moosvi et al. 2007). Contrary to the result reported by Tan et al. (2013), in which azo dye could be decolorized by the aerobic microbial community without any additional carbon source, and microorganisms could utilize azo dye as carbon sources. Microbial consortiums which capable of decolorizing dye were given in Table 2.7.

Tabel 2.6. Decolorization of dye compounds by microbial strains in pure culture

Microbial strain	Dye compound	Decolorization	References
<i>Aeromonas</i> sp.	Bordeaux S	98%	Hayase et al., 2000
	Methyl Orange	95%	
	Orange II	90%	
	Tartrazine	83%	
	Remazol Brilliant Blue R	25%	
	Acid Blue 45	18%	
	Reactive Blue 5	9%	
	Acid Blue 74	96%	
	Poly R-478	7%	
	Nigrosine	2%	
Crystal Violet	86%		
<i>Aeromonas hydrophila</i>	Reactive Red 198,	82–86%	Hsueh et al., 2009
	Reactive Black 5,	62–67%	
	Reactive Red 141,	10–17%	
	Reactive Blue 171,	13–15%	
	Reactive Yellow 84	20–28%	
<i>Aeromonas</i> sp.	Methyl Orange	100%	Du et al., 2015
<i>Klebsiella oxytoca</i>	Methyl Red	95%	Yu et al., 2014
<i>Comamonas</i> sp.	Direct Red 5B	72%	Jadhav et al., 2008
	Direct Brown MR	93%	
	Direct Orange T4	87%	
	Direct Yellow 5GL	93%	
	Disperse Golden Yellow	95%	
	Brilliant Blue GRL	73%	
	Reactive Blue HERD	95%	
	Golden Yellow HER	90%	
	Blue 2RNL	78%	
	Navy Blue 2GL	80%	
	Navy Blue HE2R	73%	
	DK Red 2B	75%	
	Navy Blue RX	70%	
Red HE8B	65%		
<i>Bacillus</i> sp.	Reactive Orange 16	88%	Telke et al., 2009
<i>Bacillus</i> sp.	Reactive Black 5	95%	Wang et al., 2013
<i>Pseudomonas</i> sp.	Reactive Orange 16	>75%	Meerbergen et al., 2018
<i>Klebsiella</i> sp.		35–75%	
<i>Acinetobacter</i> sp.		>35%	
<i>Pseudomonas</i> sp.	Reactive Green 19	>35%	
<i>Klebsiella</i> sp.		>35%	
<i>Acinetobacter</i> sp.		>35%	
<i>Shewanella</i> sp.	Reactive Black-5	50-90%	Imran et al., 2016
	Direct Red-81	37–99%	
	Acid Red-88	34–94%	
<i>Shewanella aquimarina</i>	Acid Red 27	>97%	Meng et al., 2012
<i>Enterobacter</i> sp.	Reactive Black 5	79–85%	Chen et al., 2011
<i>Sphingomonas paucimobilis</i>	Methylene Blue	>85%	Noraini et al., 2012
<i>Brevibacterium</i> sp.	Reactive Yellow 107	99%	Franciscon et al., 2012
	Reactive Black 5	99%	

Table 2.7 Bacterial consortiums capable of decolorization of dye

Microbial consortium	Dye compound	Decolorization	References
<i>Brevibacillus panacihumi</i> strain ZB1, <i>Lysinibacillus fusiformis</i> strain ZB2, <i>Enterococcus faecalis</i> strain ZL	Acid Orange 7	98%	Bay et al., 2014
Six different classes: α -, β -, and γ -proteobacteria, Bacilli, Cytophagia, and Nitrospirales.	Reactive Red 3BS Reactive Violet KN-4R Acid Brilliant Scarlet GR Acid Red B Acid Orange II	>95% >90% >75% >80% >90%	Tan et al., 2013
<i>Bacillus vallismortis</i> , <i>Bacillus pumilus</i> , <i>Bacillus cereus</i> , <i>Bacillus subtilis</i> , <i>Bacillus megaterium</i>	Congo red Bordeaux Ranocid Fast Blue Blue BCC	96% 90% 81% 83%	Tony et al., 2009
<i>Paenibacillus polymyxa</i> , <i>Micrococcus luteus</i> , <i>Micrococcus</i> sp.	Reactive Violet 5R	94%	Moosvi et al., 2007
<i>Zobellella taiwanensis</i> strain AT 1–3, <i>Bacillus pumilus</i> strain HKG212	Reactive green-19	>97%	Das and Mishra, 2017

Degradation of azo dye under anaerobic conditions has been widely reported by many studies (Ong et al., 2012; Spagnoli et al., 2012; Wang et al., 2015; Dai et al., 2018). Anaerobic conditions are more favorable for dye decolorization compared to aerobic conditions. Anaerobic degradation of azo dye is mediated by azoreductase enzymes which cause the reductive azo bond cleavage resulting in the formation of intermediate products, such as aromatic amines, that are potentially toxic and resistant to further degradation under anaerobic conditions (Saratale et al., 2011). Anaerobic decolorization of azo dye is strongly dependent on organic co-substrate addition as electron donor. Donlon et al. (2007) found that decolorization of an azo dye, Mordant Orange 1, failed in a continuous up-flow anaerobic sludge blanket (UASB) reactor without co-substrate addition, and azo dye decolorization can be achieved in the reactor supplemented with either glucose or a volatile fatty acids mixture (acetate, propionate, butyrate). Organic substrates, for example glucose, could serve as electron donor to enzyme cofactors, e.g., via NAD(P)H or reduced FAD(H)₂, which subsequently transferring electrons for azo dye reduction mediated by specific enzymes, such as azoreductase. Removal of dye using various bioreactor systems under both aerobic and anaerobic conditions were summarized in Table 2.8.

Table 2.8 Removal of dye in various bioreactors

System	Dye compound	Conditions	Decolorization	References
Aerobic granular sludge-sequencing batch reactors (AGS-SBR)	Yellow Dye	Microaerophilic	89–100%	Sarvajith et al., 2018
Down flow microaerophilic fixed film bioreactor	A mixture of azo dyes: Reactive Red 2, Reactive Red 198, Reactive Red 120, Reactive Blue 160, Reactive Blue 13, Reactive Blue 172	Microaerophilic	99.5%	Balapure et al., 2015
Sequencing batch biofilter	Acid red 151	Aerobic	99%	Buitron et al., 2004
Membrane-aerated biofilm reactor	Acid Orange 7	Aerobic	98%	Wang et al., 2012
Hydrolysis acidification (HA) reactor	A mixture dye: Reactive Black 5 (RB5) Remazol Brilliant Blue R (RBBR)	Anaerobic	51%	Xie et al., 2018
Anaerobic reactor	Acid Orange 7 (AO7)	Anaerobic	93–96%	Li et al., 2017
A continuous upflow anaerobic sludge-blanket reactor	Mordant orange 1	Anaerobic	>75%	Donlon et al., 1997
A continuous stirred tank reactor (CSTR) with bioelectrochemical system	Alizarin Yellow R	Anaerobic	97%	Cui et al., 2016
Sulfidogenic anaerobic baffled reactor	Remazol Brilliant Violet 5R	Anaerobic	>90%	Ozdemir et al., 2013
Sequential anaerobic sequencing batch reactor/moving bed sequencing batch biofilm reactor	Acid Red 18	Anaerobic-aerobic	>97% in the anaerobic reactor	Hosseini Koupaie et al., 2012
Hybrid up flow anaerobic sludge-filter bed (UASFB)-aerobic activated sludge reactor	Acid Yellow 36	Anaerobic-aerobic	100%	Ahmad et al., 2010

Aromatic amines formed in anaerobic degradation of azo dye are generally not degraded and accumulate under anaerobic conditions. Aerobic treatment process has shown to be effective as post treatment for removal of aromatic amines, in which more than 80% removal of 1-naphthylamine-4-sulfonate (1N-4S), an intermediate anaerobically degradation product of Acid Red 18, can be achieved in aerobic moving bed sequencing batch biofilm reactor (MB-SBBR), and high removal efficiency is attributable to the high percentage of porosity of the biofilm structure (Hosseini Koupaie et al., 2011). Similar results have been demonstrated by Baêta et al. (2015), in which a sequential anaerobic-aerobic reactor is found to be effective to treat azo dye-containing wastewater and removal of an aromatic amine sulfanilic acid, an intermediate product of azo dye Remazol Golden Yellow RNL under anaerobic conditions, can be achieved in an aerobic reactor. Pereira et al. (2011) reported that aromatic amines, aniline and sulfanilic acid, could be degraded under denitrifying conditions in UASB reactor with nitrite and nitrate addition, while if only supplemented with nitrate, only aniline could be degraded and sulfanilic acid remains. In another study, azo dye-containing wastewater can be mineralized in a down flow microaerophilic fixed film reactor and GC-MS analysis reveals that complete degradation of aromatic amines, intermediate products of azo dyes, into aliphatic compounds (Balapure et al., 2015).

Juarez-Ramirez et al. (2012) found interesting results, in which 4-aminonaphthalene-1-sulfonic acid (4-ANS), which is recognized as recalcitrant compound, could be effectively decomposed in nitrogen-limiting fed packed-bed column reactor, and the results demonstrated that 4-ANS, could be utilized by microbial community as the sole carbon source. Some strains are isolated from the reactor, such as *Oleomonas (sagarenensis)*, *Arthrobacter* sp., *Bacillus* sp., *Nocardioides* sp, and *Microbacterium (oxydans)*, which probably contribute to the 4-ANS degradation. In more recent study by Juarez-Ramirez et al. (2015), the mixture of 4-aminobenzene sulfonic acid (4-ABS) and 4-aminonaphthalene-1-sulfonic acid (4-ANS) could be removed in volcanic stone packed-bed column continuous reactor, and six microbial strains are isolated from the reactor which belong to the genera *Variovorax*, *Pseudomonas*, *Bacillus*, *Arthrobacter*, *Nocardioides* and *Microbacterium*. In addition to degradation of aromatic amines by mixed microbial culture in a reactor, degradation of sulfonated aromatic amine, 4-aminobenzene sulfonic acid (4-ABS), could be achieved by aerobic microbial consortium, which consists of *Pseudomonas pseudoalcaligenes*, *Pseudomonas citronellolis* and *Pseudomonas testosterone* (Barsing et al., 2011). Many previous studies also reported some microbial strains in pure culture have ability to degrade aniline, the simplest aromatic amine,

such as *Erwinia* sp. strain HSA 6 (Li and Yu, 2010), *Dietzia natronolimnaea* JQ-AN (Jin et al., 2012), and *Pigmentiphaga daeguensis* (Huang et al., 2018). According to the previous studies above, a wide range of microbes are able to decompose aromatic amines, and their ability is also influenced by other important factors, such as nutrient availability (carbon, nitrogen, sulfur), pH, and also the biodegradability characteristics of aromatic amine compounds.

However, only a few azo dyes have been completely mineralized through aerobic degradation. Jonstrup et al. (2011) shows that aromatic amines are produced during anaerobic degradation of Remazol Red RR, but only partial degradation of aromatic amines is observed, and sulfonated aromatic amines seem to be resistant. The poor biodegradability of aromatic amines under anaerobic and aerobic conditions have been reported by Tan et al. (2005), who found that from the total of ten tested aromatic amine compounds, including 2-aminobenzenesulfonic acid (2-ABS), 3-aminobenzenesulfonic acid (3-ABS), 4-aminobenzenesulfonic acid (4-ABS), 2,4-diaminobenzenesulfonic acid (2,4-DABS), 3-amino-4-hydroxybenzenesulfonic acid (3-A-4-HBS), 1-aminonaphthalene-4-sulfonic acid (1-AN-4-S), 1-aminonaphthalene-5-sulfonic acid (1-AN-5-S), 2-aminonaphthalene-1,5-disulfonic acid (2-AN-1,5-DS), 3-aminonaphthalene-2,7-disulfonic acid (3-AN-2,7-DS), and 8-aminonaphthalene-3,6-disulfonic acid (8-ANO-3,6-DS), only two aminobenzene-sulfonic acid isomers (2- and 4-ABS) can be degraded, and their degradation process only occur under aerobic conditions. The presence of sulfonated structure in aromatic amine compounds cause highly soluble resulted in the lower biodegradability.

References

- Abu Hasan, H., Sheikh Abdullah, S.R., Tan Kofli, N., Kamarudin, S.K., 2012. Effective microbes for simultaneous bio-oxidation of ammonia and manganese in biological aerated filter system. *Bioresour. Technol.* 124, 355–363. <https://doi.org/10.1016/j.biortech.2012.08.055>
- Ahmad, R., Mondal, P.K., Usmani, S.Q., 2010. Hybrid UASFB-aerobic bioreactor for biodegradation of acid yellow-36 in wastewater. *Bioresour. Technol.* 101, 3787–3790. <https://doi.org/10.1016/j.biortech.2009.12.116>
- Akob, D.M., Bohu, T., Beyer, A., Schäffner, F., Händel, M., Johnson, C.A., Merten, D., Büchel, G., Totsche, K.U., Küsel, K., 2014. Identification of Mn(II)-oxidizing bacteria from a low-pH contaminated former uranium mine. *Appl. Environ. Microbiol.* 80, 5086–5097. <https://doi.org/10.1128/AEM.01296-14>
- Anderson, C.R., Davis, R.E., Bandolin, N.S., Baptista, A.M., Tebo, B.M., 2011. Analysis of in situ manganese(II) oxidation in the Columbia River and offshore plume: Linking

- Aurantimonas* and the associated microbial community to an active biogeochemical cycle. Environ. Microbiol. 13, 1561–1576. <https://doi.org/10.1111/j.1462-2920.2011.02462.x>
- Baêta, B.E.L., Lima, D.R.S., Silva, S.Q., Aquino, S.F., 2015. Evaluation of soluble microbial products and aromatic amines accumulation during a combined anaerobic/aerobic treatment of a model azo dye. Chem. Eng. J. 259, 936–944. <https://doi.org/10.1016/j.cej.2014.08.050>
- Bai, Y., Chang, Y., Liang, J., Chen, C., Qu, J., 2016. Treatment of groundwater containing Mn(II), Fe(II), As(III) and Sb(III) by bioaugmented quartz-sand filters. Water Res. 106, 126–134. <https://doi.org/10.1016/j.watres.2016.09.040>
- Balapure, K., Bhatt, N., Madamwar, D., 2015. Mineralization of reactive azo dyes present in simulated textile wastewater using down flow microaerophilic fixed film bioreactor. Bioresour. Technol. 175, 1–7. <https://doi.org/10.1016/j.biortech.2014.10.040>
- Barboza, N.R., Morais, M.M.C.A., Queiroz, P.S., Amorim, S.S., Guerra-Sá, R., Leão, V.A., 2017. High manganese tolerance and biooxidation ability of *Serratia marcescens* isolated from manganese mine water in Minas Gerais, Brazil. Front. Microbiol. 8, 1–11. <https://doi.org/10.3389/fmicb.2017.01946>
- Barsing, P., Tiwari, A., Joshi, T., Garg, S., 2011. Application of a novel bacterial consortium for mineralization of sulphonated aromatic amines. Bioresour. Technol. 102, 765–771. <https://doi.org/10.1016/j.biortech.2010.08.098>
- Bay, H.H., Lim, C.K., Kee, T.C., Ware, I., Chan, G.F., Shahir, S., Ibrahim, Z., 2014. Decolourisation of Acid Orange 7 recalcitrant auto-oxidation coloured by-products using an acclimatised mixed bacterial culture. Environ. Sci. Pollut. Res. 21, 3891–3906. <https://doi.org/10.1007/s11356-013-2331-4>
- Bhunja, F., Saha, N.C., Kaviraj, A., 2003. Effects of aniline-An aromatic amine to some freshwater organisms. Ecotoxicology 397–404. <https://doi.org/10.1023/A:1026104205847>
- Blöthe, M., Wegorzewski, A., Müller, C., Simon, F., Kuhn, T., Schippers, A., 2015. Manganese-cycling microbial communities inside deep-sea manganese nodules. Environ. Sci. Technol. 49, 7692–7700. <https://doi.org/10.1021/es504930v>
- Boughriet, A., Ouddane, B., Wartel, M., Lalou, C., Gengembreg, L., 1996. On the oxidation states of Mn and Fe in polymetallic oxide oxyhydroxide crusts from the Atlantic Ocean. Deep. Res. 43, 321–343.
- Buitrón, G., Quezada, M., Moreno, G., 2004. Aerobic degradation of the azo dye acid red 151 in a sequencing batch biofilter. Bioresour. Technol. 92, 143–149. <https://doi.org/10.1016/j.biortech.2003.09.001>
- Burdige, D.J., 1993. The biogeochemistry of manganese and iron reduction in marine sediments. Earth-Science Rev. 35, 249–284.
- Cao, L.T.T., Koder, H., Abe, K., Imachi, H., Aoi, Y., Kindaichi, T., Ozaki, N., Ohashi, A., 2015. Biological oxidation of Mn(II) coupled with nitrification for removal and recovery of minor metals by downflow hanging sponge reactor. Water Res. 68, 545–553. <https://doi.org/10.1016/j.watres.2014.10.002>
- Carmichael, M.J., Carmichael, S.K., Santelli, C.M., Strom, A., Bräuer, S.L., 2013. Mn(II)-oxidizing bacteria are abundant and environmentally relevant members of

- ferromanganese deposits in caves of the upper Tennessee River Basin. *Geomicrobiol. J.* 30, 779–800. <https://doi.org/10.1080/01490451.2013.769651>
- Carmichael S.K. and Bräuer S.L., 2015. Microbial Diversity and Manganese Cycling: A Review of Manganese-oxidizing Microbial Cave Communities, in: Engel A.S. (Ed.), *Microbial Life of Cave Systems. Life in Extreme Environments*. Walter de Gruyter GmbH & Co KG, Boston, MA, pp. 137–160. <https://doi.org/10.1515/9783110339888-009>
- Cerrato, J.M., Falkinham, J.O., Dietrich, A.M., Knocke, W.R., McKinney, C.W., Pruden, A., 2010. Manganese-oxidizing and -reducing microorganisms isolated from biofilms in chlorinated drinking water systems. *Water Res.* 44, 3935–3945. <https://doi.org/10.1016/j.watres.2010.04.037>
- Chalmin, E., Vignaud, C., Salomon, H., Farges, F., Susini, J., Menu, M., 2006. Minerals discovered in paleolithic black pigments by transmission electron microscopy and micro-X-ray absorption near-edge structure. *Appl. Phys. A Mater. Sci. Process.* 83, 213–218. <https://doi.org/10.1007/s00339-006-3510-7>
- Chang, R., 2010. *Chemistry*, 10th ed. McGraw-Hill, New York.
- Chen, G., Huang, M. hong, Chen, L., Chen, D. hui, 2011. A batch decolorization and kinetic study of Reactive Black 5 by a bacterial strain *Enterobacter* sp. GY-1. *Int. Biodeterior. Biodegrad.* 65, 790–796. <https://doi.org/10.1016/j.ibiod.2011.05.003>
- Clarke, C., Upson, S., 2017. A global portrait of the manganese industry—A socioeconomic perspective. *Neurotoxicology* 58, 173–179. <https://doi.org/10.1016/j.neuro.2016.03.013>
- Cloutier, M.L.C., Carmichael, S.K., Carson, M.A., Madritch, M.D., Bräuer, S.L., 2017. Carbon quantity and quality drives variation in cave microbial communities and regulates Mn(II) oxidation. *Biogeochemistry* 134, 77–94. <https://doi.org/10.1007/s10533-017-0343-8>
- Crafton, E., Pritchard, C., Guo, L., Senko, J.M., Cutright, T.J., 2019. Dynamics of Mn removal in an acid mine drainage treatment system over 13 years after installation. *Environ. Earth Sci.* 78, 1–9. <https://doi.org/10.1007/s12665-018-8008-z>
- Cui, M., Cui, D., Gao, L., Cheng, H., Wang, A., 2016. Efficient azo dye decolorization in a continuous stirred tank reactor (CSTR) with built-in bioelectrochemical system. *Bioresour. Technol.* 218, 1307–1311. <https://doi.org/10.1016/j.biortech.2016.07.135>
- Dai, R., Chen, X., Xiang, X., Wang, Y., Wang, F., 2018. Understanding azo dye anaerobic bio-decolorization with artificial redox mediator supplement: Considering the methane production. *Bioresour. Technol.* 249, 799–808. <https://doi.org/10.1016/j.biortech.2017.10.072>
- Das, A., Mishra, S., 2017. Removal of textile dye reactive green-19 using bacterial consortium : Process optimization using response surface methodology and kinetics study. *J. Environ. Chem. Eng.* 5, 612–627. <https://doi.org/10.1016/j.jece.2016.10.005>
- de Oliveira Neto, G.C., Ferreira Correia, J.M., Silva, P.C., de Oliveira Sanches, A.G., Lucato, W.C., 2019. Cleaner Production in the textile industry and its relationship to sustainable development goals. *J. Clean. Prod.* 228, 1514–1525. <https://doi.org/10.1016/j.jclepro.2019.04.334>
- De Schampelaire, L., Rabaey, K., Boon, N., Verstraete, W., Boeckx, P., 2007. Minireview: The potential of enhanced manganese redox cycling for sediment oxidation. *Geomicrobiol. J.* 24, 547–558. <https://doi.org/10.1080/01490450701670137>

- Donlon, B., Razo-Flores, E., Luijten, M., Swarts, H., Lettinga, G., Field, J., 1997. Detoxification and partial mineralization of the azo dye mordant orange 1 in a continuous upflow anaerobic sludge-blanket reactor. *Appl. Microbiol. Biotechnol.* 47, 83–90. <https://doi.org/10.1007/s002530050893>
- Dorer, C., Vogt, C., Neu, T.R., Stryhanyuk, H., Richnow, H.H., 2016. Characterization of toluene and ethylbenzene biodegradation under nitrate-, iron(III)- and manganese(IV)-reducing conditions by compound-specific isotope analysis. *Environ. Pollut.* 211, 271–281. <https://doi.org/10.1016/j.envpol.2015.12.029>
- Ekici, P., Leupold, G., Parlar, H., 2001. Degradability of selected azo dye metabolites in activated sludge systems. *Chemosphere* 44, 721–728. [https://doi.org/10.1016/S0045-6535\(00\)00345-3](https://doi.org/10.1016/S0045-6535(00)00345-3)
- Fandeur, D., Juillot, F., Morin, G., Livi, L., Cognigni, A., Webb, S.M., Ambrosi, J.P., Fritsch, E., Guyot, F., Brown, G.E., 2009. XANES evidence for oxidation of Cr(III) to Cr(VI) by Mn-oxides in a lateritic regolith developed on serpentinized ultramafic rocks of New Caledonia. *Environ. Sci. Technol.* 43, 7384–7390. <https://doi.org/10.1021/es900498r>
- Francis, A.J., Dodge, C.J., 1988. Anaerobic microbial dissolution of transition and heavy metal oxides. *Appl. Environ. Microbiol.* 54, 1009–10014.
- Francis, C.A., Tebo, B.M., 2002. Enzymatic manganese(II) oxidation by metabolically dormant spores of diverse *Bacillus* species. *Appl. Environ. Microbiol.* 68, 874–880. <https://doi.org/10.1128/AEM.68.2.874-880.2002>
- Franciscon, E., Grossman, M.J., Augusto, J., Paschoal, R., Guillermo, F., Reyes, R., Durrant, L.R., 2012. Decolorization and biodegradation of reactive sulfonated azo dyes by a newly isolated *Brevibacterium* sp. strain VN-15. *Springerplus* 1, 1–10.
- Furgal, K.M., Meyer, R.L., Bester, K., 2014. Removing selected steroid hormones, biocides and pharmaceuticals from water by means of biogenic manganese oxide nanoparticles in situ at ppb levels. *Chemosphere* 136, 321–326. <https://doi.org/10.1016/j.chemosphere.2014.11.059>
- Geszvain, K., Butterfield, C., Davis, R.E., Madison, A.S., Lee, S.-W., Parker, D.L., Soldatova, A., Spiro, T.G., Luther, G.W., Tebo, B.M., 2012. The molecular biogeochemistry of manganese(II) oxidation. *Biochem. Soc. Trans.* 40, 1244–1248. <https://doi.org/10.1042/BST20120229>
- Ghattas, A.K., Fischer, F., Wick, A., Ternes, T.A., 2017. Anaerobic biodegradation of (emerging) organic contaminants in the aquatic environment. *Water Res.* 116, 268–295. <https://doi.org/10.1016/j.watres.2017.02.001>
- Gounot, A.M., 1994. Microbial oxidation and reduction of manganese. *FEMS Microbiol. Rev.* 14, 339–349.
- Hallberg, K.B., Johnson, D.B., 2005. Biological manganese removal from acid mine drainage in constructed wetlands and prototype bioreactors. *Sci. Total Environ.* 338, 115–124. <https://doi.org/10.1016/j.scitotenv.2004.09.011>
- He, Z., Zhang, Q., Wei, Z., Wang, S., Pan, X., 2019a. Multiple-pathway arsenic oxidation and removal from wastewater by a novel manganese-oxidizing aerobic granular sludge. *Water Res.* 157, 83–93. <https://doi.org/10.1016/j.watres.2019.03.064>

- He, Z., Wei, Z., Zhang, Q., Zou, J., Pan, X., 2019b. Metal oxyanion removal from wastewater using manganese-oxidizing aerobic granular sludge. *Chemosphere* 236, 124353. <https://doi.org/10.1016/j.chemosphere.2019.124353>
- Henkel, J. V., Dellwig, O., Pollehne, F., Herlemann, D.P.R., Leipe, T., Schulz-Vogt, H.N., 2019. A bacterial isolate from the Black Sea oxidizes sulfide with manganese(IV) oxide. *Proc. Natl. Acad. Sci. U. S. A.* 116, 12153–12155. <https://doi.org/10.1073/pnas.1906000116>
- Hosseini Koupaie, E., Alavi Moghaddam, M.R., Hashemi, S.H., 2012. Investigation of decolorization kinetics and biodegradation of azo dye Acid Red 18 using sequential process of anaerobic sequencing batch reactor/moving bed sequencing batch biofilm reactor. *Int. Biodeterior. Biodegrad.* 71, 43–49. <https://doi.org/10.1016/j.ibiod.2012.04.002>
- Hosseinkhani, B., Emtiazi, G., 2011. Synthesis and characterization of a novel extracellular biogenic manganese oxide (bixbyite-like Mn₂O₃) nanoparticle by isolated *Acinetobacter* sp. *Curr. Microbiol.* 63, 300–305. <https://doi.org/10.1007/s00284-011-9971-8>
- Hsueh, C.C., Chen, B.Y., Yen, C.Y., 2009. Understanding effects of chemical structure on azo dye decolorization characteristics by *Aeromonas hydrophila*. *J. Hazard. Mater.* 167, 995–1001. <https://doi.org/10.1016/j.jhazmat.2009.01.077>
- Huang, J., Ling, J., Kuang, C., Chen, J., Xu, Y., Li, Y., 2018. Microbial biodegradation of aniline at low concentrations by *Pigmentiphaga daeguensis* isolated from textile dyeing sludge. *Int. Biodeterior. Biodegrad.* 129, 117–122. <https://doi.org/10.1016/j.ibiod.2018.01.013>
- Hulth, S., Aller, R.C., Gilbert, F., 1999. Coupled anoxic nitrification/manganese reduction in marine sediments. *Geochim. Cosmochim. Acta* 63, 49–66. [https://doi.org/10.1016/S0016-7037\(98\)00285-3](https://doi.org/10.1016/S0016-7037(98)00285-3)
- Hyun, J.H., Kim, S.H., Mok, J.S., Cho, H., Lee, T., Vandieken, V., Thamdrup, B., 2017. Manganese and iron reduction dominate organic carbon oxidation in surface sediments of the deep Ulleung Basin, East Sea. *Biogeosciences* 14, 941–958. <https://doi.org/10.5194/bg-14-941-2017>
- Imran, M., Arshad, M., Negm, F., Khalid, A., Shaharoon, B., Hussain, S., Mahmood Nadeem, S., Crowley, D.E., 2016. Yeast extract promotes decolorization of azo dyes by stimulating azoreductase activity in *Shewanella* sp. strain IFN4. *Ecotoxicol. Environ. Saf.* 124, 42–49. <https://doi.org/10.1016/j.ecoenv.2015.09.041>
- Jin, Q., Hu, Z., Jin, Z., Qiu, L., Zhong, W., Pan, Z., 2012. Biodegradation of aniline in an alkaline environment by a novel strain of the halophilic bacterium, *Dietzia natronolimnaea* JQ-AN. *Bioresour. Technol.* 117, 148–154. <https://doi.org/10.1016/j.biortech.2012.04.068>
- Jones, M.E., Nico, P.S., Ying, S., Regier, T., Thieme, J., Keiluweit, M., 2018. Manganese-driven carbon oxidation at oxic-anoxic interfaces. *Environ. Sci. Technol.* 52, 12349–12357. <https://doi.org/10.1021/acs.est.8b03791>
- Jonstrup, M., Kumar, N., Murto, M., Mattiasson, B., 2011. Sequential anaerobic-aerobic treatment of azo dyes: Decolourisation and amine degradability. *Desalination* 280, 339–346. <https://doi.org/10.1016/j.desal.2011.07.022>

- Juárez-Ramírez, C., Velázquez-García, R., Ruiz-Ordaz, N., Galíndez-Mayer, J., Ramos Monroy, O., 2012. Degradation kinetics of 4-amino naphthalene-1-sulfonic acid by a biofilm-forming bacterial consortium under carbon and nitrogen limitations. *J. Ind. Microbiol. Biotechnol.* 39, 1169–1177. <https://doi.org/10.1007/s10295-012-1123-z>
- Juárez-Ramírez, C., Galíndez-Mayer, J., Ruiz-Ordaz, N., Ramos-Monroy, O., Santoyo-Tepole, F., Poggi-Varaldo, H., 2015. Steady-state inhibition model for the biodegradation of sulfonated amines in a packed bed reactor. *N. Biotechnol.* 32, 379–386. <https://doi.org/10.1016/j.nbt.2014.07.010>
- Karim, M.E., Dhar, K., Hossain, M.T., 2018. Decolorization of Textile Reactive Dyes by Bacterial Monoculture and Consortium Screened from Textile Dyeing Effluent. *J. Genet. Eng. Biotechnol.* 16, 375–380. <https://doi.org/10.1016/j.jgeb.2018.02.005>
- Krishnan, J., Arvind Kishore, A., Suresh, A., Madhumeetha, B., Gnana Prakash, D., 2017. Effect of pH, inoculum dose and initial dye concentration on the removal of azo dye mixture under aerobic conditions. *Int. Biodeterior. Biodegrad.* 119, 16–27. <https://doi.org/10.1016/j.ibiod.2016.11.024>
- Langenhoff, A.A.M., Zehnder, A.J.B., Schraa, G., 1996. Behaviour of toluene, benzene and naphthalene under anaerobic conditions in sediment columns. *Biodegradation* 7, 267–274. <https://doi.org/10.1007/BF00058186>
- Learman, D.R., Voelker, B.M., Vazquez-Rodriguez, A.I., Hansel, C.M., 2011. Formation of manganese oxides by bacterially generated superoxide. *Nat. Geosci.* 4, 95–98. <https://doi.org/10.1038/ngeo1055>
- Learman, D.R., Voelker, B.M., Madden, A.S., Hansel, C.M., 2013. Constraints on superoxide mediated formation of manganese oxides. *Front. Microbiol.* 4, 1–11. <https://doi.org/10.3389/fmicb.2013.00262>
- Lee, E.Y., Noh, S.R., Cho, K.S., Ryu, H.W., 2001. Leaching of Mn, Co, and Ni from manganese nodules using an anaerobic bioleaching method. *J. Biosci. Bioeng.* 92, 354–359. [https://doi.org/10.1016/S1389-1723\(01\)80239-5](https://doi.org/10.1016/S1389-1723(01)80239-5)
- Li, S., Cao, Y., Bi, C., Zhang, Y., 2017. Promoting electron transfer to enhance anaerobic treatment of azo dye wastewater with adding Fe(OH)₃. *Bioresour. Technol.* 245, 138–144. <https://doi.org/10.1016/j.biortech.2017.08.066>
- Li, H.P., Daniel, B., Creeley, D., Grandbois, R., Zhang, S., Xu, C., Ho, Y.F., Schwehr, K.A., Kaplan, D.I., Santschi, P.H., Hansel, C.M., Yeager, C.M., 2014. Superoxide production by a manganese-oxidizing bacterium facilitates iodide oxidation. *Appl. Environ. Microbiol.* 80, 2693–2699. <https://doi.org/10.1128/AEM.00400-14>
- Li, J., Jin, Z., Yu, B., 2010. Isolation and characterization of aniline degradation slightly halophilic bacterium, *Erwinia* sp. Strain HSA 6. *Microbiol. Res.* 165, 418–426. <https://doi.org/10.1016/j.micres.2009.09.003>
- Liang, G., Yang, Y., Wu, S., Jiang, Y., Xu, Y., 2017. The generation of biogenic manganese oxides and its application in the removal of As(III) in groundwater. *Environ. Sci. Pollut. Res.* 24, 17935–17944. <https://doi.org/10.1007/s11356-017-9476-5>
- Lin, H., Taillefert, M., 2014. Key geochemical factors regulating Mn(IV)-catalyzed anaerobic nitrification in coastal marine sediments. *Geochim. Cosmochim. Acta* 133, 17–33. <https://doi.org/10.1016/j.gca.2014.01.025>

- Liu, W., Sutton, N.B., Rijnaarts, H.H.M., Langenhoff, A.A.M., 2018. Anaerobic biodegradation of pharmaceutical compounds coupled to dissimilatory manganese (IV) or iron (III) reduction. *J. Hazard. Mater.* <https://doi.org/10.1016/j.jhazmat.2018.04.078>
- Lovley, D.R., 1991. Dissimilatory Fe(III) and Mn(IV) reduction. *Microbiol. Rev.* 55, 259–287.
- Matsushita, S., Komizo, D., Cao, L.T.T., Aoi, Y., Kindaichi, T., Ozaki, N., Imachi, H., Ohashi, A., 2018. Production of biogenic manganese oxides coupled with methane oxidation in a bioreactor for removing metals from wastewater. *Water Res.* 130, 224–233. <https://doi.org/10.1016/j.watres.2017.11.063>
- Mayanna, S., Peacock, C.L., Schäffner, F., Grawunder, A., Merten, D., Kothe, E., Büchel, G., 2015. Biogenic precipitation of manganese oxides and enrichment of heavy metals at acidic soil pH. *Chem. Geol.* 402, 6–17. <https://doi.org/10.1016/j.chemgeo.2015.02.029>
- Meng, X., Liu, G., Zhou, J., Shiang Fu, Q., Wang, G., 2012. Azo dye decolorization by *Shewanella aquimarina* under saline conditions. *Bioresour. Technol.* 114, 95–101. <https://doi.org/10.1016/j.biortech.2012.03.003>
- Mishra, D., Srivastava, R.R., Sahu, K.K., Singh, T.B., Jana, R.K., 2011. Leaching of roast-reduced manganese nodules in NH₃-(NH₄)₂CO₃ medium. *Hydrometallurgy* 109, 215–220. <https://doi.org/10.1016/j.hydromet.2011.07.006>
- Mogollón, J.M., Mewes, K., Kasten, S., 2016. Quantifying manganese and nitrogen cycle coupling in manganese-rich, organic carbon-starved marine sediments: Examples from the Clarion-Clipperton fracture zone. *Geophys. Res. Lett.* 43, 7114–7123. <https://doi.org/10.1002/2016GL069117>
- Moosvi, S., Kher, X., Madamwar, D., 2007. Isolation, characterization and decolorization of textile dyes by a mixed bacterial consortium JW-2. *J. Dyepig.* 74, 723–729. <https://doi.org/10.1016/j.dyepig.2006.05.005>
- Murray, K.J., Tebo, B.M., 2007. Cr(III) is indirectly oxidized by the Mn(II)-oxidizing bacterium *Bacillus* sp. strain SG-1. *Environ. Sci. Technol.* 41, 528–533. <https://doi.org/10.1021/es0615167>
- Myers, C.R., Nealson, K.H., 1988. Microbial reduction of manganese oxides: Interactions with iron and sulfur. *Geochim. Cosmochim. Acta* 52, 2727–2732. [https://doi.org/10.1016/0016-7037\(88\)90041-5](https://doi.org/10.1016/0016-7037(88)90041-5)
- Namgung, S., Chon, C.M., Lee, G., 2018. Formation of diverse Mn oxides: a review of bio/geochemical processes of Mn oxidation. *Geosci. J.* 22, 373–381. <https://doi.org/10.1007/s12303-018-0002-7>
- Nealson, K.H., Myers, C.R., Wimpee, B.B., 1991. Isolation and identification of manganese-reducing bacteria and estimates of microbial Mn(IV)-reducing potential in the Black Sea. *Deep. Res. Part A* 38, S907–S920. [https://doi.org/10.1016/S0198-0149\(10\)80016-0](https://doi.org/10.1016/S0198-0149(10)80016-0)
- Nelson, Y.M., Lion, L.W., Ghiorse, W.C., Shuler, M.L., 1999. Production of biogenic Mn oxides by *Leptothrix discophora* SS-1 in a chemically defined growth medium and evaluation of their Pb adsorption characteristics. *Appl. Environ. Microbiol.* 65, 175–180.
- Ng, I.S., Chen, T., Lin, R., Zhang, X., Ni, C., Sun, D., 2014. Decolorization of textile azo dye and Congo red by an isolated strain of the dissimilatory manganese-reducing bacterium *Shewanella xiamenensis* BC01. *Appl. Microbiol. Biotechnol.* 98, 2297–2308. <https://doi.org/10.1007/s00253-013-5151-z>

- Nguyen, M.T., Majumdar, D., Leszczynski, J., Roszak, S., 2011. Structure and Bonding of Simple Manganese-Containing Compounds, PATAI'S Chemistry of Functional Groups. John Wiley & Sons, Ltd. <https://doi.org/10.1002/9780470682531.pat0535>
- Ning, X.A., Liang, J.Y., Li, R.J., Hong, Z., Wang, Y.J., Chang, K.L., Zhang, Y.P., Yang, Z.Y., 2015. Aromatic amine contents, component distributions and risk assessment in sludge from 10 textile-dyeing plants. *Chemosphere* 134, 367–373. <https://doi.org/10.1016/j.chemosphere.2015.05.015>
- Noraini, C.H.C., Morad, N., Norli, I., Teng, T.T., Ogugbue, C.J., 2012. Methylene blue degradation by *sphingomonas paucimobilis* under aerobic conditions. *Water. Air. Soil Pollut.* 223, 5131–5142. <https://doi.org/10.1007/s11270-012-1264-8>
- Palermo, C., Dittrich, M., 2016. Evidence for the biogenic origin of manganese-enriched layers in Lake Superior sediments. *Environ. Microbiol. Rep.* 8, 179–186. <https://doi.org/10.1111/1758-2229.12364>
- Pereira, R., Pereira, L., van der Zee, F.P., Madalena Alves, M., 2011. Fate of aniline and sulfanilic acid in UASB bioreactors under denitrifying conditions. *Water Res.* 45, 191–200. <https://doi.org/10.1016/j.watres.2010.08.027>
- Post, J.E., 1999. Manganese oxide minerals: Crystal structures and economic and environmental significance. *Proc Natl Acad Sci USA* 96, 3447–3454.
- Queiroz, P.S., Barboza, N.R., Cordeiro, M.M., Leão, V.A., Guerra-sá, R., 2018. Rich growth medium promotes an increased on Mn (II) removal and manganese oxide production by *Serratia marcescens* strains isolates from wastewater. *Biochem. Eng. J.* 140, 148–156. <https://doi.org/10.1016/j.bej.2018.09.018>
- Randhawa, N.S., Hait, J., Jana, R.K., 2016. A brief overview on manganese nodules processing signifying the detail in the Indian context highlighting the international scenario. *Hydrometallurgy* 165, 166–181. <https://doi.org/10.1016/j.hydromet.2015.09.013>
- Rasik J. Chudgar, 2000. *Kirk-Othmer Encyclopedia of Chemical Technology*. John Wiley & Sons, Inc.
- Richter, K., Schicklberger, M., Gescher, J., 2012. Dissimilatory reduction of extracellular electron acceptors in anaerobic respiration. *Appl. Environ. Microbiol.* 78, 913–921. <https://doi.org/10.1128/AEM.06803-11>
- Santelli, C.M., Pfister, D.H., Lazarus, D., Sun, L., Burgos, W.D., Hansel, C.M., 2010. Promotion of Mn(II) oxidation and remediation of coal mine drainage in passive treatment systems by diverse fungal and bacterial communities. *Appl. Environ. Microbiol.* 76, 4871–4875. <https://doi.org/10.1128/AEM.03029-09>
- Saratale, R.G., Saratale, G.D., Chang, J.S., Govindwar, S.P., 2011. Bacterial decolorization and degradation of azo dyes: A review. *J. Taiwan Inst. Chem. Eng.* 42, 138–157. <https://doi.org/10.1016/j.jtice.2010.06.006>
- Saratovsky, I., Wightman, P.G., Pastén, P.A., Gaillard, J.F., Poepelmeier, K.R., 2006. Manganese oxides: Parallels between abiotic and biotic structures. *J. Am. Chem. Soc.* 128, 11188–11198. <https://doi.org/10.1021/ja062097g>
- Sarvajith, M., Kumar, G.K., Nancharaiah, Y. V, 2018. Textile dye biodecolourization and ammonium removal over nitrite in aerobic granular sludge sequencing batch reactors. *J. Hazard. Mater.* 342, 536–543. <https://doi.org/10.1016/j.jhazmat.2017.08.064>

- Schmidt, N., Page, D., Tiehm, A., 2017. Biodegradation of pharmaceuticals and endocrine disruptors with oxygen, nitrate, manganese (IV), iron (III) and sulfate as electron acceptors. *J. Contam. Hydrol.* 203, 62–69. <https://doi.org/10.1016/j.jconhyd.2017.06.007>
- Shaul, G.M., Holdsworth, T.J., Dempsey, C.R., Dostal, K.A., 1991. Fate of water soluble azo dyes in the activated sludge process. *Chemosphere* 22, 107–119. [https://doi.org/10.1016/0045-6535\(91\)90269-J](https://doi.org/10.1016/0045-6535(91)90269-J)
- Shi, L., Squier, T.C., Zachara, J.M., Fredrickson, J.K., 2007. Respiration of metal (hydr)oxides by *Shewanella* and *Geobacter*: A key role for multihaem c-type cytochromes. *Mol. Microbiol.* 65, 12–20. <https://doi.org/10.1111/j.1365-2958.2007.05783.x>
- Shiraishi, F., Matsumura, Y., Chihara, R., Okumura, T., Itai, T., Kashiwabara, T., Kano, A., Takahashi, Y., 2019. Depositional processes of microbially colonized manganese crusts, Sambe hot spring, Japan. *Geochim. Cosmochim. Acta* 258, 1–18. <https://doi.org/10.1016/j.gca.2019.05.023>
- Sjöberg, S., Callac, N., Allard, B., Smittenberg, R.H., Dupraz, C., 2018. Microbial Communities Inhabiting a Rare Earth Element Enriched Birnessite-Type Manganese Deposit in the Ytterby Mine, Sweden. *Geomicrobiol. J.* 35, 657–674. <https://doi.org/10.1080/01490451.2018.1444690>
- Soldatova, A. V., Butterfield, C., Oyerinde, O.F., Tebo, B.M., Spiro, T.G., 2012. Multicopper oxidase involvement in both Mn(II) and Mn(III) oxidation during bacterial formation of MnO₂. *J. Biol. Inorg. Chem.* 17, 1151–1158. <https://doi.org/10.1007/s00775-012-0928-6>
- Sparenberg, O., 2019. A historical perspective on deep-sea mining for manganese nodules, 1965–2019. *Extr. Ind. Soc.* 0–1. <https://doi.org/10.1016/j.exis.2019.04.001>
- Su, J. feng, Luo, X. xin, Wei, L., Ma, F., Zheng, S. chen, Shao, S. cheng, 2016. Performance and microbial communities of Mn(II)-based autotrophic denitrification in a Moving Bed Biofilm Reactor (MBBR). *Bioresour. Technol.* 211, 743–750. <https://doi.org/10.1016/j.biortech.2016.03.101>
- Su, J., Deng, L., Huang, L., Guo, S., Liu, F., He, J., 2014. Catalytic oxidation of manganese(II) by multicopper oxidase CueO and characterization of the biogenic Mn oxide. *Water Res.* 56, 304–313. <https://doi.org/10.1016/j.watres.2014.03.013>
- Sulu-Gambari, F., Seitaj, D., Behrends, T., Banerjee, D., Meysman, F.J.R., Slomp, C.P., 2016. Impact of cable bacteria on sedimentary iron and manganese dynamics in a seasonally-hypoxic marine basin. *Geochim. Cosmochim. Acta* 192, 49–69. <https://doi.org/10.1016/j.gca.2016.07.028>
- Swathi, D., Sabumon, P.C., Maliyekkal, S.M., 2017. Microbial mediated anoxic nitrification-denitrification in the presence of nanoscale oxides of manganese. *Int. Biodeterior. Biodegrad.* 119, 499–510. <https://doi.org/10.1016/j.ibiod.2016.10.043>
- Tan, L., Ning, S., Xia, H., Sun, J., 2013. Aerobic decolorization and mineralization of azo dyes by a microbial community in the absence of an external carbon source. *Int. Biodeterior. Biodegrad.* 85, 210–216. <https://doi.org/10.1016/j.ibiod.2013.02.018>
- Tan, N.C.G., Van Leeuwen, A., Van Voorthuizen, E.M., Slenders, P., Prenafeta-Boldú, F.X., Temmink, H., Lettinga, G., Field, J.A., 2005. Fate and biodegradability of sulfonated aromatic amines. *Biodegradation* 16, 527–537. <https://doi.org/10.1007/s10532-004-6593-x>

- Tebo, B.M., Bargar, J.R., Clement, B.G., Dick, G.J., Murray, K.J., Parker, D., Verity, R., Webb, S.M., 2004. Biogenic manganese oxides: Properties and mechanisms of formation. *Annu. Rev. Earth Planet. Sci.* 32, 287–328.
<https://doi.org/10.1146/annurev.earth.32.101802.120213>
- Tebo, B.M., Johnson, H.A., McCarthy, J.K., Templeton, A.S., 2005. Geomicrobiology of manganese(II) oxidation. *Trends Microbiol.* 13, 421–428.
<https://doi.org/10.1016/j.tim.2005.07.009>
- Thamdrup, B., Finster, K., Hansen, J.W., Bak, F., 1993. Bacterial disproportionation of elemental sulfur coupled to chemical reduction of iron or manganese. *Appl. Environ. Microbiol.* 59, 101–108.
- Tobiason, J.E., Bazilio, A., Goodwill, J., Mai, X., Nguyen, C., 2016. Manganese removal from drinking water sources. *Curr. Pollut. Reports* 2, 168–177. <https://doi.org/10.1007/s40726-016-0036-2>
- Tony, B.D., Goyal, D., Khanna, S., 2009. Decolorization of textile azo dyes by aerobic bacterial consortium. *Int. Biodeterior. Biodegradation* 63, 462–469.
<https://doi.org/10.1016/j.ibiod.2009.01.003>
- Tran, T.N., Kim, D.G., Ko, S.O., 2018. Synergistic effects of biogenic manganese oxide and Mn(II)-oxidizing bacterium *Pseudomonas putida strain MnB1* on the degradation of 17 A-ethinylestradiol. *J. Hazard. Mater.* 344, 350–359.
<https://doi.org/10.1016/j.jhazmat.2017.10.045>
- Tutu, H., McCarthy, T.S., Cukrowska, E., 2008. The chemical characteristics of acid mine drainage with particular reference to sources, distribution and remediation: The Witwatersrand Basin, South Africa as a case study. *Appl. Geochemistry* 23, 3666–3684.
<https://doi.org/10.1016/j.apgeochem.2008.09.002>
- USGS, 2015 Mineral Yearbook, <https://www.usgs.gov/centers/nmic/manganese-statistics-and-information>, accessed on 17 May 2019
- Vacchi, F.I., Von der Ohe, P.C., Albuquerque, A.F. de, Vendemiatti, J.A. de S., Azevedo, C.C.J., Honório, J.G., Silva, B.F. da, Zanoni, M.V.B., Henry, T.B., Nogueira, A.J., Umbuzeiro, G. de A., 2016. Occurrence and risk assessment of an azo dye - The case of Disperse Red 1. *Chemosphere* 156, 95–100. <https://doi.org/10.1016/j.chemosphere.2016.04.121>
- Vandieken, V., Pester, M., Finke, N., Hyun, J.H., Friedrich, M.W., Loy, A., Thamdrup, B., 2012. Three manganese oxide-rich marine sediments harbor similar communities of acetate-oxidizing manganese-reducing bacteria. *ISME J.* 6, 2078–2090.
<https://doi.org/10.1038/ismej.2012.41>
- Villatoro-Monzón, W.R., Morales-Ibarria, M.G., Velázquez, E.K., Ramírez-Saad, H., Razo-Flores, E., 2008. Benzene biodegradation under anaerobic conditions coupled with metal oxides reduction. *Water. Air. Soil Pollut.* 192, 165–172. <https://doi.org/10.1007/s11270-008-9643-x>
- Wang, H., Lv, Z., Song, Y., Wang, Y. nan, Zhang, D., Sun, Y., Tsang, Y.F., Pan, X., 2019. Adsorptive removal of Sb(III) from wastewater by environmentally-friendly biogenic manganese oxide (BMO) materials: Efficiency and mechanisms. *Process Saf. Environ. Prot.* 124, 223–230. <https://doi.org/10.1016/j.psep.2019.02.022>
- Wang, J., Yan, J., Xu, W., 2015. Treatment of dyeing wastewater by MIC anaerobic reactor. *Biochem. Eng. J.* 101, 179–184. <https://doi.org/10.1016/j.bej.2015.06.001>

- Wang, J., Liu, G.F., Lu, H., Jin, R.F., Zhou, J.T., Lei, T.M., 2012. Biodegradation of Acid Orange 7 and its auto-oxidative decolorization product in membrane-aerated biofilm reactor. *Int. Biodeterior. Biodegrad.* 67, 73–77.
<https://doi.org/10.1016/j.ibiod.2011.12.003>
- Wang, Z.W., Liang, J.S., Liang, Y., 2013. Decolorization of Reactive Black 5 by a newly isolated bacterium *Bacillus* sp. YZU1. *Int. Biodeterior. Biodegrad.* 76, 41–48.
<https://doi.org/10.1016/j.ibiod.2012.06.023>
- Wright, M.H., Farooqui, S.M., White, A.R., Greene, A.C., 2016. Production of manganese oxide nanoparticles by *Shewanella* Species. *Appl. Environ. Microbiol.* 82, 5402–5409.
<https://doi.org/10.1128/aem.00663-16>
- Xie, X., Liu, N., Ping, J., Zhang, Q., Zheng, X., Liu, J., 2018. Illumina MiSeq sequencing reveals microbial community in HA process for dyeing wastewater treatment fed with different. *Chemosphere* 201, 578–585.
<https://doi.org/10.1016/j.chemosphere.2018.03.025>
- Yu, L., Zhang, X. Yu, Xie, T., Hu, J. Mei, Wang, S., Li, W. Wei, 2015. Intracellular azo decolorization is coupled with aerobic respiration by a *Klebsiella oxytoca* strain. *Appl. Microbiol. Biotechnol.* 99, 2431–2439. <https://doi.org/10.1007/s00253-014-6161-1>
- Zeng, X., Zhang, M., Liu, Y., Tang, W., 2018. Manganese(II) oxidation by the multi-copper oxidase CopA from *Brevibacillus panacihumi* MK-8. *Enzyme Microb. Technol.* 117, 79–83. <https://doi.org/10.1016/j.enzmictec.2018.04.011>
- Zhang, Y., Tang, Y., Qin, Z., Luo, P., Ma, Z., Tan, M., Kang, H., Huang, Z., 2019. A novel manganese oxidizing bacterium-*Aeromonas hydrophila* strain DS02: Mn(II) oxidization and biogenic Mn oxides generation. *J. Hazard. Mater.* 367, 539–545.
<https://doi.org/10.1016/j.jhazmat.2019.01.012>
- Zhao, X., Wang, X., Liu, B., Xie, G., Xing, D., 2018. Characterization of manganese oxidation by *Brevibacillus* at different ecological conditions. *Chemosphere* 205, 553–558.
<https://doi.org/10.1016/j.chemosphere.2018.04.130>
- Zhou, D., Kim, D., Ko, S., 2015. Heavy metal adsorption with biogenic manganese oxides generated by *Pseudomonas putida* strain MnB1. *J. Ind. Eng. Chem.* 24, 132–139.
<https://doi.org/10.1016/j.jiec.2014.09.020>

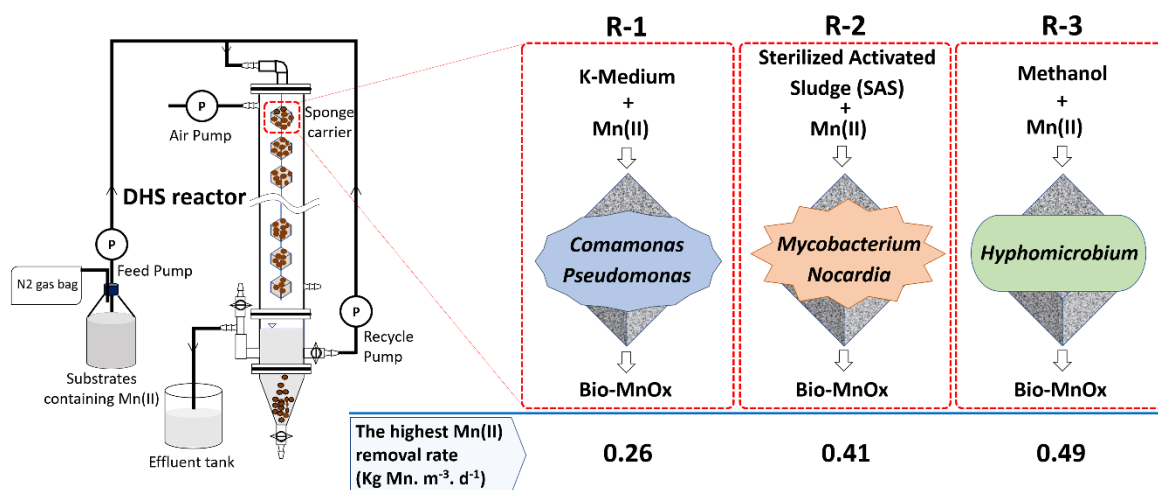
This page is intentionally left blank

Chapter 3: Multiple organic substrates support Mn(II) removal with enrichment of Mn(II)-oxidizing bacteria

This chapter has been published as;

“Multiple organic substrates support Mn(II) removal with enrichment of Mn(II)-oxidizing bacteria”, Ahmad Shoiful, Taiki Ohta, Hiromi Kambara, Shuji Matsushita, Tomonori Kindaichi, Noriatsu Ozaki, Yoshiteru Aoi, Hiroyuki Imachi and Akiyoshi Ohashi*. *Journal of Environmental Management* xxx xxxx, accepted on 23 October 2019 (Elsevier, IF = 4.865).

Graphical abstract



Abstract

Three different organic substrates, K-medium, sterilized activated sludge (SAS), and methanol, were examined for utility as substrates for enriching manganese-oxidizing bacteria (MnOB) in an open bioreactor. The differences in Mn(II) oxidation performance between the substrates were investigated using three down-flow hanging sponge (DHS) reactors continuously treating artificial Mn(II)-containing water over 131 days. The results revealed that all three substrates were useful for enriching MnOB. Surprisingly, we observed only slight differences in Mn(II) removal between the substrates. The highest Mn(II) removal rate for the SAS-supplied reactor was $0.41 \text{ kg Mn}\cdot\text{m}^{-3}\cdot\text{d}^{-1}$, which was greater than that of K-medium, although the SAS performance was unstable. In contrast, the methanol-supplied reactor had more stable performance and the highest Mn(II) removal rate. We conclude that multiple genera of *Comamonas*, *Pseudomonas*, *Mycobacterium*, *Nocardia* and *Hyphomicrobium* play a role in Mn(II) oxidation and that their relative predominance was dependent on the substrate. Moreover, the initial inclusion of abiotic-MnO₂ in the reactors promoted early MnOB enrichment.

Keywords: biological manganese oxidation, down-flow hanging sponge reactor, K-medium, manganese-oxidizing bacteria, methanol, sterilized activated sludge

3.1 Introduction

A wide variety of organisms, including bacteria, fungi, algae, and plants, have been used in bioremediation processes to remove heavy metals and hazardous organics from contaminated waters and wastewaters (Bahar et al., 2016; Jaiswal et al., 2018; Zeraatkar et al., 2016; Yin et al., 2017). Of all microbes used, manganese-oxidizing bacteria (MnOB) are gaining attention for their unique characteristics that promote the removal of heavy metals. Heterotrophic MnOB, capable of oxidizing Mn(II) to Mn(III/IV), yield manganese oxides, which also are referred to as biogenic manganese oxides (Bio-MnO_x) (Francis and Tebo, 2002). Bio-MnO_x can adsorb cationic metals and oxidize inorganic contaminants because of their poorly crystalline-layered materials that have many vacant sites (Meng et al., 2009; Droz et al., 2015; Tang et al., 2014; Bai et al., 2016a). MnOB are ubiquitous and widespread in nature; they have been detected in oligotrophic environments including caves (Cloutier et al., 2017), deep oceanic sediments (Blothe et al., 2015), and river estuaries (Anderson et al., 2011). They play a key role not only

in the biogeochemical cycle of manganese (Tebo et al., 2005) but also in carbon (Jones et al., 2018), nitrogen (Lin and Taillefert, 2014) and sulfur (Geszvain et al., 2012) cycles in nature.

Exploiting these characteristics of Bio-MnO_x in MnOB-enriched bioreactors is promising for water and wastewater treatments. Therefore, many studies on the applications of MnOB for removal of heavy metals have been reported. In most previous studies, pure MnOB cultures were employed for batch-scale and column experiments (Meng et al., 2009; Bai et al., 2016b). Pure cultures present problems for large-scale use, because it is difficult to prevent contamination by other bacteria in open systems. Even if bacterial contamination occurs, it is essential to maintain the presence and prevalence of MnOB. A previous study successfully enriched MnOB in an opened down-flow hanging sponge (DHS) reactor to continuously remove the minor metals, nickel (Ni)(II) and cobalt (Co)(II), from synthetic wastewater by coupling nitrification (Cao et al., 2015). The growth of MnOB was promoted by providing a natural substrate of soluble microbial products (SMPs) generated by nitrifying bacteria. However, a long time was required to confirm significant Mn(II) oxidation. MnO₂ inhibited bacterial activity due to its toxicity (Matsushita et al., 2018). By slowly but steadily increasing the accumulation of produced Bio-MnO_x over time, the activity of MnOB might be gradually enhanced by the MnO_x inhibition of growth of other bacteria. I hypothesized that starting with a large amount of MnO₂ would provide early MnOB enrichment and high Mn(II) oxidation performance in a shorter time.

There is little information on organic substrates that promote the enrichment of MnOB. K-medium, consisting of peptone and yeast extract, has been widely used for MnOB growth in pure cultures (Yang et al., 2013). Methanol is a promising substrate because Matsushita et al. (2018) successfully enriched methanol-utilizing MnOB in a methane oxidation reactor, where methanol was generated as a utilization-associated product (UAP) of methanotrophs. Methanol is abundant in nature and is produced in soils from the decomposition of dead plants (Kolb S., 2009). Matsushita et al. (2018) also found that Mn(II) oxidation occurred under starvation conditions without exogenous methane and concluded that MnOB could utilize biomass-associated products (BAPs) derived from cell lysis in biofilms. The bulk liquid from dead microbes contains high concentrations of proteins, carbohydrates and lipids (Ramstedt et al., 2011). Combined, these reports suggest that activated sludge is a good candidate substrate for MnOB enrichment.

This study aims to clarify whether it is possible to use methanol and sterilized activated sludge (SAS) as substrates for MnOB enrichment. I also set out to evaluate the performance of Mn(II) oxidation relative to that of K-medium through a continuous Mn(II) removal experiment. A unique DHS reactor, with abiotic MnO₂ initially installed, was employed with the goal of promoting early MnOB growth. Microbial community analyses of each retained biomass were performed to identify the predominant MnOB related to the Mn(II) oxidation performance.

3.2 Materials and methods

3.2.1 Reactor configurations, inoculation, and operational conditions

Enrichments of MnOB were conducted in three DHS reactors of 75 cm height and 5 cm diameter, in which a set of 20 polyurethane sponge cubes (each 2 × 2 × 2 cm³, total volume of 160 cm³) were hung diagonally in series on a nylon string (Fig. 3.1). The sponge carriers were inoculated with activated sludge from the aeration tank of a municipal sewage treatment plant in Higashihiroshima, by squeezing and soaking in its suspension liquid mixed with abiotic-MnO₂ 100 g·L⁻¹ (Kishida Chemical Co. Ltd., Japan). The activated sludge, consisting of a large variety of microorganisms, was expected to contain MnOB (Abu Hasan et al., 2012). Prior to using abiotic-MnO₂ for inoculation, it was pretreated by Mn(II) adsorption to equilibrium, allowing us to judge whether the Mn(II) removal performance of the reactors was caused by the oxidation or the adsorption. The reactors were placed in a dark room at 26 °C.

The reactors, R-1, R-2, and R-3, were supplied with different organic substrates: K-medium, sterilized activated sludge (SAS) and methanol, respectively. K-medium is composed of peptone and yeast extract (4:1, w/w). SAS was made by heating activated sludge at 100 °C for 24 hours in a drying oven (DVS 602 Yamato Scientific Co., Ltd., Japan). The concentrations of organic substrates in the influent are provided in Table 3.1, except for SAS, because the concentration of SAS in the influent was adjusted based on the COD concentration of SAS stock solution. The substrates contained Mn(II) (MnCl₂·4H₂O), minerals (CaCl₂·2H₂O 0.05 mg·L⁻¹, MgSO₄·7H₂O 0.2 mg·L⁻¹, Fe₂SO₄·5H₂O 0.1 mg·L⁻¹, KH₂PO₄ 1.156 mg·L⁻¹, Na₂HPO₄·7H₂O 49.08 mg·L⁻¹), and trace elements (CuSO₄·5H₂O 0.025 mg·L⁻¹, NaSeO₄ 0.005 mg·L⁻¹, NiCl₂·6H₂O 0.019 mg·L⁻¹, CoCl₂·6H₂O 0.024 mg·L⁻¹, Na₂MoO₄·2H₂O 0.022 mg·L⁻¹, H₃BO₃ 0.001 mg·L⁻¹, ZnSO₄·7H₂O 0.043 mg·L⁻¹), all final concentration. Before the substrates were supplied to the respective reactors, the substrate tanks were purged with nitrogen gas. Air

was provided to the reactors at a flow rate of $15.6 \text{ L}\cdot\text{h}^{-1}$ to create aerobic conditions. The organic and Mn(II) loading rates were set by controlling the hydraulic retention time (HRT) based on the sponge volumes and concentrations (Table 1). The reactor operation was conducted for 131 days and the condition was divided into three phases. The effluent waters were recirculated at a ratio of 1:10 (Q influent:Q recirculation).

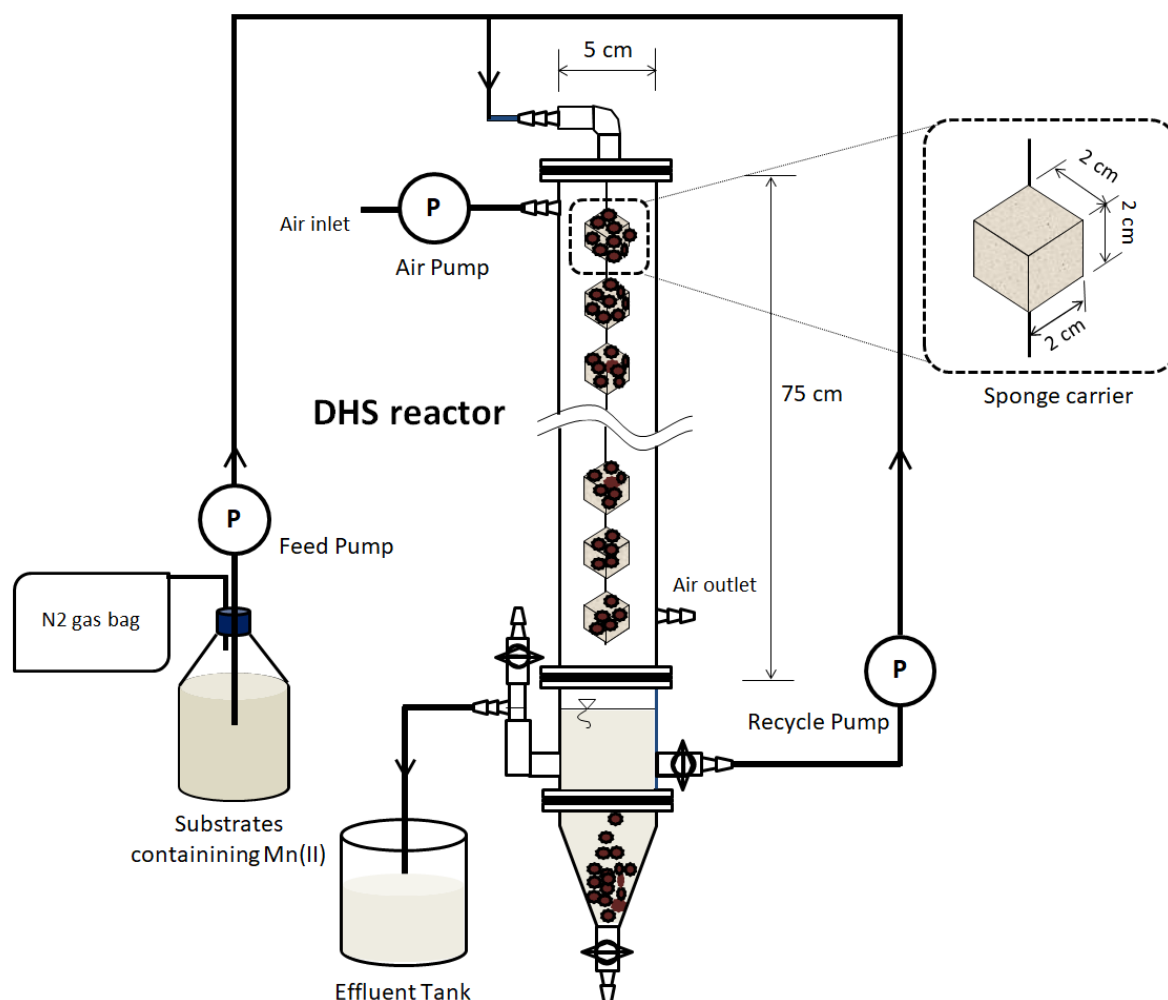


Figure 3.1 Reactor configuration.

Table 3.1 Operational conditions of the three DHS reactors

Reactor	R-1			R-2			R-3		
Phase	Phase 1	Phase 2	Phase 3	Phase 1	Phase 2	Phase 3	Phase 1	Phase 2	Phase 3
Period (d)	0–30	31–59	60–131	0–42d	43–59	60–131	0–36	37–59	60–131
COD ($\text{mg}\cdot\text{L}^{-1}$)	8–50	5	10	8–50	5	10	8–50	5	10
Mn(II) ($\text{mg}\cdot\text{L}^{-1}$)	5	5	5	5–7.5	7.5	7.5	5–7.5	7.5	7.5
HRT (h)	4.2–0.6	0.4	0.4	4.2–0.6	0.4	0.4	4.2–0.6	0.4	0.4

3.2.2 Analytical methods

Water samples were filtered through a 0.45- μm membrane filter (Advantec, Tokyo, Japan). Mn(II) and chemical oxygen demand (COD) concentrations were determined by the colorimetric method using a Hach DR2800 spectrophotometer (Hach Co., Loveland, CO, USA).

3.2.3 Microbial community analysis

Biomass samples were collected by squeezing sponge carriers taken from the upper, middle and lower portions of each reactor at the end of Phase 2 (day 60) and Phase 3 (day 131), namely R1-d60 (R-1, day 60), R1-d131 (R-1, day 131), R2-d60 (R-2, day 60), R2-d131 (R-2, day 131), R3-d60 (R-3, day 131), and R3-d131 (R-3, day 131). DNA was extracted using a Fast DNA spin kit for soil (MP Biomedicals, Irvine, CA, USA). Polymerase chain reaction (PCR) amplification of the 16S rRNA gene was performed using the primer sets 341F (5'-CCTACGGGGNGGCWGCAG) and 805R (5'-GGACTACCAGGGTATCTAATCC). The PCR conditions were as follows: 3 min of initial denaturation at 95 °C followed by 30 cycles of 30 s at 95 °C, 30 s at 55 °C and 30 s at 72 °C, and then final extension at 72 °C for 5 min. The PCR products were purified using an Agencourt AMPure XP (Beckman Coulter, CA, USA) and subsequently sent to Hokkaido System Science Co. Ltd (Sapporo, Japan) for DNA sequencing by Illumina MiSeq platform with a MiSeq Reagent Kit v3 (Illumina Inc., San Diego, CA, USA). Sequence data were analyzed using QIIME software version 1.8.0 (Caporaso et al., 2010). Sequences showing more than 97% identity of DNA were grouped into the same operational taxonomic units (OTUs) using the UCLUST method (Edgar, 2010) and the OTUs were classified using MiDAS v1.20 database (McIlroy et al., 2015).

3.2.4 Data analysis

Alpha-diversity indexes including Simpson's index of diversity (1-D), Shannon (H), Evenness and Chao-1 were calculated using PAST (PAleontological STatistics) 3.20 software (Hammer et al., 2001). One-way analysis of variance (ANOVA) was performed using Microsoft Excel to measure statistical significance between the Mn(II) oxidation performance of the three reactors.

3.3 Results

3.3.1 Reactor performances

The performance data are shown in Figure 3.2. Mn(II) removal was immediately observed for all reactors, although the Mn(II) loading rate was very low for each. Since the influent Mn(II) concentration of $5 \text{ mg Mn(II)·L}^{-1}$ was reduced to almost zero in the effluent, we gradually increased the Mn(II) loading rate by reducing HRT and increasing the influent Mn(II) concentration to find the maximum Mn(II) oxidation potentials in Phase 1, with the COD loading rate set at approximately $0.3 \text{ kg COD·m}^{-3}·\text{d}^{-1}$. The Mn(II) removal rates steadily increased to result in effluent concentrations of less than $0.5 \text{ mg Mn(II)·L}^{-1}$. At the end of Phase 1, R-1 (day 30), R-2 (day 38) and R-3 (day 36) achieved Mn(II) removal rates of 0.26, 0.41 and $0.49 \text{ kg Mn·m}^{-3}·\text{d}^{-1}$, respectively, at a HRT of 0.4 h, with effluent Mn(II) concentrations exceeding $0.5 \text{ mg Mn(II)·L}^{-1}$. Thus, as expected, Mn(II) removal with oxidation was successful with K-medium, SAS, or methanol used as substrate, although Mn(II) oxidation potential was different for each substrate at almost the same COD removal rate. In addition, a slight decrease in the effluent pH was observed in three reactors because of Mn(II) oxidation.

In Phase 2, the operational conditions were kept the same as the last conditions in Phase 1 to investigate performance stability. With elapsed time, the effluent Mn(II) concentration tended to increase for all three reactors. It was difficult to maintain stable reactor performance at high Mn(II) loading, resulting in a deterioration of the Mn(II) removal rate to 0.23, 0.36, and $0.34 \text{ kg Mn·m}^{-3}·\text{d}^{-1}$ on average for R-1, R-2 and R-3, respectively (Figs. 3.2 and 3.3).

Mn(II) removal performance of the reactor should be related to the population size of microbes with manganese oxidation ability. I expected that the Mn(II) removal rate would be improved by increasing COD loading rate. In Phase 3, I therefore doubled the COD loading rate to $0.6 \text{ kg COD·m}^{-3}·\text{d}^{-1}$ and increased the Mn(II) concentration from 5 to 10 mg L^{-1} in the influent without changing the Mn(II) loading rate of the reactors. Despite the change, the Mn(II) removal rates did not improve, although the COD removal rates were slightly higher. In R-1 and R-3, although the Mn(II) removal rates fluctuated greatly, their averages were almost the same as those achieved at the end of Phase 2 (Figs. 3.2 and 3.3). In R-2, in contrast, Mn(II) removal gradually deteriorated over time (Fig. 3.2). Therefore, to restore the Mn(II) removal performance in R-2, I decreased the influent Mn(II) concentration for the last 5 days because I hypothesized that high concentrations of Mn(II) were inhibiting removal. However, the deterioration of Mn(II) removal performance did not stop and therefore, this attempt failed. The results in Phase 3 suggested that the COD loading rate was less important in MnOB enrichment.

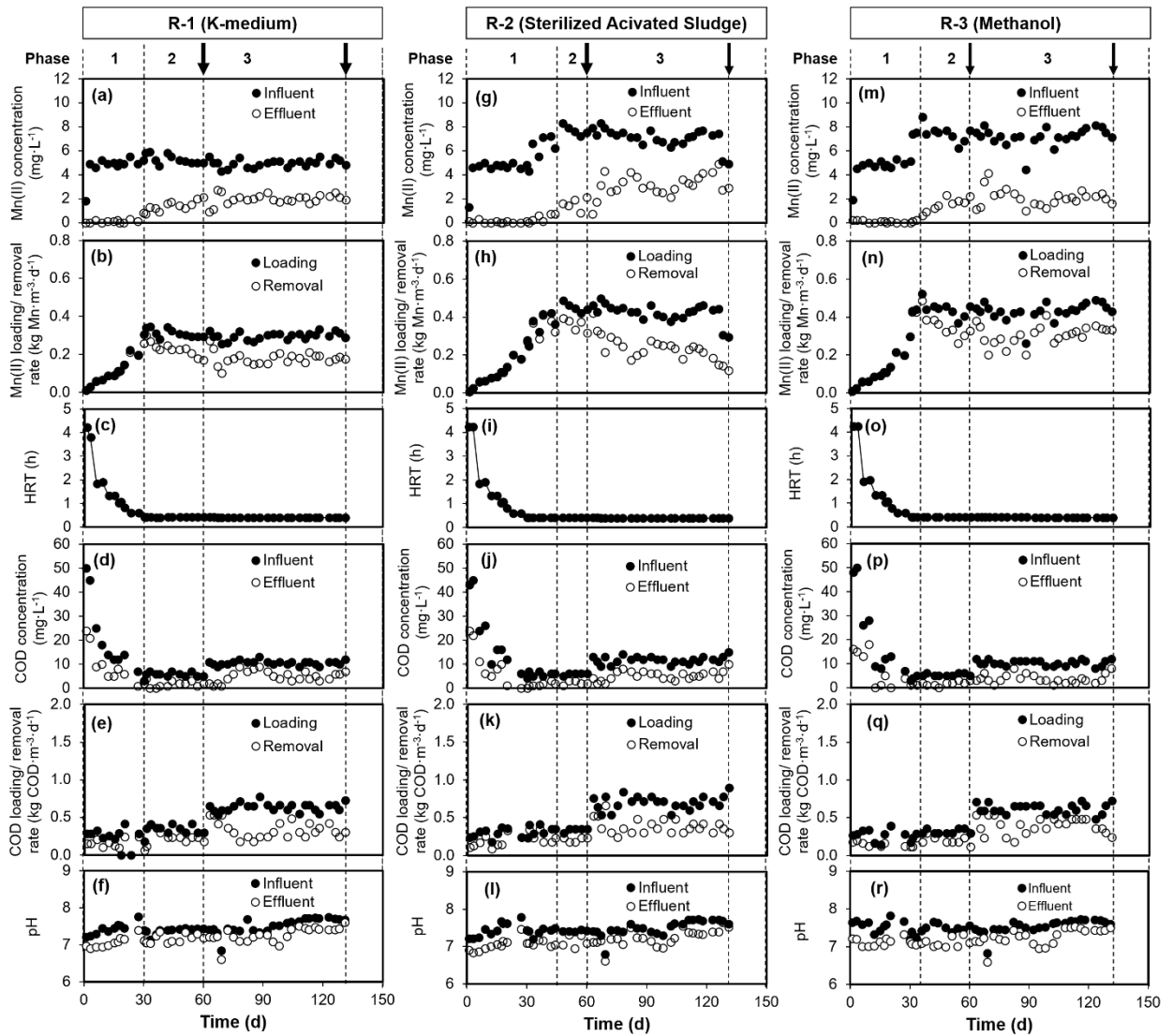


Figure 3.2 The performance of R-1, R-2, and R-3. The arrows indicate biofilm sampling on day-60 and day-131.

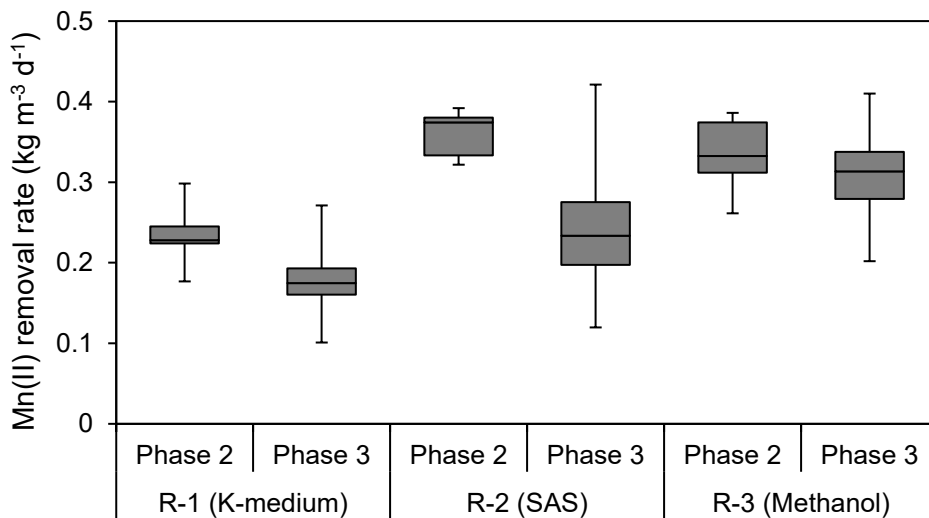


Figure 3.3 Mn(II) removal rates of each reactor during Phase 2 and 3

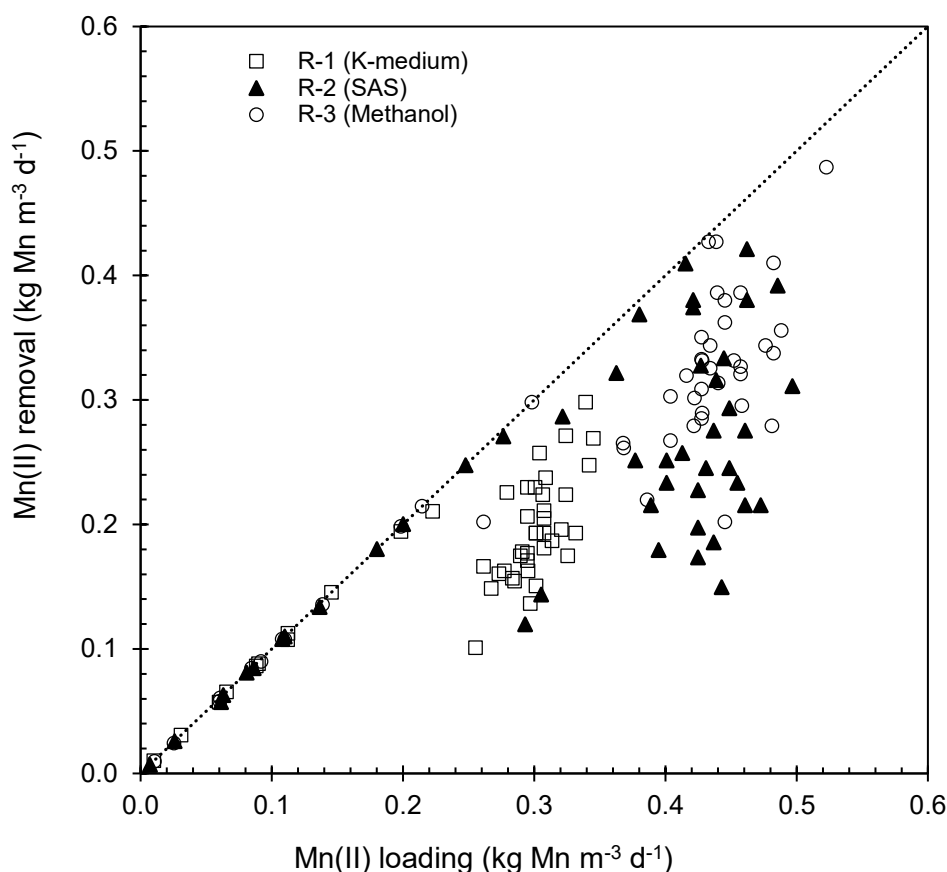


Figure 3.4 Relationship between Mn(II) loading and removal rate.

Until the low Mn(II) loading rate of approximately $0.25 \text{ kg Mn} \cdot \text{m}^{-3} \cdot \text{d}^{-1}$, three reactors could completely remove Mn(II), as shown in the plots on the line of slope 1 in Fig. 3.4. Higher Mn(II) loading rates resulted in incomplete Mn(II) removal and unstable performance. Surprisingly, the SAS substrate of R-2 yielded higher Mn(II) removal than K-medium, which is usually used for MnOB cultivation (Fig. 3.4). Thus, it can be concluded that SAS is a useful substrate for enriching MnOB. As expected, the methanol in R-3 was a preferred substrate for Mn(II) removal and yielded high and stable performance. During the operation, a black particulate precipitate was observed at the bottoms of all reactors, consistent with the removal of Mn(II) by oxidation, yielding Bio-MnO_x.

3.3.2 Microbial community

In the microbial community analysis of the six biomass samples, more than 90,000 reads were obtained, and the number of OTUs, which were defined based on the 97% similarity threshold of the 16S rRNA gene sequences, exceeded 1,600 for each sample (Table 3.2). Microbial diversity was assessed by alpha-diversity indices of Simpson (1-D), Shannon (H), Evenness,

and Chao-1 estimator (Table 3.2). No significant difference ($p < 0.05$) was found in comparisons of the diversity among the three reactors, suggesting that the difference in organic substrate had little effect on the diversity of the microbial community.

Table 3.2 Sequence reads, total number of OTU and diversity of each reactor

Sample	R-1		R-2		R-3	
	day-60	day-131	day-60	day-131	day-60	day-131
Total reads	91349	96131	96718	92321	95826	90335
Total OTU ¹⁾	1798	1675	1896	2029	1906	1633
Simpson (1-D) ²⁾	0.95	0.97	0.98	0.98	0.98	0.98
Shannon (H) ³⁾	4.61	4.97	4.99	5.25	4.98	4.85
Evenness ⁴⁾	0.06	0.09	0.08	0.09	0.08	0.08
Chao-1 ⁵⁾	2920	2685	3162	2940	2891	2616

¹⁾ Operational taxonomic unit (OTU) are defined at a 97% similarity threshold of the 16S gene sequences.

²⁾ Simpson's index of diversity (1-D). A higher number represents more diversity.

³⁾ Shannon (H) diversity index. A higher number represents more diversity.

⁴⁾ Evenness. A higher number represents more evenness.

⁵⁾ Chao-1. A higher number represents higher richness estimation.

There was little difference in microbial composition among the six samples, even in phylum level (Fig. 3.5). Of the 17 phyla identified, which were the major microbial communities with a relative abundance greater than 1% of the total sequence reads, Proteobacteria, Chloroflexi and Bacteroidetes were found to be dominant in all samples. However, the difference in microbial composition among the three reactors was clearly observed in the genus level. The genera, which had relative abundances of more than 3% in the sequence reads, are shown for each sample in Fig. 3.6. Predominant genera were *Comamonas*, unclassified *Caldilineaceae* and *Methylobacter* in the R-1 reactor. In R-2, although unclassified *Caldilineaceae* dominated, *Comamonas* was barely present. In R-3, *Hyphomicrobium* and *Methylobacterium* were detected as the predominant genera. Thus, the microbial community was strongly influenced by composition of the organic substrates even though the high Mn(II) oxidation was performed. The effect of the organic loading rate on the microbial community was also observed, but it was insignificant compared to the effect of the substrates of the three reactors (samples on days 60 and 131 in Fig. 3.6).

Phylum	R-1 (K-medium)		R-2 (SAS)		R-3 (Methanol)	
	R1-d60	R1-d131	R2-d60	R2-d131	R3-d60	R3-d131
Acidobacteria	1.6%	2.4%	1.9%	3.8%	1.8%	4.3%
Actinobacteria	5.7%	3.0%	7.0%	9.6%	3.1%	6.6%
Aerophobetes	1.5%	0.0%	0.5%	0.1%	0.0%	0.0%
Armatimonadetes	1.0%	0.6%	4.6%	1.9%	2.0%	3.9%
Bacteroidetes	11.6%	9.3%	4.9%	11.3%	11.7%	10.2%
Chlamydiae	0.4%	0.5%	0.6%	1.2%	0.9%	1.0%
Chlorobi	1.4%	1.4%	4.7%	0.6%	3.7%	4.3%
Chloroflexi	13.3%	7.1%	13.6%	13.9%	13.0%	7.6%
Firmicutes	0.3%	0.9%	1.0%	2.2%	0.5%	0.2%
Gemmatimonadetes	0.2%	0.8%	0.2%	2.0%	0.0%	0.6%
Latescibacteria	0.1%	0.7%	1.3%	2.4%	0.5%	1.8%
Nitrospirae	1.0%	1.1%	1.2%	2.8%	0.1%	0.8%
Planctomycetes	2.4%	0.9%	1.8%	2.6%	0.6%	0.5%
Proteobacteria	52.1%	65.9%	42.3%	35.8%	53.1%	53.8%
Saccharibacteria	0.1%	0.4%	0.9%	2.0%	1.8%	0.5%
Verrucomicrobia	4.2%	1.9%	10.4%	3.5%	5.3%	2.3%
WCHB1-60	0.0%	0.6%	0.2%	1.6%	0.0%	0.0%
Others	3.0%	2.6%	3.0%	2.7%	1.9%	1.6%

Figure 3.5 Microbial community at the phyla level. Phyla with relative abundance <1% were grouped as “Others”.

Phylum	Genus	R-1 (K-medium)		R-2 (SAS)		R-3 (Methanol)	
		R1-d60	R1-d131	R2-d60	R2-d131	R3-d60	R3-d131
Actinobacteria	Mycobacterium	3.8%	1.2%	2.8%	2.0%	1.4%	2.3%
	Nocardia	0.3%	0.4%	0.9%	3.2%	0.4%	2.5%
Bacteroidetes	Chitinophagaceae uncultured	1.5%	1.7%	0.9%	4.4%	1.4%	2.5%
	Cytophagaceae uncultured	2.8%	3.2%	1.3%	1.5%	1.9%	1.0%
	Saprospiraceae uncultured	2.7%	0.0%	0.5%	0.0%	5.5%	2.1%
Chloroflexi	Caldilineaceae uncultured	11.8%	4.5%	6.3%	9.2%	4.0%	0.6%
	Candidatus Defluviifilum	0.4%	0.3%	4.0%	1.2%	3.9%	1.1%
	Kouleothrix	0.5%	1.3%	1.5%	1.4%	3.6%	4.4%
Proteobacteria	Comamonas	15.9%	1.9%	0.7%	0.2%	0.4%	0.3%
	Hypomicrobium	0.6%	0.7%	1.5%	1.2%	6.9%	11.1%
	Methylobacter	1.8%	10.3%	0.4%	2.7%	2.4%	0.0%
	Methylobacterium	0.0%	0.0%	0.0%	0.0%	0.1%	8.4%
	Methylocaldum	0.6%	3.5%	0.2%	0.9%	0.9%	0.0%
	Methylophilus	0.1%	0.7%	0.1%	0.3%	5.8%	1.7%
	Pseudomonas	2.8%	4.7%	0.4%	0.4%	0.1%	1.6%
Verrucomicrobia	Zymomonas	1.3%	0.6%	3.0%	1.5%	1.8%	2.4%
	Prostheco bacter	2.8%	0.9%	9.5%	1.5%	4.3%	1.3%

Figure 3.6 Most dominant genera in the reactors with relative abundance >3% of the total sequence reads in each sample.

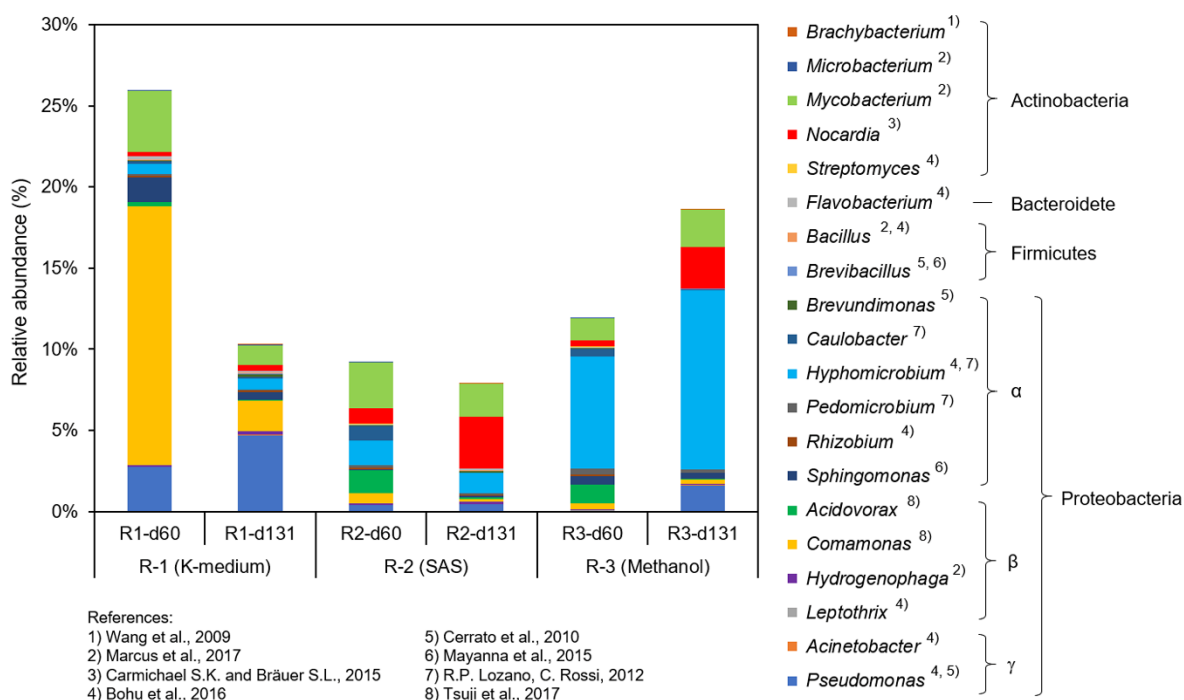


Figure 3.7 Relative abundance of putative manganese-oxidizing bacteria.

During Mn(II) removal, certain MnOB should have played a role in Mn(II) oxidation. Unfortunately, I was unable to identify enrichment for known MnOB in any of the reactors because of a limitation of DNA sequence data obtained in this study and the probable presence of unknown MnOB. However several genera that contain strains previously identified as MnOB were detected, so I tentatively refer to them as “putative MnOB” responsible for Mn(II) oxidation, with the caveat that not all putative MnOB are able to oxidize Mn(II) (Francis and Tebo, 2001; Francis and Tebo, 2002). Many putative MnOB were detected (Fig. 3.7); comprising 8–25% of the total bacteria. Most putative MnOB in R-1 belonged to either *Comamonas* or *Pseudomonas*. In R-2, multiple genera including *Mycobacterium*, *Nocardia*, and *Hyphomicrobium* were identified as putative MnOB. *Hyphomicrobium* were the dominant putative MnOB genus in R-3. These results indicated that even though three kinds of substrate used in this study were completely different, high Mn(II) oxidation rates were possible because different MnOB were highly enriched depending on the substrate

3.4 Discussion

The microbial community analysis showed that the three reactors were dominated by different putative MnOB genera (Fig. 3.7). These genera have been reported to inhabit different environments. *Comamonas testosteroni*, belonging to Proteobacteria phylum, have been found

to contribute to the formation of Bio-MnO_x on the leaf surface of submerged aquatic plants in a lake (Tsuji et al., 2017). *Pseudomonas* and *Mycobacterium* have been reported to play a major role in manganese removal in drinking water systems (Cerrato et al., 2010; Marcus et al., 2017). *Nocardia* and *Hyphomicrobium* have been detected in ferromanganese deposits in a cave (Carmichael and Brauer, 2015; Lozano and Rossi, 2012), and *Hyphomicrobium* have been found to oxidize Mn(II) in a methane-fed reactor (Matsushita et al., 2018). It can be presumed that different environments provide different available nutrients leading to differences in the microbial community. This study revealed that the distinct putative MnOB community among the three reactors was due to the adaptation of microbial communities to the different substrates.

The results showed that all three substrates used in this study supported MnOB communities (Fig. 3.7). It is unsurprising that *Comamonas* and *Pseudomonas* dominated in R-1, as they perform ammonification and nitrogen removal, because K-medium containing peptone and yeast extract has been commonly used to culture MnOB (Yang et al., 2013). In addition, MnOB have been successfully enriched even during the nitrification process (Cao et al., 2015). Both the *Mycobacterium* and the *Nocardia* belonging to Actinobacteria were suggested to be the predominant putative MnOB in the R-2 fed with SAS. The genus *Mycobacterium* can use a wide range of organic compounds as carbon sources, including recalcitrant compounds such as polycyclic aromatic hydrocarbons (PAHs) (Hartmans, et al., 2006; Zeng et al., 2010); it was also detected in similar abundance in all reactors. The DHS reactor employed in this study has a longer sludge retention time and allows a higher degree of sludge autolysis because of a biofilm system that results in reduced sludge generation (Tandukar et al., 2007). Even though different substrates were provided, *Mycobacterium* probably utilized the generated cell lysate in biofilm as a nutrient source. A previous study reported that in a methane providing reactor, *Hyphomicrobium* played a role in M(II) oxidation by growing on methanol associated with the metabolism of methanotrophic bacteria (Matsushita et al., 2018). As I expected, putative MnOB belonging to *Hyphomicrobium* were enriched with the methanol substrate of R-3. Our results demonstrate that a wide variety of organic substrates can be used for Mn(II) removal and MnO₂ production in engineered ecosystems, since MnOB are diverse and ubiquitous in natural environments.

The presence of MnO₂ has been reported to shorten the acclimation period of MnOB in biofilter and inhibit the activity of non-MnOB by its toxicity (Zhang et al., 2015; Matsushita et al., 2018). In this study, the sponge carriers combined with abiotic-MnO₂ in the hope of

enhancing MnOB enrichment by inhibiting the growth other bacteria. Our results showed that the maximum Mn(II) removal rate was achieved within 42 days in all three reactors (Fig. 3.2a, g and m). In contrast, studies using sponge carriers without abiotic-MnO₂ took a longer time to achieve similar results, even for Mn(II) removal (Cao et al., 2015; Matsushita et al., 2018). Not only higher initial Mn(II) removal performance but also much higher Mn(II) oxidation rates were obtained with sponge carriers with abiotic-MnO₂ relative to those without abiotic-MnO₂. The highest Mn(II) oxidation rates of 0.26 and 0.41 kg Mn·m⁻³·d⁻¹ for R-1 and R-2, respectively (Fig. 3.2b and 1h), were almost 10-fold higher than those of 0.048 and 0.011 kg Mn·m⁻³·d⁻¹, which were achieved by other groups in Mn(II) oxidation reactors combined with nitrification (Cao et al., 2015) and methane oxidation under marine conditions (Kato et al., 2017), respectively. Interestingly, however, the highest Mn(II) oxidation rate of 0.49 kg Mn·m⁻³·d⁻¹ in R-3 was almost the same as the highest rate in a DHS reactor coupled with methane oxidation in a freshwater environment, even though it took a long time to reach that rate (Matsushita et al. 2018). These similar Mn(II) oxidation rates might be caused by having the same predominant MnOB, *Hypromicrobium* in both reactors. Once significant Bio-MnO_x is produced, Mn(II) oxidation might reach a similar rate regardless of the initial installation of abiotic-MnO₂.

Although R-2 had a significantly lower proportion of putative MnOB relative to the other reactors (Fig. 3.7), their respective Mn(II) removal rates were almost the same (Fig. 3.3). Since many uncultured bacteria were detected, unknown MnOB might be included in them and play a major role in Mn(II) removal in R-2. Two factors, the amount of MnOB retained in the reactor and their Mn(II) oxidation potential, should directly affect the Mn(II) removal performance of the reactor. Even if the proportion of MnOB is low, a high Mn(II) removal performance will be obtained when MnOB possess high Mn(II) oxidation potentials. In addition, interactions between two non-MnOB in co-culture could induce Mn(II)-oxidizing activity (Liang et al., 2016). If such interactions occurred in R-2, the high Mn(II) removal would be expected even if unknown MnOB did not exist. It is hard to explain why so little difference in Mn(II) removal performance was observed among the three reactors despite of the feasible reasons mentioned above.

An unstable Mn(II) oxidation rate was observed at higher Mn(II) loading rates of greater than approximately 0.25 kg Mn·m⁻³·d⁻¹ in Phase 3 (Fig. 3.4). This instability could be explained by decreased Mn(II) transfer into biomass with increased production of Bio-MnO_x

covering MnOB by mass transfer resistance, resulting in deterioration of Mn(II) oxidation, as reported elsewhere (Jiang et al., 2010). These investigators also reported that the Mn(II) concentration would respond to the instability. Microorganisms have different tolerances for Mn(II) (Zhou et al., 2016). The residual Mn(II) concentration should depend on an Mn(II) loading rate due to incomplete oxidation. As shown in Fig. 3.2, Mn(II) oxidation rate tended to decrease with increased effluent Mn(II) concentration in Phase 3 of R-2. Thus, high Mn(II) loading rates would affect the stability of Mn(II) oxidation performance.

Our proposed bioreactor having high Mn(II) oxidative capacity could be applied for remediation of water contaminated by high concentrations of Mn(II), such as acid-mine drainage (Tutu et al., 2008). However, because MnOB are heterotrophs, organic substrates have to be provided to MnOB enriched bioreactors to remove heavy metals or to recover minor metals from wastewaters containing low or no organics. This study demonstrated that multiple substrates enriched MnOB and produced Bio-MnO_x at a high rate. Methanol would be preferred over K-medium for its low cost, and somewhat higher Mn(II) oxidation performance. In addition, if combined with the treatment of methanol-containing wastewaters generated from methanol production plants (G. Cao et al., 2015) or pulp and paper mills (Meyer and Edwards, 2014), MnOB enrichment of using waste methanol is preferable. The employment of SAS may also be very attractive. SAS is the most cost-effective and eco-friendly solution for the disposal of large amounts of sewage sludge. Nevertheless, our trial of SAS had the minor disadvantage of unstable Mn(II) oxidation performance. However, if I could identify the cause of instability and overcome the disadvantage, SAS becomes the most promising substrate for MnOB enrichment. SAS is the bulk of dead cells, which consist of cell walls and cytoplasm. It is unclear whether the cell wall or cytoplasm is preferable for MnOB enrichment. If I could determine the preferable substrate for MnOB enrichment, Mn(II) oxidation performance could be enhanced. Future experiments on SAS as a substrate for MnOB are therefore promising

3.5 Conclusions

Three different organic substrates, K-medium, SAS and methanol, successfully enriched MnOB with high Mn(II) oxidation rates during continuous operation of a DHS reactor employing sponge carriers initially combined with abiotic-MnO₂. Microbial analysis revealed that the major MnOB players were significantly different at the genus level among the substrates. I found that organic substances other than K-medium could enrich MnOB. Methanol

was most effective in achieving the highest Mn(II) removal with stability. Our data suggest that SAS is a promising substrate for MnOB enrichment, despite less-stable performance. To better understand the instability, a study on the effect of Mn(II) concentration on MnOB activity is necessary.

Acknowledgments

This research was supported by the Japan Society for the Promotion of Science as a Grant-in-Aid for Scientific Research (A) Grant Number JP23241029, and the Environment Research and Technology Development Fund (2-3K133004) of the Ministry of the Environment, Japan. We thank the Ministry of Research, Technology and Higher Education of the Republic of Indonesia through Riset-Pro for PhD scholarship (World Bank Loan No. 8245-ID) to AS.

References

- Abu Hasan, H., Sheikh Abdullah, S.R., Tan Kofli, N., Kamarudin, S.K., 2012. Effective microbes for simultaneous bio-oxidation of ammonia and manganese in biological aerated filter system. *Bioresour. Technol.* 124, 355–363. <https://doi.org/10.1016/j.biortech.2012.08.055>
- Anderson, C.R., Davis, R.E., Bandolin, N.S., Baptista, A.M., Tebo, B.M., 2011. Analysis of *in situ* manganese(II) oxidation in the Columbia River and offshore plume: Linking *Aurantimonas* and the associated microbial community to an active biogeochemical cycle. *Environ. Microbiol.* 13, 1561–1576. <https://doi.org/10.1111/j.1462-2920.2011.02462.x>
- Bai, Y., Yang, T., Liang, J., Qu, J., 2016a. The role of biogenic Fe-Mn oxides formed in situ for arsenic oxidation and adsorption in aquatic ecosystems. *Water Res.* 98, 119–127. <https://doi.org/10.1016/j.watres.2016.03.068>
- Bai, Y., Chang, Y., Liang, J., Chen, C., Qu, J., 2016b. Treatment of groundwater containing Mn(II), Fe(II), As(III) and Sb(III) by bioaugmented quartz-sand filters. *Water Res.* 106, 126–134. <https://doi.org/10.1016/j.watres.2016.09.040>
- Bahar M. M., Megharaj, M., Naidu, R., 2016. Oxidation of arsenite to arsenate in growth medium and groundwater using a novel arsenite-oxidizing diazotrophic bacterium isolated from soil. *Int. Biodeterior. Biodegrad.*, 106:178-182. Doi 10.1016/j.ibiod.2015.10.019
- Blöthe, M., Wegorzewski, A., Müller, C., Simon, F., Kuhn, T., Schippers, A., 2015. Manganese-cycling microbial communities inside deep-sea manganese nodules. *Environ. Sci. Technol.* 49, 7692–7700. <https://doi.org/10.1021/es504930v>
- Bohu, T., Akob, D.M., Abratis, M., Lazar, C.S., 2016. Biological Low-pH Mn(II) oxidation in a manganese deposit influenced by metal-rich groundwater. *Appl. Environ. Microbiol.* 82, 3009–3021. <https://doi.org/10.1128/AEM.03844-15>

- G. Cao, Zhang, Y., Chen, L., Liu, J., Mao, K., Li, K., Zhou, J., 2015. Production of a biofloculant from methanol wastewater and its application in arsenite removal. *Chemosphere* 141, 274–281. <https://doi.org/10.1016/j.chemosphere.2015.08.009>
- Cao, L.T.T., Kodera, H., Abe, K., Imachi, H., Aoi, Y., Kandaichi, T., Ozaki, N., Ohashi, A., 2015. Biological oxidation of Mn(II) coupled with nitrification for removal and recovery of minor metals by downflow hanging sponge reactor. *Water Res.* 68, 545–553. <https://doi.org/10.1016/j.watres.2014.10.002>
- Caporaso, J.G., Kuczynski, J., Stombaugh, J., Bittinger, K., Bushman, F.D., Costello, E.K., Fierer, N., Peña, A.G., Goodrich, K., Gordon, J.I., Huttley, G.A., Kelley, S.T., Knights, D., Jeremy, E., Ley, R.E., Lozupone, C.A., McDonald, D., Muegge, B.D., Reeder, J., Sevinsky, J.R., Turnbaugh, P.J., Walters, W.A., 2010. QIIME allows analysis of high-throughput community sequencing data. *Nat Methods* 7(5): 335–336. <https://doi.org/10.1038/nmeth.f.303>
- Carmichael S.K. and Bräuer S.L., 2015. Microbial diversity and manganese cycling: A review of manganese-oxidizing microbial cave communities, in: Engel A.S. (Ed.), *Microbial life of cave systems. life in extreme environments*. Walter de Gruyter GmbH & Co KG, Boston, MA, pp. 137–160. <https://doi.org/10.1515/9783110339888-009>
- Cerrato, J.M., Falkinham, J.O., Dietrich, A.M., Knocke, W.R., McKinney, C.W., Pruden, A., 2010. Manganese-oxidizing and -reducing microorganisms isolated from biofilms in chlorinated drinking water systems. *Water Res.* 44, 3935–3945. <https://doi.org/10.1016/j.watres.2010.04.037>
- Cloutier, M.L.C., Carmichael, S.K., Carson, M.A., Madritch, M.D., Bräuer, S.L., 2017. Carbon quantity and quality drives variation in cave microbial communities and regulates Mn(II) oxidation. *Biogeochemistry* 134, 77–94. <https://doi.org/10.1007/s10533-017-0343-8>
- Droz, B., Dumas, N., Duckworth, O.W., Peña, J., 2015. A comparison of the sorption reactivity of bacteriogenic and mycogenic Mn oxide nanoparticles. *Environ. Sci. Technol.* 49, 4200–4208. <https://doi.org/10.1021/es5048528>
- Edgar, R.C., 2010. Search and clustering orders of magnitude faster than BLAST. *Bioinformatics* 26, 2460–2461. <https://doi.org/10.1093/bioinformatics/btq461>
- Francis, C.A., Tebo, B.M., 2001. cumA multicopper oxidase genes from diverse Mn(II)-oxidizing and non-Mn(II)-oxidizing *Pseudomonas* strains. *Appl. Environ. Microbiol.* 67, 4272–4278. <https://doi.org/10.1128/AEM.67.9.4272-4278.2001>
- Francis, C.A., Tebo, B.M., 2002. Enzymatic manganese(II) oxidation by metabolically dormant spores of diverse *Bacillus* species. *Appl. Environ. Microbiol.* 68, 874–880. <https://doi.org/10.1128/AEM.68.2.874-880.2002>
- Geszvain, K., Butterfield, C., Davis, R.E., Madison, A.S., Lee, S.-W., Parker, D.L., Soldatova, A., Spiro, T.G., Luther, G.W., Tebo, B.M., 2012. The molecular biogeochemistry of manganese(II) oxidation. *Biochem. Soc. Trans.* 40, 1244–1248. <https://doi.org/10.1042/BST20120229>
- Hammer, Ø., Harper, D.A.T., Ryan, P.D., 1999. PAST: Paleontological Statistics Software Package. *Palaeontol. Electron.* 4, 9. <https://doi.org/10.1016/j.bcp.2008.05.025>

- Hartmans S., de Bont J.A.M., Stackebrandt E. 2006. The Genus *Mycobacterium*-Nonmedical. In: Dworkin M., Falkow S., Rosenberg E., Schleifer KH., Stackebrandt E. (eds) The Prokaryotes. Springer, New York, NY
- Jaiswal, V., Saxena, S., Kaur, I., Dubey, P., Nand, S., Naseem, M., Singh, S.B., Srivastava, P.K., Barik, S.K., 2018. Application of four novel fungal strains to remove arsenic from contaminated water in batch and column modes. *J. Hazard. Mater.* 356, 98–107. <https://doi.org/10.1016/j.jhazmat.2018.04.053>
- Jiang, S., Kim, D.-G., Kim, J.-H., Ko, S.-O., 2011. Characterization of the biogenic manganese oxides produced by *Pseudomonas putida* strain MnB1. *Environ. Eng. Res.* 15, 183–190. <https://doi.org/10.4491/eer.2010.15.4.183>
- Jones, M.E., Nico, P.S., Ying, S., Regier, T., Thieme, J., Keiluweit, M., 2018. Manganese-driven carbon oxidation at oxic-anoxic interfaces. *Environ. Sci. Technol.* 52, 12349–12357. <https://doi.org/10.1021/acs.est.8b03791>
- Kato, S., Miyazaki, M., Kikuchi, S., Kashiwabara, T., Saito, Y., Tasumi, E., Suzuki, K., Takai, K., Cao, L.T.T., Ohashi, A., Imachi, H., 2017. Biotic manganese oxidation coupled with methane oxidation using a continuous-flow bioreactor system under marine conditions. *Water Sci. Technol.* 76, 1781–1795. <https://doi.org/10.2166/wst.2017.365>
- Kolb, S., 2009. Aerobic methanol-oxidizing bacteria in soil. *FEMS Microbiol. Lett.* 300, 1–10. <https://doi.org/10.1111/j.1574-6968.2009.01681.x>
- Liang, J., Bai, Y., Hu, C., Qu, J., 2016. Cooperative Mn(II) oxidation between two bacterial strains in an aquatic environment. *Water Res.* 89, 252–260. <https://doi.org/10.1016/j.watres.2015.11.062>
- Lin, H., Taillefert, M., 2014. Key geochemical factors regulating Mn(IV)-catalyzed anaerobic nitrification in coastal marine sediments. *Geochim. Cosmochim. Acta* 133, 17–33. <https://doi.org/10.1016/j.gca.2014.01.025>
- Lozano, R.P., Rossi, C., 2012. Exceptional preservation of Mn-oxidizing microbes in cave stromatolites (El Soplao, Spain). *Sediment. Geol.* 255–256, 42–55. <https://doi.org/10.1016/j.sedgeo.2012.02.003>
- Marcus, D.N., Pinto, A., Anantharaman, K., Ruberg, S.A., Kramer, E.L., Raskin, L., Dick, G.J., 2017. Diverse manganese(II)-oxidizing bacteria are prevalent in drinking water systems. *Environ. Microbiol. Rep.* 9, 120–128. <https://doi.org/10.1111/1758-2229.12508>
- Matsushita, S., Komizo, D., Cao, L.T.T., Aoi, Y., Kindaichi, T., Ozaki, N., Imachi, H., Ohashi, A., 2018. Production of biogenic manganese oxides coupled with methane oxidation in a bioreactor for removing metals from wastewater. *Water Res.* 130, 224–233. <https://doi.org/10.1016/j.watres.2017.11.063>
- Mayanna, S., Peacock, C.L., Schäffner, F., Grawunder, A., Merten, D., Kothe, E., Büchel, G., 2015. Biogenic precipitation of manganese oxides and enrichment of heavy metals at acidic soil pH. *Chem. Geol.* 402, 6–17. <https://doi.org/10.1016/j.chemgeo.2015.02.029>
- McIlroy, S.J., Saunders, A.M., Albertsen, M., Nierychlo, M., McIlroy, B., Hansen, A.A., Karst, S.M., Nielsen, J.L., Nielsen, P.H., 2015. MiDAS: the field guide to the microbes of activated sludge. Database 2015, bav062. <https://doi.org/10.1093/database/bav062>
- Meng, Y.T., Zheng, Y.M., Zhang, L.M., He, J.Z., 2009. Biogenic Mn oxides for effective adsorption of Cd from aquatic environment. *Environ. Pollut.* 157, 2577–2583. <https://doi.org/10.1016/j.envpol.2009.02.035>

- Meyer, T., Edwards, E.A., 2014. Anaerobic digestion of pulp and paper mill wastewater and sludge. *Water Res.* 65, 321–349. <https://doi.org/10.1016/j.watres.2014.07.022>
- Ramstedt, M., Nakao, R., Wai, S.N., Uhlin, B.E., Boily, J.F., 2011. Monitoring surface chemical changes in the bacterial cell wall: Multivariate analysis of cryo-X-ray photoelectron spectroscopy data. *J. Biol. Chem.* 286, 12389–12396. <https://doi.org/10.1074/jbc.M110.209536>
- Tandukar, M., Ohashi, A., Harada, H., 2007. Performance comparison of a pilot-scale UASB and DHS system and activated sludge process for the treatment of municipal wastewater. *Water Res.* 41, 2697–2705. <https://doi.org/10.1016/j.watres.2007.02.027>
- Tang, Y., Webb, S.M., Estes, E.R., Hansel, C.M., 2014. Chromium(III) oxidation by biogenic manganese oxides with varying structural ripening. *Environ. Sci. Process. Impacts* 16, 2127–2136. <https://doi.org/10.1039/C4EM00077C>
- Tebo, B.M., Johnson, H.A., McCarthy, J.K., Templeton, A.S., 2005. Geomicrobiology of manganese(II) oxidation. *Trends Microbiol.* 13, 421–428. <https://doi.org/10.1016/j.tim.2005.07.009>
- Tsuji, K., Asayama, T., Shiraki, N., Inoue, S., Okuda, E., Hayashi, C., Nishida, K., Hasegawa, H., Harada, E., 2017. Mn accumulation in a submerged plant *Egeria densa* (Hydrocharitaceae) is mediated by epiphytic bacteria. *Plant Cell Environ.* 40, 1163–1173. <https://doi.org/10.1111/pce.12910>
- Tutu, H., McCarthy, T.S., Cukrowska, E., 2008. The chemical characteristics of acid mine drainage with particular reference to sources, distribution and remediation: The Witwatersrand Basin, South Africa as a case study. *Appl. Geochemistry* 23, 3666–3684. <https://doi.org/10.1016/j.apgeochem.2008.09.002>
- Wang, W., Shao, Z., Liu, Y., Wang, G., 2009. Removal of multi-heavy metals using biogenic manganese oxides generated by a deep-sea sedimentary bacterium - *Brachybacterium* sp. strain Mn32. *Microbiology* 155, 1989–1996. <https://doi.org/10.1099/mic.0.024141-0>
- Yang, W., Zhang, Z., Zhang, Z., Chen, H., Liu, J., Ali, M., Liu, F., Li, L., 2013. Population structure of manganese-oxidizing bacteria in stratified soils and properties of manganese oxide aggregates under manganese-complex medium enrichment. *PLoS One* 8. <https://doi.org/10.1371/journal.pone.0073778>
- Yin, T., Chen, H., Reinhard, M., Yi, X., He, Y., Gin, K.Y.H., 2017. Perfluoroalkyl and polyfluoroalkyl substances removal in a full-scale tropical constructed wetland system treating landfill leachate. *Water Res.* 125, 418–426. <https://doi.org/10.1016/j.watres.2017.08.071>
- Zeng, J., Lin, X., Zhang, J., Li, X., 2010. Isolation of polycyclic aromatic hydrocarbons (PAHs)-degrading *Mycobacterium* spp. and the degradation in soil. *J. Hazard. Mater.* 183, 718–723. <https://doi.org/10.1016/j.jhazmat.2010.07.085>
- Zeraatkar, A.K., Ahmadzadeh, H., Talebi, A.F., Moheimani, N.R., McHenry, M.P., 2016. Potential use of algae for heavy metal bioremediation, a critical review. *J. Environ. Manage.* 181, 817–831. <https://doi.org/10.1016/j.jenvman.2016.06.059>
- Zhang, Y., Zhu, H., Szewzyk, U., Geissen, S.U., 2015. Removal of pharmaceuticals in aerated biofilters with manganese feeding. *Water Res.* 72, 218–226. <https://doi.org/10.1016/j.watres.2015.01.009>

Zhou, H., Pan, H., Xu, J., Xu, W., Liu, L., 2016. Acclimation of a marine microbial consortium for efficient Mn(II) oxidation and manganese containing particle production. *J. Hazard. Mater.* 304, 434–440. <https://doi.org/10.1016/j.jhazmat.2015.11.019>

**Chapter 4: Residual Mn(II)
concentrations affect the Mn(II) oxidation
performance of the reactor**

Abstract

This study investigated the effect of residual Mn(II) on the Mn(II) oxidation performance of the reactors. Two DHS reactors were established; R-1 was supplied with low Mn(II) concentration and complete Mn(II) oxidation was ascertained, and R-2 was supplied with high Mn(II) concentration and residual Mn(II) was observed. Both reactors were fed with methanol as the sole carbon source, which have been shown to be the most effective substrate for MnOB enrichment. The high initial Mn(II) concentration caused microbial stress led to the declining Mn(II) oxidation ability. The maximum Mn(II) oxidation rate in R-1 and R-2 was 0.91 and 0.61 kg m⁻³ d⁻¹, respectively. Microbial community analysis demonstrated that the relative abundance of putative MnOB *Hyphomicrobium* in R-1 was remarkably higher than that of R-2. These results revealed that residual Mn(II) in the reactor not only inhibited Mn(II) oxidation ability but also MnOB population in the reactor. Therefore, to achieve a sustainable high Mn(II) oxidation performance in the bioreactor, the residual Mn(II) concentration should be monitored at a low level (<0.5 mg L⁻¹).

Keywords: Biological manganese oxidation, manganese-oxidizing bacteria, residual Mn(II), inhibition, *Hyphomicrobium*

4.1 Introduction

Manganese (Mn) is an essential element in small amounts for the growth of organisms, include humans, animals, plants, and microorganisms. However, high concentration of manganese can be poisonous and cause toxic effects to human health and plants (O'Neal and Zheng, 2015; Santos et al., 2017). The effects of Mn(II) to microbial activities have been previously investigated. Cheung et al. (1982) reported that a high concentration of manganese could inhibit the growth and sporulation of *Bacillus steavothevmophilus*, and the manganese concentration in the medium for optimum condition is between 10–30 µM. In more recent study, a high concentration of manganese can adversely affect magnesium-dependent enzyme activities of *Bradyrhizobium japonicum* (Hohle and O'Brian, 2014). The different microbial strains should have different tolerance levels for Mn(II). *D. vulgaris* and *Desulfovibrio* sp., which are widely known as sulfate reducing bacteria (SRB), have tolerance to high manganese concentration up to 10 ppm (Cabrera et al., 2006). A high Mn(II) concentration (4,000 mg L⁻¹) can promote the growth of *Ralstonia pickettii*, and this strain is able to survive under an extreme Mn(II) concentration of 1,000 mg L⁻¹ (Huang et al., 2018). The effect of Mn(II) on the mixed

microbial culture, such as biological sludge, have been investigated by Aragon et al. (2010), in which the addition of 1 mg L^{-1} Mn(II) improves the cellular metabolism of microorganisms in activated sludge as reflected by higher values of the specific oxygen uptake rate (SOUR) and lower COD values, while a higher dosage of Mn(II) (2 mg L^{-1}) have a negative effect on the respiratory activity and capacity to decompose organic matter.

Based on the results of Chapter 3, the residual Mn(II) have been observed may lead to the deterioration of Mn(II) oxidation performance of the reactor. The effects of Mn(II) to manganese-oxidizing bacteria (MnOB) have been reported in some studies. Small amounts of Mn(II) (less than $5 \text{ }\mu\text{M}$) have been found to accelerate oxidation of Cr(III) by and a higher concentration of Mn(II) (above $5 \text{ }\mu\text{M}$) inhibited Cr(III) oxidation activity, but does not affects its ability to oxidize Mn(II) (Murray and Tebo, 2007). Microbial strains, *Serratia marcescens*, isolated from manganese mine Water in Minas Gerais, Brazil have been shown to oxidize manganese, and possess a high manganese tolerance up to 1200 mg/L (Barboza et al., 2017). Mn(II)-oxidation ability of *Pseudomonas putida* strain MnB1, a widely known manganese-oxidizing bacterium, is inhibited at Mn(II) concentration of 20 mg L^{-1} , but the growth is not affected at 100 mg L^{-1} (Jiang et al., 2010). Previous study reported that a high manganese concentration ($185 \text{ }\mu\text{M}$) inhibits manganese oxidation rate in in the water column of Saanich Inlet, British Columbia, Canada (Tebo and Emerson, 1985). However, little information concerning the effects of Mn(II) on the Mn(II)-oxidation performance of microbial mixed culture in the reactor.

This study aims to investigate the effects of residual Mn(II) on the Mn(II) oxidation performance of the reactor. Two reactors are established; the first reactor is supplied with low Mn(II) concentration, in which complete manganese oxidation is warranted, while the second reactor is fed with high concentration of Mn(II), where residual Mn(II) is observed in the effluent. Microbial community analysis of biomass samples was performed to characterize the microbial community profiles and the predominant putative MnOB related to the Mn(II) oxidation performance.

4.2 Materials and methods

4.2.1 Reactor configurations, inoculation, and operational conditions

Two DHS reactors (each column size: 75 cm in height, 5 cm in diameter), in which a set of 20 polyurethane sponge cubes (each $2 \times 2 \times 2 \text{ cm}^3$, total volume of 160 cm^3) were connected

diagonally in series on a nylon string (Fig. 4.1). The sponge carriers were inoculated by squeezing and soaking in suspension liquid mixed of abiotic-MnO₂ 100 g·L⁻¹ (Kishida Chemical Co. Ltd., Japan) in activated sludge, which was taken from the aeration tank of municipal sewage treatment plant in Higashihiroshima. Prior to using abiotic-MnO₂ for inoculation, it was pretreated with a Mn(II) adsorption until reaching an equilibrium, to ascertain that removal of Mn(II) during reactor operation was not by abiotic-MnO₂ through chemical adsorption. The reactors were then placed in a dark and temperature-controlled room at 25 °C.

The reactors were supplied with substrate which consists of methanol, Mn(II) (MnCl₂·4H₂O), minerals (CaCl₂·2H₂O 0.05 mg·L⁻¹, MgSO₄·7H₂O 0.2 mg·L⁻¹, Fe₂SO₄·5H₂O 0.1 mg·L⁻¹, KH₂PO₄ 1.156 mg·L⁻¹, Na₂HPO₄·7H₂O 49.08 mg·L⁻¹), and trace elements (CuSO₄·5H₂O 0.025 mg·L⁻¹, NaSeO₄ 0.005 mg·L⁻¹, NiCl₂·6H₂O 0.019 mg·L⁻¹, CoCl₂·6H₂O 0.024 mg·L⁻¹, Na₂MoO₄·2H₂O 0.022 mg·L⁻¹, H₃BO₃ 0.001 mg·L⁻¹, ZnSO₄·7H₂O 0.043 mg·L⁻¹). Methanol was selected as the sole carbon source because the results of Chapter 3 demonstrated that methanol was the most preferred organic source for MnOB growth achieving the highest Mn(II)-oxidation rate compared with K-medium and sterilized activated sludge. The substrate was prepared with tap water in 20-L polypropylene tank and was purged with nitrogen gas before supplied to the reactors. Aerobic conditions of the reactors were maintained by continuously supplying the air to the reactors. The Mn(II) loading rates were set by controlling the hydraulic retention time (HRT) based on the sponge volumes and Mn(II) concentrations. The reactor operational conditions are shown in Table 4.1.

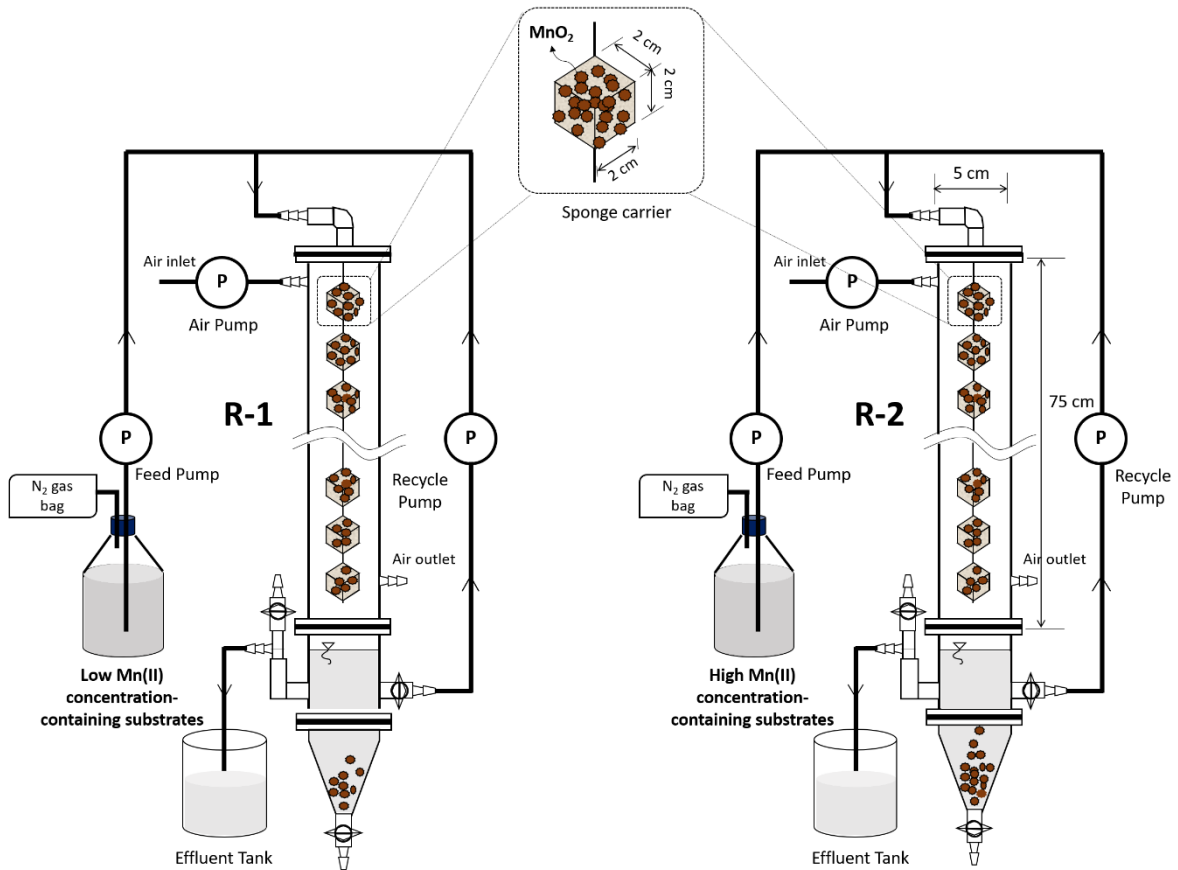


Figure 4.1 Configuration of the DHS reactors.

Table 4.1 Operational conditions of the DHS reactors.

Parameter	R-1			R-2		
	Phase 1 (0–38d)	Phase 2 (39–112d)	Phase 3 (113–210d)	Phase 1 (0–38d)	Phase 2 (39–112d)	Phase 3 (113–210d)
COD (mg·L ⁻¹)	5–50	5	5	5–50	5	5
Mn(II) (mg·L ⁻¹)	5	3–10	5–7.5	10–15	5	5–20
HRT (h)	0.36–3.8	0.4	0.2	0.2–3.8	0.4	0.4

4.2.2 Analytical methods

The samples were collected from the effluent of R-1 and R-2 two or times per week. The samples were filtered through a 0.45 μm membrane filter (Advantec, Tokyo, Japan). Mn(II) and Chemical Oxygen Demand (COD) concentrations were analyzed by the colorimetric method using a Hach DR2800 spectrophotometer (Hach Co., Loveland, CO, USA).

4.2.3 Microbial community analysis

Biomass samples were taken from the sponge carriers (the upper, middle and lower portions of the reactor) of R-1 and R-2 on days 112 and 210. A total of four biomass were analyzed for microbial community. DNA was extracted using FastDNA® SPIN Kit for Soil (MP188 Biomedicals, Ohio, USA) following manufacturer's instructions. DNA concentration was determined by Qubit fluorometer and the minimum concentration required for sequencing is 10 ng/uL. The DNA samples were sent to Hokkaido System Science Co. Ltd (Sapporo, Japan) for PCR amplification with a primer set of the V3-V4 region: 341F (5'-CCTACGGGGNGGCWGCAG-3') and 805R (5'-GGACTACHVGGGTATCTAATCC-3'), and sequenced using the Illumina MiSeq platform with a Miseq Reagent Kit v3 (Illumina Inc., San Diego, CA, USA).

The raw sequence data were trimmed to remove adapter sequences and primers from sequencing reads with the default minimum overlap length of 3 and the default maximum allowed error rate of 0.2 using the Cutadapt software (version 1.1) (Martin, 2011). Noise and low-quality sequence reads were removed by Trimmomatic (version 0.32) (Bolger et al., 2014) when the quality per base dropped below 20 bp in a sliding window of 20 bp (SLIDINGWINDOW:20:20) and the minimum length of the reads were below 50 bp (MINLEN:50). The clean reads were assembled using fastq-join software (version 1.1.2-537) (Aronesty, 2013) and analyzed using the QIIME pipeline software (version 1.8.0) (Caporaso, et al., 2010). The sequences having greater than 97% similarity were clustered into the same operational taxonomic units (OTUs) using the UCLUST method (Edgar R.C., 2010), which were subsequently classified using MiDAS taxonomy (version 1.20) (McIlroy et al., 2015).

4.2.4 Data analysis

Alpha-diversity indices in terms of Simpson's index of diversity (1-D), Shannon (H), Evenness and Chao-1 were calculated using PAST (PAleontological STatistics) 3.20 software to analyze the impact of residual Mn(II) on the microbial diversity of the reactor based on the OTUs (Hammer et al., 2001).

4.3 Results

4.3.1 Reactor performances

The performances of the reactor of R-1 and R-2 are shown in Fig. 4.2. In Phase 1, R-1 and R-2 was initially fed with Mn(II) at 5 and 10 mg L⁻¹, respectively. The results showed that Mn(II) could be completely oxidized in both reactors. Therefore, Mn(II) loading rate was increased by reducing the HRT of both reactors. At Mn(II) loading rate of 0.5 kg m⁻³ d⁻¹, both reactors could completely oxidize Mn(II). Mn(II) loading rate was kept at constant level, while Mn(II) loading rate in R-2 was elevated to 2 kg m⁻³ d⁻¹ by increasing Mn(II) concentration to 15 mg L⁻¹. At this condition, residual Mn(II) was observed in R-2. Even though Mn(II) loading rate was decreased to 1 kg m⁻³ d⁻¹, no Mn(II) removal was observed.

In Phase 2, Mn(II) concentration was gradually increased from 5 mg L⁻¹ to 10 mg L⁻¹ (Mn(II) loading rate = 0.33 – 0.6 kg m⁻³ d⁻¹) in R-1, while Mn(II) concentration in R-2 was set at 10 mg L⁻¹ (Mn(II) loading rate = 0.6 kg m⁻³ d⁻¹), which was lower than the last condition in Phase 1. As the results, Mn(II) removal performance of R-1 could be maintained, while no improvement on Mn(II) removal in R-2 was observed. Even both reactors were fed the same Mn(II) loading rate of 0.6 kg m⁻³ d⁻¹, the distinct Mn(II) oxidation ability between two reactors was obviously observed, in which R-1 could completely oxidize Mn(II), while R-2 could not. The loss of Mn(II)-oxidation ability of R-2 may due to inhibition by high residual Mn(II). In addition, declining pH was observed in R-1 along with an increase in Mn(II) removal rate, while in R-2, no Mn(II)-oxidation was observed, the pH did not change. Therefore, it can be concluded that the decreasing pH in R-1 was due to Mn(II)-oxidation activity.

In Phase 3, Mn loading rate of R-1 was kept at about 0.6 kg m⁻³ d⁻¹, while Mn loading rate of R-2 was reduced by half to be 0.25 kg m⁻³ d⁻¹ and then gradually increased to about 1.0 kg m⁻³ d⁻¹ (Mn(II) = 20 mg L⁻¹) during this phase. Interestingly, Mn(II)-oxidation ability of R-2 was observed at low Mn(II) loading rate after a period of long-time operation, in which Mn(II) could be completely oxidized. When Mn(II) loading rate was increased to 1.0 kg m⁻³ d⁻¹, Mn(II)-oxidation ability of R-2 gradually decreased. The maximum Mn(II)-oxidation rate of R-2 was 0.61 kg m⁻³ d⁻¹, which was lower than that of R-1 as 0.91 kg m⁻³ d⁻¹. These results indicated that Mn(II)-oxidation ability of R-2 was inhibited by residual Mn(II), and its Mn(II)-oxidation ability could be recovered if a lower Mn(II) loading rate was applied. Decreasing pH was also observed in R-2, as consequence of microbial Mn(II)-oxidation activity.

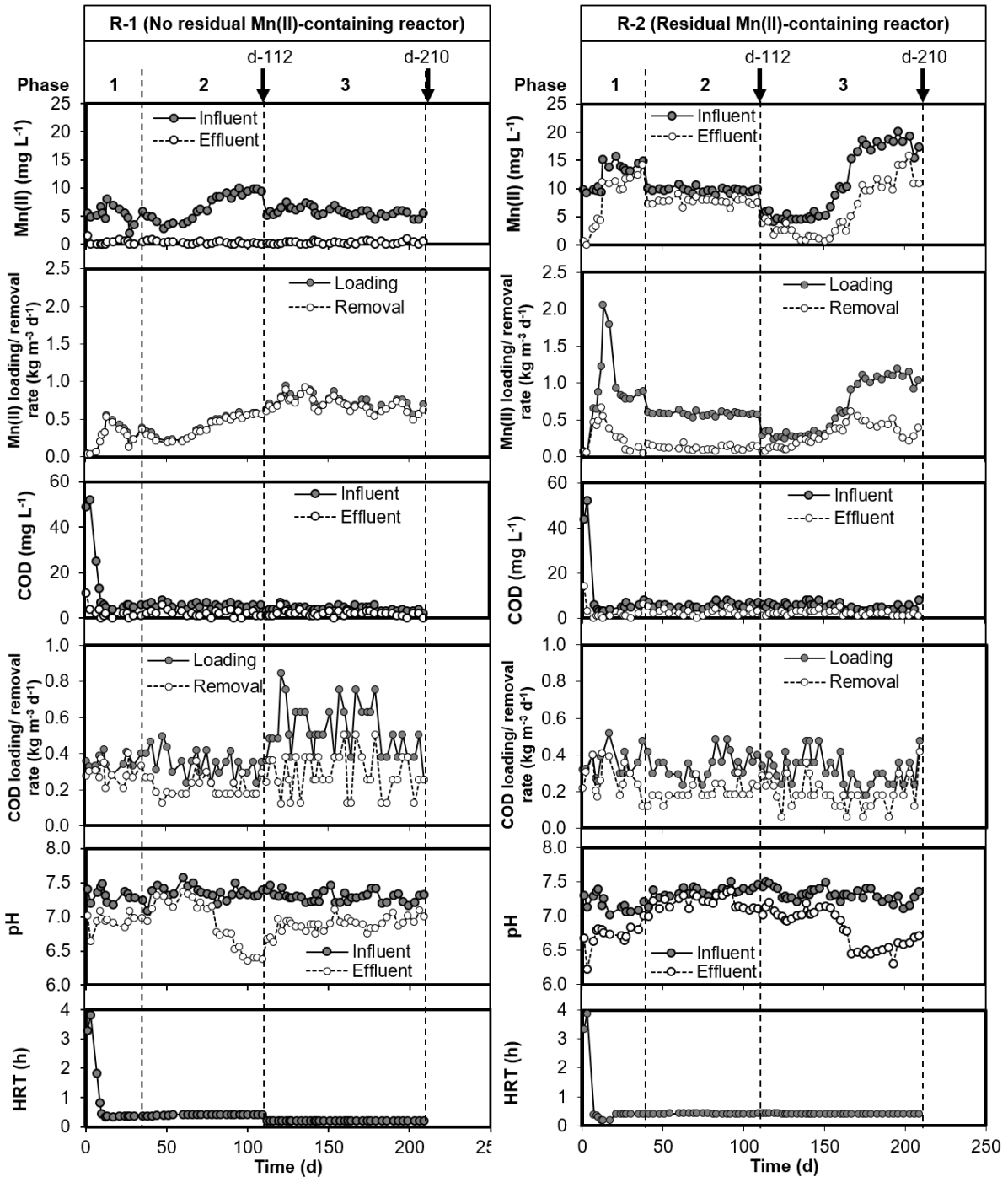


Figure 4.2 The performance of R-1 and R-2.

4.3.2 Microbial community

From the microbial community analysis of the four biomass samples, a total of more than 59,000 sequence reads were obtained, which were assigned to more than 2000 OTUs for each sample (Table 4.2). Microbial diversity was assessed by alpha-diversity indices of Simpson (1-D), Shannon (H), Evenness, and Chao-1 estimator (Table 4.2). generally, no remarkable

difference was found in comparisons between two reactors, suggesting that residual Mn(II) had little effect on the diversity of the microbial community.

Table 4.2 Sequence reads, total number of OTU and diversity of each sample

Sample	d-112_R1	d-112_R2	d-210_R1	d-210_R2
Total reads	63176	62750	63077	59873
Total OTU ¹⁾	2240	2097	2090	2077
Simpson (1-D) ²⁾	0.98	0.98	0.97	0.99
Shannon (H) ³⁾	5.18	5.22	4.91	5.11
Evenness ⁴⁾	0.079	0.088	0.065	0.079
Chao-1 ⁵⁾	5188	4770	4729	5741

¹⁾ Operational taxonomic units (OTUs) are defined as similarity thresholds of the 16S gene sequences at 97%.

²⁾ Simpson's index of diversity (1-D). A higher value indicates more diversity.

³⁾ Shannon (H) diversity index. A higher value indicates more diversity.

⁴⁾ Evenness. A higher value indicates more evenness.

⁵⁾ Chao-1. A higher value indicates a higher estimated richness.

The sequence reads having a relative abundance greater than 1% were identified into 15 phyla. There was little difference between four samples in term of microbial profile at the phylum level (Fig. 4.3), in which Proteobacteria was found to be the most dominant phylum in all samples. In R-1, the relative abundance of Acidobacteria, Chloroflexi, and Actinobacteria decreased, while Chlorobi and Bacteroidetes increased over the operation time. In R-2, even though dominant, the relative abundance of Bacteroidetes decreased, while Chloroflexi and Actinobacteria increased at day 210.

The identified genera, which had relative abundances greater than 3% of the total sequence reads, are shown in Figure 4.4. The widely known methanol-utilizing bacteria, such as *Hyphomicrobium*, *Methylibium*, *Methylobacterium* and *Methylophilus*, were detected in all reactors. Members of *Rhizobiales*, which have been found as methanol-degrading bacteria (Linz et al., 2018), were also detected at a high relative abundance. Methanol-utilizing bacteria are phylogenetically diverse and affiliate with Proteobacteria, Bacteroidetes, Verrucomicrobia, Actinobacteria and Firmicutes (Morawe et al., 2017). The relative abundance of methylotrophs seemed to be increase over the time. As expected, the microbial community was strongly influenced by methanol as the sole carbon source. Methylotrophs utilized methanol generating organic compounds that can be utilized as nutrient sources by other predominant bacteria resulting in the high relative abundance.

Phylum	d-112_R1	d-112_R2	d-210_R1	d-210_R2
Acidobacteria	9.5%	3.5%	6.5%	4.9%
Actinobacteria	7.7%	6.9%	4.6%	9.3%
Armatimonadetes	3.6%	9.4%	2.9%	2.4%
Bacteroidetes	5.2%	16.0%	8.3%	7.6%
Chlamydiae	5.1%	2.6%	3.6%	2.2%
Chlorobi	0.8%	1.6%	10.7%	5.5%
Chloroflexi	8.1%	7.8%	5.0%	9.5%
Cyanobacteria	1.2%	1.3%	0.9%	1.3%
Gemmatimonadetes	0.9%	1.1%	0.2%	2.2%
Nitrospirae	1.1%	1.8%	2.0%	3.3%
Planctomycetes	5.9%	5.4%	6.1%	4.1%
Proteobacteria	38.5%	32.3%	36.2%	33.3%
Saccharibacteria	2.2%	1.2%	7.3%	4.3%
Verrucomicrobia	1.1%	2.1%	1.0%	2.2%
WCHB1-60	0.5%	1.3%	0.0%	0.4%
Others	4.5%	3.4%	2.1%	2.8%
Unassigned	4.3%	2.5%	2.5%	4.8%

Figure 4.3 Microbial community at the phyla level. Phyla with relative abundance <1% were classified as “Others”.

Both reactors demonstrated the Mn(II) removal ability, which indicated that certain MnOB community exist and played an important role in the Mn(II)-oxidation in both reactors. The “putative” MnOB which had relative abundances greater than 1% of the total sequence reads, are shown in Figure 4.4. It should be noted that identification of putative MnOB was based on the strains that previously reported as MnOB, and not all strains belonging to putative MnOB are able to oxidize Mn(II). Only three MnOB were detected including *Mycobacterium*, *Nocardia*, and *Hyphomicrobium* with total relative abundance of 6–9% of the total bacteria. The higher relative abundance of *Hyphomicrobium* in R-1 than R-2 indicated that this strain may be inhibited by high residual Mn(II) in R-2.

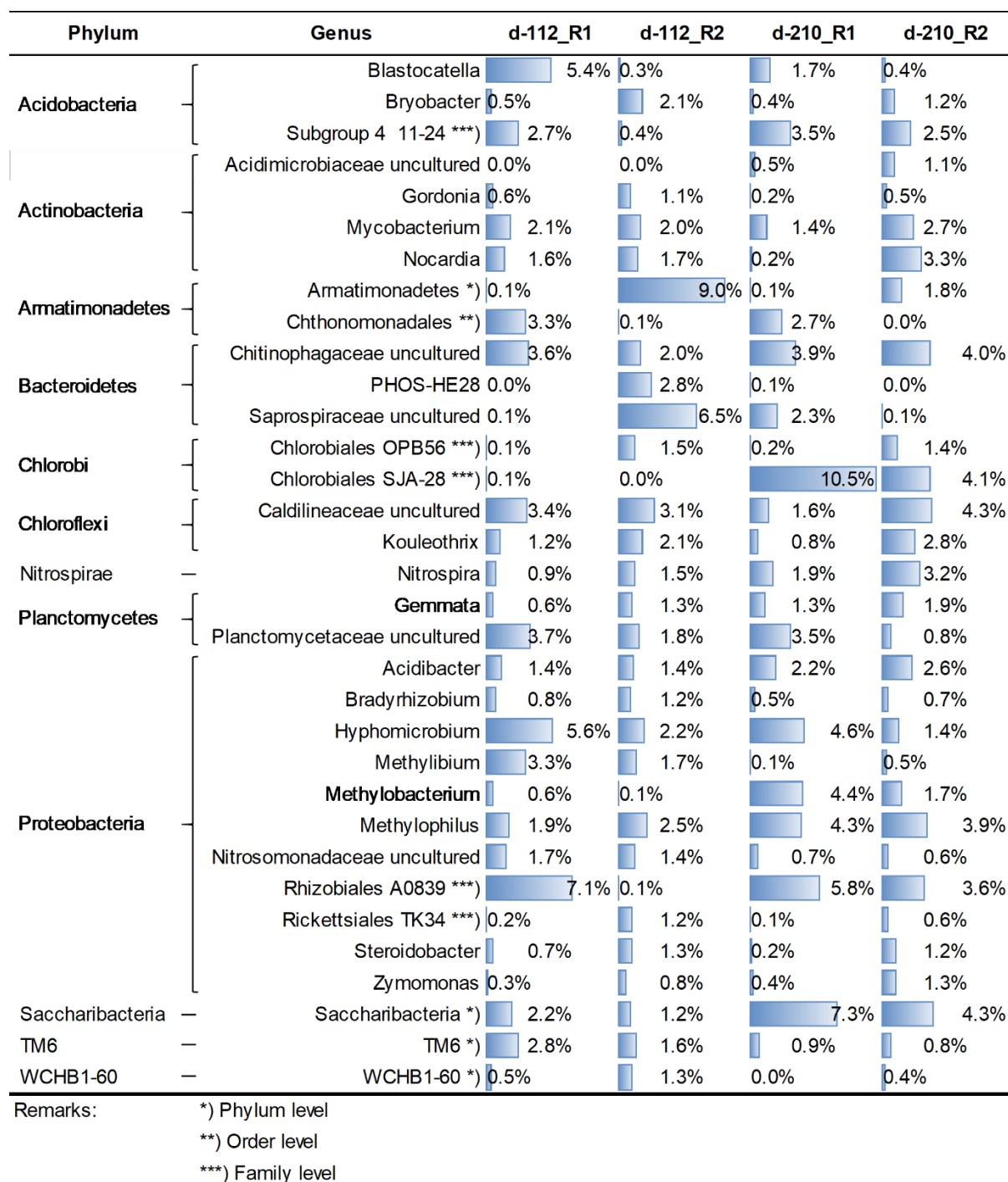


Figure 4.4 Most dominant genera in the reactors with relative abundance >1% of the total sequence reads in each sample.

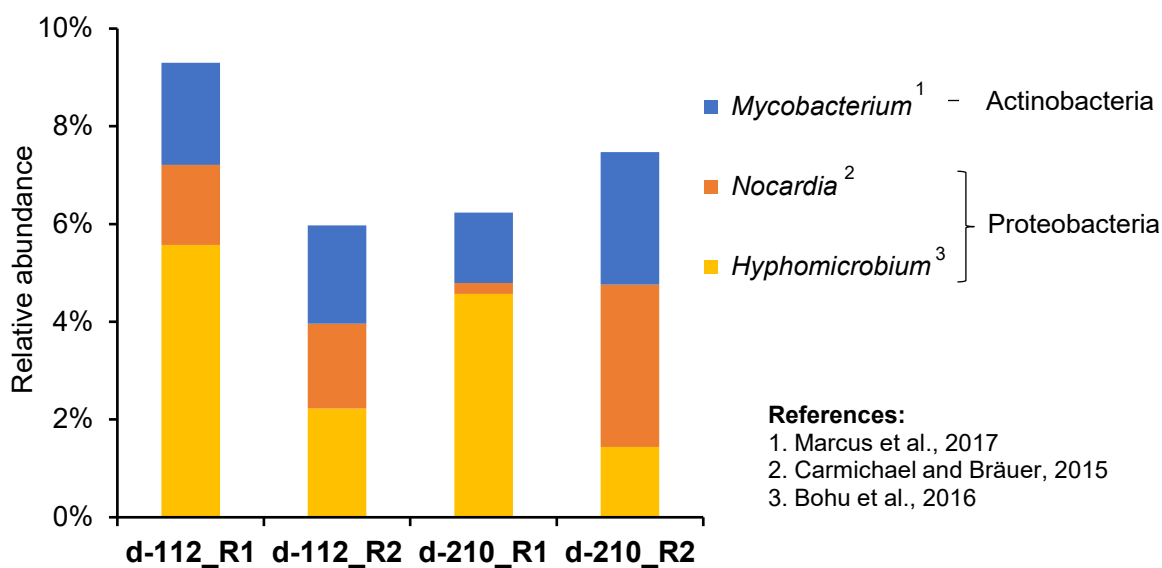


Figure 4.5 Relative abundance of putative manganese-oxidizing bacteria with relative abundance greater than 1%.

4.4 Discussion

This study demonstrated that residual Mn(II) in the reactor R-2 was found to inhibit Mn(II) oxidation activity of microorganisms led to the declining Mn(II) oxidation performance. The reactor R-2 was able to completely oxidize Mn(II) at low Mn(II) loading ($< 0.61 \text{ kg m}^{-3} \text{ d}^{-1}$), however, if a higher Mn(II) loading was applied, Mn(II) was only partially oxidized resulted in the residual Mn(II) in the reactor R-2. In Phase 2, Even though R-2 was supplied by the same Mn(II) loading rate as that R-1, no Mn(II) removal was observed in R-2, but completely oxidized in R-1. Based on the results from Figure 4.2, the relationships between residual Mn(II) and Mn(II) oxidation performance can be drawn in the Figure 4.6. The Mn(II) oxidation performance of R-1 was higher than those R-2. The higher Mn(II)-oxidation can be achieved if residual Mn(II) is kept at low concentration, while the high residual Mn(II) concentrations adversely affect the Mn(II) oxidation performances. Mn(II) have been shown to possess toxic effects to some microbial strains (Jiang et al., 2010; Zhao et al., 2018). In addition, Tu et al. (2014) found that the high initial Mn(II) concentration not only inhibits the growth of *Pseudomonas* sp. G7, but also decreases the formation of bio-MnO_x.

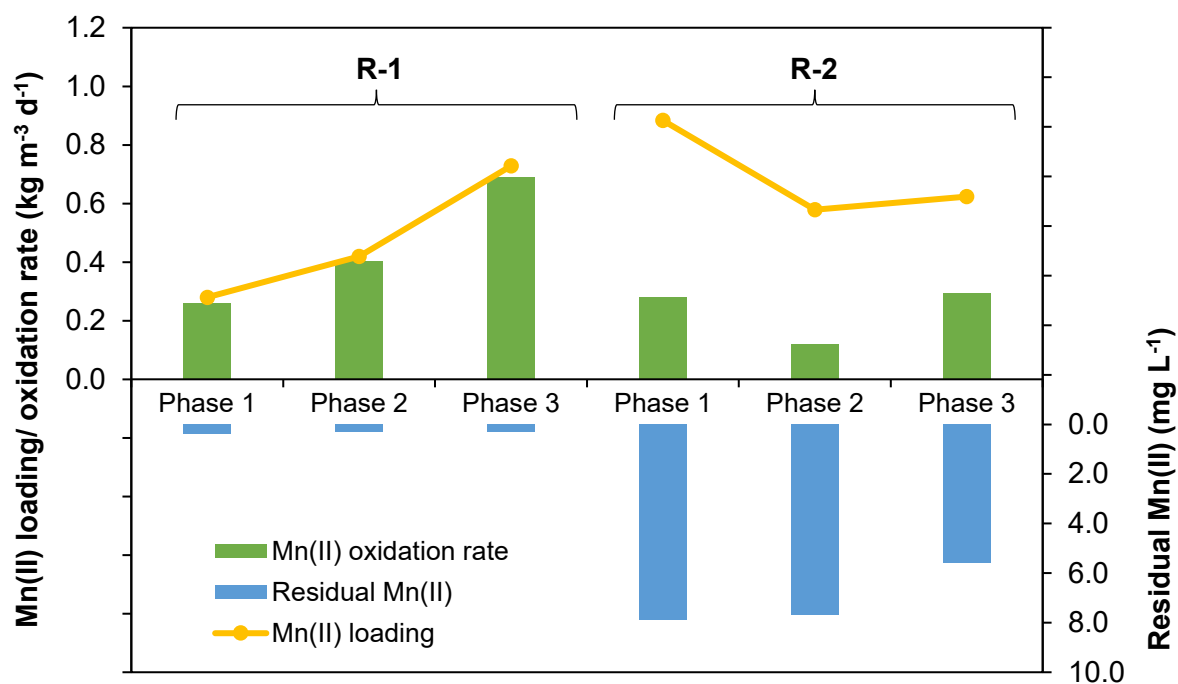


Figure 4.6 Relationship between Mn(II) oxidation performance and residual Mn(II) concentration at each phase.

The results of Phase 1 demonstrated that, R- 2 initially could completely oxidize Mn(II) at low Mn(II) loading ($< 0.61 \text{ kg m}^{-3} \text{ d}^{-1}$), however, when Mn(II) loading was remarkably increased ($2 \text{ kg m}^{-3} \text{ d}^{-1}$), MnOB were unable to fully oxidize Mn(II), resulting in the high concentration of residual Mn(II). Mn(II)-oxidation activity by microorganism is a protection mechanism against toxic environments, such as heavy metal, reactive oxygen species, and UV light (Tebo et al., 2005). Several environmental factors, such as pH, temperature, initial Mn(II) concentration, and dissolved oxygen, could affect microbial Mn(II) oxidation activity (Paccini et al., 2005; Jiang et al., 2010; Zhao et al., 2018). In addition, MnOB is suppressed lead to the lost their ability to oxidize Mn(II) in the presence of environmental stressors, for example, a microbial manganese-oxidizing strain, *Arthrobacter* sp. NI-2, was not able to oxidize Mn(II) under low temperature condition (Nakayama et al., 2019). In this study, high Mn(II) loading rate may induce MnOB stress led to the decreasing Mn(II) oxidation ability. When Mn(II) loading rate, the stressor, was reduced, for example in Phase 3, Mn(II) oxidation ability of R-2 can be recovered.

Microbial analysis results revealed that among detected putative MnOB, *Hyphomicrobium*, that affiliated with methanol-utilizing bacteria were found to be the predominant in this study. This result in agreement with the results of Chapter 3 that

Hyphomicrobium was detected as the predominant MnOB in the methanol-fed reactor. Mn(II)-oxidation of the reactor corresponded to the relative abundance of *Hyphomicrobium*. R-1 that had a higher Mn(II)-oxidation rate possessed higher relative abundance of *Hyphomicrobium* than R-2, that have lower Mn(II)-oxidation ability. In addition to *Hyphomicrobium*, increasing *Mycobacterium* and *Nocardia* indicated that these strains were more resistant to high Mn(II) concentration than *Hyphomicrobium*.

4.5 Conclusions

This study demonstrated the effect of residual Mn(II) concentration on the Mn(II)-oxidation performance of the reactors. High Mn(II)-oxidation can be achieved if residual Mn(II) concentration was kept at low levels. High concentration of residual Mn(II) caused adversely effects on the Mn(II)-oxidation performances. Microbial analysis revealed that the relative abundance of the predominant putative MnOB, *Hyphomicrobium*, corresponded to the Mn(II) oxidation ability of the reactors, and this genus was obviously inhibited by high residual Mn(II) exposure. This study provided useful information on application of Mn-oxidation bioreactor in practical level, where to achieve high Mn(II) oxidation performance, the residual Mn(II) concentration should be kept at low level.

References

- Aragón, C., Coello, M.D., Quiroga, J.M., 2010. Effect of manganese(II) on the respiratory activity of biological sludge from wastewater treatment plant. *Chem. Eng. Res. Des.* 88, 641–646. <https://doi.org/10.1016/j.cherd.2009.10.006>
- Aronesty, E., 2013. Comparison of sequencing utility programs. *Open Bioinforma. J.* 7, 1–8. <https://doi.org/10.2174/1875036201307010001>
- Barboza, N.R., Morais, M.M.C.A., Queiroz, P.S., Amorim, S.S., Guerra-Sá, R., Leão, V.A., 2017. High manganese tolerance and biooxidation ability of *Serratia marcescens* Isolated from manganese mine Water in Minas Gerais, Brazil. *Front. Microbiol.* 8, 1–11. <https://doi.org/10.3389/fmicb.2017.01946>
- Bohu, T., Akob, D.M., Abratis, M., Lazar, C.S., 2016. Biological low-pH Mn(II) oxidation in a manganese deposit influenced by metal-rich groundwater. *Appl. Environ. Microbiol.* 82, 3009–3021. <https://doi.org/10.1128/AEM.03844-15>
- Bolger, A.M., Lohse, M., Usadel, B., 2014. Trimmomatic: A flexible trimmer for Illumina sequence data. *Bioinformatics* 30, 2114–2120. <https://doi.org/10.1093/bioinformatics/btu170>

- Cabrera, G., Pérez, R., Gómez, J.M., Ábalos, A., Cantero, D., 2006. Toxic effects of dissolved heavy metals on *Desulfovibrio vulgaris* and *Desulfovibrio* sp. strains. *J. Hazard. Mater.* 135, 40–46. <https://doi.org/10.1016/j.jhazmat.2005.11.058>
- Caporaso, J.G., Kuczynski, J., Stombaugh, J., Bittinger, K., Bushman, F.D., Costello, E.K., Fierer, N., Peña, A.G., Goodrich, K., Gordon, J.I., Huttley, G.A., Kelley, S.T., Knights, D., Jeremy, E., Ley, R.E., Lozupone, C.A., McDonald, D., Muegge, B.D., Reeder, J., Sevinsky, J.R., Turnbaugh, P.J., Walters, W.A., 2010. QIIME allows analysis of high-throughput community sequencing data. *Nat Methods* 7(5): 335–336. <https://doi.org/10.1038/nmeth.f.303>.
- Carmichael S.K. and Bräuer S.L., 2015. Microbial diversity and manganese cycling: A review of manganese-oxidizing microbial cave communities, in: Engel A.S. (Ed.), *Microbial life of cave systems. life in extreme environments*. Walter de Gruyter GmbH & Co KG, Boston, MA, pp. 137–160. <https://doi.org/10.1515/9783110339888-009>
- Cheung, H.Y., Vitkovič, L., Brown, M.R.W., 1982. Toxic effect of manganese on growth and sporulation of *Bacillus stearothermophilus*. *J. Gen. Microbiol.* 128, 2395–2402. <https://doi.org/10.1099/00221287-128-10-2395>
- Edgar, R.C., 2010. Search and clustering orders of magnitude faster than BLAST. *Bioinformatics* 26, 2460–2461. <https://doi.org/10.1093/bioinformatics/btq461>
- Hohle, T.H., O’Brian, M.R., 2014. Magnesium-dependent processes are targets of bacterial manganese toxicity. *Mol. Microbiol.* 93, 736–747. <https://doi.org/10.1111/mmi.12687>
- Huang, H., Zhao, Y., Xu, Z., Ding, Y., Zhang, W., Wu, L., 2018. Biosorption characteristics of a highly Mn(II) resistant *Ralstonia pickettii* strain isolated from Mn ore. *PLoS One* 13, 1–17. <https://doi.org/10.1371/journal.pone.0203285>
- Jiang, S., Kim, D.-G., Kim, J.-H., Ko, S.-O., 2010. Characterization of the biogenic manganese oxides produced by *Pseudomonas putida* strain MnB1. *Environ. Eng. Res.* 15, 183–190. <https://doi.org/10.4491/eer.2010.15.4.183>
- Marcus, D.N., Pinto, A., Anantharaman, K., Ruberg, S.A., Kramer, E.L., Raskin, L., Dick, G.J., 2017. Diverse manganese(II)-oxidizing bacteria are prevalent in drinking water systems. *Environ. Microbiol. Rep.* 9, 120–128. <https://doi.org/10.1111/1758-2229.12508>
- Martin, M., 2011. Cutadapt removes adapter sequences from high-throughput sequencing reads. *EMBnet.journal* 17, 10–12. <https://doi.org/10.14806/ej.17.1.200>.
- McIlroy, S.J., Saunders, A.M., Albertsen, M., Nierychlo, M., McIlroy, B., Hansen, A.A., Karst, S.M., Nielsen, J.L., Nielsen, P.H., 2015. MiDAS: the field guide to the microbes of activated sludge. *Database* 2015, bav062. <https://doi.org/10.1093/database/bav062>
- Murray, K.J., Tebo, B.M., 2007. Cr(III) is indirectly oxidized by the Mn(II)-oxidizing bacterium *Bacillus* sp. strain SG-1. *Environ. Sci. Technol.* 41, 528–533. <https://doi.org/10.1021/es0615167>
- O’Neal, S.L., Zheng, W., 2015. Manganese toxicity upon overexposure: a Decade in review. *Curr. Environ. Heal. reports* 2, 315–328. <https://doi.org/10.1007/s40572-015-0056-x>
- Pacini, V.A., Ingallinella, A.M., Sanguinetti, G., 2005. Removal of iron and manganese using biological roughing up flow filtration technology. *Water Res.* 39, 4463–4475. <https://doi.org/10.1016/j.watres.2005.08.027>
- Santos, E.F., Kondo Santini, J.M., Paixão, A.P., Júnior, E.F., Lavres, J., Campos, M., Reis, A.R. dos, 2017. Physiological highlights of manganese toxicity symptoms in soybean

- plants: Mn toxicity responses. *Plant Physiol. Biochem.* 113, 6–19.
<https://doi.org/10.1016/j.plaphy.2017.01.022>
- Tebo, B.M., Emerson, S., 1986. Microbial manganese(II) oxidation in the marine environment: a quantitative study. *Biogeochemistry* 2, 149–161.
<https://doi.org/10.1007/BF02180192>
- Tebo, B.M., Johnson, H.A., McCarthy, J.K., Templeton, A.S., 2005. Geomicrobiology of manganese(II) oxidation. *Trends Microbiol.* 13, 421–428.
<https://doi.org/10.1016/j.tim.2005.07.009>
- Tu, J., Yang, Z., Hu, C., Qu, J., 2014. Characterization and reactivity of biogenic manganese oxides for ciprofloxacin oxidation. *J. Environ. Sci. (China)* 26, 1154–1161.
[https://doi.org/10.1016/S1001-0742\(13\)60505-7](https://doi.org/10.1016/S1001-0742(13)60505-7)
- Zhao, X., Wang, X., Liu, B., Xie, G., Xing, D., 2018. Characterization of manganese oxidation by *Brevibacillus* at different ecological conditions. *Chemosphere* 205, 553–558. <https://doi.org/10.1016/j.chemosphere.2018.04.130>

Chapter 5: Aerobic decolorization of Acid Orange 7 (AO7) dye coupled with Mn(II) oxidation

Abstract

This study investigated decolorization of azo dye coupled with Mn(II) oxidation under aerobic conditions. The enrichment of MnOB was enhanced in the installed abiotic-MnO₂ reactor, achieving higher Mn(II) removal compared with the devoid of abiotic-MnO₂ reactor. When sodium acetate was supplemented to keep pH at neutral, enhancement of decolorization of AO7 was observed along with increasing Mn(II) oxidation activity in the abiotic-MnO₂ containing reactor, however decolorization performance suddenly decreased when sodium acetate concentration was elevated. It remained unclear whether the decreasing decolorization performance was caused by increasing sodium acetate concentration or high Mn(II) oxidation activity and the high abundance of generated bio-MnO_x which may be toxic to dye-decolorizing bacteria. Microbial community analysis revealed that putative MnOB enriched in the abiotic-MnO₂-containing reactor, and the isolates of this reactor have shown Mn(II) oxidation ability but no AO7 removal ability. MnOB and Mn(II) oxidation activity had less effect on the AO7 removal. In addition, when sodium acetate was supplied, the abiotic-MnO₂-containing reactor was more efficient to decompose organic substances than the devoid of abiotic-MnO₂ reactor. Thus, Mn(II) oxidation could enhance degradation of organic substances other than azo dye.

Keywords: Azo dye, decolorization, abiotic-MnO₂, biological manganese oxidation, manganese-oxidizing bacteria, sodium acetate

5.1 Introduction

Dye is one of the problem contaminants in textile wastewater due to their stable and resist under environmental conditions. Most of dyes are non-biodegradable due to their synthetic nature and structure mainly aromatic. Moreover, various dyes have carcinogenic or causing adverse health effects on human (Rawat et al., 2016). Previous studies reported that chemical methods, such as adsorption, electrochemical with catalyst and advanced oxidation by electro-fenton have been successfully applied to treat an azo dye compound, acid orange 7 (AO7) (Cai et al., 2014; Elizalde-González and Hernández-Montoya, 2009; Özcan et al., 2009). In this study, the author employed biological process which has several significant advantages, such as, low initial cost, do not require chemical consumption, less sludge and secondary pollutant generation.

Biological decolorization of AO7 by microbial strain in pure culture (Mutafov et al., 2007) and mixed cultures batch test (Bay et al., 2014), as well as using a specific electrogenic

microorganism in bioelectrochemical system (Gao et al., 2016), or continuous bioreactor system (Coughlin et al., 2003), have been widely reported in previous studies. However, decolorization of AO7 using manganese oxidizing bacteria (MnOB) has never been investigated yet. MnOB are able to oxidize soluble Mn(II) generating insoluble Mn(III/IV) or biogenic manganese oxide (bio-MnO_x), and play important role in the redox cycling of manganese in the environment (Spiro et al., 2010). Bio-MnO_x has attracted attention for its potential application in environmental remediation through adsorption of inorganic contaminant because it has a high surface area (Wang et al., 2009; Watanabe et al., 2013), and also capable of oxidizing various organic pollutants, such as pharmaceutical products (Forrez et al., 2010; Forrez et al., 2011; Furgal et al., 2014; Zhang et al., 2015). Removal of organic pollutant can be through oxidation by biogenic manganese oxides generating Mn(II) and intermediate products. Wu et al. (2017) found semicarbazide as intermediate product of 1,2,4-triazole degradation by biogenic manganese oxides in biofilter reactor.

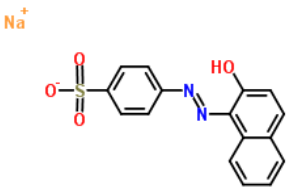
The present study aims to investigate performance of enriched MnOB in DHS reactor for decolorization of AO7. This is first report on the application of manganese oxidizing bacteria and biogenic manganese oxides for decolorization of dye. The effect of initially added abiotic-MnO₂ in the sponge media was investigated whether could accelerate MnOB enrichment or not, was also investigated. Isolation of dye-decolorizing bacteria from the reactor and microbial structure analysis were performed to identify bacteria which contribute to the decolorization of dye and oxidation of Mn(II) in the reactor. Microbial community analysis was also conducted to characterize microbial profiles of the reactors.

5.2 Materials and methods

5.2.1 Chemicals and reagents

Peptone, yeast extract and agar powder were purchased from Wako Chemical Ltd. (Tokyo, Japan). Abiotic-MnO₂ was purchased from Kishida Chemical Co. Ltd., (Tokyo, Japan). A single dye compound Acid Orange 7 (AO7) obtained from Nacalai Tesque, Japan, was used as the model in this study. The physico-chemical properties of AO7 were given in Table 5.1 as follows.

Table 5.1 Physico-chemical properties of Acid Orange 7 (AO7)

Chemical structure	Parameter	Value
 <p>Orange II (Acid Orange 7)</p>	CAS	000573-89-7
	Molecular Formula	C ₁₆ H ₁₁ N ₂ NaO ₄ S
	Average mass	328.35
	Water solubility	50000 mg/L
	Log P (oct-water)	2.35
	Henry's Law Constant	7.01.10 ⁻¹² atm-m ³ /mol

Source: SRC PhysProp Database <http://esc.srcinc.com/fatepointer/search.asp/>

5.2.2 Batch decolorization of AO7 by abiotic-MnO₂

Abiotic-MnO₂ (Kishida Chemical Co. Ltd., Japan) (0.1 – 0.5 mg) was placed to 50 mL of a solution of AO7 (10 – 500 mg/L) in a glass tube with a parafilm-covered screw cap. The tube was shaken in a horizontal shaker (MMS-1, EYELA, Tokyo, Japan) at 120 rpm and room temperature in the dark condition. The liquid was sampled at predetermined time intervals and the AO7 concentration was determined.

5.2.3 Synthetic dye-containing wastewater

A synthetic wastewater medium containing AO7 was designed to simulate textile wastewater. The substrate consists of AO7, Mn (II) (MnCl₂.4H₂O), K-medium ((made of peptone casein (Nacalai Tesque Inc., Kyoto, Japan) and extract yeast dried (Nacalai Tesque Inc., Kyoto, Japan) (4:1, w/w)), phosphate buffer (KH₂PO₄ (0.602 mg L⁻¹), and Na₂HPO₄ (6.22 mg L⁻¹)), Mn(II) (MnCl₂.4H₂O), minerals (CaCl₂.2H₂O (0.05 mg L⁻¹), MgSO₄.7H₂O (0.2 mg L⁻¹), Fe₂SO₄.5H₂O (0.1 mg L⁻¹)), and trace elements (CuSO₄.5H₂O (0.025 mg L⁻¹), NaSeO₄ (0.005 mg L⁻¹), NiCl₂.6H₂O (0.019 mg L⁻¹), CoCl₂.6H₂O (0.024 mg L⁻¹), Na₂MoO₄.2H₂O (0.022 mg L⁻¹), H₃BO₃ (0.001 mg L⁻¹), ZnSO₄.7H₂O (0.043 mg L⁻¹)). The substrate tank was purged with nitrogen and connected to a nitrogen-filled gas bag during the experiment.

5.2.4 Reactor configurations and operational conditions

Two identical cylindrical DHS reactors with size of 45 cm in height and 5 cm in diameter were set up (Fig. 5.1). The reactor was filled with 10 polyurethane sponge cubes (2 x 2 x 2 cm) which were connected diagonally in series to each other. The sponge media of the first reactor (R-3), as a control, were inoculated with activated sludge taken from aeration tank of municipal

sewage treatment plant in Higashihiroshima, Japan, while the sponge media of another reactor (R-4) were inoculated using suspension of 50 g abiotic-MnO₂ (Kishida Chemical Co. Ltd., Japan) in 500 mL activated sludge taken from the same source for inoculation of R-3. Commercial abiotic-MnO₂ was used to enhance MnOB growth. The reactors were placed in dark and temperature-controlled room at 26 °C. The air was supplied to the reactors at flowrate of 2.6 L h⁻¹ to maintain dissolved oxygen concentration above 7 mg L⁻¹. The reactors were placed in a controlled room at 26 °C and dark condition to avoid the decomposition of AO7 by effect of light. The operational conditions of the reactor were provided in detail in Table 5.2 as follows.

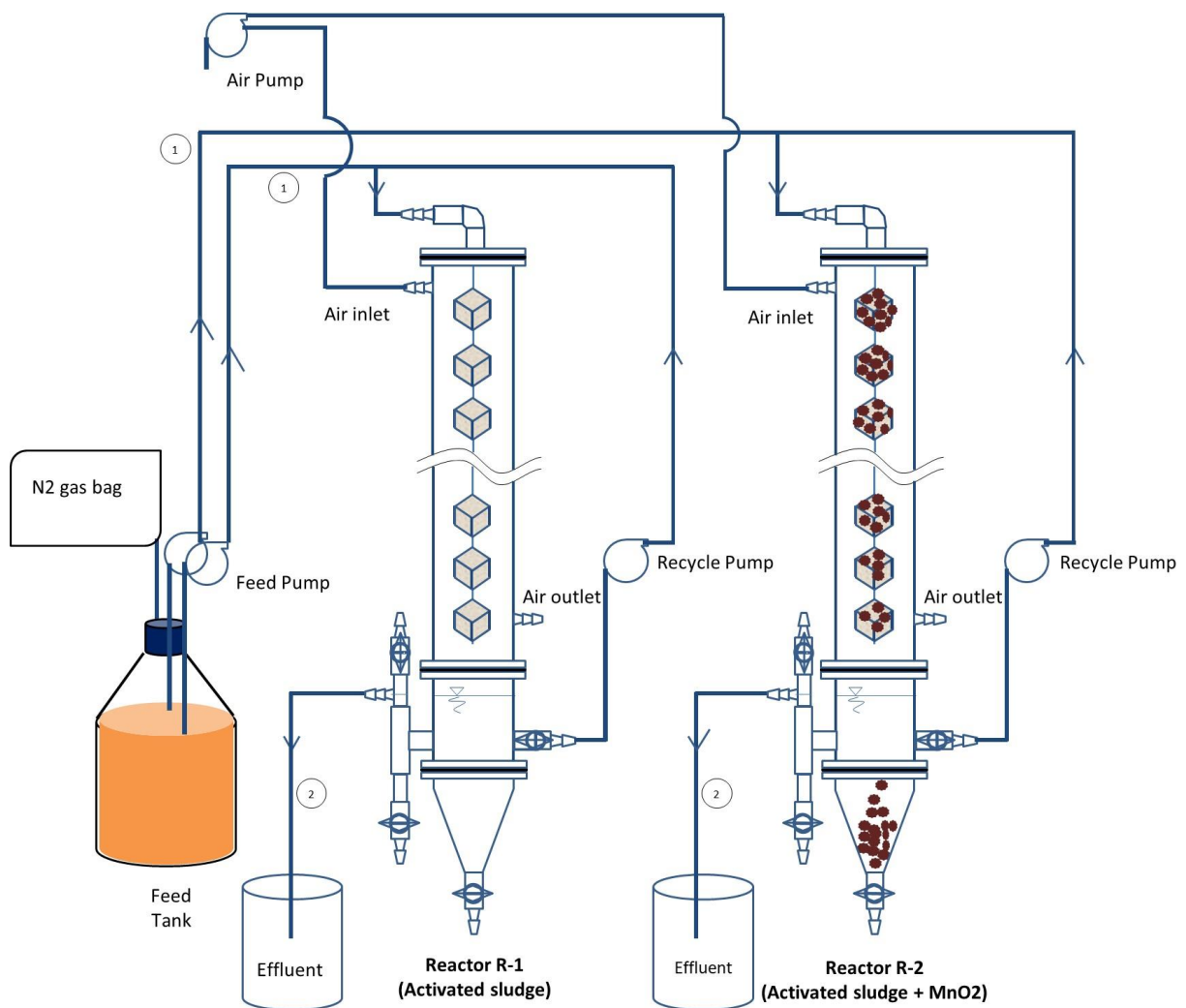


Figure 5.1 DHS reactor configurations.

Table 5.2. Reactor operational conditions

STAGE 1										
Phase	Phase 1	Phase 2	Phase 3	Phase 4	Phase 5	Phase 6	Phase 7	Phase 8	Phase 9	Phase 10
Period (day)	0-11	12 -18	19 -25	26 -32	33- 37	38-39	40-46	47-55	56-57	58-67
AO7 (mg/L)	-	10	10	10	10	10	10	10	10	10
Mn (II) (mg/L)	5	5	7.5	7.5	10	10	10	10	10	10
Organic										
Yeast extract	20	20	20	40	40	40	20	20	20	20
Peptone	5	5	5	10	10	10	5	5	5	5
Phosphate Buffer	0.2mM	0.2mM	0.2mM	0.2mM	0.2mM	0.4mM	0.4mM	0.2mM	0.2mM	0.2mM
KH ₂ PO ₄ (mg/L)	1.156	1.156	1.156	1.156	1.156	2.312	2.312	1.442		1.442
Na ₂ HPO ₄ ·7H ₂ O (mg/L)	49.08	49.08	49.08	49.08	49.08	98.16	98.16			
Na ₂ HPO ₄ (mg/L)								26.09	85.23	28.41
Q (L/d)	0.79	0.79	0.79	0.79	0.79	0.79	0.79	0.79	0.79	0.79
HRT (h)	2.4	2.4	2.4	2.4	2.4	2.4	2.4	2.4	2.4	2.4
ART (h)	0.4	0.4	0.4	0.3	0.3	0.3	0.3	0.3	0.3	0.3

Table 5.2. (continued)

STAGE 1									
Phase	Phase 11	Phase 12	Phase 13	Phase 14	Phase 15	Phase 16	Phase 17	Phase 18	Phase 19
Period (day)	68-85	85-88	89-99	100-101	102-113	114-116	116-123	124-131	132-151
AO7 (mg/L)	10	10	10	10	10	10	10	10	10
Mn (II) (mg/L)	12	12	7.5	7.5	10	10	12	10	7.5
Organic									
Yeast extract	20	20	20	20	20	20	20	40	40
Peptone	5	5	5	5	5	5	5	10	10
Phosphate Buffer pH=8	0.2mM	pH=7.8 0.2mM	pH=7.8 0.2mM	pH=7.8 0.2mM	pH=7.8 0.2mM	pH=7.8 0.2mM			
KH ₂ PO ₄ (mg/L)	1.442	1.205	1.205	1.205	1.205	1.205	pH=7.8 0.2mM		
Na ₂ HPO ₄ ·7H ₂ O (mg/L)							1.205	1.205	1.205
Na ₂ HPO ₄ (mg/L)	28.41	12.44	12.44	12.44	12.44	12.44			
Na ₂ CO ₃ 1mM → pH=8			0.04mM				12.44	12.44	12.44
NaOH				0.05mM	0.05mM		0.79	0.79	0.79
Q (L/d)	0.79	0.79	0.79	0.79	0.79	0.79	2.4	2.4	2.4
HRT (h)	2.4	2.4	2.4	2.4	2.4	2.4	0.3	0.3	0.3
ART (h)	0.3	0.3	0.3	0.3	0.3	0.3			

Table 5.2. (continued)

STAGE 2									
Phase	Phase 20	Phase 21	Phase 22	Phase 23	Phase 24	Phase 25	Phase 26	Phase 27	Phase 28
Period (day)	152-158	159-165	166-173	174-181	182-193	194-197	198-205	206-211	212-215
AO7 (mg/L)	10	10	10	10	10	10	10	10	10
Mn (II) (mg/L)	7.5	10	12	15	18	18	20	20	20
Organic (mg/L)									
Yeast extract	5	5	5	5	5	5	3.4	7.5	3.4
Peptone	20	20	20	20	20	20	13.6	30	13.6
Sodium acetate	32	32	32	32	32	64	42.24	48	42.24
COD value (ratio)	50 (1:1)	50 (1:1)	50 (1:1)	50 (1:1)	50 (1:1)	75 (1:2)	50 (1:2)	75 (1:1)	50 (1:2)
Phosphate Buffer									
KH ₂ PO ₄ (mg/L)	1.205	0.602	0.602	0.602	0.602	0.602	0.602	0.602	0.602
Na ₂ HPO ₄ (mg/L)	12.44	6.22	6.22	6.22	6.22	6.22	6.22	6.22	6.22
Q (L/d)	0.79	0.79	0.79	0.79	0.79	0.79	0.79	0.79	0.79
HRT (h)	2.4	2.4	2.4	2.4	2.4	2.4	2.4	2.4	2.4
ART (h)	0.3	0.3	0.3	0.3	0.3	0.3	0.3	0.3	0.3

Table 5.2. (continued)

STAGE 2					
Phase	Phase 29	Phase 30	Phase 31	Phase 32	Phase 33
Period (day)	216-220	221-228	229-242	243-258	259-277
AO7 (mg/L)	10	10	10	10	10
Mn (II) (mg/L)	22	24	12	15	0
Organic (mg/L)					
Yeast extract	3.4	2	5	5	5
Peptone	13.6	8	20	20	20
Sodium acetate	42.24	51.2	32	32	32
COD value (ratio)	50 (1:2)	50 (1:4)	50 (1:1)	50 (1:1)	50 (1:1)
Phosphate Buffer					
KH ₂ PO ₄ (mg/L)	0.602	0.602	0.602	0.602	0.602
Na ₂ HPO ₄ (mg/L)	6.22	6.22	6.22	6.22	6.22
Q (L/d)	0.79	0.79	0.79	0.79	0.79
HRT (h)	2.4	2.4	2.4	2.4	2.4
ART (h)	0.3	0.3	0.3	0.3	0.3

Table 5.2. (continued)

STAGE 3					
Phase	Phase 34	Phase 35	Phase 36	Phase 37	Phase 38
Period (day)	278-312	313-326	327-347	348-354	355-368
AO7 (mg/L)	10	10	5	5	10
Mn (II) (mg/L)	0	5	2.5	5	5 (R4)
Organic (mg/L)					0 (R3)
Yeast extract	10	10	5	5	5
Peptone	40	40	20	20	20
Sodium acetate	-	-	-	-	-
COD value (ratio)	50 (1:0)	50 (1:0)	25 (1:0)	25 (1:0)	25 (1:0)
Phosphate Buffer					
KH ₂ PO ₄ (mg/L)	0.602	0.602	0.602	0.602	0.602
Na ₂ HPO ₄ (mg/L)	6.22	6.22	6.22	6.22	6.22
Q (L/d)	0.79	0.79	1.44	1.44	1.44
HRT (h)	2.4	2.4	1.2	1.2	1.2
ART (h)	0.3	0.3	0.3	0.3	0.3

Table 5.2. (continued)

STAGE 4						
Phase	Phase 39	Phase 40	Phase 41	Phase 42	Phase 43	Phase 44
Period (day)	369-384	385-396	397-404	405-410	411-424	425-431
AO7 (mg/L)	10	10	10	10	10	10
Mn (II) (mg/L)	5 (R4)	10 (R4)	15 (R4)	15 (R4)	15	15
	0 (R3)	0 (R3)	0 (R3)	0 (R3)		
Organic (mg/L)						
Yeast extract	2.5	5	5	2.5	5	15
Peptone	10	20	20	10	20	60
Sodium acetate	16	32	32	64	32	96
COD value (ratio)	25 (1:1)	50 (1:1)	50 (1:1)	50 (1:2)	50 (1:1)	150 (1:1)
Phosphate Buffer						
KH ₂ PO ₄ (mg/L)	0.602	0.602	0.602	0.602	0.602	0.602
Na ₂ HPO ₄ (mg/L)	6.22	6.22	6.22	6.22	6.22	6.22
NaOH 0.1M (pH=8) R-4						
Q (L/d)	1.44	0.79	0.79	0.79	0.79	0.79
HRT (h)	1.2	2.4	2.4	2.4	2.4	2.4
ART (h)	0.3	0.3	0.3	0.3	0.3	0.3

Table 5.2. (continued)

STAGE 5					
Phase	Phase 45	Phase 46	Phase 47	Phase 48	Phase 49
Period (day)	432-446	447-521	522-533	534-577	578-593
AO7 (mg/L)	10	10	10	10	10
Mn (II) (mg/L)	10	10 (R4) 0 (R3)	15 (R4) 0 (R3)	15 (R4) 0 (R3)	0 (R4) 0 (R3)
Organic (mg/L)					
Yeast extract	-	-	-	10	10
Peptone	-	-	-	40	40
Sodium acetate	-	-	-	-	-
COD value (ratio)	-	-	-	50 (1:0)	50 (1:0)
Phosphate Buffer					
KH ₂ PO ₄ (mg/L)	0.602	0.602	0.602	0.602	0.602
Na ₂ HPO ₄ (mg/L)	6.22	6.22	6.22	6.22	6.22
NaOH 0.1M (pH=8) R-4	2ml	2ml	2ml	2ml	2ml
Q (L/d)	0.79	0.79	0.79	0.79	0.79
HRT (h)	2.4	2.4	2.4	2.4	2.4
ART (h)	0.3	0.3	0.3	0.3	0.3

5.2.5 Analytical methods

The decolorization of AO7 was determined colorimetrically at the maximum absorption wavelength (λ_{\max} =484 nm) of influent and effluent samples using a UV-visible spectrophotometer UV-1800 (Shimadzu, Japan). The samples were pre-filtered by 0.45 μ m membrane filter (Advantec, Japan) prior to analysis of dissolved organic carbon (DOC) as non-purgeable organic carbon (NPOC) by the TOC analyzer (TOC-VCSH, Shimadzu, Japan). Mn(II) was analyzed by the inductively coupled plasma emission spectrometer ICPE-9000 (Shimadzu, Japan) after filtered through a 0.2 μ m membrane filter (Advantec, Japan).

5.2.6 Isolation, screening and identification of microorganism

The streak-plate procedure was used to isolate single pure dye decolorizing bacteria and manganese-oxidizing bacteria from the R-4 reactor. Sponge media from upper, middle and bottom parts of the R-4 reactor on day-180 was squeezed and spread on media agar plate and incubated at 28 °C. Composition of agar medium was identical with the reactor substrate. The isolated colonies were picked up and transferred to liquid medium. Isolation was repeated from agar medium to liquid medium until single pure culture was obtained.

5.2.7 Dye decolorization and manganese oxidation ability of the isolates

A 10 mg/l of AO7-containing liquid medium was inoculated with bacterial culture (5% v/v) and incubated at 30 °C under shaking condition. Samples were withdrawn at different time intervals and analyzed for the growth using HACH spectrophotometer DR2800 (Hach Lange, Dusseldorf, Germany) at wavelength (λ) of 600 nm, and decolorization ability using UV-Vis spectrophotometer UV-1800 (Shimadzu, Kyoto, Japan) at wavelength (λ) of 484 nm.

A 10 mg/L Mn(II)-containing liquid medium was inoculated with bacterial culture (5% v/v) and incubated at 30 °C under shaking condition. After 7 days incubation, generated biogenic manganese oxides was identified using leucoberbelin blue (LBB) method (Krumbein and Altmann, 1973; Akob et al., 2014). Briefly, 500 μ l of 0.04% LBB-1 (Sigma Aldrich, Japan) in a 45 mM acetic acid was added to 1 ml culture after cultivated with 10 mg/l of Mn(II) for 3 months.

5.2.8 Molecular characterization of isolates

Polymerase chain reaction (PCR) of the 16S rRNA gene sequence of the isolates bacteria was amplified using a KOD FX Neo (Toyobo Lifescience, Japan) with universal primers of 27F (5'-AGAGTTTGATCCTGGCTCAG-3') and 1492R (5'-GGTTACCTTGTTACGACTT-3'). PCR reactions were performed by thermal cycler GeneAmp PCR System 9700 (Applied Biosystem, CA, USA) and the conditions were set as follows; 5 min of initial denaturation at 94 °C followed by 35 cycles of 30 s at 94 °C, 30 s at 55 °C, and 1 min at 72 °C with final extension at 72 °C for 7 min and keep in 4 °C. The PCR product was purified using FastGene® Gel/PCR extraction kit (Nippon Genetics Co. Ltd., Japan). The amplified products were then sent to Eurofins Genomics (Tokyo, Japan) for sequencing. The sequences were aligned and computed using chromas software and sequence homologies were determined by using BLAST database (<https://blast.ncbi.nlm.nih.gov/Blast.cgi>).

5.2.9 Microbial community analysis

Biomass samples taken from the sponge carriers (the upper, middle and lower portions) of R-3 and R-4 on days 252 and 592. The samples taken from the three portions of the reactor on each day were pooled to obtain one sample and four biomass samples in total were analyzed for microbial community. The DNA of the samples was extracted using the FastDNA® SPIN Kit for Soil (MP188 Biomedicals, Ohio, USA) according to the method reported by Noorain et

al. (2019). The DNA samples were sent to Hokkaido System Science Co. Ltd (Sapporo, Japan) for PCR amplification with a primer set of the V3-V4 region: 341F (5'-CCTACGGGGNGGCWGCAG-3') and 805R (5'-GGACTACHVGGGTATCTAATCC-3'), and sequenced using the Illumina MiSeq platform with a Miseq Reagent Kit v3 (Illumina Inc., San Diego, CA, USA).

The adapter sequences and primers were removed from sequence data using the Cutadapt software (version 1.1) (Martin, 2011) with the default minimum overlap length of 3 and the default maximum allowed error rate of 0.2. The noise and low-quality sequence reads, when the quality per base dropped below 20 bp in a sliding window of 20 bp (SLIDINGWINDOW:20:20) and the minimum length of the reads were below 50 bp (MINLEN:50), were removed using Trimmomatic (version 0.32) (Bolger et al., 2014). The assembling of the clean reads was performed using Fastq-join software (version 1.1.2-537) (Aronesty, 2013), which were then analyzed using the QIIME pipeline software (version 1.8.0) (Caporaso, et al., 2010). the UCLUST method was used to assign sequences having similarity greater than 97% into the same operational taxonomic units (OTUs) (Edgar R.C., 2010), which were subsequently classified using MiDAS taxonomy (version 1.20) (McIlroy et al., 2015).

5.3 Results

5.3.1 Batch decolorization of AO7 by abiotic-MnO₂

Batch experiment of AO7 removal by abiotic-MnO₂ is presented in Fig 5.2. The results showed that removal capacity of AO7 by abiotic-MnO₂ was approximately 70 mg/g abiotic-MnO₂, which revealed that chemical adsorption or oxidation of AO7 by abiotic-MnO₂ was found to occur.

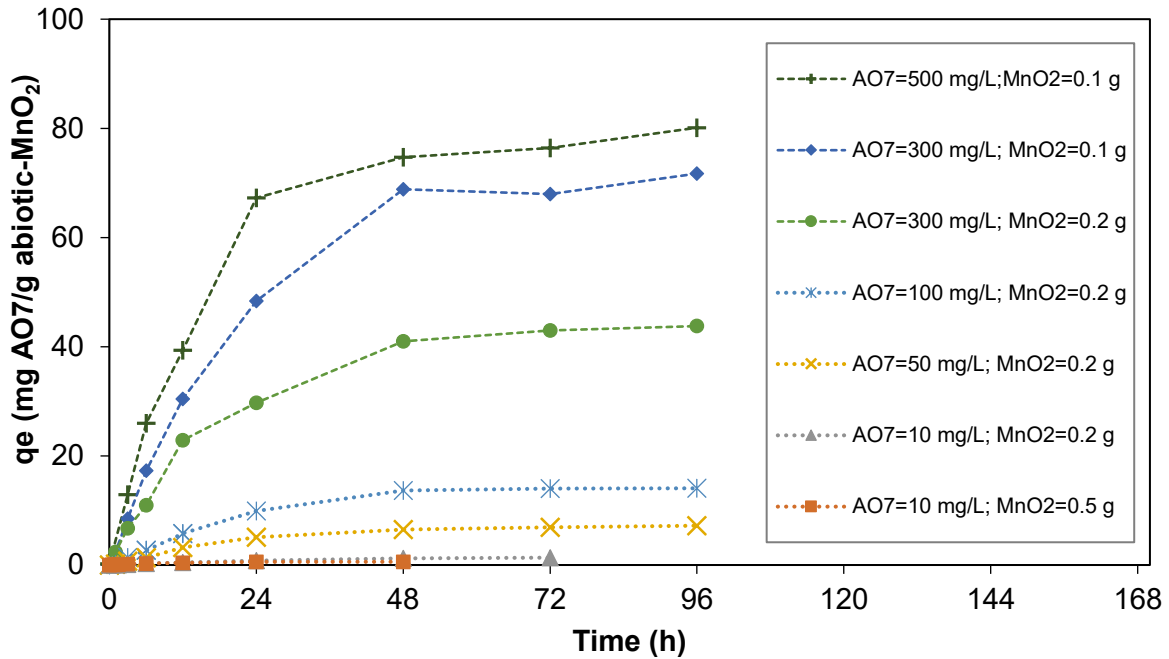


Figure 5.2 Capacity of abiotic-MnO₂ for removal of AO7 in batch experiments.

5.3.2 Reactor performances

The performance of R-3 (without MnO₂) and R-4 (with MnO₂) were presented in Fig 5-3. To simplify the process description, the operational condition of the reactors was divided into five stages.

Stage 1 (day 1 – 151):

After inoculation, the reactors were initially operated without AO7 load until day-12, to allow for microbial growth and attached well in the sponge media. The reactors were then supplemented with AO7 at a constant load of 0.1 kg Mn.m⁻³.d⁻¹. The AO7 removal was observed in R-4 and its performance gradually decreased, suggesting that chemical adsorption of AO7 onto abiotic- MnO₂) has occurred. While no removal of AO7 was observed in R-3.

No Mn(II) oxidation was observed in R-3 during this period. Mn(II) oxidation was found to occur in R-4 from first day operation, and 5 mg/L Mn(II) could be completely oxidized, therefore, Mn(II) loading was increased gradually obtain maximum Mn(II) oxidation capacity. Unfortunately, increasing Mn(II) loading caused a drop in pH and deterioration of Mn(II) performance as indicated by residual Mn(II) in the effluent.

Stage 2 (day 152 – 277):

Because Mn(II) oxidation is favorable at neutral pH, during this period, sodium acetate was added to the substrates to control pH at neutral, and the COD concentration of the substrate was kept at the same value by controlling ratio of sodium acetate to K-medium. The ratio of sodium acetate to K-medium was initially set as 1:1, and COD concentration was 50 mg/L. The results showed that AO7 removal in R-3 was slightly increased to 20% during this stage, but no Mn(II) oxidation was observed. Sodium acetate addition was found to be effective in controlling pH at neutral in R-4, and Mn(II) oxidation performance could be improved. During the period of Stage 2, Mn(II) loading was gradually elevated by increasing Mn(II) concentration from 7.5 mg/L to 10 mg/L, and then 12 mg/L. Because increasing the Mn(II) oxidation decreases the pH, the ratio of sodium acetate was raised with increasing Mn(II) concentration to keep the pH at neutral level.

Interestingly, the improvement of AO7 removal was observed along with increasing Mn(II) oxidation performance. When Mn(II) concentration was increased to 15 mg/L, and the ratio of sodium to K-medium to 4:1, the higher than 60% AO7 removal could be achieved in R-4, while only about 20% removal was observed in R-3. Unfortunately, the AO7 removal performance in R-4 could not be maintained and gradually tended to decrease, even though the Mn(II) oxidation was improved and 20 mg/L Mn(II) was completely oxidized. The performance could not be recovered even though the ratio of sodium to K-medium was reduced to 1:1, as the same with the previous conditions. I suspected that the decreasing AO7 removal was due to the toxicity of high concentration of Mn(II). Therefore, Mn(II) supplementation was discontinued at the end of the period. The results demonstrated that improvement of AO7 removal was not observed and the performance of AO7 removal was about 20%, and there was no different between R-3 and R-4.

Another interesting finding was observed during this period, in which TOC removal of R-4 was higher than R-3. This result suggested that Mn(II)-oxidation reactor (R-4) was more effective to degrade organic matters than without Mn(II)-oxidation reactor (R-3).

Stage 3 (day 278 – 368):

Sodium acetate supplementation was stopped, only K-medium was supplied as co-substrate. Mn(II) loading was gradually increased from zero (without Mn(II)) to 0.1 kg Mn.m⁻³.d⁻¹. As the results, AO7 removal in R-4 could be slightly improved to 40% when Mn(II) loading was 0.05 kg Mn.m⁻³.d⁻¹, but AO7 removal decreased with decreasing HRT. The same phenomenon

with Stage 1, where Mn(II) oxidation caused the pH drop. At the end of phase 3, the substrate tank was provided separately between R-3 and R-4, and R-3 was not supplemented with Mn(II). There was no change in pH between influent and effluent of R-3 (without Mn-oxidation), which evidenced that the decreasing of pH was caused by Mn-oxidation process.

Stage 4 (day 369 – 431):

Sodium acetate was supplied again in expectation to obtain the same results as in the Stage 2, and Mn(II) loading was increased step by step. As the results, the pH can be controlled even though Mn(II) oxidation was increased in R-4. Unfortunately, the high AO7 removal could not be achieved again, and the performance of R-3 and R-4 were almost similar in the range 20-40%.

Stage 5 (day 432 – 593):

Sodium acetate and K-medium were not supplemented, and only AO7 was provided as carbon source in the substrate tank during the period of day-432 to 533. Interestingly, the result showed that R-4 could oxidize Mn(II) without organic substrate addition, but AO7 removal was stable at 20%. This result suggest that MnOB seemed to utilize dead cells rather than AO7 as carbon source.

When K-medium was supplied again on day-534, AO7 removal in R-3 (without Mn(II)-oxidation) was enhanced, but no improvement was observed in R-4 (with Mn(II)-oxidation). Even though having high Mn(II)-oxidation ability, R-4 could not remove AO7. The removal of AO7 in R-4 may be inhibited by Mn(II) oxidation and/or the presence of highly abundant bio-MnOx formed during Mn(II)-oxidation.

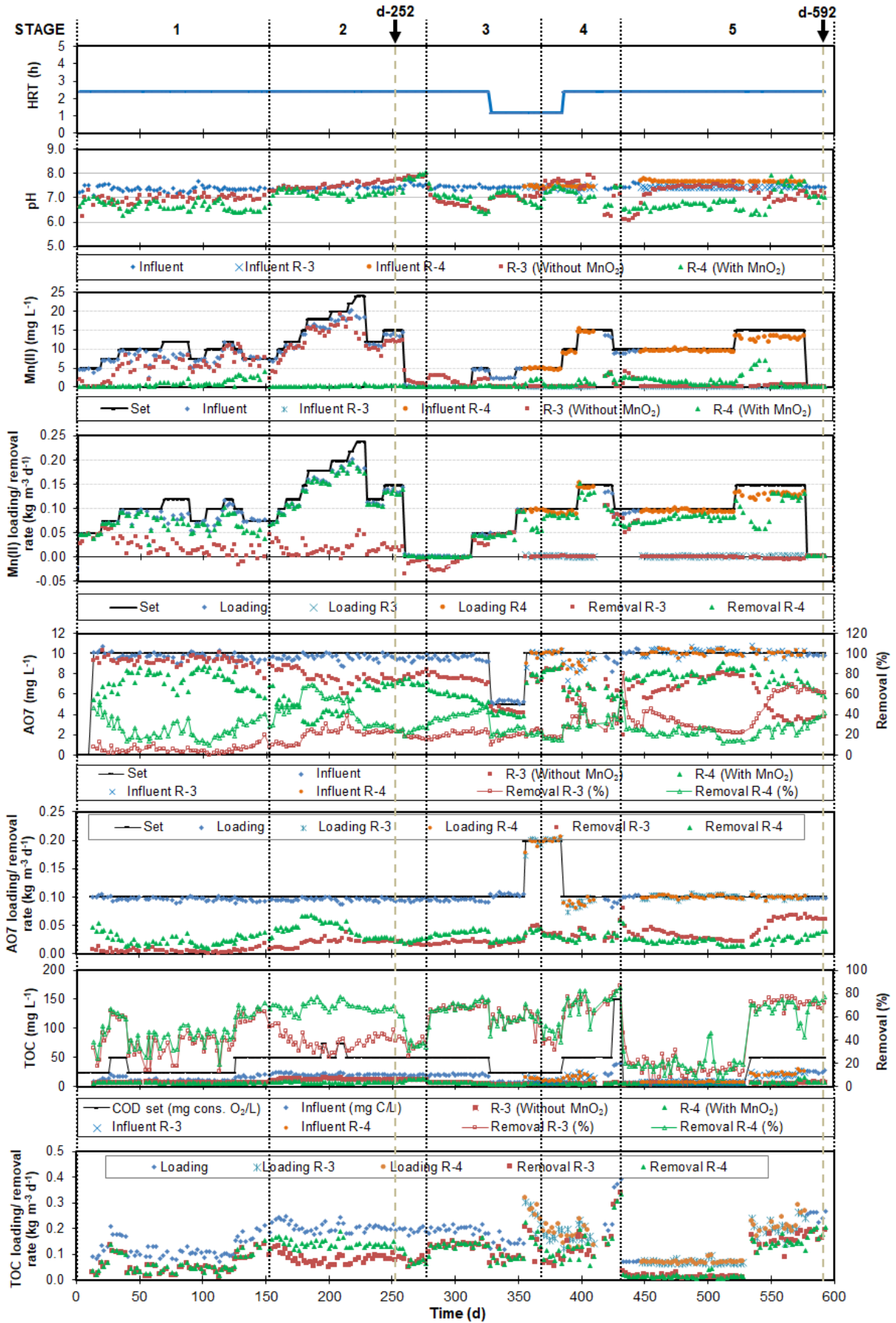


Figure 5.3 DHS reactor performances.

5.3.3 Microbial community of the reactors

A total of 4 biomass samples from two reactors were analyzed for compositions of microbial community. The total number of reads in each sample was more than 60,000, and the total number of operational taxonomic units (OTU) was more than 1,900 in each sample. Microbial diversity in the two reactors was assessed by alpha-diversity indices, include Simpson (1-D), Shannon (H), Evenness and Chao-1 estimator (Table 5.3). Comparisons between two reactors revealed no significant difference of the diversity in term of Simpson (1-D), Shannon (H), Evenness and Chao-1 estimator, suggesting that different Mn(II)-oxidation ability did not cause any significant effects on microbial diversity in each reactor.

Table 5.3 Sequence reads, total numbers of OTUs and diversities of the reactors

Sample	R3-d252	R4-d252	R3-d594	R4-d594
Total reads	61626	60033	60749	65662
Total OTU ¹⁾	2505	2189	1988	2177
Simpson (1-D) ²⁾	0.99	0.98	0.99	0.99
Shannon (H) ³⁾	5.68	5.14	5.29	5.57
Evenness ⁴⁾	0.12	0.08	0.10	0.12
Chao-1 ⁵⁾	5258	4428	4406	5092

¹⁾ Operational taxonomic units (OTUs) are defined as similarity thresholds of the 16S gene sequences at 97%.

²⁾ Simpson's index of diversity (1-D). A higher value indicates more diversity.

³⁾ Shannon (H) diversity index. A higher value indicates more diversity.

⁴⁾ Evenness. A higher value indicates more evenness.

⁵⁾ Chao-1. A higher value indicates a higher estimated richness.

Microbial community of the two reactors at phylum level can be seen in Figure 5.4. The major microbial communities with a relative abundance greater than 1% of total sequence reads were assigned into 15 phyla. The results showed that there were no significant differences between microbial community in the two reactors at the phylum level. Proteobacteria, Acidobacteria, Actinobacteria, Planctomycetes and Bacteroidetes were found to be the dominant phyla in all reactors, which accounted for more than 72% of the total bacterial composition.

The major genera whose relative abundance more than 1% of total sequence reads, were shown in Figure 5.5. A distinct microbial composition was observed between two reactors at the genus level. *Blastocatella* was the most dominant genus in R-3 d-252 sample (7.6%), followed by *Gordonia* (3.5%), and *Mycobacterium* (3.0%). While, R-4 d-252 sample was dominated by *Gordonia* (7.0%), *Nocardia* (6.1%), *Obscuribacterales* (4.6%), *Bradyrhizobium*

(4.3%) and *Rhodococcus* (3.6%). The microbial community altered on d-594, where the dominant genus in R-3 was *Acidobacteria Subgroup 2* (6.1%), followed by *Woodsholea* (5.1%), *Rhodococcus* (5.0%), and *Caldilineaceae uncultured* (3.0%). While the dominant genera in R-4 were *Blastocatella* (7.1%), *Woodsholea* (5.5%), *Nitrospira* (3.9%), and *Acidobacteria Subgroup 2* (3.5%). Both reactors were exposed with the same level of AO7 and Mn(II), regardless in some phases. The differences in microbial community profiles at the genus level might be influenced by the initially added abiotic-MnO₂ in R-4 which led to enhancement of Mn(II)-oxidation.

Phyla	R3-d252	R4-d252	R3-d594	R4-d594
Acidobacteria	12.8%	6.7%	9.2%	15.0%
Actinobacteria	9.7%	23.3%	10.5%	7.8%
Armatimonadetes	2.5%	0.1%	0.5%	0.2%
Bacteroidetes	7.5%	7.0%	6.1%	5.2%
Chlamydiae	1.4%	2.9%	2.2%	1.8%
Chlorobi	2.8%	0.1%	0.4%	1.4%
Chloroflexi	4.8%	3.2%	3.8%	3.6%
Cyanobacteria	0.3%	0.2%	2.3%	1.3%
Firmicutes	0.3%	0.7%	2.3%	2.2%
Gemmatimonadetes	1.9%	1.3%	1.8%	2.9%
Nitrospirae	2.0%	0.6%	2.6%	3.7%
Planctomycetes	9.6%	5.6%	9.1%	9.3%
Proteobacteria	32.9%	37.7%	42.2%	37.8%
Saccharibacteria	2.5%	6.5%	0.2%	1.2%
Verrucomicrobia	6.5%	2.0%	3.9%	2.4%
Unassigned	1.5%	1.6%	1.6%	2.2%
Others	1.3%	0.6%	1.2%	2.2%

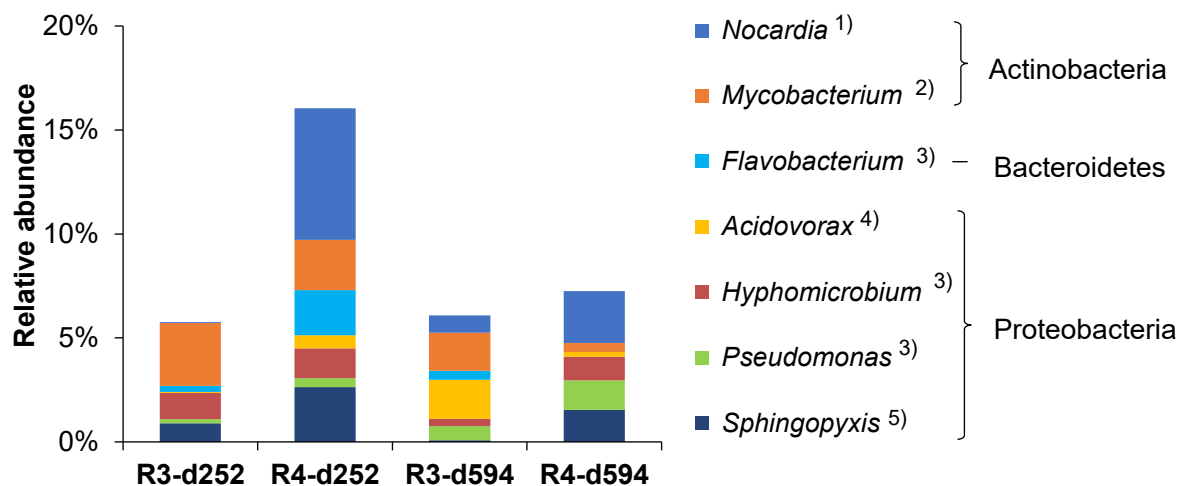
Figure 5.4 Microbial community at the phylum level, the phylum with relative abundance below 1% were grouped in “others”.

The performance of R-4 in Mn(II) removal exhibited that a certain microbial population exists and plays a key role in Mn(II) oxidation. Several genera that those strains have been previously reported as manganese-oxidizing bacteria, were identified in the reactors. However, it should be noted that not all strains belonging to these genera have the capability of oxidizing Mn(II). In this study, these genera were then referred to as “putative MnOB”. Seven putative MnOB were detected in the reactors with relative abundance greater than 1%, including *Nocardia*, *Mycobacterium*, *Flavobacterium*, *Acidovorax*, *Hyphomicrobium*, *Pseudomonas*, and *Spingophyxis*. The total relative abundance of identified putative MnOB in the reactors were presented in Figure 5.6.

Phylum	Genus	R3-d252	R4-d252	R3-d594	R4-d594
Acidobacteria	Acidobacteria Subgroup 2	2.1%	2.4%	6.1%	3.5%
	Blastocatella	7.6%	1.7%	1.1%	7.1%
Actinobacteria	Gordonia	3.5%	7.0%	1.4%	2.0%
	Mycobacterium	3.0%	2.3%	1.8%	0.4%
	Nocardia	0.0%	6.1%	0.8%	2.6%
	Rhodococcus	0.3%	3.6%	5.0%	0.5%
Armatimonadetes	Armatimonadales	0.4%	0.1%	0.4%	1.3%
Bacteroidetes	Flavobacterium	0.3%	2.1%	0.4%	0.0%
Chlorobi	SJA-28	2.3%	0.2%	0.3%	0.5%
Chloroflexi	Caldilineaceae uncultured	1.2%	2.1%	3.0%	1.5%
Cyanobacteria	Obscuribacterales	1.5%	4.6%	0.0%	0.9%
Nitrospirae	Nitrospira	2.0%	0.5%	2.6%	3.9%
Parcubacteria	Parcubacteria	1.5%	0.2%	0.4%	0.3%
Planctomycetes	WD2101 soil group	0.5%	1.7%	0.7%	1.0%
Proteobacteria	Acidibacter	1.1%	3.0%	0.8%	1.2%
	Acidovorax	0.1%	0.6%	1.8%	0.2%
	Bradyrhizobium	2.1%	4.3%	0.6%	1.3%
	Haliangium	0.2%	0.0%	2.1%	0.0%
	Meganema	1.1%	0.3%	0.2%	1.9%
	Myxococcales P3OB-42	0.0%	0.1%	0.3%	1.1%
	Myxococcales uncultured	0.0%	0.0%	1.1%	0.5%
	Nitrosomonadaceae uncultured	0.7%	0.1%	1.9%	1.1%
	Nordella	1.9%	0.9%	1.2%	0.9%
	Pseudomonas	0.2%	0.4%	0.7%	1.5%
	Rhizomicrobium	0.5%	2.2%	1.0%	0.8%
	Rhodanobacter	1.3%	0.2%	0.0%	0.2%
	Rivicola	0.0%	0.0%	1.4%	0.0%
	Rudaea	0.2%	1.4%	0.1%	0.3%
	SM1B06	0.0%	0.0%	1.3%	0.0%
	Sphingomonadaceae uncultured	1.6%	1.0%	2.4%	1.1%
	Sphingopyxis	0.9%	2.5%	0.1%	1.6%
	TA18	0.2%	0.5%	0.2%	2.4%
	Variibacter	0.2%	1.0%	0.5%	0.9%
	Woodsholea	0.3%	1.8%	5.1%	5.5%
Xanthomonadales uncultured	0.7%	0.6%	1.5%	0.1%	
Zymomonas	0.6%	0.2%	2.7%	0.5%	
Verrucomicrobia	OPB35 soil group	2.8%	0.9%	1.4%	1.2%

Figure 5.5 Microbial community at the genus level with relative abundances >1%

In addition to the identified putative MnOB community contributing to Mn(II) oxidation ability, microbial analysis results demonstrated that microbial communities at the genus level having ability to degrade azo dye under aerobic conditions, such as *Pseudomonas*, *Bacillus*, *Aeromonas*, and *Comamonas* (Meerbergen et al., 2018; Du et al., 2015; Cui et al., 2012; Jadhav et al., 2008), were detected at very low relative abundance (less than 2% of the total community) in both reactors.

**References:**

1) Carmichael and Bräuer, 2015

4) Tsuji et al., 2017

2) Marcus et al., 2017

5) Piazza et al., 2019

3) Bohu et al., 2016

Figure 5.6 Putative MnOB community with relative abundance >1%.

5.3.4 Isolation, screening and identification of microorganisms

The total of 20 bacterial strains were isolated and identified from R-4. The isolates belong to several genera, such as *Brevibacillus sp.*, *Ochrobactrum sp.*, *Sphingomonas sp.*, *Bacillus sp.*, *Serratia sp.*, and *Rhizobium sp.*. The isolates were then tested for their decolorization and Mn(II)-oxidation ability. Of the total isolates, all tested isolates did not have decolorization ability. Figure 5.8 showed that all isolates were only able to remove AO7 less than 20%, which indicated that the removal of AO7 was due to adsorption to onto cells rather than degradation by microbial.

By addition LBB-1 in culture tube, several isolates demonstrated Mn(II)-oxidation ability, as shown by the blue color appearance of the culture, indicated that biogenic manganese oxides (Mn(III) or (IV)) were formed (Fig. 5.9). Here, the amount of formed Mn-oxides was indicated by the blue color intensity, for example light blue color corresponded to the small amount of bio-MnO_x, and dark blue color indicated the high abundant of bio-MnO_x. Of the total 20 isolates, nine isolates possessed high Mn(II)-oxidizing ability, four isolates possess low Mn(II)-oxidizing ability, and the remaining isolates do not have Mn(II)-oxidizing ability. Characterization of the isolates and their decolorization and Mn(II)-oxidation ability were summarized in Table 5.2.

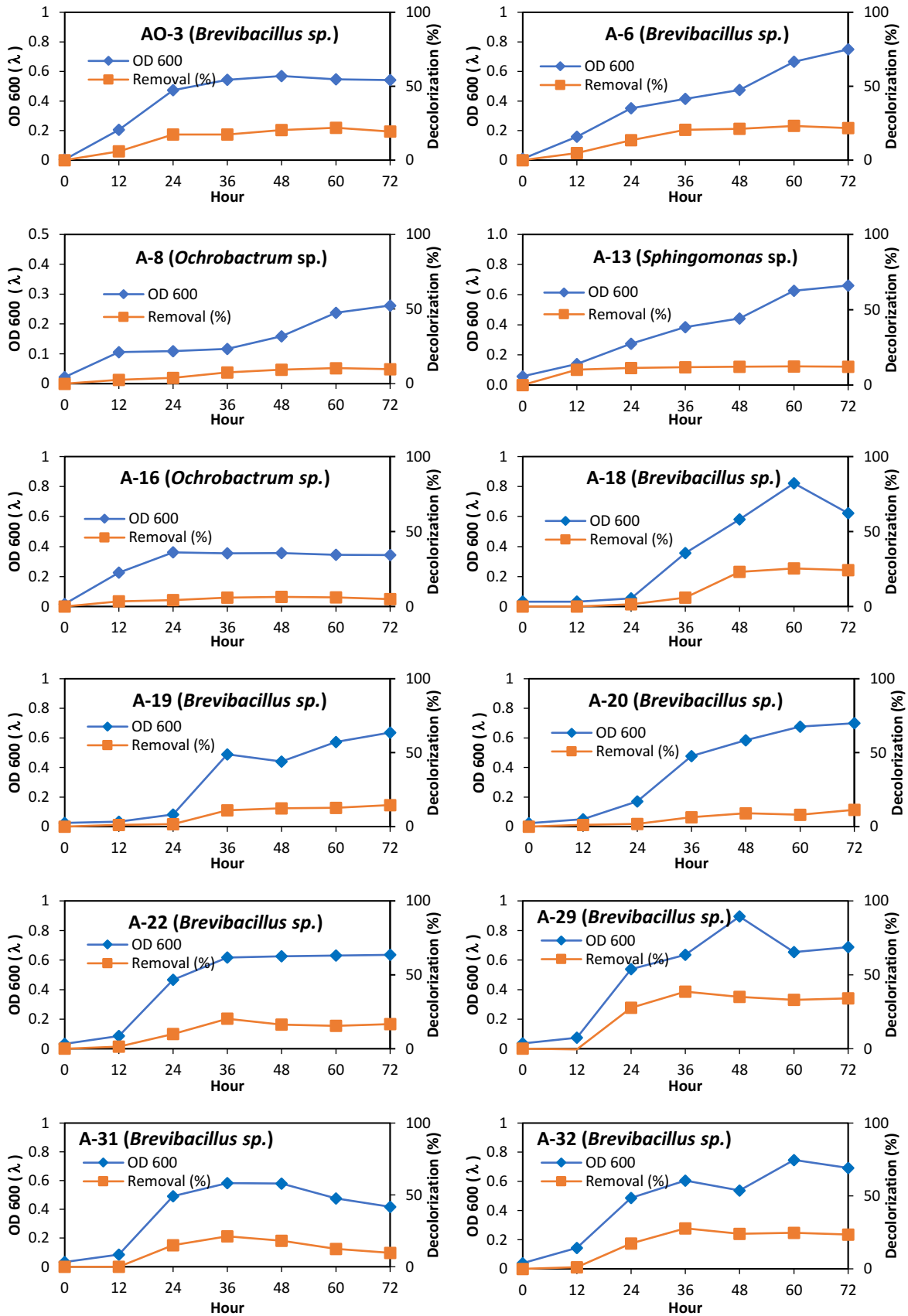


Figure 5.7 Decolorization ability of isolates and their growth

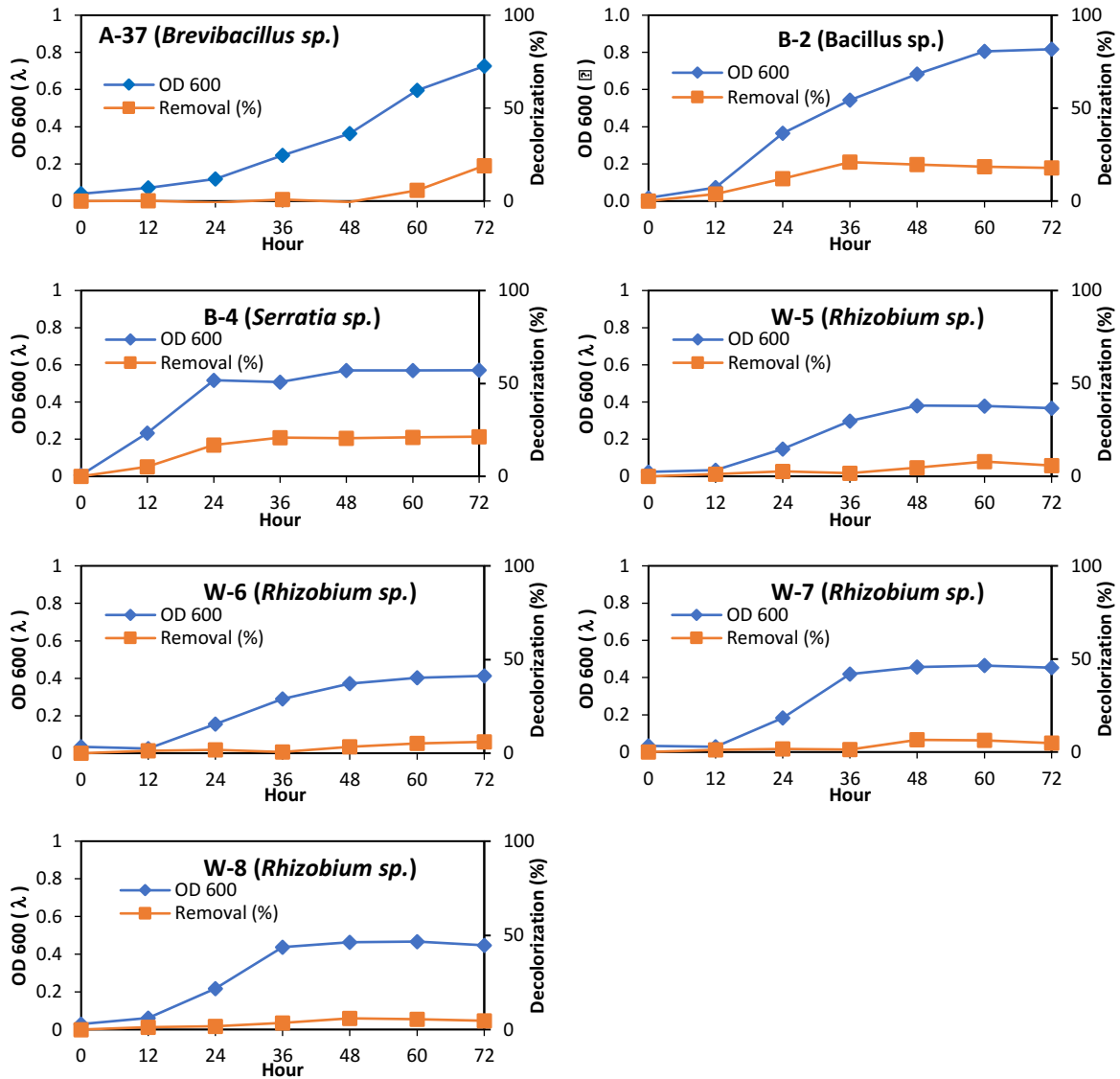


Figure 5.7 (continued)

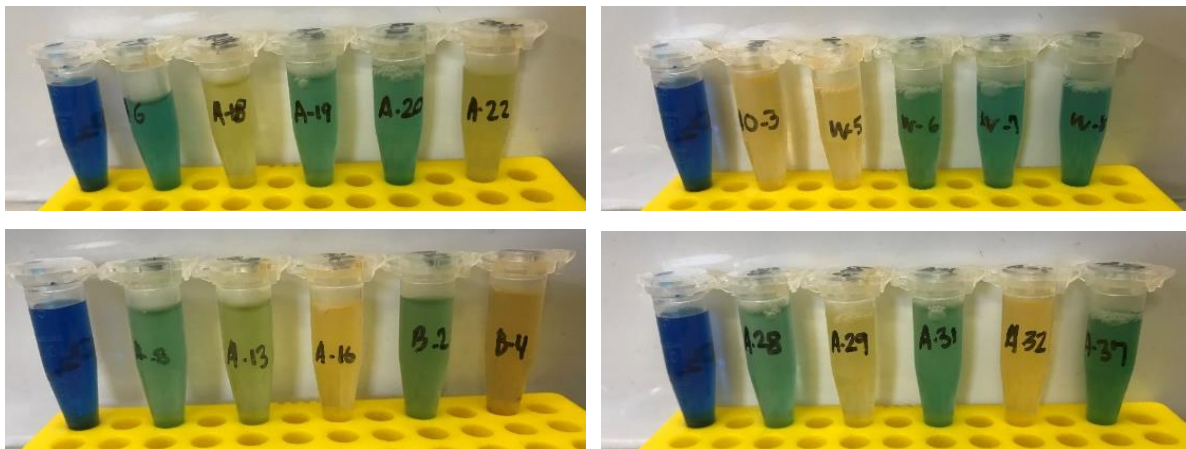


Figure 5.8 Mn-oxidizing ability test of isolates using LBB-1, the left-most tube of each photo is using abiotic-MnO₂ as control.

Table 5.4 Characterization of identified bacterial isolates

Sample name	Identified	Phylum	Similarity	Colony color	Decolorization ability	Mn-oxidation ability
AO-3	<i>Brevibacillus</i> sp.	Firmicutes	100%	Orange	-	-
A-6	<i>Brevibacillus</i> sp.	Firmicutes	99%	Orange	-	++
A-8	<i>Ochrobactrum</i> sp.	Proteobacteria	100%	White	-	++
A-13	<i>Sphingomonas</i> sp.	Proteobacteria	100%	Yellow	-	+
A-16	<i>Ochrobactrum</i> sp.	Proteobacteria	100%	White	-	++
A-18	<i>Brevibacillus</i> sp.	Firmicutes	99%	Yellow	-	-
A-19	<i>Brevibacillus</i> sp.	Firmicutes	99%	White	-	++
A-20	<i>Brevibacillus</i> sp.	Firmicutes	99%	White	-	++
A-22	<i>Brevibacillus</i> sp.	Firmicutes	99%	Orange	-	-
A-28	<i>Brevibacillus</i> sp.	Firmicutes	99%	Orange	na	+
A-29	<i>Brevibacillus</i> sp.	Firmicutes	99%	Orange	-	-
A-31	<i>Brevibacillus</i> sp.	Firmicutes	99%	Orange	-	+
A-32	<i>Brevibacillus</i> sp.	Firmicutes	99%	Orange	-	-
A-37	<i>Brevibacillus</i> sp.	Firmicutes	99%	Yellow	-	++
B-2	<i>Bacillus</i> sp.	Firmicutes	100%	White	-	+
B-4	<i>Serratia</i> sp.	Proteobacteria	99%	Orange	-	-
W-5	<i>Rhizobium</i> sp.	Proteobacteria	99%	White	-	-
W-6	<i>Rhizobium</i> sp.	Proteobacteria	100%	White	-	++
W-7	<i>Rhizobium</i> sp.	Proteobacteria	99%	White	-	++
W-8	<i>Rhizobium</i> sp.	Proteobacteria	99%	White	-	++

Remarks:

- : no ability (decolorization < 20%, or no blue color appear for LBB test)
- + : low ability (LBB test showing light blue color)
- ++ : high ability (LBB test showing dark blue color)
- n.a. : not tested

5.4 Discussion

5.4.1 Reactor performances

The reactor performance results demonstrated that high Mn(II)-oxidation ability can be achieved at early stage of operation in R-4 which was initially installed with abiotic-MnO₂. While, Mn(II)-oxidation ability was not observed in R-3. Abiotic-MnO₂ installed in the sponge carrier media could effectively induce MnOB and inhibit other-MnOB growth in the reactor. Mn-based materials, such as manganese carbonate (MnCO₃), have been reported to accelerate MnOB growth in the biofilter reactor (Zhang et al., 2015). Due to its toxicity, the presence of MnO₂ has been reported to inhibit non-MnOB activity (Matsushita et al., 2018). Unfortunately, Mn(II) oxidation activity led to the decreasing pH, which was identical with that observed in Chapter 4. The lower pH is not an ideal condition for biological Mn(II) oxidation, which is optimum at neutral to higher pH (Tebo et al., 2005). Even though some studies reported that biological oxidation by some bacterial strains was possible at low pH or acidic conditions

(Mayanna et al, 2015; Bohu et al., 2016), in this study, it was observed that decreasing pH caused the disruption of manganese oxidation ability, such as the condition occurred at Stage 1, 3 and 5, as shown by the detection of residual Mn(II) in the effluent (Fig. 5.3).

It seemed that enhancement of AO7 removal could be achieved at the Stage 2 along with increasing Mn(II) oxidation, and neutral pH can be maintained by sodium acetate addition. We therefore increased Mn(II) concentration to 22 mg/L, and the ratio of sodium acetate to K-medium was increased to 4:1. Unfortunately, the AO7 removal performance suddenly decreased. Even though Mn(II) oxidation was kept at high rate, AO7 removal continued to decline. Therefore, decolorization mechanisms are likely controlled by different process, not by Mn(II) oxidation. There are several mechanisms that may contribute to the decreasing removal of AO7 at these conditions. First, increasing the ratio of sodium acetate to K-medium may affect the enzyme activity that responsible for decolorization of AO7. The availability of organic co-substrate is one of important factors in decolorizing azo dye under aerobic conditions, and different substrate types influence the decolorization ability of the microorganisms (Moosvi et a., 2007). Enzymatic azo dye decolorization under aerobic conditions has been proposed by Yu et al. (2015), in which metabolism of organic substrate is essential for generation of NADH, which is then catalyzed by azoreductase enzyme coupling with azo dye reduction. Therefore, the available organic substrate plays an important role in supplying NADH as cofactor for redox reaction with azo dye. In this study, increasing sodium acetate ratio to K-medium gave poor decolorization efficiency, regardless of Mn(II)-oxidation ability. Moosvi et al. (2007) also found lower decolorization efficiency when supplying with sodium acetate as the sole organic carbon source compared with peptone or yeast extract.

Another plausible reason for declining decolorization efficiency is the generated bio-MnO_x from oxidation of Mn(II) may inhibit microbial decolorization activity. Previous studies reported that bio-MnO_x could inhibit methane-oxidizing activity and biodegradation of dichlorophenyl phosphine (Matsushita et al., 2018; He et al., 2019). In this study, even though the substrate composition of R-4 in Phase 4 was set the same as the substrate composition of Phase 2, the same AO7 removal efficiency could not be attained. It can be concluded that decolorization of AO7 was not regulated by Mn(II) oxidation. The difference between R-3 and R-4 was the presence of initially added abiotic-MnO₂ and generated bio-MnO_x in R-4. Zhao et al. (2019) reported that the presence of insoluble material, such as iron (hydr)oxides, at the bacterial outer membrane could inhibit the contact between cell membranes and azo dye lead

to the deterioration of removal ability. At the end of Stage 5, R-3 (without Mn(II)-oxidation), has shown higher decolorization efficiency than R-4 (with Mn(II)-oxidation). It therefore can be presumed that the presence of abiotic-MnO₂ and the generated bio-MnO_x covered the cell membranes resulting in the low decolorization ability. However, increasing decolorization of AO7 at initial period of Stage 2 remained unclear whether due to Mn(II)-oxidation, adsorption onto biomass or other mechanisms.

The results showed that R-4 was more effectively to decompose organic substrate than R-3 during Stage 1 and Stage 2. The presence of MnO_x in R-4 may contributed to removal of organic substances. Previous study reported that acetate does not react abiotically with Mn(IV) but can be oxidized completely to CO₂ by biological reaction coupled with Mn(IV) reduction (Lovely, 1991). The presence of manganese oxides could stimulate decomposition of complex organic substances, such as humic acid into lower molecular organic compounds which are more degradable and suitable as substrate for microbial growth (Sunda and Kieber, 1994). Keiluweit et al. (2015) has shown that Mn-redox cycling was linked to the decomposition of litter in forest ecosystems. Mn(II) provided by fresh plant litter was biologically oxidized to insoluble oxidative species Mn(III or IV) which act as oxidizer for the breakdown of litter.

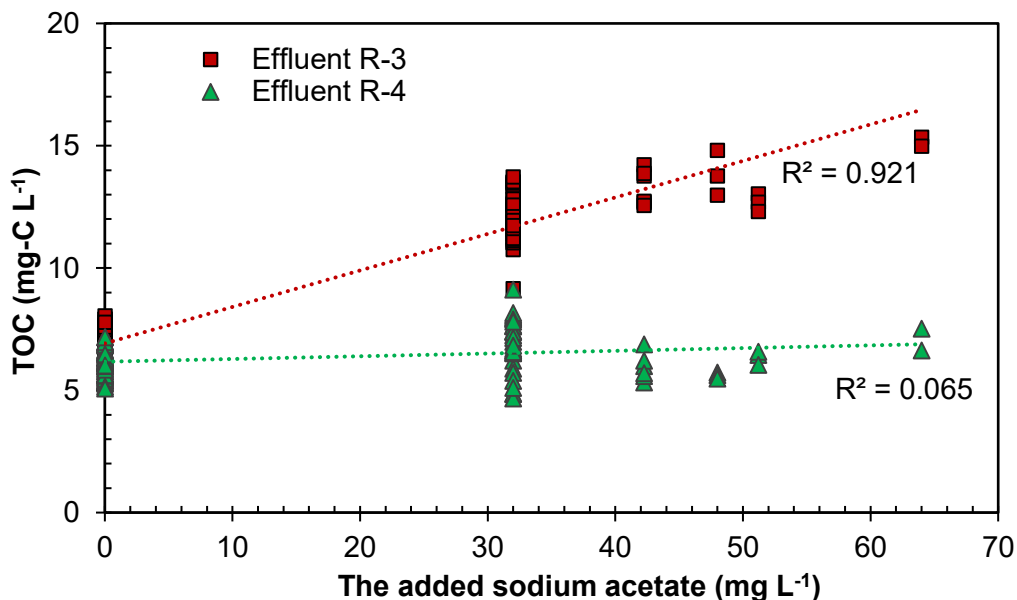


Figure 5.9 TOC concentration during Stage 1 and Stage 2. The Mn-oxidation reactor (R-4) more effectively decompose organic substances than the reactor without Mn-oxidation (R-3).

In Stage 5, both reactors were supplemented with AO7 as sole carbon source without any organic co-substrate addition for a long period operation. The results showed that R-4 exhibited

good performance in Mn-oxidation ability, but no decolorization of AO7 was observed, indicated that MnOB community in R-4 did not utilize AO7 as carbon source. Good Mn(II) removal performance of the reactor without organic feeding has been reported previously, which indicated that MnOB could survive by utilizing biomass associated products (BAPs) from dead cells (Matsushita et al., 2018). The results of Chapter 3 also demonstrated that MnOB could utilize activated sludge as energy source performing Mn(II) oxidation ability. Thus, during this period, the biomass preferred to utilize dead cells rather than AO7.

5.4.2 Microbial community and isolates

Azo dyes are generally resistant to aerobic degradation. The poor decolorization performance of the reactors were attributable to the low abundance of azo dye-degrading bacteria community in the reactors. *Blastocatella*, *Gordonia*, *Nocardia*, *Woodsholea*, and *Rhodococcus* were the most dominant genera in both reactors. *Blastocatella*, an aerobic chemoorganotrophic bacterium, have been detected in high abundant in biofilm membrane bioreactor (BF-MBR) treating petroleum refinery wastewater (Jiang et al., 2019), but their occurrence in azo dye treatment process have never been reported. *Gordonia* in consortium has been reported to degrade azo dye under anaerobic conditions but poorly under aerobic conditions (Eskandari et al., 2019). *Nocardia corallina* has been demonstrated to degrade a triphenylmethane dye (Yatome et al., 1993), but no studies on degradation of azo dye by *Nocardia* have been reported. *Rhodococcus* strain UCC 0016 has shown to capable of degrading azo dye methyl red under static condition (Maniyam et al., 2018). Thus, considering the decolorization performance of the reactors, these dominant genera did not have ability to decolorize azo dye. Even though MnOB were enriched in the reactor R-4, such as *Nocardia*, *Mycobacterium*, *Hyphomicrobium* and *Sphingopyxis*, enhancement of AO7 removal was not observed. Some isolates showed their ability to oxidize Mn(II), such as *Brevibacillus* sp., *Ochrobactrum* sp., *Sphingomonas* sp., *Bacillus* sp., and *Rhizobium* sp., but decolorization test revealed that none of them was capable of decolorizing AO7.

5.5 Conclusions

This study presented the application of enriched MnOB in DHS reactor for decolorization of an azo dye AO7. The enrichment of MnOB was accelerated by installing abiotic-MnO₂ in the sponge media of the reactor, achieving higher Mn(II) removal compared with the reactor devoid of abiotic-MnO₂. However, no significant removal of AO7 was observed in the abiotic-

MnO₂-containing reactor. Microbial community analysis revealed that putative MnOB enriched in the abiotic-MnO₂-containing reactor, and bacterial strains isolated from abiotic-MnO₂ containing reactor demonstrated Mn(II)-oxidation ability but not AO7 removal. Thus, MnOB and Mn(II) oxidation activity had less effect on AO7 removal. Further studies are required to investigate the phenomena of enhancement of AO7 removal and suddenly decline in the abiotic-MnO₂-containing reactor at Stage 2, and the increase in AO7 removal in the devoid of abiotic-MnO₂ reactor at the end of Stage 5, whether decolorization of AO7 was inhibited by Mn(II) oxidation activity or toxic effects of generated bio-MnO_x.

References

- Akob, D.M., Bohu, T., Beyer, A., Schäffner, F., Händel, M., Johnson, C.A., Merten, D., Büchel, G., Totsche, K.U., Küsel, K., 2014. Identification of Mn(II)-oxidizing bacteria from a Low-pH contaminated former uranium mine. *Appl. Environ. Microbiol.* 80, 5086–5097. <https://doi.org/10.1128/AEM.01296-14>
- Aronesty, E., 2013. Comparison of sequencing utility programs. *Open Bioinforma. J.* 7, 1–8. <https://doi.org/10.2174/1875036201307010001>
- Bay, H.H., Lim, C.K., Kee, T.C., Ware, I., Chan, G.F., Shahir, S., Ibrahim, Z., 2014. Decolourisation of Acid Orange 7 recalcitrant auto-oxidation coloured by-products using an acclimatised mixed bacterial culture. *Environ. Sci. Pollut. Res.* 21, 3891–3906. <https://doi.org/10.1007/s11356-013-2331-4>
- Bohu, T., Akob, D.M., Abratis, M., Lazar, C.S., 2016. Biological low-pH Mn (II) oxidation in a manganese deposit. *Appl. Environ. Microbiol.* 82, 3009–3021. <https://doi.org/10.1128/AEM.03844-15>.
- Bolger, A.M., Lohse, M., Usadel, B., 2014. Trimmomatic: A flexible trimmer for Illumina sequence data. *Bioinformatics* 30, 2114–2120. <https://doi.org/10.1093/bioinformatics/btu170>
- Cai, C., Zhang, H., Zhong, X., Hou, L., 2014. Electrochemical enhanced heterogeneous activation of peroxydisulfate by Fe-Co/SBA-15 catalyst for the degradation of Orange II in water. *Water Res.* 66, 473–485. <https://doi.org/10.1016/j.watres.2014.08.039>
- Cao L.T., Kodera H., Abe K., Imachi H., Aoi Y., Kindaichi T., Ozaki T., Ohashi A., 2015. Biological oxidation of Mn(II) coupled with nitrification for removal and recovery of minor metals by downflow hanging sponge reactor. *Water Res.* 68: 545-53.
- Caporaso, J.G., Kuczynski, J., Stombaugh, J., Bittinger, K., Bushman, F.D., Costello, E.K., Fierer, N., Peña, A.G., Goodrich, K., Gordon, J.I., Huttley, G. a, Kelley, S.T., Knights, D., Jeremy, E., Ley, R.E., Lozupone, C. a, Mcdonald, D., Muegge, B.D., Reeder, J., Sevinsky, J.R., Turnbaugh, P.J., Walters, W. a, 2010. QIIME allows analysis high-throughput community sequencing data. *Nat. Methods* 7, 335–336. <https://doi.org/10.1038/nmeth.f.303>.
- Coughlin, M.F., Kinkle, B.K., Bishop, P.L., 2003. High performance degradation of azo dye Acid Orange 7 and sulfanilic acid in a laboratory scale reactor after seeding with

- cultured bacterial strains. *Water Res.* 37, 2757–2763. [https://doi.org/10.1016/S0043-1354\(03\)00069-1](https://doi.org/10.1016/S0043-1354(03)00069-1)
- Cui, D., Li, G., Zhao, D., Gu, X., Wang, C., Zhao, M., 2012. Microbial community structures in mixed bacterial consortia for azo dye treatment under aerobic and anaerobic conditions. *J. Hazard. Mater.* 221–222, 185–192. <https://doi.org/10.1016/j.jhazmat.2012.04.032>
- Du, L.N., Li, G., Zhao, Y.H., Xu, H.K., Wang, Y., Zhou, Y., Wang, L., 2015. Efficient metabolism of the azo dye methyl orange by *Aeromonas* sp. strain DH-6: Characteristics and partial mechanism. *Int. Biodeterior. Biodegrad.* 105, 66–72. <https://doi.org/10.1016/j.ibiod.2015.08.019>
- Edgar, R.C., 2010. Search and clustering orders of magnitude faster than BLAST. *Bioinformatics* 26, 2460–2461. <https://doi.org/10.1093/bioinformatics/btq461>
- Elizalde-González, M.P., Hernández-Montoya, V., 2009. Removal of acid orange 7 by guava seed carbon: A four parameter optimization study. *J. Hazard. Mater.* 168, 515–522. <https://doi.org/10.1016/j.jhazmat.2009.02.064>
- Eskandari, F., Shahnavaaz, B., Mashreghi, M., 2019. Optimization of complete RB-5 azo dye decolorization using novel cold-adapted and mesophilic bacterial consortia. *J. Environ. Manage.* 241, 91–98. <https://doi.org/10.1016/j.jenvman.2019.03.125>
- Forrez, I., Carballa, M., Verbeken, K., Vanhaecke, L., Michael Schlusener, M.S., Ternes, T., Boon, N., Verstraete, W., 2010. Diclofenac oxidation by biogenic manganese oxides. *Environ. Sci. Technol.* 44, 3449–3454. <https://doi.org/10.1021/es9027327>
- Forrez, I., Carballa, M., Fink, G., Wick, A., Hennebel, T., Vanhaecke, L., Ternes, T., Boon, N., Verstraete, W., 2011. Biogenic metals for the oxidative and reductive removal of pharmaceuticals, biocides and iodinated contrast media in a polishing membrane bioreactor. *Water Res.* 45, 1763–1773. <https://doi.org/10.1016/j.watres.2010.11.031>
- Furgal, K.M., Meyer, R.L., Bester, K., 2014. Removing selected steroid hormones, biocides and pharmaceuticals from water by means of biogenic manganese oxide nanoparticles in situ at ppb levels. *Chemosphere* 136, 321–326. <https://doi.org/10.1016/j.chemosphere.2014.11.059>
- Gao, S.H., Peng, L., Liu, Y., Zhou, X., Ni, B.J., Bond, P.L., Liang, B., Wang, A.J., 2016. Bioelectrochemical reduction of an azo dye by a *Shewanella oneidensis* MR-1 formed biocathode. *Int. Biodeterior. Biodegrad.* 115, 250–256. <https://doi.org/10.1016/j.ibiod.2016.09.005>
- He, Z., Zhang, Q., Wei, Z., Zhao, Y., Pan, X., 2019. Cultivation of a versatile manganese-oxidizing aerobic granular sludge for removal of organic micropollutants from wastewater. *Sci. Total Environ.* 690, 417–425. <https://doi.org/10.1016/j.scitotenv.2019.06.509>
- Jadhav, U.U., Dawkar, V. V., Ghodake, G.S., Govindwar, S.P., 2008. Biodegradation of Direct Red 5B, a textile dye by newly isolated *Comamonas* sp. UVS. *J. Hazard. Mater.* 158, 507–516. <https://doi.org/10.1016/j.jhazmat.2008.01.099>
- Lovley, D.R., 1991. Dissimilatory Fe(III) and Mn(IV) reduction. *Microbiol. Rev.* 55, 259–287.

- Marcus, D.N., Pinto, A., Anantharaman, K., Ruberg, S.A., Kramer, E.L., Raskin, L., Dick, G.J., 2017. Diverse manganese(II)-oxidizing bacteria are prevalent in drinking water systems. *Environ. Microbiol. Rep.* 9, 120–128. <https://doi.org/10.1111/1758-2229.12508>
- Martin, M., 2011. Cutadapt removes adapter sequences from high-throughput sequencing reads. *EMBnet.journal* 17, 10–12. <https://doi.org/10.14806/ej.17.1.200>.
- McIlroy, S.J., Saunders, A.M., Albertsen, M., Nierychlo, M., McIlroy, B., Hansen, A.A., Karst, S.M., Nielsen, J.L., Nielsen, P.H., 2015. MiDAS: the field guide to the microbes of activated sludge. *Database* 2015, bav062. <https://doi.org/10.1093/database/bav062>
- Moosvi, S., Kher, X., Madamwar, D., 2007. Isolation, characterization and decolorization of textile dyes by a mixed bacterial consortium JW-2. *J. Environ. Sci.* 74, 723–729. <https://doi.org/10.1016/j.dyepig.2006.05.005>
- Mutafov, S., Avramova, T., Stefanova, L., Angelova, B., 2007. Decolorization of Acid Orange 7 by bacteria of different tinctorial type: A comparative study. *World J. Microbiol. Biotechnol.* 23, 417–422. <https://doi.org/10.1007/s11274-006-9241-2>
- Noorain, R., Kindaichi, T., Ozaki, N., Aoi, Y., Ohashi, A., 2019. Integrated biological–physical process for biogas purification effluent treatment. *J. Environ. Sci.* 83, 110–122. <https://doi.org/10.1016/j.jes.2019.02.028>
- Özcan, A., Oturan, M.A., Oturan, N., Şahin, Y., 2009. Removal of Acid Orange 7 from water by electrochemically generated Fenton’s reagent. *J. Hazard. Mater.* 163, 1213–1220. <https://doi.org/10.1016/j.jhazmat.2008.07.088>
- Jiang, Y., Khan, A., Huang, H., Tian, Y., Yu, X., Xu, Q., Mou, L., Lv, J., Zhang, P., Liu, P., Deng, L., Li, X., 2019. Using nano-attapulgitic clay compounded hydrophilic urethane foams (AT/HUFs) as biofilm support enhances oil-refinery wastewater treatment in a biofilm membrane bioreactor. *Sci. Total Environ.* 646, 606–617. <https://doi.org/10.1016/j.scitotenv.2018.07.149>
- Keiluweit, M., Nico, P., Harmon, M.E., Mao, J., Pett-Ridge, J., Kleber, M., 2015. Long-term litter decomposition controlled by manganese redox cycling. *Proc. Natl. Acad. Sci. U. S. A.* 112, E5253–E5260. <https://doi.org/10.1073/pnas.1508945112>
- Krumbein, W.E., Altmann, H.J., 1973. A new method for the detection and enumeration of manganese oxidizing and reducing microorganisms. *Helgoländer Wissenschaftliche Meeresuntersuchungen* 25, 347–356. <https://doi.org/10.1007/BF01611203>
- Maniyam, M.N., Ibrahim, A.L., Cass, A.E.G., 2018. Decolourization and biodegradation of azo dye methyl red by *Rhodococcus* strain UCC 0016. *Environ. Technol.* 1–15. <https://doi.org/10.1080/09593330.2018.1491634>
- Matsushita, S., Komizo, D., Cao, L.T.T., Aoi, Y., Kindaichi, T., Ozaki, N., Imachi, H., Ohashi, A., 2018. Production of biogenic manganese oxides coupled with methane oxidation in a bioreactor for removing metals from wastewater. *Water Res.* 130, 224–233. <https://doi.org/10.1016/j.watres.2017.11.063>
- Mayanna, S., Peacock, C.L., Schäffner, F., Grawunder, A., Merten, D., Kothe, E., Büchel, G., 2015. Biogenic precipitation of manganese oxides and enrichment of heavy metals at acidic soil pH. *Chem. Geol.* 402, 6–17. <https://doi.org/10.1016/j.chemgeo.2015.02.029>
- Meerbergen, K., Willems, K.A., Dewil, R., Van Impe, J., Appels, L., Lievens, B., 2018. Isolation and screening of bacterial isolates from wastewater treatment plants to

- decolorize azo dyes. *J. Biosci. Bioeng.* 125, 448–456.
<https://doi.org/10.1016/j.jbiosc.2017.11.008>
- Rawat Deepak, Vandana Mishra, Radhey Shyam Sharma. 2016. Detoxification of azo dyes in the context of environmental processes. *Chemosphere* 155, 591-605
- Spiro, Thomas G., John R. Bargar, Garrison Sposito, and Bradley M. Tebo , 2010. Bacteriogenic manganese oxides. *Accounts of Chemical Research*, Vol. 43, No. 1, 2–9.
- Sunda, W.G., Kieber, D.J., 1994. Oxidation of humic substances by manganese oxides yields low-molecular-weight organic substrates. *Nature* 367, 62–64.
<https://doi.org/10.1038/367062a0>
- Tebo, B.M., Johnson, H.A., McCarthy, J.K., Templeton, A.S., 2005. Geomicrobiology of manganese(II) oxidation. *Trends Microbiol.* 13, 421–428.
<https://doi.org/10.1016/j.tim.2005.07.009>
- Wang, W., Shao, Z., Liu, Y., Wang, G., 2009. Removal of multi-heavy metals using biogenic manganese oxides generated by a deep-sea sedimentary bacterium - *Brachybacterium* sp. strain Mn32. *Microbiology* 155, 1989–1996. <https://doi.org/10.1099/mic.0.024141-0>
- Watanabe, J., Tani, Y., Chang, J., Miyata, N., Naitou, H., Seyama, H., 2013. As(III) oxidation kinetics of biogenic manganese oxides formed by *Acremonium strictum* strain KR21-2. *Chem. Geol.* 347, 227–232. <https://doi.org/10.1016/j.chemgeo.2013.03.012>
- Wu, R., Wu, H., Jiang, X., Shen, J., Faheem, M., Sun, X., Li, J., Han, W., Wang, L., Liu, X., 2017. The key role of biogenic manganese oxides in enhanced removal of highly recalcitrant 1,2,4-triazole from bio-treated chemical industrial wastewater. *Environ. Sci. Pollut. Res.* 24, 10570–10583. <https://doi.org/10.1007/s11356-017-8641-1>
- Yatome, C., Yamada, S., Ogawa, T., Matsui, M., 1993. Degradation of Crystal violet by *Nocardia corallina*. *Appl. Microbiol. Biotechnol.* 38, 565–569.
<https://doi.org/10.1007/BF00242956>
- Yu, L., Zhang, X. yu, Xie, T., Hu, J. mei, Wang, S., Li, W. wei, 2015. Intracellular azo decolorization is coupled with aerobic respiration by a *Klebsiella oxytoca* strain. *Appl. Microbiol. Biotechnol.* 99, 2431–2439. <https://doi.org/10.1007/s00253-014-6161-1>
- Zhang, Y., Zhu, H., Szewzyk, U., Geissen, S.U., 2015. Removal of pharmaceuticals in aerated biofilters with manganese feeding. *Water Res.* 72, 218–226.
<https://doi.org/10.1016/j.watres.2015.01.009>
- Zhao, G., Li, E., Li, J., Liu, Feifei, Liu, Fei, Xu, M., 2019. Goethite hinders azo dye bioreduction by blocking terminal reductive sites on the outer membrane of shewanella decolorationisS12. *Front. Microbiol.* 10, 1–9. <https://doi.org/10.3389/fmicb.2019.01452>

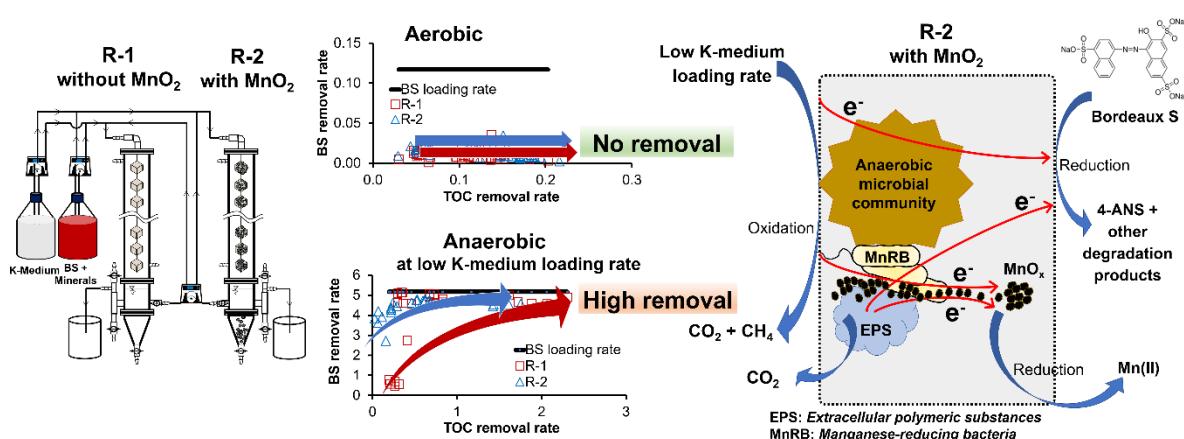
This page is intentionally left blank

Chapter 6: Decolorization of an azo dye Bordeaux S under manganese-oxidizing and manganese-oxides-reducing conditions

Part of the research contained within this chapter has been published as:

“*Mn(II) oxidation and manganese-oxide reduction on the decolorization of an azo dye*”, Ahmad Shoiful, Hiromi Kambara, Linh Thi Thuy Cao, Shuji Matsushita, Tomonori Kindaichi, Yoshiteru Aoi, Noriatsu Ozaki, and Akiyoshi Ohashi*. *International Biodeterioration & Biodegradation* 146, 104820, accepted on 14 October 2019 (Elsevier, IF=3.824).

Graphical abstract



Abstract

The development of biological processes for treating azo-dye-contaminated waters is an important objective. Herein, we investigated the effects of Mn(II) oxidation and manganese-oxide reduction on the removal of the azo dye, Bordeaux S (BS), under aerobic and anaerobic conditions using two reactors, one with installed abiotic-MnO₂, and one devoid of abiotic-MnO₂. Under aerobic conditions, very little BS was removed, even at the highest Mn(II) oxidation rate (0.22 kg Mn(II) m⁻³ d⁻¹), indicating that Mn(II) oxidation has essentially no effect on azo-dye removal. In contrast, under anaerobic conditions, the reduction and/or presence of MnO_x was found to have an effect. Although BS decolorization increased with increasing K-medium loading, and the decolorization rate of 4.75 kg m⁻³ d⁻¹ was achieved using both reactors, the reactor with abiotic-MnO₂ performed better at low K-medium loading rates. The presence of MnO_x induced higher secretion of extracellular polymeric substances, which serve as electron donors for the decolorization of BS under K-medium-deficient conditions. BS decolorization is caused by the simple cleavage of the azo bond to the 4-amino-1-naphthalenesulfonic acid moiety, and further degradation did not occur under anaerobic conditions. Although methane was produced even in the presence of MnO_x, we conclude that *Methanosaeta* were inhibited.

Keywords: decolorization, azo dye, manganese oxidation, manganese-oxide reduction, *Methanosaeta*, methane production

6.1 Introduction

The textile industry sector significantly contributes to the economic growth of developing countries (Hossain et al., 2018); however, the wastewater discharged by textile industries is considered to be a major cause of river-water pollution. In general manufacturing, approximately 90% of the textile dyes bind to woven fabrics, with 10% discharged as effluent (Nimkar, 2018). Azo dyes, which are among the most widely used dyes in textile industries, persist with little degradation in the natural environment, and their degradation products are potentially mutagenic and carcinogenic, and are major health concerns (Imran et al., 2015; Brüsweiler and Merlot, 2017). The general population is also generally concerned about exposure to colored water. Therefore, the development of eco-friendly and cost-effective technologies to treat azo-dye-containing wastewater and to decolorize it to harmless products is important.

Biological processes are very attractive for treating azo-dye-contaminated waters, which is due to advantages that include lower operational costs and lower amounts of chemical reagents when compared to physicochemical methods (Saratale et al., 2011). The treatment of azo dye-containing wastewaters using bioreactors has been extensively studied under aerobic and anaerobic conditions (Kolekar et al., 2012; Spagni et al., 2012). Anaerobic conditions are reportedly more effective for decolorizing azo dyes than aerobic conditions (Saratale et al., 2011). However, it is impossible to achieve complete mineralization of azo dyes under anaerobic conditions because persistent metabolites are produced.

Manganese oxides are present in large quantities in the natural environments, such as in soils and sediments; these oxides are naturally formed through the biological oxidation of Mn(II) by manganese-oxidizing bacteria (MnOB) under aerobic conditions and are referred to hereinafter as “biogenic manganese oxides” (bio-MnO_x) (Tebo et al., 2004). To the best of our knowledge, the ability of bio-MnO_x to decolorize azo dyes has never been investigated. However, biological Mn(II) oxidation and the reduction of Mn(IV) play important roles in the biogeochemical cycles of organic carbon, nitrogen, sulfur, and many elements, and bio-MnO_x catalyzes the degradation of organic contaminants through redox processes (Tebo et al., 2005; Borch et al., 2010; Hyun et al., 2017). Some reports on the effects of bio-MnO_x exist. Tran et al. (2018) reported that the presence of MnOB coupled with the generated bio-MnO_x enhances the degradation of organic pollutants. Bio-MnO_x have particular poor crystalline structures and chemical properties, which facilitate the removal of organic and inorganic compounds, including methylene blue, through redox reactions and/or adsorption processes (Furgal et al., 2014; Bai et al., 2016; Zhou et al., 2016). Not only have bio-MnO_x been reported to oxidize and adsorb several dyes, but abiotic-MnO₂ does so too (Chen et al., 2013; Das and Bhattacharyya, 2014; Clarke et al., 2013; Remucal et al., 2014; Islam et al., 2019). We reported the successful enrichment of MnOB in a DHS reactor for the continuous production of bio-MnO_x particles (Cao et al., 2015; Matsushita et al., 2018). The enzymatic generation of extracellular superoxide radicals has been identified to be responsible for the indirect oxidation of Mn(II) to bio-MnO_x (Learman et al., 2011). We expect that the generated superoxide radicals not only play important roles in Mn(II) oxidation but also simultaneously attack the azo dye. The continuous generation of superoxide radicals with the production of bio-MnO_x in the bioreactor may contribute to the decolorization of the azo dye during wastewater treatment. Therefore, we hypothesize that MnOB together with Mn(II) oxidation and the generated bio-MnO_x, can biodegrade azo dyes.

Manganese oxides are the second-most abundant electron acceptors for microbial respiration in the environment after Fe(III) (Lovley, 2011). Under anaerobic conditions, MnO_x can act as electron acceptors during the degradation of organic compounds such as BTEX (benzene, toluene, ethylbenzene, and xylenes), naphthalene, and pharmaceuticals by dissimilatory metal-reducing bacteria (Langenhoff et al., 1996; Villatoro-Monzón et al., 2003; Dorer et al., 2016; Ghattas et al., 2017; Liu et al., 2018a), and direct extracellular electron transfer (DEET) has been reported to play a key role in the degradation mechanism (Lovley, 2011). Ng et al. (2014) reported that *Shewanella xiamenensis*, a widely known dissimilatory manganese-reducing bacterium, is capable of decolorizing azo dye, and this capability was improved by the addition of manganese. In a more-recent study, *Geobacter sulfurreducens*, an electroactive bacterium (EAB) that can respire on extracellular electron acceptors, is able to decolorize the methyl orange azo dye, exhibiting a higher decolorization ability than other decolorizing microbial strains, even though this strain does not contain azo reductase genes (Liu et al., 2017). In addition, the presence of metal oxides such as $Fe(OH)_3$ and Fe_3O_4 , reportedly enhances electron-transfer activity, leading to high performance for the decolorization of azo dye (Li et al., 2017; Sharma et al., 2016; Wang et al., 2018). Even under anoxic conditions, manganese oxides promote the abiotic degradation of diclofenac through redox chemistry (Liu et al., 2018b). Consequently, we expect that the reduction of manganese oxides to Mn(II) will enhance the degradation of azo dyes under anaerobic conditions.

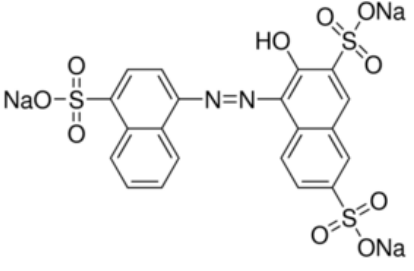
In this study, we investigated the effects of Mn(II) oxidation and MnO_x reduction on the removal of an azo dye through batch and continuous experiments. The batch experiment was initially conducted to determine the effects of abiotic- MnO_2 on azo-dye removal by chemical adsorption and/or oxidation. The continuous experiments, which used two down-flow hanging sponge (DHS) reactors, were performed over the long term under aerobic and anaerobic conditions, and the difference in the biological azo-dye-removal efficiencies of the systems in the presence and absence of abiotic- MnO_2 was determined. Abiotic- MnO_2 was installed with the expectation that it will enrich MnOB in the reactor, resulting in enhanced biological Mn(II) oxidation under aerobic conditions, and to act as a conductive material that accelerates electron transfer, and as an oxidizing agent or electron acceptor under anaerobic conditions.

6.2 Materials and methods

6.2.1 Azo dye

Bordeaux S (BS), which was purchased from Fujifilm Wako Pure Chemical Co., Ltd. (Tokyo, Japan), was used as the sole azo dye in this study. The chemical structure and properties of BS are provided in Table 6.1 as follows.

Table 6.1 Chemical structure and properties of Bordeaux S.

Chemical structure	Properties	
	CAS	915-67-3
	Molecular Formula	C ₂₀ H ₁₁ N ₂ Na ₃ O ₁₀ S ₃
	Average mass	604.47
	Water solubility	60000 mg L ⁻¹
	Log P (oct-water)	-5.13
	Henry's Law Constant	2.68E-30 atm·m ³ /mol

Source: SRC PhysProp Database

6.2.2 Batch experiments

6.2.2.1 Chemical batch experiment with MnO₂

Abiotic-MnO₂ (0.5 g) (Kishida Chemical Co. Ltd., Japan) was added to 50 mL of a 10 mg L⁻¹ solution of BS in a glass tube with a parafilm-covered screw cap. The tube was shaken in a horizontal shaker (MMS-1, EYELA, Tokyo, Japan) at 120 rpm and room temperature in the dark. The liquid was sampled at predetermined time intervals and the BS concentration was determined. The batch experiments were performed in triplicate.

6.2.2.2 Abiotic anaerobic experiment

Abiotic anaerobic experiment was performed to investigate whether decolorization of BS was obtained by biological reaction or chemical reaction. A 50 mL of BS (50 mg/L) in 50 mL glass tube with silicone rubber and aluminum cap was added with trace elements, K-medium, or MnO₂. To create anaerobic conditions, the glass tube was degassed (vacuum) the head space (5 min), and then purged with nitrogen gas (5 min). This degassed-purged cycle was performed for three times. The glass tubes were placed in a dark chamber. BS concentration was measured at predetermined time intervals.

6.2.2.3 Chemical reduction by a reducing agent sodium sulfide (Na₂S)

Chemical reduction of BS by sodium sulfide was conducted to investigate whether the decolorization of BS under anaerobic conditions was caused by reducing conditions or

mediated by biological reaction of microbes. A 50 mL of BS (240 mg/L) in 50 mL glass tube with silicone rubber and aluminum cap was added with trace elements, K-medium, or MnO₂. The glass tube was degassed (vacuum) the head space (5 min) and then purged with nitrogen gas (5 min). This degassed-purged cycle was performed for three times. A 0.01M Na₂S₉H₂O was injected to the glass tube. The glass tubes were subsequently shaken at 120 rpm, dark conditions and room temperature (MMS-1, EYELA, Tokyo, Japan). BS concentration was determined by UV spectrophotometer at predetermined time intervals.

6.2.3 Continuous azo dye treatment

6.2.3.1 Synthetic dye wastewater

The synthetic dye wastewater used in this study was composed of BS, K-medium (consisting of peptone casein (Nacalai Tesque Inc., Kyoto, Japan) and dried yeast extract (Nacalai Tesque Inc., Kyoto, Japan) (4:1, w/w)), minerals and trace elements. To avoid the precipitation of the K-medium and BS, the author prepared two substrate tanks. One tank contained K-medium and phosphate buffer (KH₂PO₄ (0.602 mg L⁻¹), and Na₂HPO₄ (6.22 mg L⁻¹)). The other tank contained BS, Mn(II) (MnCl₂·4H₂O), minerals (CaCl₂·2H₂O (0.05 mg L⁻¹), MgSO₄·7H₂O (0.2 mg L⁻¹), Fe₂SO₄·5H₂O (0.1 mg L⁻¹)), and trace elements (CuSO₄·5H₂O (0.025 mg L⁻¹), NaSeO₄ (0.005 mg L⁻¹), NiCl₂·6H₂O (0.019 mg L⁻¹), CoCl₂·6H₂O (0.024 mg L⁻¹), Na₂MoO₄·2H₂O (0.022 mg L⁻¹), H₃BO₃ (0.001 mg L⁻¹), ZnSO₄·7H₂O (0.043 mg L⁻¹)). The substrate tanks were purged with nitrogen and connected to a nitrogen-filled gas bag during the experiment, prior to providing the substrates to the reactors.

6.2.3.2 Bioreactor set-up and operational conditions

Two identical DHS reactors were used in this study (Fig. 6.1). One reactor (R-1) was devoid of abiotic-MnO₂, while the other reactor (R-2) contained abiotic-MnO₂. Each reactor consisted of a column (height: 75 cm; inner diameter: 4 cm) and a string of 20 polyurethane sponge cubes (volume: 2 × 2 × 2 cm each; total volume: 160 cm³) that were diagonally interconnected in series. Activated sludge collected from the aeration tank of a municipal sewage treatment plant in Higashihiroshima was used as the inoculum. Before setting up the DHS reactors, the sponges in R-1 were soaked in activated sludge. For R-2, the sponges were squeezed and soaked in 1 L of a suspension of activated sludge containing 100 g of abiotic-MnO₂ that was used for

inoculation and MnO_2 installation. The reactors were placed in a dark room at 26 °C to avoid any effect of light on the decomposition of BS.

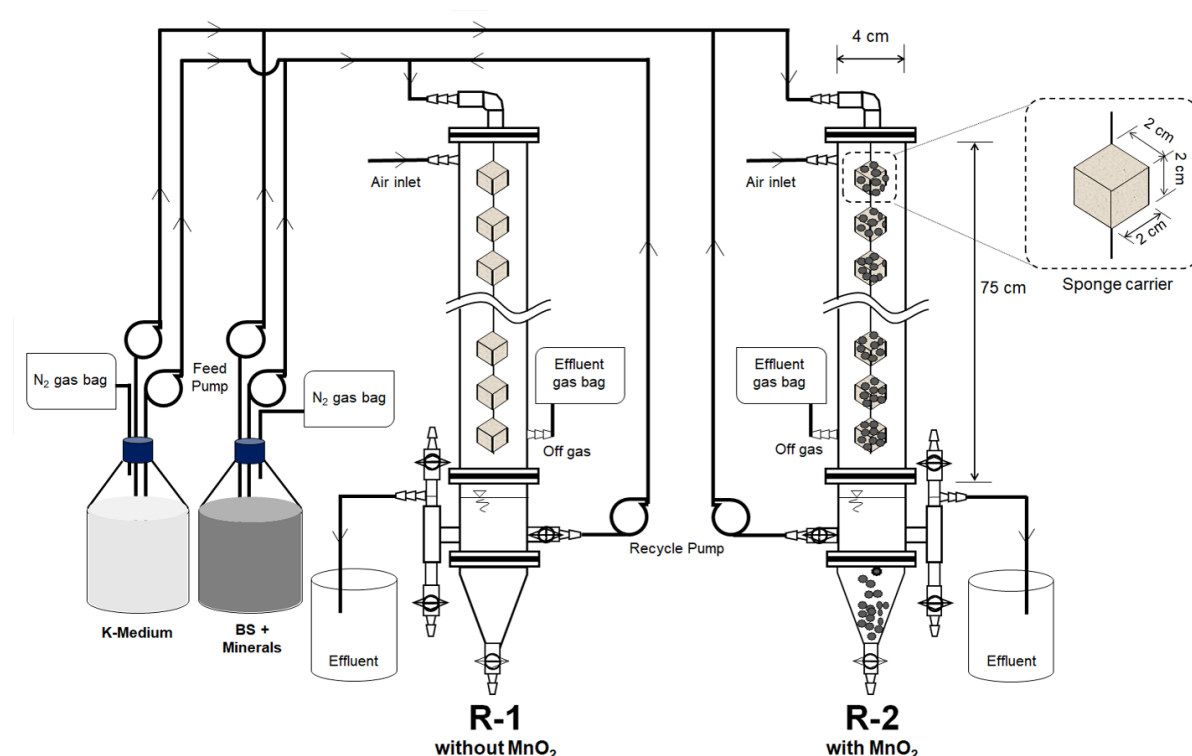


Figure 6.1 DHS reactor configurations.

Table 6.2 Operational conditions of the DHS reactors.

Conditions	Aerobic		Anaerobic			
	1	2	3	4	5	6
Phase						
Operation time (d)	0–24	25–116	117–355	356–404	405–472	473–534
Bordeaux S (mg L^{-1})	0	5–10	5–30	60	120	240
K-medium (mg COD L^{-1})	25	25–50	0–100	100–350	25–350	25–350
Mn (II) (mg L^{-1})	5–10	5–20	0	0	0	0
HRT (h)	2.1	2.1	1–2.1	1	1	1
Q air (L h^{-1})	1.6	1.6	0	0	0	0

The reactors were operated for 534 d over six phases, as summarized in Table 1. Under aerobic conditions (Phases 1 and 2), the reactors were supplied with air at a flow rate of 1.6 L h^{-1} . Anaerobic conditions were applied in Phases 3–6 by terminating the air supply from day 117, and replacing it with N_2 at a flow rate of 0.046 L h^{-1} from day 265. The off-gas was collected in a Smart Bag PA gas bag (GL Science Inc., Tokyo, Japan). The water effluents were recirculated at a 1:10 flow ratio of influent to recirculation.

6.2.4 Analytical methods

The water samples were filtered through 0.45- μm membrane filters (Advantec, Tokyo, Japan). The BS concentration was determined by colorimetry at its maximum absorption wavelength ($\lambda_{\text{max}} = 522 \text{ nm}$) using a UV-visible spectrophotometer (Shimadzu UV-1800, Kyoto, Japan). Total organic carbon (TOC) as non-purgeable organic carbon (NPOC) was measured using a TOC analyzer (Shimadzu TOC-VCSH, Kyoto, Japan). Chemical oxygen demand (COD) concentrations were analyzed by colorimetry using a Hach Spectrophotometer (Hach Co. DR2800, Loveland, CO, USA). Mn(II) was determined using an inductively coupled plasma emission spectrometer (Shimadzu ICPE-9000, Kyoto, Japan) after filtering through a 0.2- μm PTFE membrane filter (Advantec, Tokyo, Japan).

The effluent gas was analyzed using a gas chromatograph (GC-8A) equipped with a thermal conductivity detector (TCD) and a column packed with 5A molecular sieves (Mesh 60/80, 3.0 m in length, 3.0 mm in diameter) (all from Shimadzu, Kyoto, Japan). Helium was used as the carrier gas. The injector and detector temperatures were set to 150 °C.

The degradation products of BS were analyzed with an HPLC system consisting of an LC-10AD VP pump, a DGU-14A degasser, an SIL-10AD VP autoinjector, an SCL-10A VP controller, a CTO-10A column oven, and an SPD-10AV VP UV-Vis detector (All from Shimadzu, Kyoto, Japan) and fitted with an Inert Sustain C-18 column (5 μm , 4.6 mm x 150 mm, GL. Sciences, Tokyo, Japan). A mixture of methanol, water, and H_3PO_4 (50:49.7:0.3, v/v/v) was used as the mobile phase carrier at a flow rate of 0.6 ml min^{-1} . The UV-Vis detector was set to 220 nm.

6.2.5 Microbial community analysis

Biomass was sampled from the sponge carriers (the upper, middle and lower portions) of R-1 and R-2 on days 116, 166 and 534. The samples taken from the three portions of the reactor on each day were mixed in equal amounts to obtain one sample and six biomass samples in total were analyzed for microbial community. DNA extraction was performed using FastDNA® SPIN Kit for Soil (MP188 Biomedicals, Ohio, USA) according to the method reported by Noorain et al. (2019). The DNA samples were sent to Hokkaido System Science Co. Ltd (Sapporo, Japan) for PCR amplification with a primer set of the V3-V4 region: 341F (5'-CCTACGGGGNGGCWGCAG-3') and 805R (5'-GGACTACHVGGGTATCTAATCC-3'),

and sequenced using the Illumina MiSeq platform with a Miseq Reagent Kit v3 (Illumina Inc., San Diego, CA, USA).

The raw sequence data were trimmed using the Cutadapt software (version 1.1) (Martin, 2011) to remove adapter sequences and primers from sequencing reads with the default minimum overlap length of 3 and the default maximum allowed error rate of 0.2. Noise and low-quality sequence reads were removed by Trimmomatic (version 0.32) (Bolger et al., 2014) when the quality per base dropped below 20 bp in a sliding window of 20 bp (SLIDINGWINDOW:20:20) and the minimum length of the reads were below 50 bp (MINLEN:50). The clean reads were assembled using fastq-join software (version 1.1.2-537) (Aronesty, 2013) and then analyzed using the QIIME pipeline software (version 1.8.0) (Caporaso, et al., 2010). Sequences with greater than 97% similarity were clustered into the same operational taxonomic units (OTUs) using the UCLUST method (Edgar R.C., 2010), which were then classified using MiDAS taxonomy (version 1.20) (McIlroy et al., 2015).

The sequence data were deposited in the DDBJ database under DDBJ/EMBL/GenBank accession number DRA008483.

6.2.6 Statistical analysis

The alpha-diversity indices (Simpson's index of diversity (1-D), Shannon (H), Evenness and Chao-1) of each sample were calculated using PAST (PAleontological STatistics) software (version 3.20) (Hammer et al., 2001).

6.3 Results

6.3.1 Batch experiments

6.3.1.1 Chemical batch experiment with MnO₂

Prior to continuous biological decolorization experiments using the two reactors, we initially conducted batch decolorization experiments to investigate the inherent dye-removal ability of abiotic-MnO₂, which revealed that BS removal by chemical adsorption or oxidation does occur, but at the very low rate of approximately 0.05 mg g⁻¹ abiotic-MnO₂ (Fig. 6.2), which suggests that the contribution of abiotic-MnO₂ to BS removal in the Mn(II) oxidation reactor is negligible.

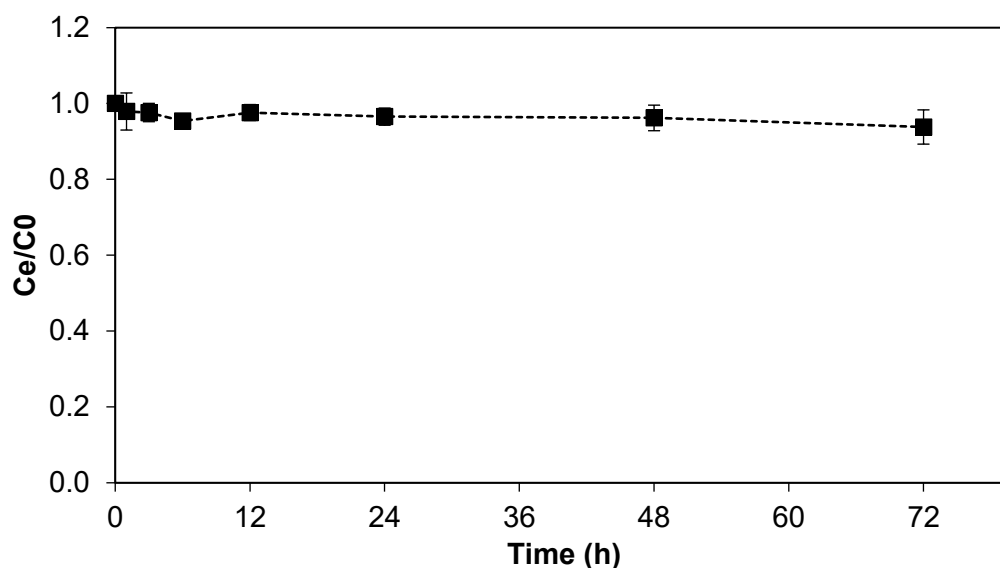


Figure 6.2 Batch decolorization experiments for BS (10 mg L^{-1}) by abiotic- MnO_2 (0.5 g).

6.3.1.2 Decolorization of BS under abiotic anaerobic conditions

Batch experiments of abiotic decolorization of BS under anaerobic conditions were performed to investigate whether decolorization of BS without any microbial activity was possible or not. The results showed that decolorization of BS under abiotic anaerobic conditions did not occur even in the presence of electron donor (K-medium) or electron acceptor (MnO_2) (Fig. 6.3).

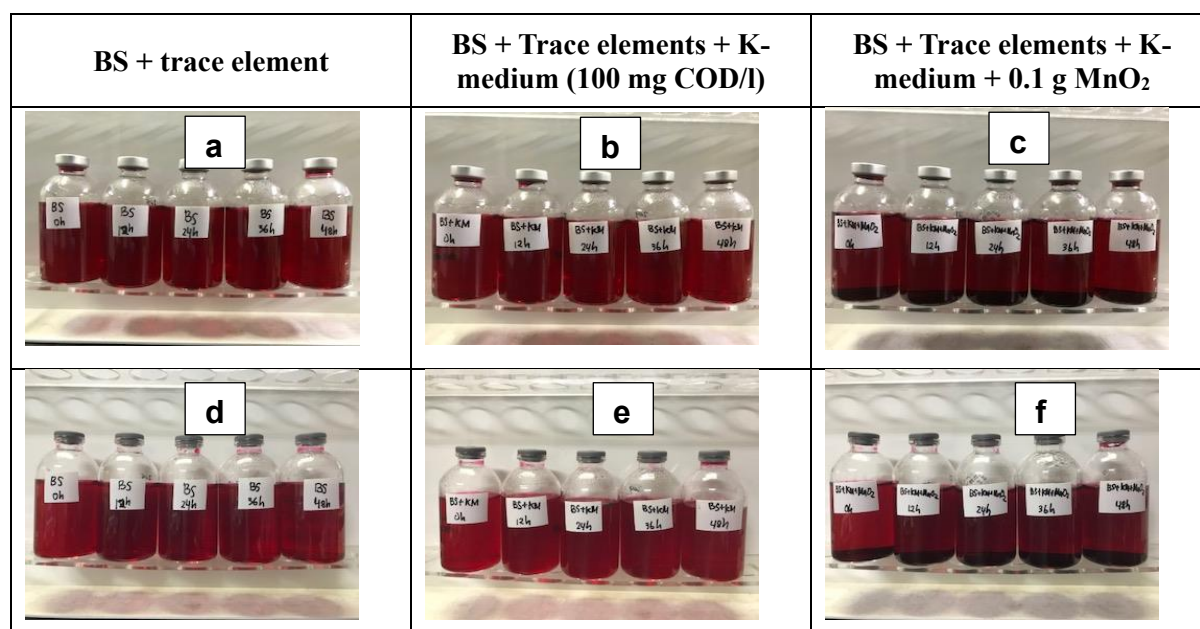


Figure 6.3 Appearance of abiotic anaerobic BS decolorization experiment with different substrates at 0 h (a-c), and after 48 h incubation (d-f).

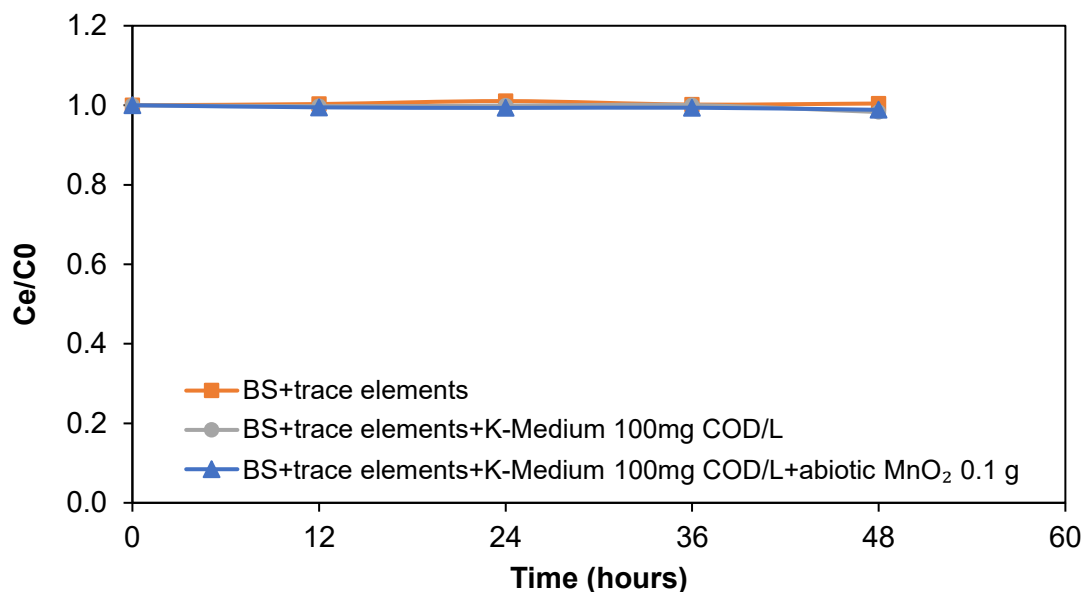


Figure 6.4 Batch decolorization of BS under abiotic anaerobic conditions with different substrate compositions.

6.3.1.3 Chemical decolorization of BS using Na₂S

Chemical decolorization of BS was performed using a strong reductant Na₂S.9H₂O (0.01M). The results showed that chemical reduction of azo dye by a strong reductant Na₂S was possible (Fig 6.5). Based on visual observation of dye solutions, black color appeared immediately after Na₂S addition, and the absorbance at 522 nm decreased (Fig 6.5.1d, 2d, 3d). If Na₂S was added to the BS solution, without any other chemical compounds, a significant decolorization was observed after 36 h, the color changed to reddish, and the color turned yellow after 48 h incubation (Fig 6.5.1c). According to the UV-Vis spectrophotometer results, the decrease of absorbance at wavelength (λ) of 522 nm was observed, and the its peak disappeared after 48 h incubation (Fig. 6.5.1d). In the presence of other chemical compounds, such as K-medium or MnO₂, no color changes were visual observed, but the absorbance at 522 nm decreased. The decolorization of BS by chemical reduction of Na₂S with different substrate compositions were shown in Figure 6.6 as follows.

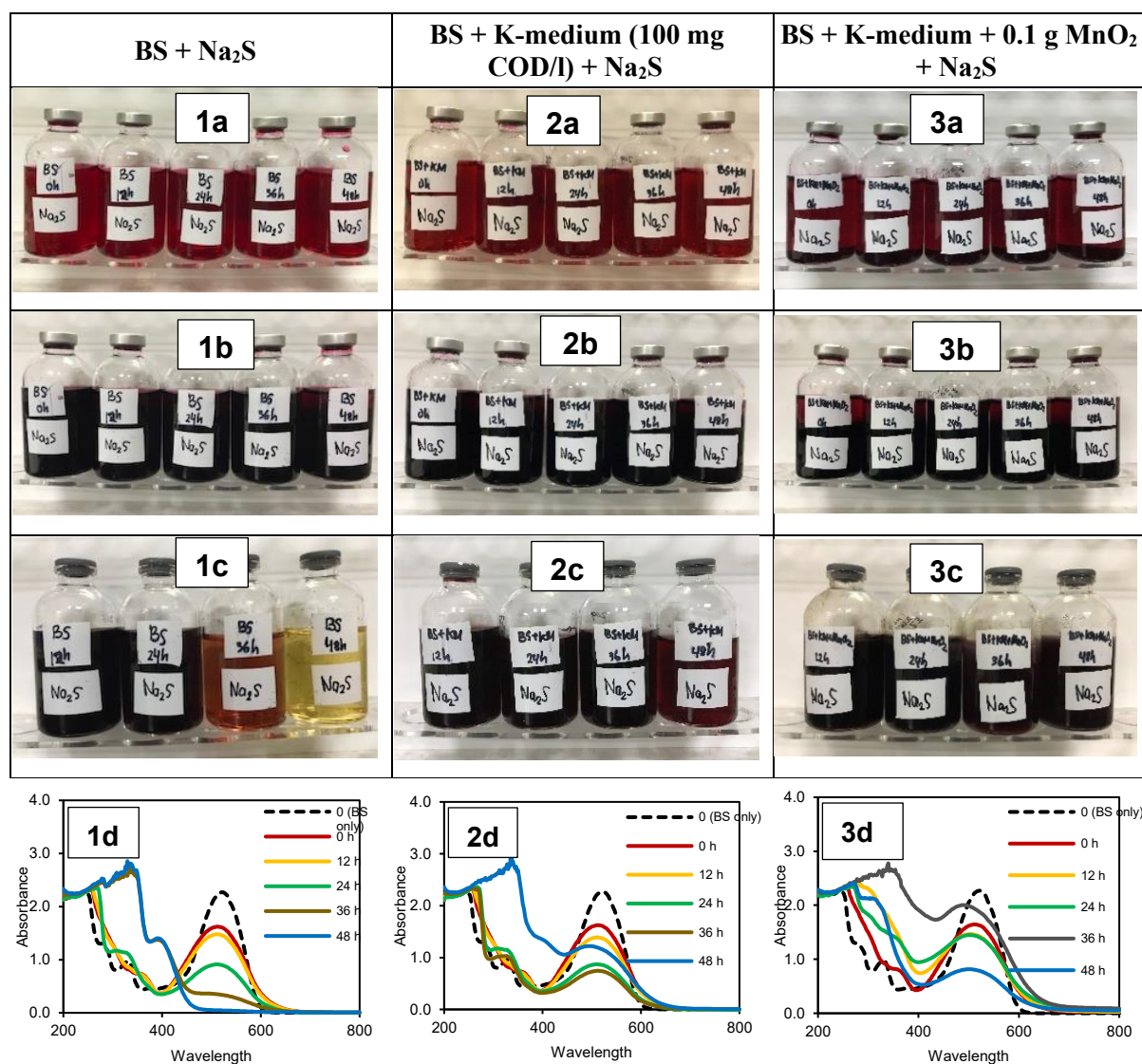


Figure 6.5 Appearance of chemical BS decolorization using 0.01M Na₂S.9H₂O with three different substrate compositions; (1): BS + Na₂S, (2): BS + K-medium (100 mg COD/l) + Na₂S, and (3): BS + K-medium + 0.1 g MnO₂ + Na₂S, at the conditions of before Na₂S.9H₂O addition (1a, 2a, 3a), immediately after addition (1b, 2b, 3b), after 48h incubation (1c, 2c, 3c), and UV-Vis spectrophotometer analysis of each condition (1d, 2d, 3d).

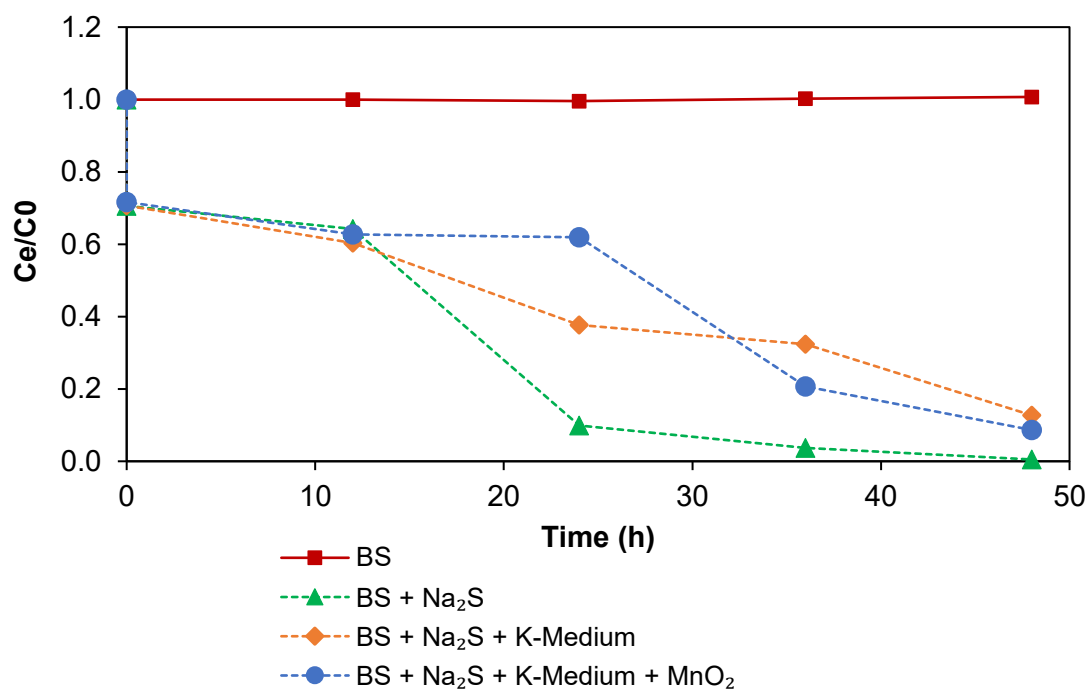


Figure 6.6 Decolorization of BS using 0.01M Na₂S·9H₂O with different substrate compositions.

6.3.2 Reactor performance

6.3.2.1 Aerobic conditions

Figure 6.7 shows the performance of reactors R-1 and R-2. The 24-d period of Phase 1 was designed to enrich MnOB especially in R-2, which contains abiotic-MnO₂. In this phase, the reactors were supplied with the organic substrate containing K-medium (25 mg COD L⁻¹ (= 10.7 mg TOC L⁻¹)) and Mn(II) (5 mg L⁻¹), but no BS. Both reactors achieved a TOC removal of approximately 80% in this phase. Mn(II) was removed even in the absence of abiotic-MnO₂ (as in R-1); the highest Mn(II)-removal rates exhibited by R-1 and R-2 were 0.065 and 0.11 kg m⁻³ d⁻¹, respectively, which indicates that MnOB was successfully enriched despite the Mn(II) oxidation potential of R-1 being significantly lower than that of R-2.

From Phase 2 onwards, BS was provided to both reactors, initially at a low loading rate of 0.11 kg m⁻³ d⁻¹. BS removal was inefficient under these conditions, with less than 20% removed from both reactors to day 87. The Mn(II) concentration was then gradually increased to 20 mg L⁻¹ with the expectation of enhancing Mn(II) oxidation, which may lead to more efficient BS removal. As expected, the Mn(II) removal rate was enhanced to 0.22 kg Mn(II) m⁻³ d⁻¹ in R-2, but BS removal was not improved. It seems that Mn(II) oxidation under aerobic

conditions hardly contributes to BS removal. Despite no BS bio-degradation occurring, higher TOC removal efficiency was observed in R-2 compared to R-1, which exhibited little Mn(II) oxidation (Fig. 6.7(d)). Mn(II) oxidation was very effective for removing the organic substances in the K-medium. In addition, the precipitation of black particles was observed at the bottom of the R-2 reactor, presumably due to Mn(II) oxidation.

6.3.2.2 Anaerobic conditions

In Phase 3, we changed the operational conditions from aerobic to anaerobic in the expectation that decolorization would occur. To create anaerobic conditions, the air supply was terminated at day 117 and nitrogen gas was provided (instead of air) from day 265 onwards. As a result, significant decolorization was observed, as expected (Fig. 6.7(a)). We believe that this decolorization is the result of the reduction of BS coupled with the oxidation of the organic substrate. To investigate this hypothesis, influent wastewater devoid of the K-medium was supplied during days 166–185; as a result, the effluent became BS colored. This short experiment revealed that the organic substance is needed to decolorize the BS. Reductive decolorization is dependent on available organic substrates as electron donors; hence we varied the K-medium concentration in the influent over the 0-100 mg COD L⁻¹ range. BS-decolorizing efficiency was observed to increase with increasing K-medium concentration, and very little difference in decolorization efficiency was observed between R-1 and R-2. Surprisingly, we observed a significant increase in the level of Mn(II) in the effluent from each reactor, although the Mn(II) concentration gradually decreased with elapsed time. This observation is consistent with the reduction of the manganese oxides (MnO_x) that were initially installed (abiotic-MnO₂) or produced (bio-MnO_x) during Phase 2 in these reactors. Notably, no direct relationship between MnO_x reduction and BS removal was observed.

Phases 4 – 6 were conducted in order to investigate the BS-removal potential and the effect of organic substances on removal. The influent BS concentration was increased in a stepwise fashion to 60, 120 and 240 mg L⁻¹ in Phases 4, 5 and 6, respectively, which correspond to BS loading rates of 1.44, 2.88 and 5.76 kg m⁻³ d⁻¹. High BS removal efficiencies were observed through Phases 4 – 6, except for the time spent under lower K-medium loading conditions. The highest BS removal rate of approximately 5 kg m⁻³ d⁻¹ was attained at high a K-medium concentration, with approximately 90% of the BS removed at the end of Phase 6,

and very little difference observed between R-1 and R-2 (Fig. 6.7(a)). Hence, the results reveal that it is possible to decolorize BS at high removal rates under anaerobic conditions.

To investigate the effect of K-medium on BS removal, the influent K-medium was gradually decreased from 350 to 50 mg COD L⁻¹ during Phase 5 and increased in Phase 6. The relationships between the BS-removal rates and COD-removal rates are shown in Figure 6.8. We found that a certain COD-removal rate was needed to achieve high BS-removal efficiency; the BS-removal efficiency declined along with the decreasing level of supplied K-medium. This tendency was observed for both R-1 and R-2, and suggests that K-medium functions as an electron donor during BS removal.

On the other hand, a large difference between R-1 and R-2 was also observed under very low K-medium loading conditions, where high BS-removal efficiency was achieved in R-2 but not in R-1. For example, when a low K-medium concentration of 25 mg COD L⁻¹ was supplied, the average BS-removal efficiency was maintained at more than 70% in R-2, but was significantly lower, at 11%, in R-1 (Fig. 6.7(a)). Although MnO_x was continuously reduced until the end of experiment in R-2 (with sponge carriers containing abiotic-MnO₂), reduction in R-1 quickly stopped in the middle of Phase 3 (Fig. 6.7(c)), presumably because the accumulated bio-MnO_x had been consumed at that time. These results revealed that the presence of MnO_x affects BS removal. High BS removal rates are even expected at low COD concentrations when combined with MnO_x reduction (Fig. 6.14).

Even though BS decolorized at high rates, unfortunately good COD-removal performance was not obtained. High COD concentrations were detected in the effluents at all operational times (Fig. 6.7(e)). As shown in Figure 6.9, somewhat of a relationship was observed between COD removal and loading rate. The COD removal rate seemed to decrease linearly with decreasing COD loading rate, leading to no COD removal at COD loading rates of 3.3 and 6.6 kg m⁻³ d⁻¹ in Phases 5 and 6, respectively. These values were almost coincident with the BS loading rates, which means that the influent COD concentration of the BS was completely maintained in the effluent. Therefore, we found that, although the azo bond of the BS was certainly cleaved, further decomposition of the metabolites did not occur, irrespective of the occurrence of MnO_x reduction. HPLC revealed that BS was degraded to 4-amino-1-naphthalenesulfonic acid (Fig 6.15).

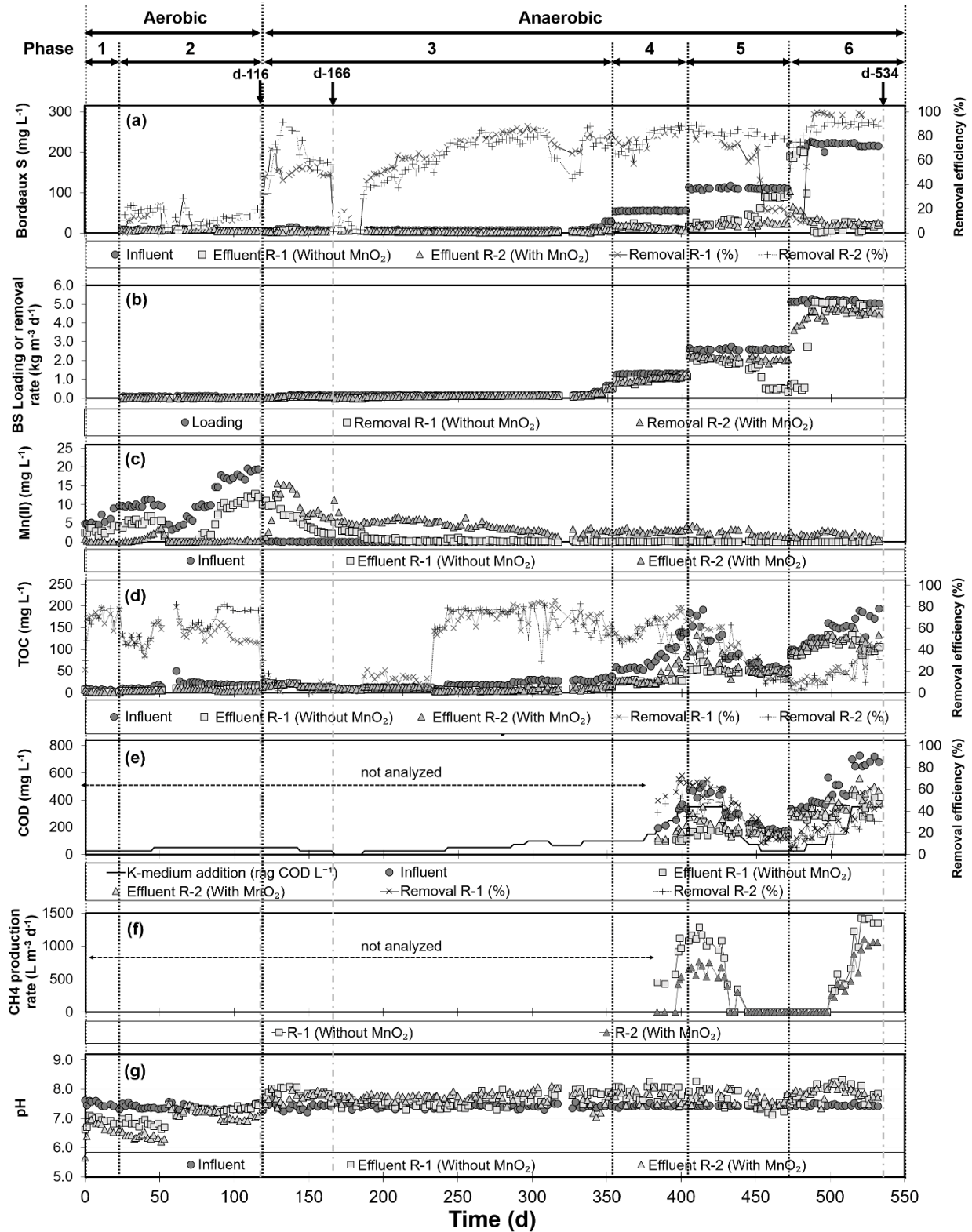


Figure 6.7 The performance of the two DHS reactors. The black arrows indicate the days when biofilm samples were taken from the reactors (day 116, 166, and 534).

Notably, Fig. 6.9 also shows that the COD removal rate of R-1 was higher than that of R-2. In general, organic substrates are finally converted into CH_4 and CO_2 when anaerobically treated. Consequently, we began to investigate CH_4 gas production in the middle of Phase 4, when a relatively high COD loading rate was imposed. Surprisingly, CH_4 was detected in R-1 and R-2, even though they were only inoculated with activated sludge, meaning that methane-producing archaea grew in these reactors during their long operating times of almost one year. Accordingly, the amount of CH_4 produced in R-1 was higher than that produced in R-2 (Fig. 6.7(f)). The existence, or not, of MnO_x and MnO_x reduction in Phases 4–6 is effectively the only difference between R-1 and R-2. These results suggest that the presence of MnO_x and/or MnO_x reduction affects the activities and/or the communities of anaerobic microbes enriched in R-2 by some mechanisms.

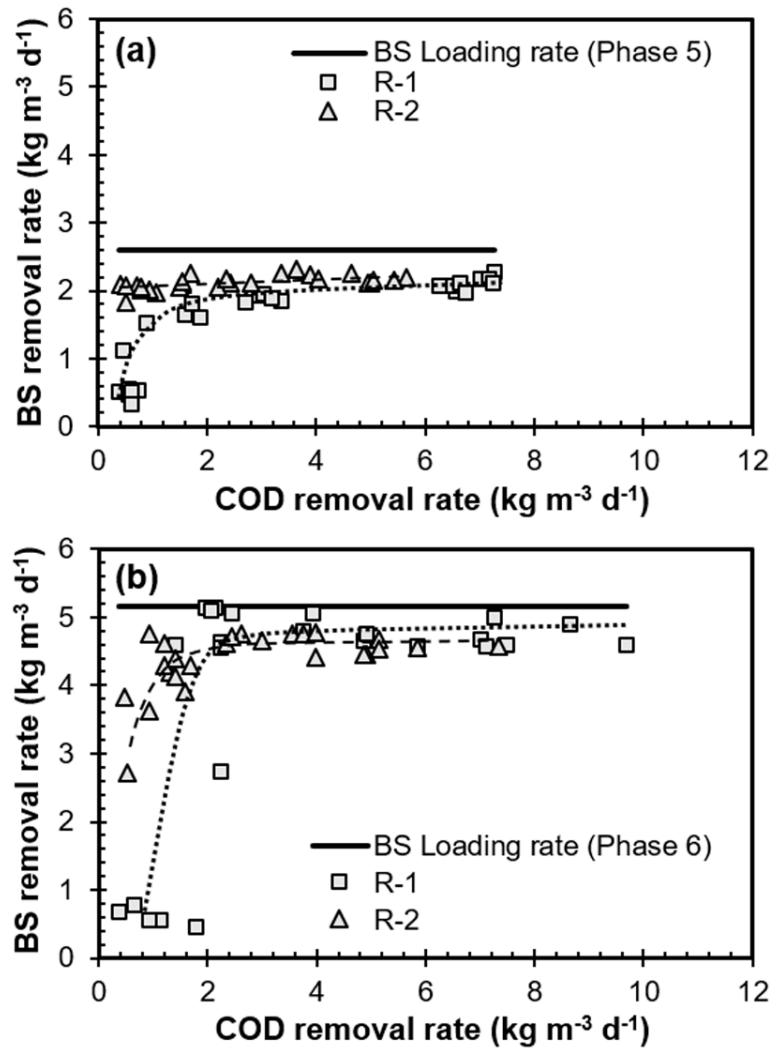


Figure 6.8 Relationships between COD removal rates and BS removal rates at different BS loading rates: (a) 2.8 $\text{kg BS m}^{-3} \text{d}^{-1}$, and (b) 5.6 $\text{kg BS m}^{-3} \text{d}^{-1}$.

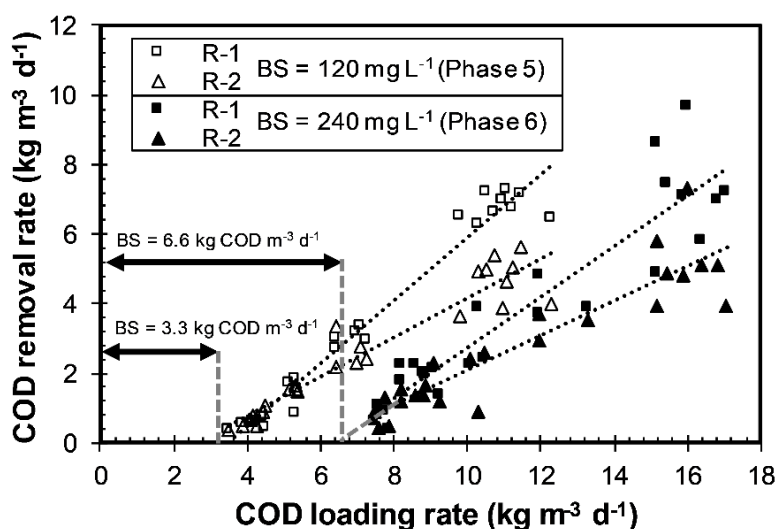


Figure 6.9 Relationships between COD loading rates and COD removal rates

6.3.3 Microbial community

During the 16S rRNA gene sequencings of the six biomass samples, more than 60,000 reads, including bacteria and archaea, were obtained, and the number of OTUs exceeded 1,700 for each sample. For these OTUs, the alpha-diversity indices of Simpson (1-D), Shannon (H), Evenness, and the Chao-1 estimator were assessed (Table 6.3). Little differences were found in the alpha diversities between the phases as well as the two reactors. Even though the operational conditions were fully changed from aerobic to anaerobic, high levels of diversity were mostly maintained.

Table 6.3 Sequence reads, total numbers of OTUs and diversities of both reactors under aerobic and anaerobic conditions

Sample	Aerobic		Anaerobic			
	R1-d116	R2-d116	R1-d166	R2-d166	R1-d534	R2-d534
Total reads	60535	64942	66520	64725	64993	64121
Total OTU ¹⁾	2000	3067	2066	2838	1775	1703
Simpson (1-D) ²⁾	0.83	0.99	0.97	0.99	0.97	0.96
Shannon (H) ³⁾	3.75	5.88	4.48	5.35	4.63	4.49
Evenness ⁴⁾	0.021	0.116	0.043	0.074	0.058	0.052
Chao-1 ⁵⁾	4511	5651	4328	6392	3869	3950

¹⁾ Operational taxonomic units (OTUs) are defined as similarity thresholds of the 16S gene sequences at 97%.

²⁾ Simpson's index of diversity (1-D). A higher value indicates more diversity.

³⁾ Shannon (H) diversity index. A higher value indicates more diversity.

⁴⁾ Evenness. A higher value indicates more evenness.

⁵⁾ Chao-1. A higher value indicates a higher estimated richness.

The sequencing results reveal that bacterial and archaeal communities were detected in both reactors (Fig. 6.10). Even at the phylum and genus levels, little differences between the microbial communities in R-1 and R-2 were observed (Figs. 6.11 and 6.12). However, the microbial communities were observed to change with operational time. The population sizes of Proteobacteria and Planctomycetes, which dominated on day 116 under aerobic conditions, were significantly less dominant on day 534 under anaerobic conditions, while Bacteroidetes and Firmicutes became dominant, and Euryarchaeota appeared after longer operational times.

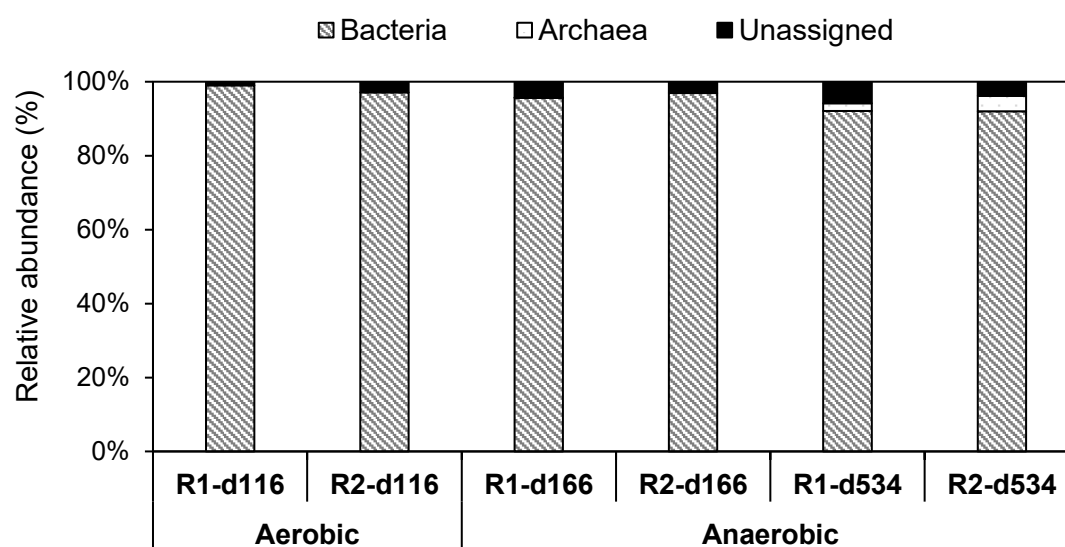


Figure 6.10 Illumina 16S rRNA gene amplicon sequencing results

	Aerobic		Anaerobic			
	R1-d116	R2-d116	R1-d166	R2-d166	R1-d534	R2-d534
Acidobacteria	2.2%	11.4%	2.3%	4.2%	2.1%	5.3%
Actinobacteria	3.9%	6.2%	0.5%	3.1%	0.2%	0.3%
Armatimonadetes	0.6%	4.5%	0.3%	2.5%	1.1%	0.3%
Bacteroidetes	15.1%	7.2%	19.9%	28.8%	26.8%	29.7%
Chlamydiae	0.7%	5.5%	0.3%	2.8%	0.4%	0.3%
Chlorobi	0.2%	1.8%	8.0%	3.4%	5.0%	2.1%
Chloroflexi	5.4%	12.7%	7.6%	6.8%	8.2%	5.9%
Cloacimonetes	0.1%	0.1%	7.0%	0.1%	0.3%	0.1%
Deinococcus-Thermus	0.1%	1.4%	0.1%	0.3%	0.0%	0.0%
Firmicutes	0.2%	0.8%	14.9%	4.9%	21.4%	22.1%
Parcubacteria	0.1%	0.2%	4.5%	1.1%	0.9%	3.1%
Planctomycetes	4.3%	11.5%	0.7%	1.7%	0.7%	0.5%
Proteobacteria	62.0%	24.3%	24.3%	29.9%	12.2%	10.2%
Saccharibacteria	0.5%	2.6%	0.1%	0.5%	1.9%	1.1%
Spirochaetae	0.2%	0.1%	1.3%	1.4%	5.6%	5.5%
Synergistetes	0.0%	0.0%	0.0%	0.0%	1.6%	2.6%
Verrucomicrobia	2.0%	3.3%	1.9%	2.9%	0.6%	0.4%
Euryarchaeota	0.0%	0.0%	0.0%	0.0%	2.1%	4.2%
Unassigned	1.0%	2.9%	4.4%	3.1%	5.8%	3.8%
Others	1.3%	3.5%	2.0%	2.5%	3.0%	2.3%

Figure 6.11 Microbial communities at the phylum level. “Others” represents all phyla that have relative abundances of less than 1%.

The detected genera that reportedly have azo-dye-decolorizing functions are listed in Table 6.4. Genera containing dye-decolorizing bacteria under aerobic conditions, such as *Pseudomonas*, *Aeromonas*, *Bacillus* and *Comamonas* were detected at very low relative abundances, which may explain why almost no BS removal was observed under the aerobic conditions. In contrast, under anaerobic conditions, *Holophagaceae uncultured*, *Desulfovibrio*, *Clostridium sensu stricto 13* and *Clostridium sensu stricto 12* were found in relatively high abundances of approximately 10% during Phase 6, which were suspiciously azo-dye-decolorizing in this study.

Chapter 6: Decolorization of an azo dye Bordeaux S (BS)

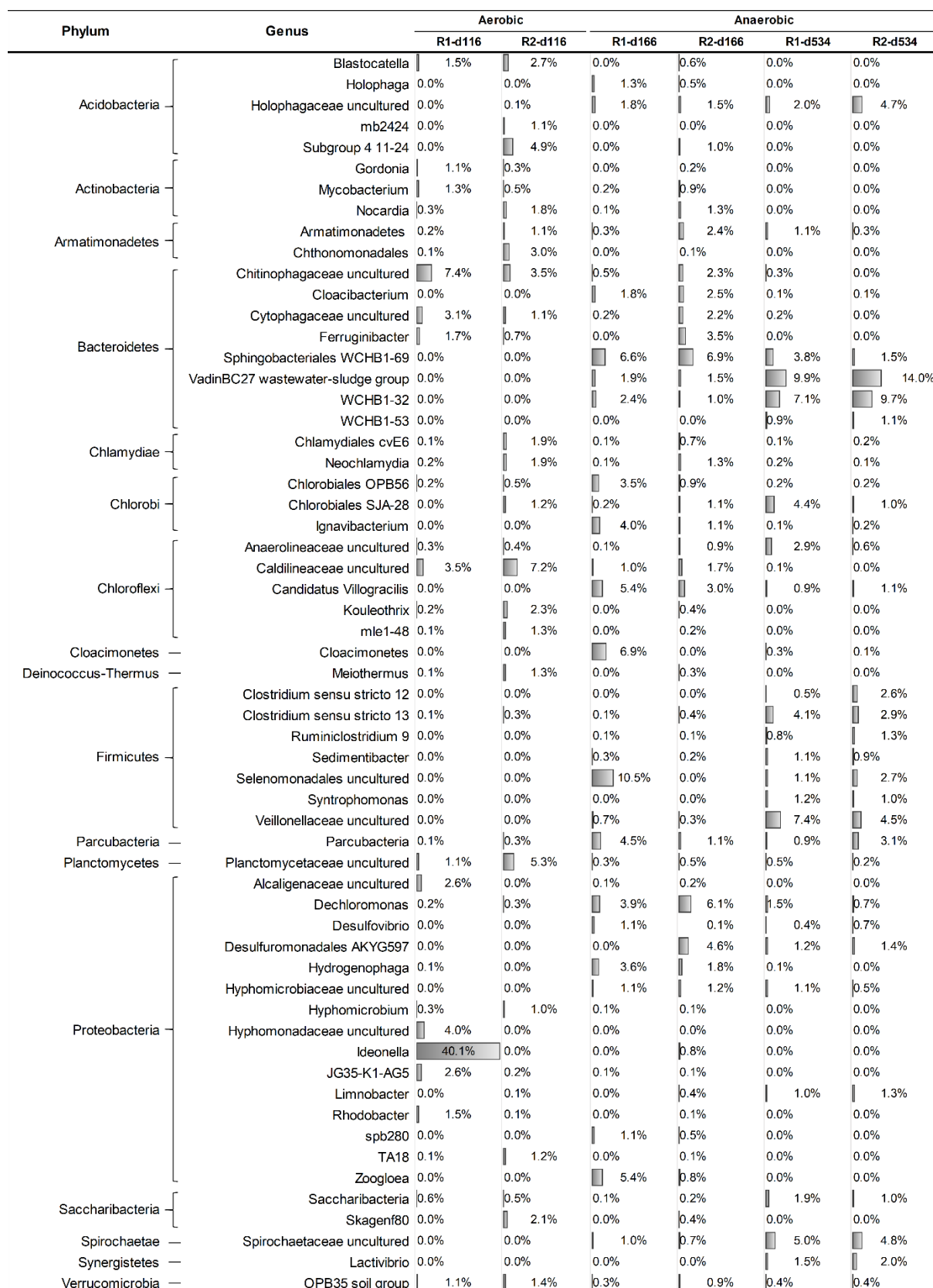


Figure 6.12 Microbial communities at the genus level with relative abundances >1%.

Table 6.4 Abundance of genera related to their functions in the DHS reactors.

Genus	Aerobic				Anaerobic						References		
	R1-d116		R2-d116		R1-d166		R2-d166		R1-d534			R2-d534	
	No of Seq.	(%)	No of Seq.	(%)	No of Seq.	(%)	No of Seq.	(%)	No of Seq.	(%)		No of Seq.	(%)
Dye-decolorizing bacteria													
Pseudomonas	1	0.0	121	0.2									Meerbergen et al., 2018
Aeromonas	5	0.0	90	0.1									Du et al., 2015
Bacillus	4	0.0	36	0.1									Telke et al., 2009
Comamonas	35	0.1	27	0.0									Jadhav et al., 2008
Total	45	0.1	274	0.4									
Holophagaceae uncultured					1189	1.8	960	1.5	1291	2.0	3029	4.7	Xie et al., 2018
Desulfovibrio					761	1.1	61	0.1	253	0.4	418	0.7	Xie et al., 2016
Clostridium sensu stricto 13					78	0.1	285	0.4	2679	4.1	1865	2.9	Zhu et al., 2018
Clostridium sensu stricto 12					0	0.0	6	0.0	346	0.6	1678	2.6	Zhu et al., 2018
Total					2028	3.0	1312	2.0	4569	7.0	6990	10.9	
Manganese-oxidizing bacteria													
Mycobacterium	782	1.3	305	0.5									Marcus et al., 2017
Nocardia	153	0.3	1173	1.8									Carmichael and Bräuer, 2015
Flavobacterium	9	0.0	209	0.3									Bohu et al., 2016
Aeromonas	5	0.0	90	0.1									Zhang et al., 2019
Hyphomicrobium	168	0.3	672	1.0									Bohu et al., 2016
Pedomicrobium	79	0.1	82	0.1									Lozano and Rossi, 2012
Pseudomonas	1	0.0	121	0.2									Bohu et al., 2016
Rhizobium	142	0.2	179	0.3									Bohu et al., 2016
Rhodobacter	884	1.5	59	0.1									Brauer et al., 2011
Sphingomonas	49	0.1	155	0.2									Mayanna et al., 2015
Total	2272	3.8	3045	4.8 %									

Table 6.4 (Continued).

Genus	Aerobic				Anaerobic				References				
	R1-d116		R2-d116		R1-d166		R2-d166			R1-d534		R2-d534	
	No of Seq.	(%)	No of Seq.	(%)	No of Seq.	(%)	No of Seq.	(%)		No of Seq.	(%)	No of Seq.	(%)
Manganese-reducing bacteria													
Pseudomonas					82	0.1	33	0.1	84	0.1	102	0.2	Cerrato et al., 2010
Geobacter					38	0.1	15	0.0	188	0.3	242	0.4	Richter e al., 2012
Desulfovibrio					761	1.1	61	0.1	253	0.4	418	0.7	Reyes et al., 2017; Keller et al., 2014
Desulforhabdus					0	0.0	0	0.0	291	0.4	44	0.1	Reyes et al., 2017; Oude Elferink et al., 1995
Desulfobulbus					10	0.0	0	0.0	336	0.5	125	0.2	Reyes et al., 2017; Sass et al., 2002
Desulfomonile					0	0.0	0	0.0	492	0.8	30	0.0	Reyes et al., 2017; DeWeerd et al., 1990
Total					891	1.3	109	0.2	1644	2.5	961	1.5	
Sulfate-reducing bacteria													
Desulfovibrio					761	1.1	61	0.1	253	0.4	418	0.7	Keller et al., 2014
Desulforhabdus					0	0.0	0	0.0	291	0.4	44	0.1	Oude Elferink et al., 1995
Desulfobulbus					10	0.0	0	0.0	336	0.5	125	0.2	Sass et al., 2002
Desulfomonile					0	0.0	0	0.0	492	0.8	30	0.0	DeWeerd et al., 1990
Total					771	1.1	61	0.1	1372	2.1	617	1.0	

Although Mn(II) was oxidized in Phases 1 and 2 under aerobic conditions, it was impossible to identify the manganese-oxidizing bacteria (MnOB) from the sequencing data. However, a wide variety of genera reported to have MnOB strains were detected, as shown in Table 6.3. These genera occupy approximately 4% of the total, and some of their strains are expected to play Mn(II)-oxidation roles. Under anaerobic conditions, manganese oxides were reduced as mentioned above. There are a few reports on bacteria possessing manganese-oxide-reducing functions (hereinafter referred to “manganese-reducing bacteria” (MnRB)) (Cerrato et al., 2010; Richter et al., 2012). Genera containing MnRB exist in both of R-1 and R-2 in small populations of approximately 0.2-2.5% (Table 6.3). Of the detected genera, sulfate-reducing bacteria affiliated with *Desulfovibrio* were the most dominant; these bacteria may utilize MnO_x as an electron acceptor to produce Mn(II).

Euryarchaeota was detected with relative abundances of 2.1 and 4.2% in R-1 and R-2, respectively (Fig. 6.10), and almost all of the detected Euryarchaeota were methanogens. Although there were very few differences between R-1 and R-2 in terms of bacterial communities, a distinct difference was interestingly observed for the methanogens. The most dominant methanogen was *Methanosaeta* in R-1, while *Methanosarcina* dominated in R-2 (Fig. 4). This difference is ascribable to the presence of MnO_x, which reportedly inhibits microbial activity (Matsushita et al., 2018; Tian et al., 2019). *Methanosaeta* and *Methanoregula* are strongly inhibited by MnO_x, but *Methanosarcina* and *Methanobacterium* are highly MnO_x tolerant.

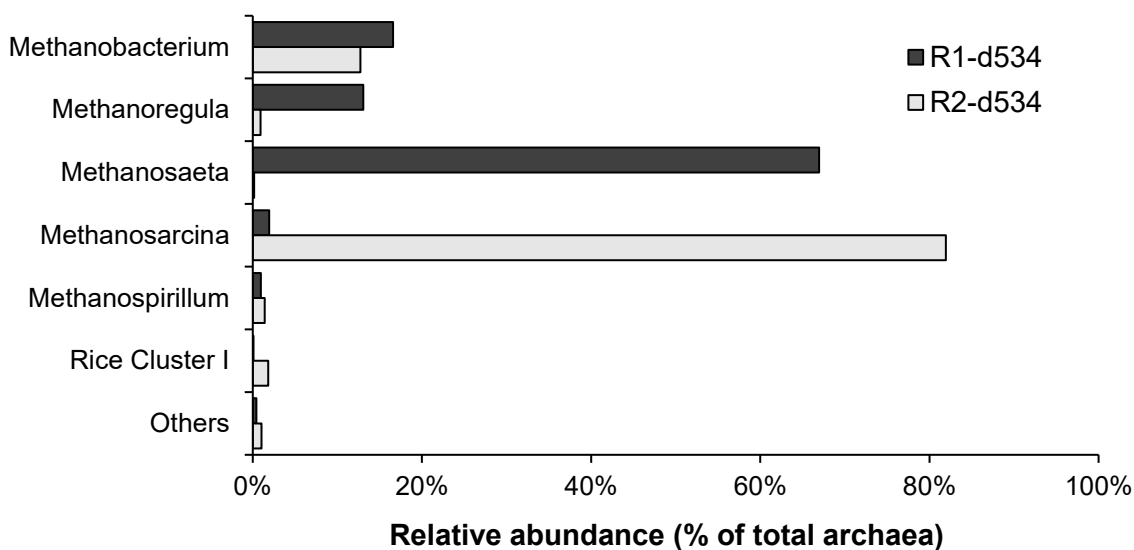


Figure 6.13 Archaeal community compositions at the genus level.

6.4 Discussion

The results show that under the aerobic conditions, the abiotic-MnO₂ initially installed on the sponge carriers of R-2 enhance biological oxidation of Mn(II). However, this installation had less effect on BS removal, and no difference in BS removal between R-1 and R-2 was observed (Fig. 6.7). Despite previous reports that some kinds of azo dye are able to be degraded by aerobic granules or some bacterial consortia under aerobic conditions (Kolekar et al., 2012; Tan et al., 2013), here, BS was unable to be degraded. The low decolorization efficiency in our experiment can be explained as arising from differences in the chemical structures of the azo dye and the microbial community. BS is a sulfonated azo dye and is highly water soluble; consequently, it is difficult for BS to pass through microbial cell membranes, which leads limited biodegradation (Telke et al., 2009). However, sulfonated azo dyes were reportedly mineralized under aerobic conditions in several pure cultures of genera, including *Pseudomonas*, *Aeromonas*, *Bacillus* and *Comamonas* (Meerbergen et al., 2018; Du et al., 2015; Cui et al., 2012; Jadhav et al., 2008). These genera were found at very low population levels in our reactors (Table 6.3), and little BS degradation was observed as a result. It would be difficult to enrich these genera in opened bioreactors under our operational conditions. On the other hand, some MnOB belong to the *Pseudomonas*, *Bacillus* or *Comamonas* genera (Bohu et al., 2016; Tsuji et al., 2017); however, it remains unclear whether or not Mn(II) oxidation affects the degradation of the azo dye.

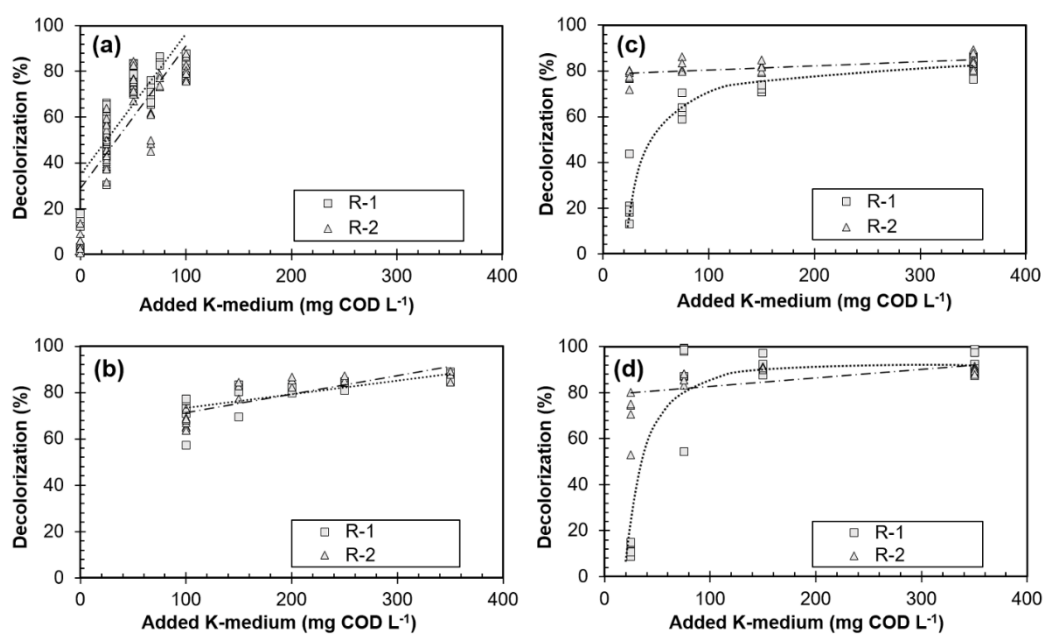


Figure 6.14 The effect of the added K-medium on the decolorization of BS under anaerobic conditions at different concentrations, (a) 7.5 mg L⁻¹, (b) 60 mg L⁻¹, (c) 120 mg L⁻¹, and (d) 240 mg L⁻¹.

In contrast, BS was decolorized under anaerobic conditions (Fig. 6.7), and was strongly dependent on the K-medium concentration (Fig. 6.14). This result is consistent with a reported study in which anaerobic decolorization efficiency was observed to be enhanced with increasing co-substrate concentration (Ong et al., 2012). The azo bonds of azo dyes are reportedly cleaved during reduction by accepting electrons released during the oxidation of organic substances by an azoreductase enzyme, which results in the decolorization of the azo dye (Singh et al., 2015). The decolorization of BS in this study reached 100% and the decolorization performance of the reactor in this study was almost similar to those the reactor of previous studies that operated under anaerobic conditions (. 4-Amino-1-naphthalenesulfonic acid is produced as the metabolite by the reductive cleave of BS (Hayase et al., 2000), which we also detected in this study (Fig 6-15). The detection of this metabolite means that, unfortunately, further degradation of BS did not proceed, and COD remained in the effluent even though the dye was sufficiently decolorized. Batch experiments revealed that microbial metabolisms played a major role in the decolorization mechanism of BS in the reactors. BS mineralization appears to be difficult in a single-only reactor under anaerobic conditions. A post-treatment system is required to further degrade anaerobic effluents, and aerobic treatment is a promising post-treatment process. A combination process that employs both anaerobic and aerobic treatments has been proposed to completely mineralize azo dyes (Hosseini Koupaie et al., 2012).

Table 6.5 A comparison of the reactor performances between this study and previous studies

System	Dye compound	Conditions	Decolorization	References
DHS reactor	Bordeaux S	Anaerobic	99% (R-1) 92% (R-2)	This study
Anaerobic reactor	Acid Orange 7 (AO7)	Anaerobic	93-96%	Li et al., 2017
A continuous upflow anaerobic sludge-blanket reactor	Mordant orange 1	Anaerobic	>75%	Donlon et al., 1997
A continuous stirred tank reactor (CSTR) with bioelectrochemical system	Alizarin Yellow R	Anaerobic	97%	Cui et al., 2016
Sulfidogenic anaerobic baffled reactor	Remazol Brilliant Violet 5R	Anaerobic	>90%	Ozdemir et al. , 2013

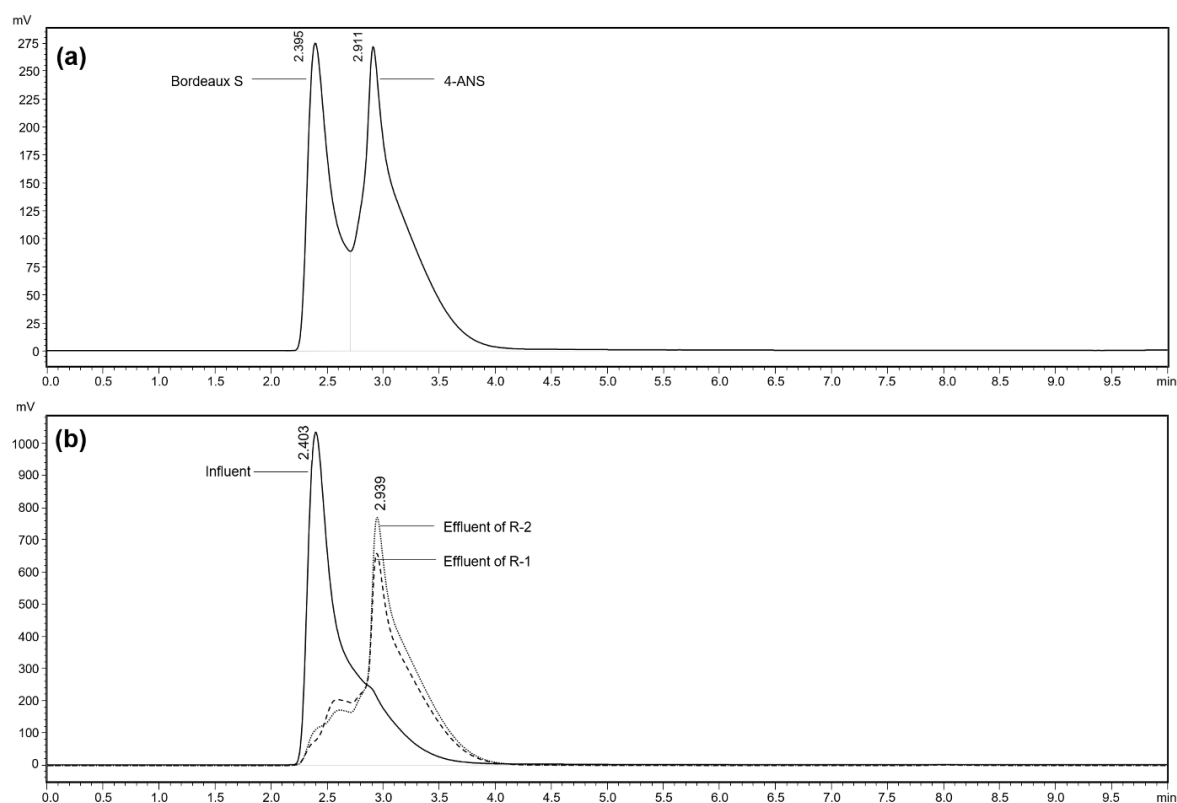


Figure 6.15 HPLC traces of (a) a standard solution of Bordeaux S (RT = 2.395) and 4-amino-1-naphthalenesulfonic acid (4-ANS) (RT = 2.911), (b) the influent, the effluent from R-1, and the effluent from R-2 on day 501.

An interesting and important phenomenon that affects decolorization performance was observed. As mentioned above, BS was more efficiently decolorized in R-2 than in R-1 at low K-medium loading rates; this observation may be attributable to the secretion of extracellular polymeric substances (EPS). Tian et al. (2019) reported that abiotic-MnO₂ stresses microbial cells, which results in an increase in EPS secretion. EPS is mainly composed of carbohydrates and proteins, and acts to protect microbes from toxic chemicals (Li et al., 2015) as well as serving as an electron donor for the reduction of Au(III) to gold nanoparticles (Kang et al., 2017). Therefore, the abiotic-MnO₂ installed in the sponge carriers stimulate the formation of higher levels of EPS that play major roles during BS decolorization as electron donors, especially when an insufficient amount of the external electron donor (K-medium in this study) is present. In contrast, the lower decolorization performance in R-1 in the absence of abiotic-MnO₂ is attributable to low levels of EPS produced in the presence of insufficient K-medium. However, the EPS matrix is complex and poorly biodegradable; hence a wide variety of enzymes are required to completely decompose the EPS (Flemming and Wingender, 2010). Sunda and Kieber (1994) reported that recalcitrant humic substances are degraded by Mn

oxides to lower-molecular-weight compounds that can be used as nutrient sources for microbial metabolism. Therefore, we expect that the abiotic-MnO₂ in R-2 decomposes EPS to more readily utilizable substrates that serve as carbon sources and electron donors for BS decolorization. Electroactive bacteria (EAB), which can respire on extracellular electron acceptors, such as electrode and minerals (Fe(III) and Mn(IV)), play major roles in the decolorization of azo dye due to their extracellular electron-transfer abilities (Liu et al., 2107). In this study, MnRB, which were identified as EAB because they can use manganese oxides as electron acceptors (Table 6.3), may be important contributors to azo-dye decolorization. In addition to EAB, electron transfer is a key process in the anaerobic treatment of azo dyes, and the addition of a conductive material may enhance azo-dye removal (Wang et al., 2018). Therefore, the presence of abiotic-MnO₂ in R-2 is not only important for EPS degradation but also as a conductive material that promotes effective electron transfer between the electron donor and the BS, resulting in enhanced BS decolorization. A simplified proposed mechanism for the decolorization of azo dyes under these conditions is presented in Fig. 6.16.

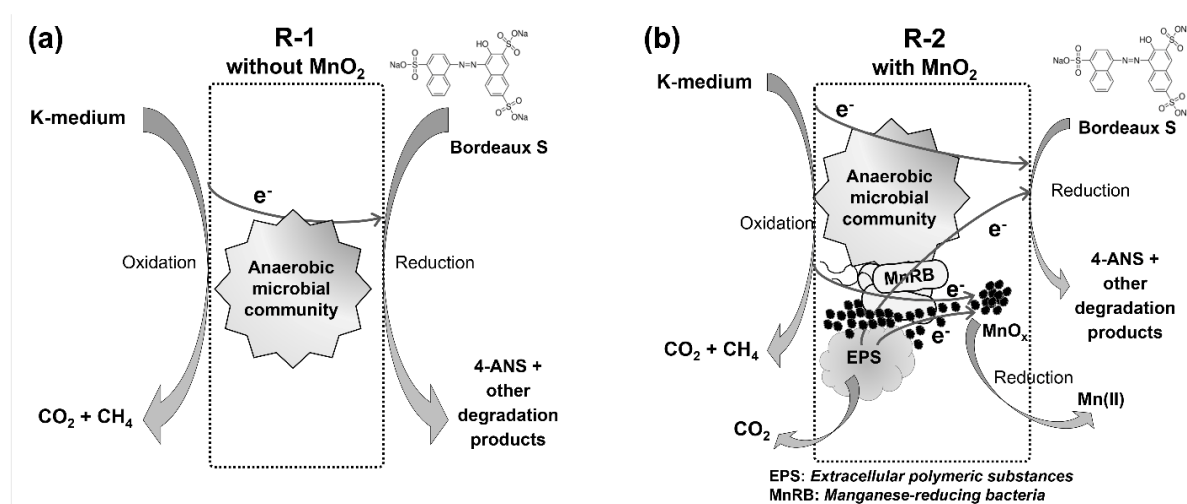


Figure 6.16 Proposed decolorization mechanism at a low K-medium loading rate in (a) R-1, and (b) R-2.

Based on the measured Mn(II) concentrations shown in Fig. 6.7, the author calculated the approximate amount of bio-MnO_x generated by Mn(II) oxidation under aerobic conditions, and the amount of reduced MnO_x generated under anaerobic conditions (Fig. 6.17). The total amount of generated bio-MnO_x in R-1 was 1,180 mg as Mn, and approximately 1,020 mg of Mn(II) was produced by MnO_x reduction until day 210 under anaerobic conditions; these total amounts of Mn(II) are almost coincidental. In contrast, the amount of generated bio-MnO_x and

reduced MnO_x in R-2 were 2,190 and 5,660 ($=2,000 + 1,770 + 1,890$) mg as Mn, respectively. This higher amount of reduced MnO_x compared to the generated bio- MnO_x reveals that part of the initial abiotic- MnO_2 ($= 16 \text{ g/reactor}$) underwent reduction to Mn(II). The time course of the Mn(II) removal rate in R-2 looks like the higher MnO_x reduction rate observed in the early stage of anaerobic operation, and its rate gradually declined until day 317, after which the reduction rate became stable. Assuming that stable Mn reduction after day 317 at the cross-point is the result of abiotic- MnO_2 and that the abiotic- MnO_2 is also reduced at the beginning of the anaerobic period, the amount of reduced bio- MnO_x to day 317 is estimated to be 2,000 mg Mn, which almost corresponds to the amount of generated bio- MnO_x (2,190 mg as Mn). These results suggest that, although both bio- MnO_x and abiotic- MnO_2 were simultaneously reduced in the early stage, the reduction rate of bio- MnO_x is higher than that of abiotic- MnO_2 . Our result is consistent with a previous study in which the reduction of bio- MnO_x by manganese-reducing bacteria was observed to occur quickly (Wright et al., 2016). Therefore, It can be concluded that the presence of abiotic- MnO_2 potentially affects the BS removal when R-2 is operated at low COD concentration during days 453–482 because the produced bio- MnO_x had almost completely disappeared and only the initial abiotic- MnO_2 remained in the reactor.

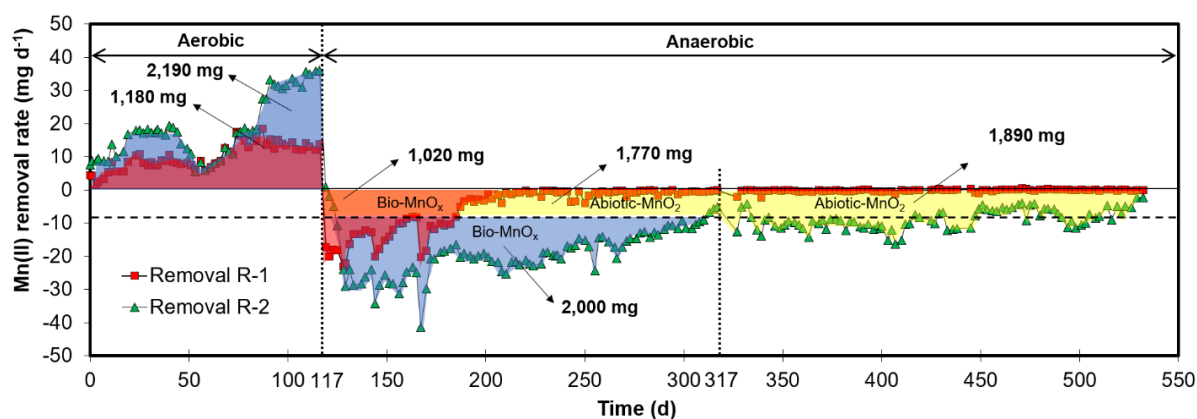


Figure 6.17 Evaluating the amounts of bio- MnO_x produced under aerobic conditions and reduced MnO_x produced under anaerobic conditions based on the Mn(II) removal-rate performance.

Even though the reactors were inoculated with activated sludge, surprisingly, CH_4 was produced at high K-medium loading rates and methanogens were detected in both reactors after long-term operation (Figs. 6.7(f) and 6.13); hence methanogens were present in the activated sludge, which supports reports in which activated sludge is applied to CH_4 -producing reactors

as an anaerobic inoculum (Fredriksson et al., 2012; Cronin and Lo, 1998). The results of this study also demonstrated that more methane is produced in R-1 than in R-2 (Fig. 6.7(f)). This difference in performance is due to the presence of MnO_x , that act as a terminal electron acceptor (Lovley, 1991; Rissanen et al., 2017) and triggers intense competition between the methanogens and Mn-reducing bacteria (MnRB) for the use of the K-medium electron donor, resulting in lower CH_4 production in R-2 (with MnO_x present). This observation is consistent with that of Tian et al. (2019), who found that CH_4 production is inhibited by nano-sized MnO_2 dosed at a high concentration.

Distinct differences between the archaeal communities in R-1 and R-2 were observed (Fig. 6.13). *Methanosaeta* dominated in R1, while *Methanosarcina* dominated in R-2 and very little *Methanosaeta* was detected. *Methanosaeta* is an obligate acetoclastic methanogen that uses only acetate to produce CH_4 . In contrast, *Methanosarcina* is also an acetoclastic methanogen, but uses acetate as well as hydrogen, methanol and methylamines (Raskin et al., 1996; De Vrieze et al., 2012). The acetate-use activity of *Methanosaeta* is greater than that of *Methanosarcina* at low acetate concentrations (De Vrieze et al., 2012). Although they exhibit these different characteristics, they do not explain the difference in the dominant methanogen observed between R-1 and R-2 because the acetate concentrations are almost same in both reactors. *Methanosarcina* reportedly has a higher tolerance to stress under extreme conditions such as exposure to oxidants (i.e. H_2O_2) and dry environments (Horne and Lessner, 2013; Anderson et al., 2012). If *Methanosarcina* is also remarkably resistant toward MnO_x compared to *Methanosaeta*, it will be the dominantly community in R-2. However, Tian et al. (2017) reported that both *Methanosaeta* and *Methanosarcina* were dominant in an anaerobic sludge digester supplemented with MnO_2 nanoparticles, which does not agree with our results. The intolerance of *Methanosaeta* toward MnO_x probably depends on the MnO_x concentration.

6.5 Conclusions

In this study, the Author investigated the effects of Mn(II) oxidation and MnO_x reduction on BS treatment. Through the longtime operation of two reactors, the author revealed that Mn(II) oxidation has little effect on BS removal under aerobic conditions, in which BS decolorization was impossible. In contrast, BS was easily decolorized under anaerobic conditions, and decolorization efficiency was enhanced with increasing K-medium loading rate. The author also found that more BS was decolorized, even at low K-medium concentrations, by the

presence of MnO_x and/or its reduction. However, the BS was decolorized through simple cleavage of azo bond to produce the 4-amino-1-naphthalenesulfonic acid metabolite; hence further BS mineralization did not occur. In addition, the presence of MnO_x significantly influences methane production and the archaeal community by its toxicity.

Acknowledgments

This research was supported by the Japan Society for the Promotion of Science as Grants-in-Aid for Scientific Research (A) Grant Number 17H01300 and Challenging Research (Exploratory) Grant Number 17H06214, and the Environment Research and Technology Development Fund (2-3K133004) of the Ministry of the Environment, Japan. We thank the Ministry of Research, Technology and Higher Education of the Republic of Indonesia through Riset-Pro (World Bank Loan No. 8245-ID) for PhD scholarship to AS.

References

- Anderson, K.L., Apolinario, E.E., Sowers, K.R., 2012. Desiccation as a long-term survival mechanism for the archaeon *Methanosarcina barkeri*. *Appl. Environ. Microbiol.* 78, 1473–1479. <https://doi.org/10.1128/AEM.06964-11>
- Aronesty, E., 2013. Comparison of sequencing utility programs. *Open Bioinf. J.* 7, 1–8. <https://doi.org/10.2174/1875036201307010001>
- Bai, Y., Yang, T., Liang, J., Qu, J., 2016. The role of biogenic Fe-Mn oxides formed in situ for arsenic oxidation and adsorption in aquatic ecosystems. *Water Res.* 98, 119–127. <https://doi.org/10.1016/j.watres.2016.03.068>
- Bohu, T., Akob, D.M., Abratis, M., Lazar, C.S., 2016. Biological Low-pH Mn (II) Oxidation in a manganese deposit. *Appl. Environ. Microbiol.* 82, 3009–3021. <https://doi.org/10.1128/AEM.03844-15>.
- Bolger, A.M., Lohse, M., Usadel, B., 2014. Trimmomatic: A flexible trimmer for Illumina sequence data. *Bioinformatics* 30, 2114–2120. <https://doi.org/10.1093/bioinformatics/btu170>
- Borch, T., Kretzschmar, R., Kappler, A., Cappellen, P. Van, Ginder-Vogel, M., Voegelin, A., Campbell, K., 2010. Biogeochemical redox processes and their impact on contaminant dynamics. *Environ. Sci. Technol.* 44, 15–23. <https://doi.org/10.1021/es9026248>
- Bräuer, S.L., Adams, C., Kranzler, K., Murphy, D., Xu, M., Zuber, P., Simon, H.M., Baptista, A.M., Tebo, B.M., 2011. Culturable *Rhodobacter* and *Shewanella* species are abundant in estuarine turbidity maxima of the Columbia River. *Environ. Microbiol.* 13, 589–603. <https://doi.org/10.1111/j.1462-2920.2010.02360.x>

- Brüschweiler, B.J., Merlot, C., 2017. Azo dyes in clothing textiles can be cleaved into a series of mutagenic aromatic amines which are not regulated yet. *Regul. Toxicol. Pharmacol.* 88, 214–226. <https://doi.org/10.1016/j.yrtph.2017.06.012>
- Cao, L.T.T., Kodera, H., Abe, K., Imachi, H., Aoi, Y., Kindaichi, T., Ozaki, N., Ohashi, A., 2015. Biological oxidation of Mn(II) coupled with nitrification for removal and recovery of minor metals by downflow hanging sponge reactor. *Water Res.* 68, 545–553. <https://doi.org/10.1016/j.watres.2014.10.002>
- Caporaso, J.G., Kuczynski, J., Stombaugh, J., Bittinger, K., Bushman, F.D., Costello, E.K., Fierer, N., Peña, A.G., Goodrich, K., Gordon, J.I., Huttley, G. a, Kelley, S.T., Knights, D., Jeremy, E., Ley, R.E., Lozupone, C. a, McDonald, D., Muegge, B.D., Reeder, J., Sevinsky, J.R., Turnbaugh, P.J., Walters, W. a, 2010. QIIME allows analysis high-throughput community sequencing data. *Nat. Methods* 7, 335–336. <https://doi.org/10.1038/nmeth.f.303>
- Carmichael S.K. and Bräuer S.L., 2015. Microbial Diversity and Manganese Cycling: A Review of manganese-oxidizing microbial cave communities, in: Engel A.S. (Ed.), *Microbial life of cave systems. Life in extreme environments.* Walter de Gruyter GmbH & Co KG, Boston, MA, pp. 137–160. <https://doi.org/10.1515/9783110339888-009>
- Cerrato, J.M., Falkinham, J.O., Dietrich, A.M., Knocke, W.R., McKinney, C.W., Pruden, A., 2010. Manganese-oxidizing and -reducing microorganisms isolated from biofilms in chlorinated drinking water systems. *Water Res.* 44, 3935–3945. <https://doi.org/10.1016/j.watres.2010.04.037>
- Chen, R., Yu, J., Xiao, W., 2013. Hierarchically porous MnO₂ microspheres with enhanced adsorption performance. *J. Mater. Chem. A* 11682–11690. <https://doi.org/10.1039/c3ta12589k>
- Clarke, C.E., Kielar, F., Johnson, K.L., 2013. The oxidation of acid azo dye AY 36 by a manganese oxide containing mine waste. *J. Hazard. Mater.* 246–247, 310–318. <https://doi.org/10.1016/j.jhazmat.2012.12.018>
- Cronin, C., Lo, K. V., 1998. Anaerobic treatment of brewery wastewater using UASB reactors seeded with activated sludge. *Bioresour. Technol.* 64, 33–38. [https://doi.org/10.1016/S0960-8524\(97\)00154-5](https://doi.org/10.1016/S0960-8524(97)00154-5)
- Cui, D., Li, G., Zhao, D., Gu, X., Wang, C., Zhao, M., 2012. Microbial community structures in mixed bacterial consortia for azo dye treatment under aerobic and anaerobic conditions. *J. Hazard. Mater.* 221–222, 185–192. <https://doi.org/10.1016/j.jhazmat.2012.04.032>
- Das, M., Bhattacharyya, K.G., 2014. Oxidation of Rhodamine B in aqueous medium in ambient conditions with raw and acid-activated MnO₂, NiO, ZnO as catalysts. *Journal Mol. Catal. A, Chem.* 391, 121–129. <https://doi.org/10.1016/j.molcata.2014.04.019>
- De Vrieze, J., Hennebel, T., Boon, N., Verstraete, W., 2012. *Methanosarcina* : The rediscovered methanogen for heavy duty biomethanation. *Bioresour. Technol.* 112, 1–9. <https://doi.org/10.1016/j.biortech.2012.02.079>
- DeWeerd, K.A., Mandelco, L., Tanner, R.S., Woese, C.R., Suflita, J.M., 1990. *Desulfomonile tiedjei* gen. nov. and sp. nov., a novel anaerobic, dehalogenating, sulfate-reducing bacterium. *Arch. Microbiol.* 154, 23–30. <https://doi.org/10.1007/BF00249173>

- Dorer, C., Vogt, C., Neu, T.R., Stryhanyuk, H., Richnow, H.H., 2016. Characterization of toluene and ethylbenzene biodegradation under nitrate-, iron(III)- and manganese(IV)-reducing conditions by compound-specific isotope analysis. *Environ. Pollut.* 211, 271–281. <https://doi.org/10.1016/j.envpol.2015.12.029>
- Du, L.N., Li, G., Zhao, Y.H., Xu, H.K., Wang, Y., Zhou, Y., Wang, L., 2015. Efficient metabolism of the azo dye methyl orange by *Aeromonas* sp. strain DH-6: Characteristics and partial mechanism. *Int. Biodeterior. Biodegrad.* 105, 66–72. <https://doi.org/10.1016/j.ibiod.2015.08.019>
- Edgar, R.C., 2010. Search and clustering orders of magnitude faster than BLAST. *Bioinformatics* 26, 2460–2461. <https://doi.org/10.1093/bioinformatics/btq461>
- Flemming, H.C., Wingender, J., 2010. The biofilm matrix. *Nat. Rev. Microbiol.* 8, 623–633. <https://doi.org/10.1038/nrmicro2415>
- Fredriksson, N.J., Hermansson, M., Wilén, B.M., 2012. Diversity and dynamics of Archaea in an activated sludge wastewater treatment plant. *BMC Microbiol.* 12, 140. <https://doi.org/10.1186/1471-2180-12-140>
- Fungal, K.M., Meyer, R.L., Bester, K., 2014. Removing selected steroid hormones, biocides and pharmaceuticals from water by means of biogenic manganese oxide nanoparticles in situ at ppb levels. *Chemosphere* 136, 321–326. <https://doi.org/10.1016/j.chemosphere.2014.11.059>
- Ghattas, A.K., Fischer, F., Wick, A., Ternes, T.A., 2017. Anaerobic biodegradation of (emerging) organic contaminants in the aquatic environment. *Water Res.* 116, 268–295. <https://doi.org/10.1016/j.watres.2017.02.001>
- Hammer, Ø., Harper, D.A.T., Ryan, P.D., 2001. PAST: Paleontological Statistics Software Package. *Palaeontol. Electron.* 4, 9.
- Hayase, N., Kouno, K., Ushio, K., 2000. Isolation and characterization of *Aeromonas* sp. B-5 capable of decolorizing various dyes. *J. Biosci. Bioeng.* 90, 570–573.
- Horne, A.J., Lessner, D.J., 2013. Assessment of the oxidant tolerance of *Methanosarcina acetivorans*. *FEMS Microbiol. Lett.* 343, 13–19. <https://doi.org/10.1111/1574-6968.12115>
- Hossain, L., Sarker, S.K., Khan, M.S., 2018. Evaluation of present and future wastewater impacts of textile dyeing industries in Bangladesh. *Environ. Dev.* 26, 23–33. <https://doi.org/10.1016/j.envdev.2018.03.005>
- Hosseini Koupaie, E., Alavi Moghaddam, M.R., Hashemi, S.H., 2012. Investigation of decolorization kinetics and biodegradation of azo dye Acid Red 18 using sequential process of anaerobic sequencing batch reactor/moving bed sequencing batch biofilm reactor. *Int. Biodeterior. Biodegrad.* 71, 43–49. <https://doi.org/10.1016/j.ibiod.2012.04.002>
- Hyun, J.H., Kim, S.H., Mok, J.S., Cho, H., Lee, T., Vandieken, V., Thamdrup, B., 2017. Manganese and iron reduction dominate organic carbon oxidation in surface sediments of the deep Ulleung Basin, East Sea. *Biogeosciences* 14, 941–958. <https://doi.org/10.5194/bg-14-941-2017>
- Imran, M., Shaharouna, B., Crowley, D.E., Khalid, A., Hussain, S., Arshad, M., 2015. The stability of textile azo dyes in soil and their impact on microbial phospholipid fatty acid

- profiles. *Ecotoxicol. Environ. Saf.* 120, 163–168.
<https://doi.org/10.1016/j.ecoenv.2015.06.004>
- Islam, M.A., Ali, I., Karim, S.M.A., Hossain Firoz, M.S., Chowdhury, A.-N., Morton, D.W., Angove, M.J., 2019. Removal of dye from polluted water using novel nano manganese oxide-based materials. *J. Water Process Eng.* 32, 100911.
<https://doi.org/10.1016/j.jwpe.2019.100911>
- Jadhav, U.U., Dawkar, V. V., Ghodake, G.S., Govindwar, S.P., 2008. Biodegradation of Direct Red 5B, a textile dye by newly isolated *Comamonas* sp. *UVS. J. Hazard. Mater.* 158, 507–516. <https://doi.org/10.1016/j.jhazmat.2008.01.099>
- Kang, F., Qu, X., Alvarez, P.J.J., Zhu, D., 2017. Extracellular saccharide-mediated reduction of Au³⁺ to gold nanoparticles: New insights for heavy metals biomineralization on microbial surfaces. *Environ. Sci. Technol.* 51, 2776–2785.
<https://doi.org/10.1021/acs.est.6b05930>
- Keller, K.L., Rapp-Giles, B.J., Semkiw, E.S., Porat, I., Brown, S.D., Wall, J.D., 2014. New model for electron flow for sulfate reduction in *Desulfovibrio alaskensis* G20. *Appl. Environ. Microbiol.* 80, 855–868. <https://doi.org/10.1128/AEM.02963-13>
- Kolekar, Y.M., Nemade, H.N., Markad, V.L., Adav, S.S., Patole, M.S., Kodam, K.M., 2012. Decolorization and biodegradation of azo dye, Reactive Blue 59 by aerobic granules. *Bioresour. Technol.* 104, 818–822. <https://doi.org/10.1016/j.biortech.2011.11.046>
- Langenhoff, A.A.M., Zehnder, A.J.B., Schraa, G., 1996. Behaviour of toluene, benzene and naphthalene under anaerobic conditions in sediment columns. *Biodegradation* 7, 267–274. <https://doi.org/10.1007/BF00058186>
- Learman, D.R., Voelker, B.M., Vazquez-Rodriguez, A.I., Hansel, C.M., 2011. Formation of manganese oxides by bacterially generated superoxide. *Nat. Geosci.* 4, 95–98.
<https://doi.org/10.1038/ngeo1055>
- Li, L.L., Tong, Z.H., Fang, C.Y., Chu, J., Yu, H.Q., 2015. Response of anaerobic granular sludge to single-wall carbon nanotube exposure. *Water Res.* 70, 1–8.
<https://doi.org/10.1016/j.watres.2014.11.042>
- Li, S., Cao, Y., Bi, C., Zhang, Y., 2017. Promoting electron transfer to enhance anaerobic treatment of azo dye wastewater with adding Fe(OH)₃. *Bioresour. Technol.* 245, 138–144. <https://doi.org/10.1016/j.biortech.2017.08.066>
- Liu, W., Sutton, N.B., Rijnaarts, H.H.M., Langenhoff, A.A.M., 2018a. Anaerobic biodegradation of pharmaceutical compounds coupled to dissimilatory manganese (IV) or iron (III) reduction. *J. Hazard. Mater.* <https://doi.org/10.1016/j.jhazmat.2018.04.078>
- Liu, W., Sutton, N.B., Rijnaarts, H.H.M., Langenhoff, A.A.M., 2018b. Anoxic conditions are beneficial for abiotic diclofenac removal from water with manganese oxide (MnO₂). *Environ. Sci. Pollut. Res.* 25, 10141–10147. <https://doi.org/10.1007/s11356-018-1569-2>
- Liu, Y., Zhang, F., Li, J., Li, D., Liu, D., Li, W., Yu, H., 2017. Exclusive extracellular bioreduction of Methyl Orange by azo reductase-free *Geobacter sulfurreducens*. *Environ. Sci. Technol.* 51, 8616–8623. <https://doi.org/10.1021/acs.est.7b02122>
- Lovley, D.R., 1991. Dissimilatory Fe(III) and Mn(IV) reduction. *Microbiol. Rev.* 55, 259–287.
- Lovley, D.R., 2011. Live wires: direct extracellular electron exchange for bioenergy and the bioremediation of energy-related contamination. *Energy Environ. Sci.* 4, 4896–4906.
<https://doi.org/10.1039/c1ee02229f>

- Lozano, R.P., Rossi, C., 2012. Exceptional preservation of Mn-oxidizing microbes in cave stromatolites (El Soplao, Spain). *Sediment. Geol.* 255–256, 42–55.
<https://doi.org/10.1016/j.sedgeo.2012.02.003>
- Marcus, D.N., Pinto, A., Anantharaman, K., Ruberg, S.A., Kramer, E.L., Raskin, L., Dick, G.J., 2017. Diverse manganese(II)-oxidizing bacteria are prevalent in drinking water systems. *Environ. Microbiol. Rep.* 9, 120–128. <https://doi.org/10.1111/1758-2229.12508>
- Martin, M., 2011. Cutadapt removes adapter sequences from high-throughput sequencing reads. *EMBnet.journal* 17, 10–12. <https://doi.org/10.14806/ej.17.1.200>.
- Matsushita, S., Komizo, D., Cao, L.T.T., Aoi, Y., Kindaichi, T., Ozaki, N., Imachi, H., Ohashi, A., 2018. Production of biogenic manganese oxides coupled with methane oxidation in a bioreactor for removing metals from wastewater. *Water Res.* 130, 224–233.
<https://doi.org/10.1016/j.watres.2017.11.063>
- Mayanna, S., Peacock, C.L., Schäffner, F., Grawunder, A., Merten, D., Kothe, E., Büchel, G., 2015. Biogenic precipitation of manganese oxides and enrichment of heavy metals at acidic soil pH. *Chem. Geol.* 402, 6–17. <https://doi.org/10.1016/j.chemgeo.2015.02.029>
- McIlroy, S.J., Saunders, A.M., Albertsen, M., Nierychlo, M., McIlroy, B., Hansen, A.A., Karst, S.M., Nielsen, J.L., Nielsen, P.H., 2015. MiDAS: the field guide to the microbes of activated sludge. *Database* 2015, bav062. <https://doi.org/10.1093/database/bav062>
- Meerbergen, K., Willems, K.A., Dewil, R., Van Impe, J., Appels, L., Lievens, B., 2018. Isolation and screening of bacterial isolates from wastewater treatment plants to decolorize azo dyes. *J. Biosci. Bioeng.* 125, 448–456.
<https://doi.org/10.1016/j.jbiosc.2017.11.008>
- Ng, I.S., Chen, T., Lin, R., Zhang, X., Ni, C., Sun, D., 2014. Decolorization of textile azo dye and Congo red by an isolated strain of the dissimilatory manganese-reducing bacterium *Shewanella xiamenensis* BC01. *Appl. Microbiol. Biotechnol.* 98, 2297–2308.
<https://doi.org/10.1007/s00253-013-5151-z>
- Nimkar, U., 2018. Sustainable chemistry: A solution to the textile industry in a developing world. *Curr. Opin. Green Sustain. Chem.* 9, 13–17.
<https://doi.org/10.1016/j.cogsc.2017.11.002>
- Noorain, R., Kindaichi, T., Ozaki, N., Aoi, Y., Ohashi, A., 2019. Integrated biological–physical process for biogas purification effluent treatment. *J. Environ. Sci.* 83, 110–122.
<https://doi.org/10.1016/j.jes.2019.02.028>
- Ong, S.A., Toorisaka, E., Hirata, M., Hano, T., 2012. Decolorization of Orange II using an anaerobic sequencing batch reactor with and without co-substrates. *J. Environ. Sci.* 24, 291–296. [https://doi.org/10.1016/S1001-0742\(11\)60766-3](https://doi.org/10.1016/S1001-0742(11)60766-3)
- Oude Elferink, S.J.W.H., Maas, R.N., Harmsen, H.J.M., Stams, A.J.M., 2006. *Desulforhabdus amnigenus* gen. nov. sp. nov., a sulfate reducer isolated from anaerobic granular sludge. *Arch. Microbiol.* 164, 119–124. <https://doi.org/10.1007/bf02525317>
- Raskin, L., Rittmann, B.E., Stahl, D.A., 1996. Competition and coexistence of sulfate-reducing and methanogenic populations in anaerobic biofilms. *Appl. Environ. Microbiol.* 62, 3847–3857.
- Reyes, C., Schneider, D., Thürmer, A., Kulkarni, A., Lipka, M., Szejtjrenzus, S.Y., Böttcher, M.E., Daniel, R., Friedrich, M.W., 2017. Potentially active iron, sulfur, and sulfate

- reducing bacteria in Skagerrak and Bothnian Bay Sediments. *Geomicrobiol. J.* 34, 840–850. <https://doi.org/10.1080/01490451.2017.1281360>
- Remucal, C.K., Ginder-Vogel, M., 2014. A critical review of the reactivity of manganese oxides with organic contaminants. *Environ. Sci. Process. Impacts* 16, 1247–66. <https://doi.org/10.1039/c3em00703k>
- Richter, K., Schicklberger, M., Gescher, J., 2012. Dissimilatory reduction of extracellular electron acceptors in anaerobic respiration. *Appl. Environ. Microbiol.* 78, 913–921. <https://doi.org/10.1128/AEM.06803-11>
- Rissanen, A.J., Karvinen, A., Nykänen, H., Peura, S., Tiirola, M., Mäki, A., Kankaala, P., 2017. Effects of alternative electron acceptors on the activity and community structure of methane-producing and consuming microbes in the sediments of two shallow boreal lakes. *FEMS Microbiol. Ecol.* 93, 1–16. <https://doi.org/10.1093/femsec/fix078>
- Saratale, R.G., Saratale, G.D., Chang, J.S., Govindwar, S.P., 2011. Bacterial decolorization and degradation of azo dyes: A review. *J. Taiwan Inst. Chem. Eng.* 42, 138–157. <https://doi.org/10.1016/j.jtice.2010.06.006>
- Sass, A., Rütters, H., Cypionka, H., Sass, H., 2002. *Desulfobulbus mediterraneus* sp. nov., a sulfate-reducing bacterium growing on mono- and disaccharides. *Arch. Microbiol.* 177, 468–474. <https://doi.org/10.1007/s00203-002-0415-5>
- Sharma, S.C.D., Sun, Q., Li, J., Wang, Y., Suanon, F., Yang, J., Yu, C.P., 2016. Decolorization of azo dye methyl red by suspended and co-immobilized bacterial cells with mediators anthraquinone-2,6-disulfonate and Fe₃O₄ nanoparticles. *Int. Biodeterior. Biodegrad.* 112, 88–97. <https://doi.org/10.1016/j.ibiod.2016.04.035>
- Singh, R.L., Singh, P.K., Singh, R.P., 2015. Enzymatic decolorization and degradation of azo dyes-A review. *Int. Biodeterior. Biodegrad.* 104, 21–31. <https://doi.org/10.1016/j.ibiod.2015.04.027>
- Spagni, A., Casu, S., Grilli, S., 2012. Decolourisation of textile wastewater in a submerged anaerobic membrane bioreactor. *Bioresour. Technol.* 117, 180–185. <https://doi.org/10.1016/j.biortech.2012.04.074>
- SRC PhysProp Database, <http://esc.syrres.com/fatepointer/search.asp>, accessed on August 17, 2018
- Sunda, W.G., Kieber, D.J., 1994. Oxidation of humic substances by manganese oxides yields low-molecular-weight organic substrates. *Nature* 367, 62–64. <https://doi.org/10.1038/367062a0>
- Tan, L., Ning, S., Xia, H., Sun, J., 2013. Aerobic decolorization and mineralization of azo dyes by a microbial community in the absence of an external carbon source. *Int. Biodeterior. Biodegrad.* 85, 210–216. <https://doi.org/10.1016/j.ibiod.2013.02.018>
- Tebo, B.M., Bargar, J.R., Clement, B.G., Dick, G.J., Murray, K.J., Parker, D., Verity, R., Webb, S.M., 2004. Biogenic manganese oxides: Properties and mechanisms of formation. *Annu. Rev. Earth Planet. Sci.* 32, 287–328. <https://doi.org/10.1146/annurev.earth.32.101802.120213>
- Tebo, B.M., Johnson, H.A., McCarthy, J.K., Templeton, A.S., 2005. Geomicrobiology of manganese(II) oxidation. *Trends Microbiol.* 13, 421–428. <https://doi.org/10.1016/j.tim.2005.07.009>
- Telke, A.A., Kalyani, D.C., Dawkar, V. V., Govindwar, S.P., 2009. Influence of organic and inorganic compounds on oxidoreductive decolorization of sulfonated azo dye C.I.

- Reactive Orange 16. *J. Hazard. Mater.* 172, 298–309.
<https://doi.org/10.1016/j.jhazmat.2009.07.008>
- Tian, T., Qiao, S., Yu, C., Tian, Y., Yang, Y., Zhou, J., 2017. Distinct and diverse anaerobic respiration of methanogenic community in response to MnO₂ nanoparticles in anaerobic digester sludge. *Water Res.* 123, 206–215. <https://doi.org/10.1016/j.watres.2017.06.066>
- Tian, T., Qiao, S., Yu, C., Zhou, J., 2019. Effects of nano-sized MnO₂ on methanogenic propionate and butyrate degradation in anaerobic digestion. *J. Hazard. Mater.* 364, 11–18. <https://doi.org/10.1016/j.jhazmat.2018.09.081>
- Tran, T.N., Kim, D.G., Ko, S.O., 2018. Synergistic effects of biogenic manganese oxide and Mn(II)-oxidizing bacterium *Pseudomonas putida* strain MnB1 on the degradation of 17 α -ethinylestradiol. *J. Hazard. Mater.* 344, 350–359.
<https://doi.org/10.1016/j.jhazmat.2017.10.045>
- Tsuji, K., Asayama, T., Shiraki, N., Inoue, S., Okuda, E., Hayashi, C., Nishida, K., Hasegawa, H., Harada, E., 2017. Mn accumulation in a submerged plant *Egeria densa* (Hydrocharitaceae) is mediated by epiphytic bacteria. *Plant Cell Environ.* 40, 1163–1173. <https://doi.org/10.1111/pce.12910>
- Villatoro-Monzón, W.R., Mesta-Howard, A.M., Razo-Flores, E., 2003. Anaerobic biodegradation of BTEX using Mn(IV) and Fe(III) as alternative electron acceptors. *Water Sci. Technol.* 48, 125–131. <https://doi.org/10.2166/wst.2003.0375>
- Wang, Z., Yin, Q., Gu, M., He, K., Wu, G., 2018. Enhanced azo dye Reactive Red 2 degradation in anaerobic reactors by dosing conductive material of ferrous oxide. *J. Hazard. Mater.* 357, 226–234. <https://doi.org/10.1016/j.jhazmat.2018.06.005>
- Wright, M.H., Farooqui, S.M., White, A.R., Greene, A.C., 2016. Production of manganese oxide nanoparticles by *Shewanella* species. *Appl. Environ. Microbiol.* 82, 5402–5409. <https://doi.org/10.1128/aem.00663-16>
- Xie, X., Liu, N., Ping, J., Zhang, Q., Zheng, X., Liu, J., 2018. Illumina MiSeq sequencing reveals microbial community in HA process for dyeing wastewater treatment fed with different co-substrates. *Chemosphere* 201, 578–585.
<https://doi.org/10.1016/j.chemosphere.2018.03.025>
- Xie, X., Liu, N., Yang, B., Yu, C., Zhang, Q., Zheng, X., Xu, L., Li, R., Liu, J., 2016. Comparison of microbial community in hydrolysis acidification reactor depending on different structure dyes by Illumina MiSeq sequencing. *Int. Biodeterior. Biodegrad.* 111, 14–21. <https://doi.org/10.1016/j.ibiod.2016.04.004>
- Zhang, Y., Tang, Y., Qin, Z., Luo, P., Ma, Z., Tan, M., Kang, H., Huang, Z., 2019. A novel manganese oxidizing bacterium-*Aeromonas hydrophila* strain DS02: Mn(II) oxidization and biogenic Mn oxides generation. *J. Hazard. Mater.* 367, 539–545.
<https://doi.org/10.1016/j.jhazmat.2019.01.012>
- Zhou, H., Pan, H., Xu, J., Xu, W., Liu, L., 2016. Acclimation of a marine microbial consortium for efficient Mn(II) oxidation and manganese containing particle production. *J. Hazard. Mater.* 304, 434–440. <https://doi.org/10.1016/j.jhazmat.2015.11.019>
- Zhu, Y., Cao, X., Cheng, Y., Zhu, T., 2018. Performances and structures of functional microbial communities in the mono azo dye decolorization and mineralization stages. *Chemosphere* 210, 1051–1060. <https://doi.org/10.1016/j.chemosphere.2018.07.083>

This page is intentionally left blank

Chapter 7: Integrated anaerobic-aerobic reactor under manganese redox cycling for degradation of azo dye-containing wastewater

Abstract

Anaerobic treatment process is unable to complete degradation of recalcitrant azo dye compound and aerobic process has been extensively reported to be effective for treating anaerobic effluent or as post treatment process. Herein, the author investigated manganese-oxidizing reactor for the treatment of anaerobic reactor effluent. The results showed that only small amounts of COD (<30%) can be decomposed in the aerobic reactor and the concentration of the remaining COD corresponded to the initial BS concentration, suggesting that intermediate products of BS were unable to further decomposed under aerobic conditions. Remarkably, nitrogen loss was observed in the anaerobic reactor, which was associated with the occurrence of manganese oxides reduction. Simultaneous nitrification-denitrification was also found to occur in the aerobic reactor, and the nitrogen removal was linked with manganese oxides reduction. The presence of manganese oxides is beneficial to the removal of nitrogen in wastewater. Integrated anaerobic-aerobic reactor would be a promising method not only to allow Mn redox cycle for generating bio-MnO_x, but also for the treatment of high organic nitrogen-containing wastewater resulting in the nitrogen removal.

Keywords: anaerobic-aerobic process, manganese redox cycling, azo dye degradation, nitrogen removal

7.1 Introduction

The azo dye-containing wastewaters are of a serious problem, particularly in developing countries. They are aesthetically unacceptable due to color appearance and harmful to the environment due their toxic content. Azo dyes and their metabolites are resistant to biological process not only in the natural environment, but also in engineered ecosystem; therefore, they are still present in the conventional wastewater treatment effluent (Shaul et al., 1991; Ekici et al., 2001), released to the river water and also remained in the sludge (Vacchi et al., 2016; Ning et al., 2015). From the toxicological point of view, the occurrence of azo dyes and their intermediate products in the environment will be poisonous to the ecosystem and human health (Bhunia et al., 2003; Skipper et al., 2010).

Based on the results obtained in Chapter 6, the effluent of anaerobic reactor still contains high organic substances, as represented by high COD concentration, including intermediate products of azo dye Bordeaux S that are generated from anaerobic decolorization.

This result agrees with previous study conducted by Hayase et al (2000), which showed that Bordeaux S is mainly degraded to 4-Amino-1-naphthalenesulfonic acid and 1-Amino-2-naphthol-3,6-disulphonic acid. Therefore, a post-treatment system is required to further degrade anaerobic effluents. The aerobic treatment has been reported as a promising post-treatment process for anaerobic effluent, and a sequence process anaerobic-aerobic treatment has been proposed to further degradation of azo dyes (Hosseini Koupaie et al., 2012). In the Chapter 4, the Mn(II) oxidation reactor more effectively decompose acetate-containing wastewater than the reactor without Mn(II) oxidation.

The manganese redox cycling in the natural environment has been reported to play a significant role in the biogeochemical cycles of organic carbon, nitrogen, sulfur and phosphorus (Tebo et al., 2005; Geszvain et al., 2012; Hyun et al., 2017). This Mn redox cycle usually occurs at the oxic-anoxic boundary, such as the sediment-water interfaces in freshwater environment (Jones et al., 2018). Under anaerobic conditions, manganese oxides undergo reduction to Mn(II), and Mn(II) would be oxidized in the presence of oxygen or aerobic conditions. Therefore, the author expected that a combination of anaerobic-aerobic reactor could not only allow Mn redox cycle (Mn(II) oxidation and manganese oxides reduction), but also enhance degradation of organic substances including azo dye and its intermediate products.

In this study, we investigated the performance of an integrated anaerobic-aerobic reactor for the degradation of an azo dye. Under anaerobic conditions, reductively cleavage the azo bond of azo dye generates intermediate products, which will be further decomposed under Mn(II) oxidation conditions in the aerobic reactor.

7.2 Materials and methods

7.2.1 Synthetic dye wastewater

Azo dye Bordeaux S (BS) (Fujifilm Wako Pure Chemical Co., Ltd. (Tokyo, Japan) was used in this study. The synthetic dye wastewater was consisted of BS, K-medium (consisting of peptone casein (Nacalai Tesque Inc., Kyoto, Japan) and dried yeast extract (Nacalai Tesque Inc., Kyoto, Japan) (4:1, w/w)), minerals and trace elements. The substrate was prepared in two separated substrate tanks. One tank contained K-medium and phosphate buffer (KH_2PO_4 (0.602 mg L^{-1}), and Na_2HPO_4 (6.22 mg L^{-1})). The other tank contained BS, Mn(II) ($\text{MnCl}_2 \cdot 4\text{H}_2\text{O}$), minerals ($\text{CaCl}_2 \cdot 2\text{H}_2\text{O}$ (0.05 mg L^{-1}), $\text{MgSO}_4 \cdot 7\text{H}_2\text{O}$ (0.2 mg L^{-1}), $\text{Fe}_2\text{SO}_4 \cdot 5\text{H}_2\text{O}$ (0.1 mg L^{-1})), and trace elements ($\text{CuSO}_4 \cdot 5\text{H}_2\text{O}$ (0.025 mg L^{-1}), NaSeO_4 (0.005 mg L^{-1}), $\text{NiCl}_2 \cdot 6\text{H}_2\text{O}$ (0.019

mg L⁻¹), CoCl₂·6H₂O (0.024 mg L⁻¹), Na₂MoO₄·2H₂O (0.022 mg L⁻¹), H₃BO₃ (0.001 mg L⁻¹), ZnSO₄·7H₂O (0.043 mg L⁻¹). The substrate tanks were purged with nitrogen gas and connected to a nitrogen-filled gas bag during the experiment.

7.2.2 Bioreactor set-up and operational conditions

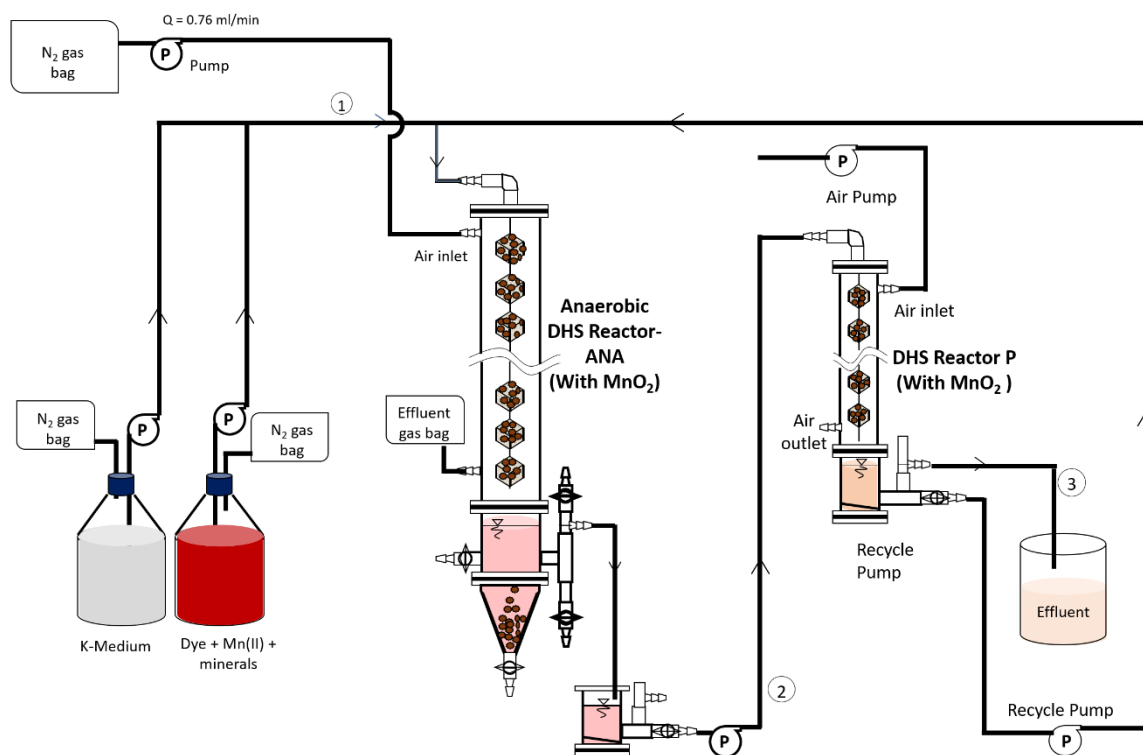


Figure 7.1 Integrated anaerobic-aerobic DHS reactor configurations.

A combination of anaerobic-aerobic DHS reactor was used in this study (Fig. 7.1). The first reactor was anaerobic reactor that has been operated for decolorization of BS in Chapter 6. The second reactor was new established aerobic reactor with size of 45 cm in height and 4 cm in diameter, filled with 10 polyurethane sponge cubes (volume: $2 \times 2 \times 2$ cm each; total volume: 80 cm³). The aerobic reactor was also inoculated with suspension of abiotic-MnO₂ in activated sludge to induce the growth of manganese-oxidizing bacteria. The reactors were then placed in a controlled temperature room at 25 °C and dark condition to avoid any effect of light on the azo dye decomposition.

Table 7.1 Operational conditions of the integrated aerobic-anaerobic DHS reactor

	Phase 1 (0-8d)	Phase 2 (9-134d)	Phase 3 (135-156d)	Phase 4 (157-162d)	Phase 5 (163-172d)	Phase 6 (173-198d)	Phase 7 (199-212d)	Phase 8 (213-223d)	Phase 9 (223-230d)
BS (mg/L)	30	30	30	60	60	60	60	60	60
Mn (II) (mg/L)	5	5	5	5	5	5	5	5	5
K-medium (mg COD/L)									
Yeast extract	100	100	100	100	100	100	20	20	-
Peptone	400	400	400	400	400	400	80	80	-
Sucrose (mg COD/L)	-	-	-	-	-	-	-	-	100
Anaerobic reactor									
Q (L/d)	0.22	0.11	0.11	0.11	0.11			0.11	0.11
HRT (h)	12.1	24.2	24.2	24.2	24.2			24.2	24.2
ART (h) N2	32.3	32.3	32.3	32.3	32.3			32.3	32.3
Aerobic reactor									
Q (L/d)	0.22	0.11	0.22	0.22	0.22			0.22	0.22
HRT (h)	6.1	12.1	6.1	6.1	6.1			6.1	6.1
ART (h)	0.3	0.3	0.3	0.3	0.3			0.3	0.3
Integrated system									
Q inf. (L/d)						0.11	0.11		
Q rec (L/d)						0.06	0.06		
Added co-substrate in the aerobic reactor									
K-medium (mg COD/L)			50	50	-	-	-	100	-
Sodium acetate (mg COD/L)			-	-	50	-	-	-	-
Sucrose (mg COD/L)			-	-	-	-	-	-	50

The reactors were operated for 230 d. The reactor operational conditions were summarized in Table 7.1. The anaerobic reactor was blown with nitrogen gas at very low flow rate (0.76 ml/min) to keep anaerobic conditions, while the aerobic reactor was aerated by continuously supplying with the air. The anaerobic reactor was supplemented with 30–60 mg/L BS, 5 mg/L Mn(II) and 100–500 mg-COD/L K-medium. The effluent of anaerobic reactor was subsequently fed to aerobic reactor. The HRT of anaerobic reactor and aerobic reactor in Phase 1 was set as 12.1 h and 6.1 h, respectively. In Phase 2, the HRT of the anaerobic and aerobic reactor was set to 24.2 h and 12.1 h, respectively. The reactors were operated in one-way system, and in Phase 6–7, recirculation system was applied.

7.2.3 Chemical oxidation of ammonium with abiotic-MnO₂

Chemical experiments with abiotic-MnO₂ were performed in batch experiment and column experiment to investigate whether removal of ammonium in the aerobic reactor was due to chemical oxidation with MnO_x or biologically mediated reaction.

7.2.3.1 Batch experiment

Batch experiment was conducted by adding 5 mg abiotic-MnO₂ in 40 mL pre-filtered of the anaerobic reactor effluent day-50, in 50 mL glass tube with a parafilm-covered screw cap. The tube was shaken in a horizontal shaker (MMS-1, EYELA, Tokyo, Japan) at 120 rpm and

room temperature. The concentration of Mn(II) and ammonium were determined after 15 h reaction using ICPE 9000 (Shimadzu, Japan) and Nessler's reagent method, respectively.

7.2.3.2 Column experiment

A glass column of 1 cm in diameter filled with abiotic-MnO₂ was used in this study (Fig 7.1). In the 1st experiment, a-30 g abiotic-MnO₂ was placed into the column, and polyurethane sponge was used to retain abiotic-MnO₂ in the column. Due to column clogging after 3 days operation, in the 2nd experiment, the amounts of abiotic-MnO₂ was reduced to 5 g and polyurethane sponge was used as an attachment structure. Three different feed solutions were used, including anaerobic reactor effluents, ammonium sulfate ((NH₄)₂SO₄), and ammonium chloride (NH₄Cl). The column conditions and feed solutions were described in the Table 7.2 as follows.

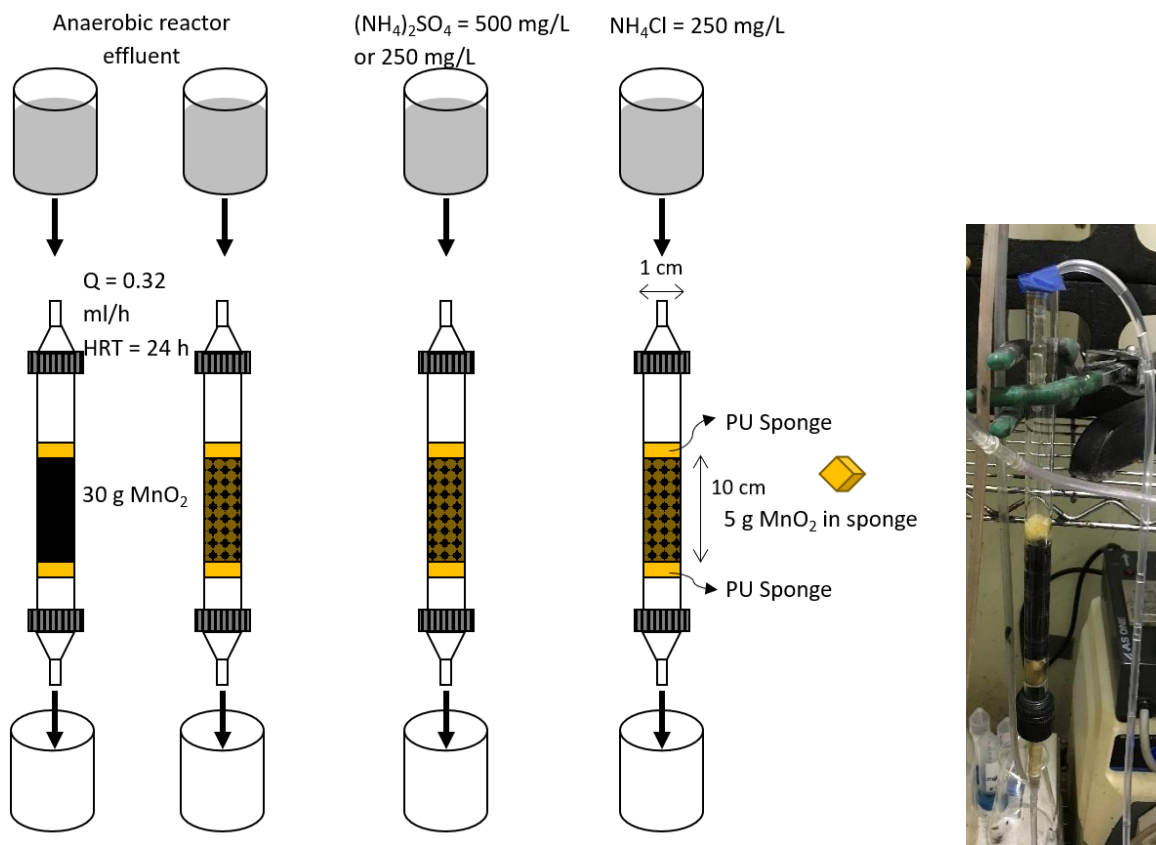


Figure 7.2 Column experiment design and photo of the column reactor

Table 7.2 Column experiment conditions and feed solution

Experiment	Feed solution	MnO ₂
1st	Anaerobic reactor effluent	30 g MnO ₂
2nd	Anaerobic reactor effluent	5 g in polyurethane foam (10 cm)
3rd	Anaerobic reactor effluent	5 g in polyurethane foam (10 cm)
4th	(NH ₄) ₂ SO ₄ = 500 mg/L	5 g in polyurethane foam (10 cm)
5th	(NH ₄) ₂ SO ₄ = 250 mg/L	5 g in polyurethane foam (10 cm)
6th	NH ₄ Cl = 250 mg/L	5 g in polyurethane foam (10 cm)

7.2.4 Analytical methods

The water samples were filtered through 0.45- μ m membrane filters (Advantec, Tokyo, Japan). The BS concentration was determined by colorimetry using a UV-visible spectrophotometer (Shimadzu UV-1800, Kyoto, Japan) at its maximum absorption wavelength ($\lambda_{\max} = 522$ nm). Total organic carbon (TOC) as non-purgeable organic carbon (NPOC) and total nitrogen (TN) was measured using a TOC analyzer (Shimadzu TOC-VCSH, Kyoto, Japan). Mn(II) was determined using an inductively coupled plasma emission spectrometer (Shimadzu ICPE-9000, Kyoto, Japan) after filtering with a 0.2- μ m PTFE membrane filter (Advantec, Tokyo, Japan). Concentration of sulfate (SO₄²⁻), Chemical oxygen demand (COD), and total nitrogen with persulfate digestion method were analyzed by colorimetry using a Hach Spectrophotometer (Hach Co. DR2800, Loveland, CO, USA). Ammonium, nitrite, and nitrate were determined using ion chromatography (Shimadzu HPLC 10A). Ammonium was also measured using Nessler's reagent method to confirm the ion chromatography results.

7.3 Results

7.3.1 Reactor performances

7.3.1.1 Anaerobic reactor

Figure 7.3 showed the performance of integrated anaerobic-aerobic reactor. In the Phase 1, pH increased in the effluent. This alkalinity was due to the high loading of K-medium in the influent. K-medium is a high organic-nitrogen substrate consisting of yeas extract and peptone. Decomposition of K-medium under anaerobic conditions generates carbon dioxides and ammonia/ammonium. The release of carbon dioxide lead to the production of carbonic acid, bicarbonate alkalinity, and carbonate alkalinity results in the raising pH. Mn(II) concentration

in the effluent was higher than influent, which indicated that manganese oxide reduction had occurred. BS was fully decolorized. COD was degraded almost completely, and the residual COD in the effluent corresponded to the concentration of BS in the influent indicating that BS was only partially decomposed.

In Phase 2, the HRT of anaerobic reactor was elevated to 24 h. Since this period, concentration of sulfate, nitrite, nitrate, ammonium and total nitrogen were measured. The results showed that the performance of anaerobic reactor was the same with previous phase in term of pH, Mn(II), BS, COD, and TOC. Sulfate (SO_4^{2-}) was detected in the effluent, but not in the influent. Since concentration of SO_4^{2-} was determined using colorimetry method, and the colored influent sample could interfere the measurement, thus the obtained data may be unreliable. Concentration of sulfate (SO_4^{2-}) gradually decreased during this period. Interestingly, nitrite and nitrate were detected at this period, and a nitrogen loss was observed according to the nitrogen mass balance calculation (Fig. 7.3 and 7.4). The formation of nitrite and nitrate under anaerobic conditions was unusual. Ammonium may be oxidized to nitrite, nitrate, and nitrogen gas, coupled with the reduction of MnO_x .

I presumed that aerobic process difficult to decompose degradation products of BS due to insufficient electron donor. Therefore, K-medium was supplied to the aerobic reactor in Phase 3–4. The result showed that COD removal was only around 50%, indicating that only K-medium was consumed, and the degradation products of BS remain in the effluent of aerobic reactor. During this phase, Mn oxides reduction still occurred which may due to the existence of higher concentration of ammonium. To avoid effects of ammonium, in Phase 5, we changed electron donor in the aerobic reactor from K-medium to sodium acetate. Even though Mn(II) oxidation occurred, no improvement in the COD removal.

To investigate the effect Mn redox processes to the degradability of intermediate products of BS, the effluent of the aerobic reactor was recirculated to the anaerobic reactor during Phase 6–7. Unfortunately, COD removal could not be enhanced. In Phase 8, recirculation was terminated and a higher concentration of K-medium (100 mg/L) was supplied to the aerobic reactor. No COD removal was observed during this period. In Phase 9, even though K-medium was changed to sucrose as co-substrate in the anaerobic and aerobic reactor, remaining COD could not be decomposed under anaerobic and aerobic reactor. Recalcitrant of degradation products of BS to biodegradation under anaerobic and aerobic process may due to its physical-chemical characteristics.

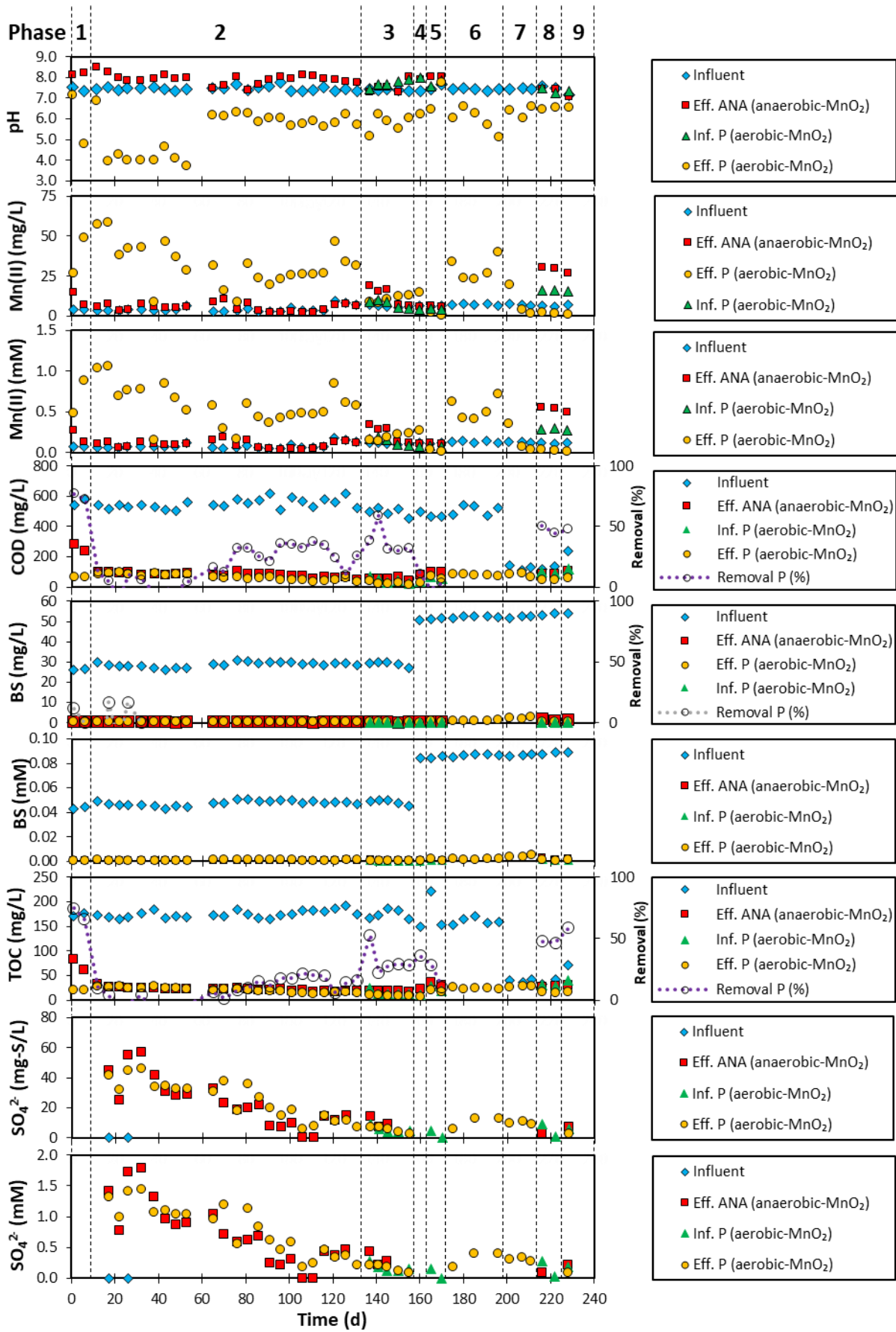


Figure 7.3 The performance of the integrated anaerobic-aerobic reactor.

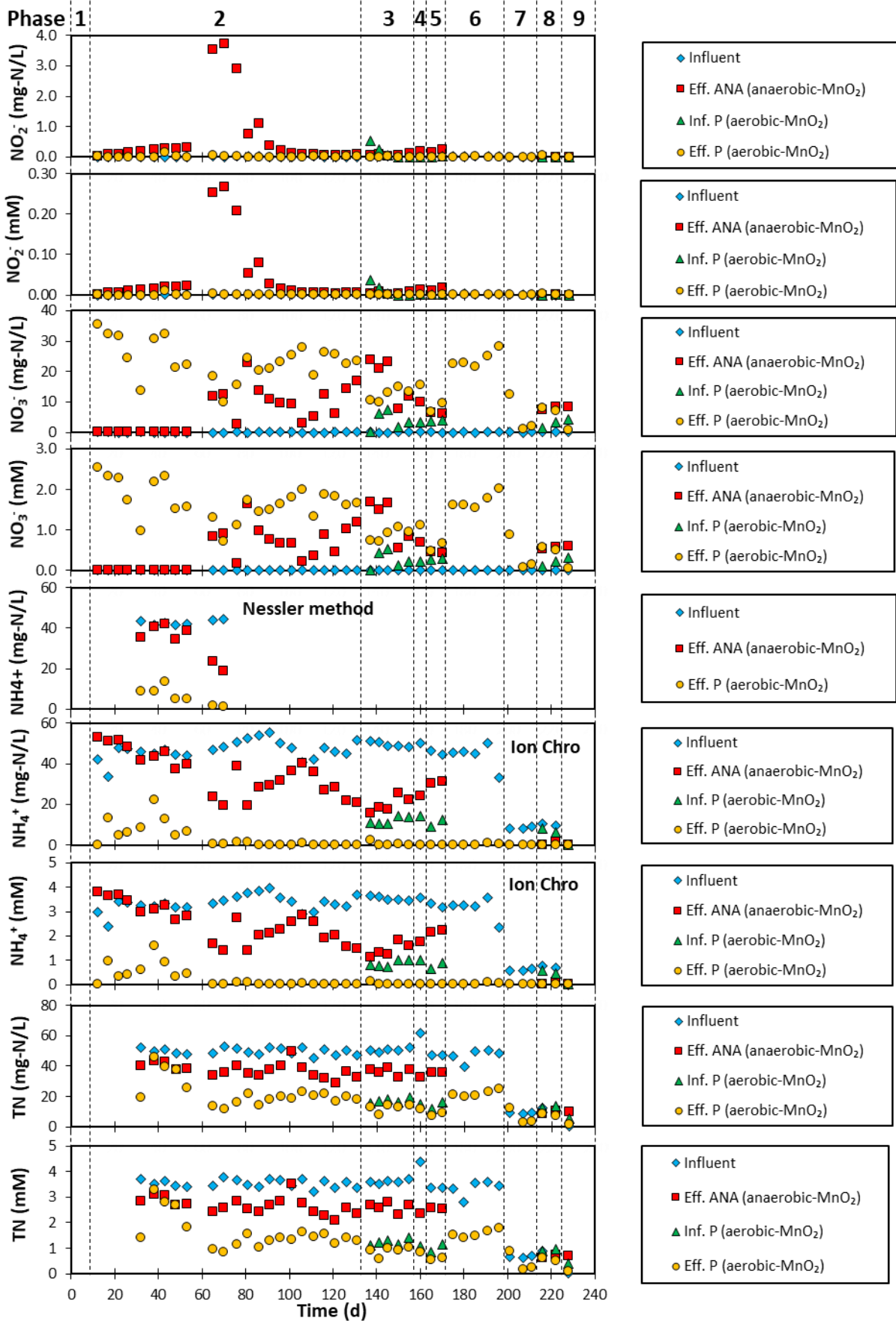


Figure 7.3 (Continued).

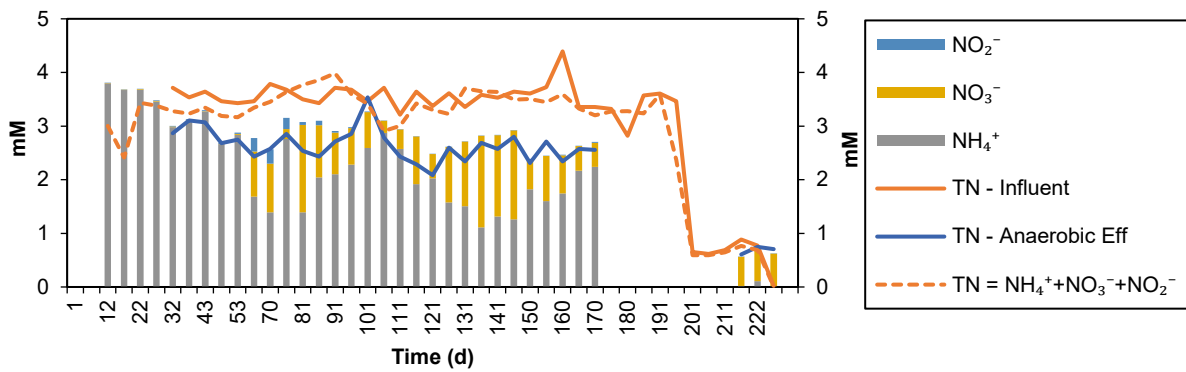


Figure 7.4 Nitrogen mass balance in the anaerobic reactor

7.3.1.2 Aerobic reactor

In the Phase 1, decreasing pH was observed in the effluent of the aerobic reactor that might be caused by nitrification process. Mn(II) was detected higher than the influent indicating that manganese oxides reduction has occurred. This was unusual because Mn(II) was oxidized under aerobic conditions and manganese oxides reduction occurred under anaerobic conditions. No further COD removal was observed at this period. Therefore, HRT will be reduced to 24 h to enhance COD removal.

In Phase 2, when HRT was reduced from 12 h to 24 h, the higher Mn(II) concentration were still detected. The enhancement of COD removal up to 30% was found after 70 days of operation, however this performance still fluctuated. Even though COD removal enhanced, the residual COD concentration corresponded to the initial concentration of BS. Some organic matters were decomposed but not for intermediate products of BS. TOC removal was found to be the same pattern with COD removal. It is widely known that ammonium is converted to nitrate under aerobic conditions. At initial period, partial oxidation of ammonium was observed, and since day-81, no residual ammonium was detected in the effluent. An interesting finding was observed, in which based on the nitrogen mass balance calculation (Fig. 7.5), the nitrogen loss has occurred. Thus, oxidation of ammonium to nitrogen gas also likely occurred even under aerobic conditions.

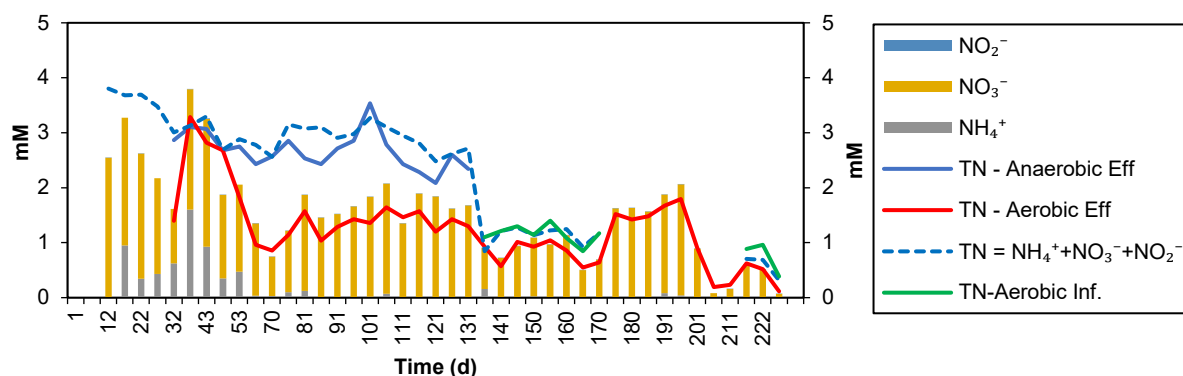


Figure 7.5 Nitrogen mass balance in the aerobic reactor

7.3.2 Batch experiment with abiotic-MnO₂

Table 7.3 The result of batch experiment with abiotic-MnO₂

Parameter	Feed solution (=anaerobic effluent d-50)	After 15 h
pH	8.124	7.553
NH ₄ ⁺ (mg-N/L)	40.60	42.5
Mn ²⁺ (mg/L)	5.99	0.255

The data from the Table 7.4 above showed that instead of slightly decrease in pH, ammonium removal was not observed after 15 h reaction. The reducing Mn(II) concentration indicated that Mn(II) was adsorbed onto abiotic-MnO₂, and no chemical reduction of manganese oxides has occurred. From the results obtained, it can be concluded that chemical reaction between abiotic-MnO₂ and ammonium did not occur.

7.3.2.1 Column experiments with abiotic-MnO₂

Table 7.4 The results of 1st experiment of column reactor

Parameter	Influent (=anaerobic effluent d-77)	Effluent of column	Effluent of Aerobic reactor (d-77)
pH	7.484	6.484	6.181
COD (mg/L)	81	143	68
Mn²⁺ (mg/L)	8.66	6.95	31.7
Total N (mg-N/L)	34	525	13.5
NH₄⁺ (mg-N/L)	23.8	410	1.6
NO ₂ ⁻ (mg-N/L)	3.55	0.3	0.07
NO ₃ ⁻ (mg-N/L)	11.79	131.4	18.45

Table 7.5 The results of 2nd experiment of column reactor

Parameter	Influent (=anaerobic effluent d-88)	Effluent of column	Effluent of Aerobic reactor (d-88)
pH	8.059	6.035	6.330
COD (mg/L)	102	780	69
Mn²⁺ (mg/L)	4.38	1.54	8.99
Total N (mg-N/L)	40	126	16
NH₄⁺ (mg-N/L)	38.7	99.7	1.4
NO ₂ ⁻ (mg-N/L)	2.9	0.85	0.03
NO ₃ ⁻ (mg-N/L)	2.59	15.7	41.6

Table 7.6 The results of 3rd experiment of column reactor

Parameter	Influent (=anaerobic effluent d-93)	Effluent of column	Effluent of Aerobic reactor (d-93)
pH	7.390	7.180	6.285
COD (mg/L)	84	137	57
Mn²⁺ (mg/L)	8.35	0.951	33
Total N (mg-N/L)	35.5	17	22
NH₄⁺ (mg-N/L)	19.46	17.7	1.68
NO ₂ ⁻ (mg-N/L)	0.74	1.1	0.01
NO ₃ ⁻ (mg-N/L)	22.9	2.0	24.52

Table 7.7 The results of 4th, 5th, and 6th experiment of column reactor

Parameter	(NH ₄) ₂ SO ₄ = 500 mg/L		(NH ₄) ₂ SO ₄ = 250 mg/L		NH ₄ Cl = 250 mg/L	
	Influent	Effluent	Influent	Effluent	Influent	Effluent
pH	5.858	7.356	5.772	6.852	5.840	6.904
COD (mg/L)	-4	171	-5	191	57	310
Mn²⁺ (mg/L)	0.241	0.525	0.947	0.526	0.297	0.293
Total N (mg-N/L)	109.5	144	53	97	57.5	184
NH₄⁺ (mg-N/L)	127	160	60.8	101	7	17.5
NO ₂ ⁻ (mg-N/L)	0	0.04	0	0.58	0	0
NO ₃ ⁻ (mg-N/L)	0	9	0	10.1	0	2.8

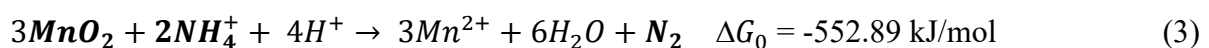
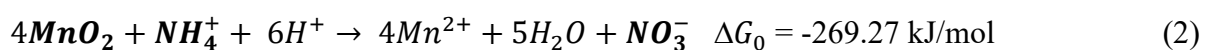
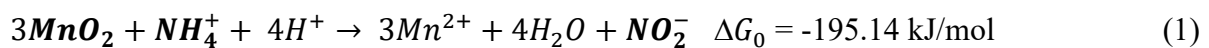
Column experiments were conducted with different feed solutions; real wastewater from anaerobic reactor effluent and synthetic wastewater (ammonium sulfate and ammonium chloride). As can be seen from the Table 7.5, 7.6, and 7.7 above, Mn(II) seemed to be adsorbed on abiotic-MnO₂. The increase of Mn(II) concentrations were also not observed when using synthetic wastewater (Table 7.8). These results indicated that abiotic-MnO₂ did not react with ammonium, which was similar to the result of batch experiment. While the concentration of

ammonium in the effluent was higher than that of the influent, which was questionable. Contamination from polyurethane was suspected; therefore, further experiment was performed by immersing polyurethane foam into 30 mL NH_4Cl (250 mg/L). After 15 h reaction, concentration of COD increased from 23 mg/L to 99 mg/L. Thus, the higher of COD concentration was due to the presence of polyurethane foam. Based on the column experiment results, it can be concluded that chemical reaction between ammonium and abiotic- MnO_2 did not occur.

7.4 Discussion

The results showed that only small fractions of the remaining COD in the anaerobic effluent could be decomposed under aerobic conditions, which indicated that intermediate products of BS still exist and are resistant to biological process. Sulfonated aromatic amines, as the main products of sulfonated azo dye degradation, are poorly degraded by biological processes under aerobic and anaerobic conditions because the presence of sulfonated structure in aromatic amine compounds cause highly soluble resulted in the lower biodegradability (Jonstrup et al., 2011; Tan et al., 2005). The organic substances (K-medium) was almost completely consumed in the anaerobic reactor, and only intermediate products were transferred to the aerobic reactor. Therefore, in the next phase, addition of co-substrate will be applied to aerobic reactor because addition extra carbon source is required for decolorization of azo dye (Moosvi et al., 2007).

Interesting results was observed in which manganese oxides reduction and nitrogen loss occurred in the both anaerobic and aerobic reactor. The interaction of manganese oxides-nitrogen in natural and engineered ecosystems has been reported previously. The presence of manganese oxides mediates nitrogen cycling in the sediment under suboxic conditions, in which ammonium generated from organic matter decomposition is oxidized by manganese oxides (Javanaud et al., 2011; Mogollón et al., 2016). In the engineered ecosystem, it has been found that the nanoscale manganese oxides act as electron acceptor for the biologically mediated anoxic nitrification-denitrification in the laboratory scale sequencing batch reactor (Swathi et al., 2017). The chemical reaction pathways of anaerobic ammonium oxidation coupled with Mn reduction proposed by Swathi et al. (2017) were given as follows.



Several microbial strains have been reported to be capable of oxidizing ammonium and utilizing manganese oxides as electron acceptor. *Marinobacter daepoensis* strain M4AY14, that has been isolated from Arcachon Bay (SW Atlantic French coast), is able to oxidize ammonium in the presence of manganese oxide (Javanaud et al., 2011). Aigle et al. (2017) demonstrated that anaerobic ammonium oxidation by a microbial strain *Shewanella algae* C6G3 coupled with manganese oxides reduction generates nitrite or nitrate. This strain utilizes nitrate or Mn(IV) as the sole electron acceptor under anaerobic conditions with faster growth. The ammonium oxidation pathway in the presence of manganese oxides proposed by Aigle et al. (2017) was presented as follows.

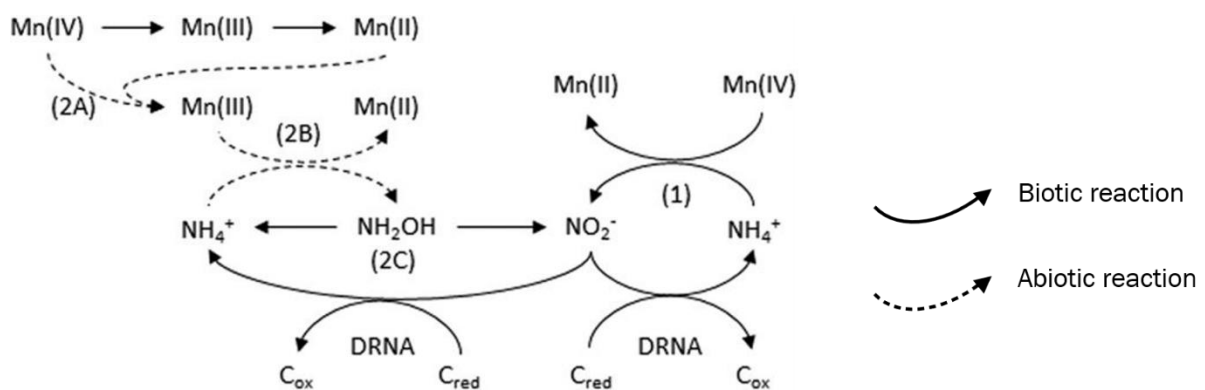
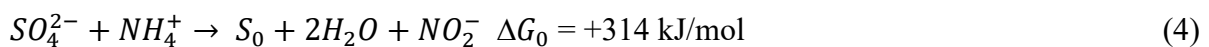
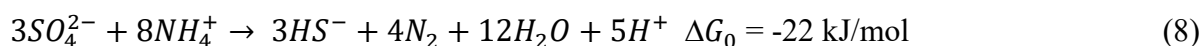
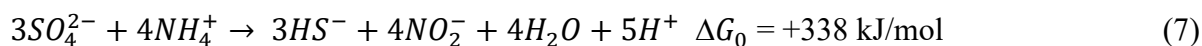


Figure 7.6 Ammonium oxidation coupled with manganese reduction mediated by a microbial strain *Shewanella algae* C6G3 (Adapted from Aigle, A. et al. 2017).

In addition to ammonium oxidation in the presence of manganese oxides, anaerobic ammonium oxidation coupled with sulfate (SO_4^{2-}) reduction was also possible to occur. The decreasing of sulfate in the anaerobic effluent might be attributed to the ammonium oxidation in the reactor. Anaerobic ammonium oxidation coupled to sulfate reduction, also known as Sulfammox, has been observed in the sediments collected from the eastern tropical North Pacific coast (Rios-Del Toro et al., 2018). This phenomenon has also been found in engineered ecosystems, such as in a moving bed biofilm reactor (MBBR) and up-flow anaerobic sludge blanket reactor (UASBR) (Rikmann et al, 2012; Yang et al., 2009). The possible reaction pathways for anaerobic manganese oxidation coupled with sulfate reduction have been proposed as follows. Equation 4-7 were proposed by Rikmann et al. (2012), and while Equation 8-9 were suggested by Yang et al. (2009).





Nitrogen loss mechanisms in the aerobic reactor remained unclear. Chemical experiment of this study in batch and column reactor revealed that abiotic reaction between ammonium and abiotic-MnO₂ did not occur. Thus, it can be suggested that manganese oxide reduction in the aerobic reactor was microbially mediated process. It is widely known that biological Mn(II) oxidation is usually occur under aerobic conditions, and manganese oxides reduction undergoes under anaerobic conditions through directly by manganese reducing microorganisms, or indirectly by dissimilatory metal reducing bacteria which utilize manganese oxides as an electron acceptor (Tebo et al., 2005; Lovely, 1991). However, previous study reported that manganese oxide reduction was found to occur in oxic regions of the Lake Vanda, Antarctica (Bratina et al., 1998). Few microbial strains have been reported capable of reducing manganese oxides under aerobic conditions, such as *Carnobacterium*, *Salmonella* strain MR4, and *Dietzia* (Bratina et al., 1998; Pak et al., 2002; Zhang et al., 2015). Thus, it can be suspected that microorganisms which capable of reducing manganese oxides under aerobic conditions were present in the aerobic reactor. The presence of ammonium might be another reason why manganese oxidation did not occur in the aerobic reactor. Tian et al. (2019) reported that the higher ammonium concentration (>1.5 mg/L) could inhibit manganese oxidation, and nitrification lead to the decreased pH, which is unfavorable for biological manganese oxidation.

The conventional nitrogen cycle theory suggests that conversion of ammonium to nitrogen gas includes nitrification, oxidation of ammonium to nitrite by ammonia-oxidizing bacteria and further transformed to nitrate by nitrite-oxidizing bacteria, which requires oxygen as electron acceptor, and denitrification, reduction of nitrate to nitrogen gas by denitrifying bacteria, which requires carbon as electron donor and less oxygen. This study demonstrated that simultaneous nitrification and denitrification occurred in the aerobic reactor in which ammonium was completely converted to nitrate and some total nitrogen loss was also achieved. This phenomenon can be explained as follows. This study used DHS reactor which utilizes polyurethane sponge as carrier media for microbial growth. This reactor has been characterized by the accumulation of biomass on the sponge surface which could lead to the decreasing of dissolved oxygen (DO) concentration from the surface to the inside of the sponge (Onodera et al., 2016). Therefore, it can be suggested that nitrification would occur on the surface, while

denitrification process takes place inside the sponge. In addition, visual observation of the sponge revealed that black color appeared over the operation time indicating that Mn(II) oxidation has occurred and manganese oxides existed on the sponge surface. While, the higher Mn(II) concentration indicated that manganese oxides reduction has also occurred. It can be suggested that nitrification-denitrification process occurred simultaneously in the aerobic reactor, and the nitrogen removal was enhanced by manganese oxide reduction activity. This phenomenon would be a promising method to remove nitrogen in one system. Therefore, further studies to investigate this phenomenon was deemed necessary, such as whether the addition of organic substrate could improve denitrification activity in the aerobic reactor or not.

7.5 Conclusions

The performance of integrated anaerobic-aerobic reactor for degradation of BS was evaluated. Through one-way flow system or recirculation system, residual organic substances in the anaerobic reactor effluent were only partially degraded, and the intermediate products of BS could not be completely decomposed under aerobic conditions. Even though addition of organic substrate was applied to the aerobic reactor, intermediate products of azo dye could not be enhanced. Remarkably, nitrogen loss was observed in both anaerobic and aerobic reactor. The conventional nitrogen cycling suggested that ammonium removal process needs two step mechanisms; nitrification under aerobic conditions and then followed by denitrification under anaerobic conditions, however, this study demonstrated that anaerobic ammonium oxidation coupled with manganese oxides reduction and sulfate reduction under anaerobic conditions were possible, and simultaneous nitrification-denitrification also occurred under manganese redox dynamics in the aerobic reactor. Further studies are required to investigate the parameters that influence the process of ammonium oxidation coupled with manganese oxides reduction, such as carbon/nitrogen (C/N) ratio, HRT, etc.

References

- Aigle, A., Bonin, P., Iobbi-Nivol, C., Méjean, V., Michotey, V., 2017. Physiological and transcriptional approaches reveal connection between nitrogen and manganese cycles in *Shewanella* algae C6G3. *Sci. Rep.* 7, 1–12. <https://doi.org/10.1038/srep44725>
- Bhunja, F., Saha, N.C., Kaviraj, A., 2003. Effects of aniline-An aromatic amine to some freshwater organisms. *Ecotoxicology* 397–404. <https://doi.org/10.1023/A:1026104205847>

- Bratina, B.J.O., Stevenson, B.S., Green, W.J., Schmidt, T.M., 1998. Manganese reduction by microbes from oxic regions of the Lake Vanda (Antarctica) water column. *Appl. Environ. Microbiol.* 64, 3791–3797.
- Ekici, P., Leupold, G., Parlar, H., 2001. Degradability of selected azo dye metabolites in activated sludge systems. *Chemosphere* 44, 721–728. [https://doi.org/10.1016/S0045-6535\(00\)00345-3](https://doi.org/10.1016/S0045-6535(00)00345-3)
- Geszvain, K., Butterfield, C., Davis, R.E., Madison, A.S., Lee, S.-W., Parker, D.L., Soldatova, A., Spiro, T.G., Luther, G.W., Tebo, B.M., 2012. The molecular biogeochemistry of manganese(II) oxidation. *Biochem. Soc. Trans.* 40, 1244–1248. <https://doi.org/10.1042/BST20120229>
- Hayase, N., Kouno, K., Ushio, K., 2000. Isolation and characterization of *Aeromonas* sp. B-5 capable of decolorizing various dyes. *J. Biosci. Bioeng.* 90, 570–573.
- Hosseini Koupaie, E., Alavi Moghaddam, M.R., Hashemi, S.H., 2012. Investigation of decolorization kinetics and biodegradation of azo dye Acid Red 18 using sequential process of anaerobic sequencing batch reactor/moving bed sequencing batch biofilm reactor. *Int. Biodeterior. Biodegrad.* 71, 43–49. <https://doi.org/10.1016/j.ibiod.2012.04.002>
- Hyun, J.H., Kim, S.H., Mok, J.S., Cho, H., Lee, T., Vandieken, V., Thamdrup, B., 2017. Manganese and iron reduction dominate organic carbon oxidation in surface sediments of the deep Ulleung Basin, East Sea. *Biogeosciences* 14, 941–958. <https://doi.org/10.5194/bg-14-941-2017>
- Javanaud, C., Michotey, V., Guasco, S., Garcia, N., Anschutz, P., Canton, M., Bonin, P., 2011. Anaerobic ammonium oxidation mediated by Mn-oxides: From sediment to strain level. *Res. Microbiol.* 162, 848–857. <https://doi.org/10.1016/j.resmic.2011.01.011>
- Jones, M.E., Nico, P.S., Ying, S., Regier, T., Thieme, J., Keiluweit, M., 2018. Manganese-driven carbon oxidation at oxic-anoxic interfaces. *Environ. Sci. Technol.* 52, 12349–12357. <https://doi.org/10.1021/acs.est.8b03791>
- Jonstrup, M., Kumar, N., Murto, M., Mattiasson, B., 2011. Sequential anaerobic-aerobic treatment of azo dyes: Decolourisation and amine degradability. *Desalination* 280, 339–346. <https://doi.org/10.1016/j.desal.2011.07.022>
- Lovley, D.R., 1991. Dissimilatory Fe(III) and Mn(IV) reduction. *Microbiol. Rev.* 55, 259–287.
- Mogollón, J.M., Mewes, K., Kasten, S., 2016. Quantifying manganese and nitrogen cycle coupling in manganese-rich, organic carbon-starved marine sediments: Examples from the Clarion-Clipperton fracture zone. *Geophys. Res. Lett.* 43, 7114–7123. <https://doi.org/10.1002/2016GL069117>
- Moosvi, S., Kher, X., Madamwar, D., 2007. Isolation, characterization and decolorization of textile dyes by a mixed bacterial consortium JW-2. *Environ. Sci. Technol.* 41, 723–729. <https://doi.org/10.1016/j.dyepig.2006.05.005>
- Ning, X.A., Liang, J.Y., Li, R.J., Hong, Z., Wang, Y.J., Chang, K.L., Zhang, Y.P., Yang, Z.Y., 2015. Aromatic amine contents, component distributions and risk assessment in sludge from 10 textile-dyeing plants. *Chemosphere* 134, 367–373. <https://doi.org/10.1016/j.chemosphere.2015.05.015>

- Onodera, T., Okubo, T., Uemura, S., Yamaguchi, T., Ohashi, A., 2016. Bioresource Technology Long-term performance evaluation of down-flow hanging sponge reactor regarding nitrification in a full-scale experiment in India. *Bioresour. Technol.* 204, 177–184. <https://doi.org/10.1016/j.biortech.2016.01.005>
- Pak, K., Lim, O., Lee, H., Choi, S., 2002. Aerobic reduction of manganese oxide by *Salmonella* sp. strain MR4. *Biotechnol. Lett.* 24, 1181–1184.
- Rikmann, E., Zekker, I., Tomingas, M., Tenno, Taavo, Menert, A., Loorits, L., Tenno, Toomas, 2012. Sulfate-reducing anaerobic ammonium oxidation as a potential treatment method for high nitrogen-content wastewater. *Biodegradation* 23, 509–524. <https://doi.org/10.1007/s10532-011-9529-2>
- Rios-Del Toro, E.E., Valenzuela, E.I., López-Lozano, N.E., Cortés-Martínez, M.G., Sánchez-Rodríguez, M.A., Calvario-Martínez, O., Sánchez-Carrillo, S., Cervantes, F.J., 2018. Anaerobic ammonium oxidation linked to sulfate and ferric iron reduction fuels nitrogen loss in marine sediments. *Biodegradation* 29, 429–442. <https://doi.org/10.1007/s10532-018-9839-8>
- Shaul, G.M., Holdsworth, T.J., Dempsey, C.R., Dostal, K.A., 1991. Fate of water soluble azo dyes in the activated sludge process. *Chemosphere* 22, 107–119. [https://doi.org/10.1016/0045-6535\(91\)90269-J](https://doi.org/10.1016/0045-6535(91)90269-J)
- Skipper, P.L., Kim, M.Y., Sun, H.P., Wogan, N., Ñ, S.R.T., 2010. Monocyclic aromatic amines as potential human carcinogens : old is new again 31, 50–58. <https://doi.org/10.1093/carcin/bgp267>
- Swathi, D., Sabumon, P.C., Maliyekkal, S.M., 2017. Microbial mediated anoxic nitrification-denitrification in the presence of nanoscale oxides of manganese. *Int. Biodeterior. Biodegrad.* 119, 499–510. <https://doi.org/10.1016/j.ibiod.2016.10.043>
- Tan, L., Ning, S., Xia, H., Sun, J., 2013. Aerobic decolorization and mineralization of azo dyes by a microbial community in the absence of an external carbon source. *Int. Biodeterior. Biodegrad.* 85, 210–216. <https://doi.org/10.1016/j.ibiod.2013.02.018>
- Tebo, B.M., Johnson, H.A., McCarthy, J.K., Templeton, A.S., 2005. Geomicrobiology of manganese(II) oxidation. *Trends Microbiol.* 13, 421–428. <https://doi.org/10.1016/j.tim.2005.07.009>
- Tian, X., Zhang, R., Huang, T., Wen, G., 2019. The simultaneous removal of ammonium and manganese from surface water by MeOx: Side effect of ammonium presence on manganese removal. *J. Environ. Sci.* 77, 346–353. <https://doi.org/10.1016/j.jes.2018.09.006>
- Vacchi, F.I., Von der Ohe, P.C., Albuquerque, A.F. de, Vendemiatti, J.A. de S., Azevedo, C.C.J., Honório, J.G., Silva, B.F. da, Zanoni, M.V.B., Henry, T.B., Nogueira, A.J., Umbuzeiro, G. de A., 2016. Occurrence and risk assessment of an azo dye - The case of Disperse Red 1. *Chemosphere* 156, 95–100. <https://doi.org/10.1016/j.chemosphere.2016.04.121>
- Yang, Z., Zhou, S., Sun, Y., 2009. Start-up of simultaneous removal of ammonium and sulfate from an anaerobic ammonium oxidation (anammox) process in an anaerobic up-flow bioreactor. *J. Hazard. Mater.* 169, 113–118. <https://doi.org/10.1016/j.jhazmat.2009.03.067>

Zhang, H., Li, Y., Wang, Xin, Lu, A., Ding, H., Zeng, C., Wang, Xiao, Wu, X., Nie, Y., Wang, C., 2015. Aerobic and anaerobic reduction of birnessite by a novel *Dietzia* strain. *Geochem. Trans.* 7–11. <https://doi.org/10.1186/s12932-015-0026-0>

Chapter 8: General conclusions, perspectives and recommendations

Textile industry sector has positive impacts on the economic growth of developing countries, on the other hand, azo dye and its intermediate products-containing textile wastewater is one of the crucial environmental issues due to its resistance to degradation in the environment, toxicity and mutagenic or carcinogenic potential. Therefore, development treatment technology to treat azo dye and its intermediate products is essential. In this PhD dissertation, degradation of an azo dye using manganese-oxidizing bacteria (MnOB) was investigated. Prior to azo dye degradation experiment, three different organic substrates as the sole carbon source for MnOB enrichment in a continuous reactor, and the effect of residual Mn(II) on the Mn(II) oxidation performance of the reactor were studied. Degradation of an azo dye under Mn(II) oxidation (aerobic conditions), and under manganese oxide reduction (anaerobic conditions) were also investigated. And the last, an integrated anaerobic-aerobic reactor was applied to obtain further degradation of azo dye and its intermediate products and also other organic substances. The results of this study were summarized in Figure 8.1 and elaborated in more detail below. Future perspectives and recommendation were also discussed.

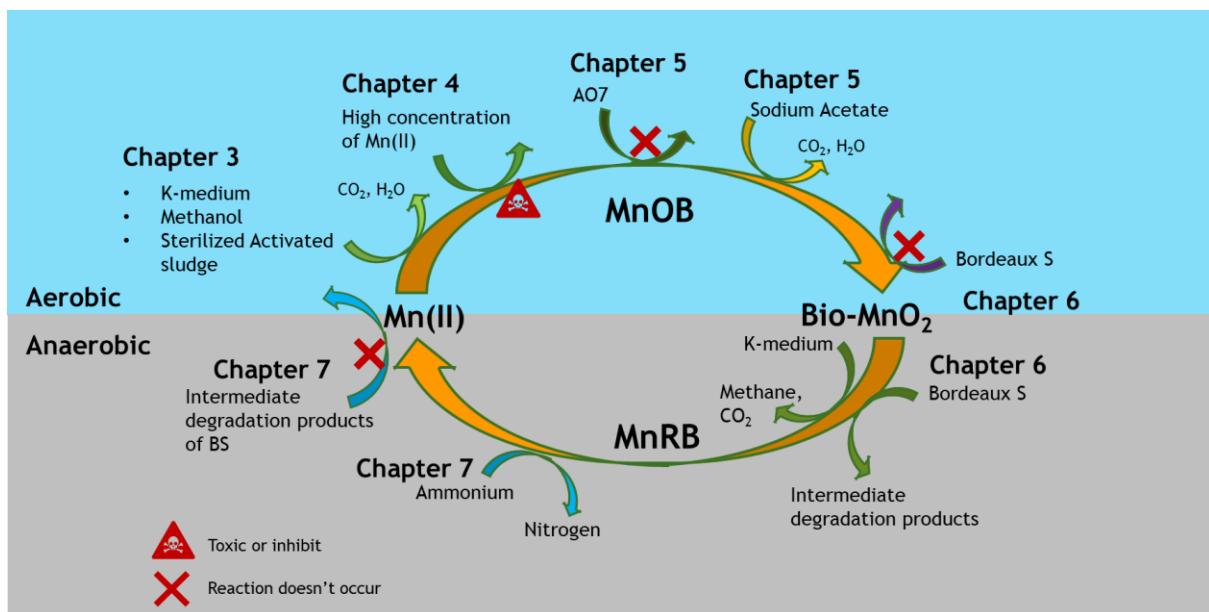


Figure 8.1 The scheme summarizing the main results of this study

8.1 Main results of this study

8.1.1 Enrichment of manganese-oxidizing bacteria in a continuous DHS reactor using different organic substrates

MnOB are diverse and widespread in natural environments. In Chapter 3, three different organic substrates; K-medium, methanol, and sterilized activated sludge (SAS), were examined

as the sole carbon source for the enrichment MnOB in a continuous reactor. All of them can be used to enrich MnOB resulted in the different Mn(II) oxidation performances. The highest Mn(II) removal rate was achieved by the reactor fed with methanol, followed by SAS, and K-medium, as 0.49, 0.41, and 0.26 kg Mn·m⁻³·d⁻¹, respectively. Remarkably, the SAS-fed reactor has higher removal rate than K-medium-supplied reactor, which was widely known as MnOB enrichment substrate. However, its performance was the most unstable compared to other reactors. The different organic substrates strongly affected microbial community of the reactors. *Comamonas*, *Caldilineaceae uncultured* and *Methylobacter* were dominant in the K-medium-fed reactor. In the SAS-supplied reactor, the dominant bacteria were *Caldilineaceae uncultured* and *Prostheco bacter*. In the methanol-fed reactor, *Hyphomicrobium* and *Methylobacterium* were detected as the predominant genera. Several genera which probably play a major role in Mn(II) oxidation were *Comamonas* and *Pseudomonas* in the K-medium-fed reactor, *Mycobacterium* and *Nocardia* in the SAS-fed reactor, and *Hyphomicrobium* in the methanol-fed reactor. In addition, initial addition of abiotic-MnO₂ in the sponge of reactor could effectively promote MnOB enrichment achieving in the high Mn(II) oxidation rate.

8.1.2 Residual Mn(II) concentrations affect the Mn(II) oxidation performance of the reactor

The results obtained in Chapter 3 demonstrated that the unstable Mn(II) oxidation performance has been shown in the reactor with high residual Mn(II). Therefore, in Chapter 4, the effect of residual Mn(II) on the Mn(II) oxidation performance of the reactor was investigated. At low Mn(II) loading rate (0.61 kg m⁻³ d⁻¹), the reactors were able to completely oxidize Mn(II). At a higher Mn(II) loading rate, the reactor was unable to oxidize completely resulted in the residual Mn(II). The reactor with low residual Mn(II) achieved Mn(II) oxidation rate (0.91 kg m⁻³ d⁻¹) higher than the reactor having high level of residual Mn(II) (0.61 kg m⁻³ d⁻¹). The relative abundance of *Hyphomicrobium*, widely known as methylotroph and Mn(II) oxidizer, was higher in the low residual Mn(II) reactor than that of the high residual Mn(II) reactor. These results demonstrated that residual Mn(II) not only inhibited Mn(II) oxidation ability but also affected microbial abundance in the reactor. Therefore, it can be suggested that to achieve a sustainable high Mn(II) oxidation performance, the low level of residual Mn(II) should be maintained in the bioreactor.

8.1.3 Aerobic decolorization of Acid Orange 7 (AO7) dye coupled with Mn(II) oxidation

MnOB and bio-MnO_x have been reported to play a significant role in biogeochemical cycles of not only manganese, but also carbon, nitrogen, and other elements. In Chapter 5, the ability of MnOB and bio-MnO_x for removal of an azo dye, as a model of organic pollutant, was investigated. MnOB enrichment were firstly accelerated in DHS reactor by installing abiotic-MnO₂ in the sponge media. Improvement of decolorization of AO7 was observed along with increasing Mn(II) oxidation activity, however its performance suddenly decreased when sodium acetate concentration was elevated. Even though Mn(II) oxidation was increased, but AO7 removal could not be recovered. The isolates of the reactor have been shown to possess Mn(II) oxidation ability but no AO7 removal ability. Therefore, it can be concluded that decolorization of AO7 was not related to the Mn(II) oxidation. The enhancement of AO7 removal along with increasing Mn(II) oxidation activity was only coincident, and AO7 removal were regulated by different mechanisms. Even though Mn(II) oxidation had no effect on decolorization of AO7, it effectively decomposed another organic substance, such as sodium acetate.

8.1.4 Decolorization of an azo dye Bordeaux S (BS) under manganese-oxidizing and manganese-oxide reducing conditions

In the Chapter 6, decolorization of another azo compound, Bordeaux S (BS) under aerobic conditions and then changed to anaerobic conditions was investigated using two DHS reactors; initially added abiotic-MnO₂ and without abiotic-MnO₂. The results revealed that Mn(II) oxidation had less effect on the decolorization of BS. Anaerobic conditions was more favorable to decolorize azo dye than aerobic conditions. Under anaerobic conditions, decolorization performance was highly dependent on organic co-substrate addition, because azo dye was reductively cleavage to intermediate products, such as 4-amino-1-naphthalenesulfonic acid, in the presence of K-medium as an electron donor. Decolorization rate of 4.75 kg m⁻³ d⁻¹ was achieved. Interestingly, decolorization efficiency in the manganese-reduction reactor was higher than that of without manganese-reduction reactor when a low organic co-substrate was applied. The presence of MnO_x (abiotic-MnO₂ and bio-MnO_x) may not only contribute to the decomposition of EPS to more degradable substrates that can be used for electron donor but also as a conductive material that enhance electron transfer between electron donor and BS.

Methane gas was produced as a result of anaerobic decomposition of K-medium. The differences in archaeal methanogen community between two reactors was observed, indicating that some microorganisms, such as *Methanosaeta* and *Methanoregula*, were inhibited by the presence of abiotic-MnO₂. Unfortunately, anaerobic decolorization of azo dye was unable to effectively remove azo dye and high COD value remained in the effluent. Therefore, further treatment process is required for further decomposition of anaerobic effluent.

8.1.5 Integrated anaerobic-aerobic reactor under manganese redox cycling for degradation of azo dye-containing wastewater

Based on the obtained results in the Chapter 6, in which a post treatment process is required for the treatment of anaerobic effluent, and Chapter 5 demonstrated effective degradation of sodium acetate in Mn(II) oxidation reactor. Therefore, in Chapter 7, integrated anaerobic-aerobic reactor under manganese redox cycling was proposed for further degradation of azo dye-containing wastewater. After 60 days operation, the aerobic reactor could only remove small amounts of COD (< 30%), and the remaining COD corresponded to the initial BS in the influent, which indicated that intermediate products of BS were resistant under microbial Mn(II) oxidation activity. Nitrogen loss was remarkably observed in the anaerobic and aerobic reactor. K-medium as co-substrate was converted to ammonium under anaerobic conditions, which was further oxidized to nitrite, nitrate or nitrogen by manganese oxides. While, under aerobic conditions, nitrification occurred, where ammonium was oxidized to nitrite then followed by oxidation nitrite to nitrate. Even though DHS reactor was operated under aerobic conditions, anaerobic conditions occur at the inside of the sponge. It was revealed by the detection of higher concentration of Mn(II) in the effluent indicating that manganese oxides reduction has occurred. This result was not common because manganese reduction usually takes place under anaerobic conditions. Simultaneous nitrification-denitrification was therefore possible to occur in the aerobic reactor. Thus, the presence of manganese oxides was important for nitrogen removal.

8.2 Perspectives

This study has broadened the knowledge on the strategy to enrich MnOB in a continuous DHS reactor achieving high Mn(II) oxidation rate and high bio-MnO_x production in a short acclimation period. A wide range of organic substrates can be used for MnOB enrichment.

Selecting preferred substrate is one of important factors to enrich MnOB, however the substrate availability and cost-effectiveness should be considered. For example, methanol was the most preferred substrate attaining the highest Mn(II) oxidation and stable performance among other organic substrates (Chapter 3). It would be feasible in practical application if coupled with the treatment of methanol-containing wastewaters, such as wastewater generated from methanol production plant or pulp and paper mills (G. Cao et al., 2015; Meyer and Edwards, 2014). Controlling favorable conditions for MnOB is another key factor to maintain Mn(II) oxidation performance of the reactor. Various environmental factors, such as pH, temperature, initial Mn(II) concentration, and dissolved oxygen, have been reported to impact biological Mn(II) oxidation activity (Paccini et al., 2005; Jiang et al., 2010; Zhao et al., 2018). Here, controlling residual Mn(II) of the effluent at a constant low level would be an important information for engineer to control the performance and stability on Mn(II) oxidation of the reactor (Chapter 4). Increasing residual Mn(II) in the effluent is an indicator for reducing Mn(II) in the influent to prevent toxic effects of Mn(II).

Even though biological Mn(II) oxidation had less effect on the degradation of azo dye and its intermediate products, some organic substances can be decomposed, such as sodium acetate (Chapter 5) and some of remaining COD from the anaerobic effluent (Chapter 7). In addition, considering MnOB can utilize activated sludge as the sole carbon source (Chapter 3), and lignin can be decomposed under manganese redox cycling (Jones et al., 2018), biological Mn(II) oxidation may have potential application for the polishing treatment of anaerobic digestion of agricultural waste which contains poorly degradable organic matter such as lignocellulose.

Anaerobic ammonium oxidation and nitrogen removal coupled with manganese oxides reduction can be an alternative option to the traditional nitrogen cycle concept for nitrogen removal from wastewaters. This concept has many advantageous, such as low energy consumption, reduce carbon source supply, and less sludge generation. However, the removal performance was strongly dependent on the presence of manganese oxides in the anaerobic reactor. By controlling the existence of manganese oxides in the anaerobic reactor, sustainable nitrogen removal can be achieved. Therefore, a combination anaerobic-aerobic reactor with recirculation system would be a promising method not only to allow Mn redox cycle for continuous generating bio-MnO_x, but also for the treatment of high organic nitrogen-containing wastewater.

8.3 Recommendations

To broaden potential application of MnOB, enrichment of MnOB using a wide range of organic substrates, from simple organic, such as sodium acetate, format, etc., to complex organic compounds such as solid sludge, humic substances, etc., need to be investigated. Application of biological Mn(II) oxidation for degradation of organic pollutants in a continuous reactor remains challenges. The decrease in pH during biological Mn(II) oxidation is one of the drawbacks of sustainable Mn(II) oxidation performance. The pH-buffering at neutral condition is required to support Mn(II) oxidation. HEPES buffer has been widely used in biological Mn(II) oxidation studies (Zhu et al., 2016; Chang et al., 2018), other Good's buffers, such as MOPSO (3-Morpholino-2-hydroxypropanesulfonic acid), MOBS (4-(N-Morpholino)butanesulfonic acid), HEPPSO (N-(2-Hydroxyethyl)piperazine-N0-(2-hydroxypropanesulfonicacid)), POPSO (perazine-1,4-bis(2-hydroxypropanesulfonic acid), can be alternative buffers since they do not react with Mn(II) and less effect to microorganisms (Ferreira et al., 2015). However, their cost should be considered when applied in a continuous reactor in order to ensure the system is economically feasible.

Even though some pharmaceutical compounds have been reported to be successfully decomposed by MnOB and/or bio-MnO_x (Furgal et al., 2014; Tran et al., 2018), their performances in a continuous reactor need to be further assessed. This study evidenced that a recalcitrant organic compound azo dye and its intermediate products were unable to be degraded by biological Mn(II) oxidation and bio-MnO_x. Degradability of the organic pollutants should be related to their chemical physical nature. Additional chemical or physical treatment process, such as advanced oxidation process (AOPs) using fenton reaction or ozone treatment, is proposed for further degradation of azo intermediate products (Punzi et al., 2015a; Punzi et al., 2015b). Identification of intermediate degradation products of azo dye using GC or LC-MS is proposed to obtain accurate identification of the compounds. In addition, since the intermediate products of azo dye can be more toxic than the original compound, the acute toxicity assay should be performed to ensure that the effluent does not have any potential toxic effects to the environment.

Anaerobic ammonium oxidation coupled with manganese oxide reduction is an interesting finding. This study also highlighted that simultaneous nitrification-denitrification and manganese oxides reduction took place in the aerobic reactor which serves as a post treatment of anaerobic effluent. Manganese oxides reduction is observed in the aerobic reactor

that usually occurs under anaerobic conditions. Further investigation using ammonium as the influent substrate in the abiotic MnO₂-containing reactor under anaerobic and aerobic conditions are proposed to clarify the role of abiotic MnO₂ in regulating ammonium removal. Denitrification activity by heterotrophic microorganisms is strongly influenced by the availability of organic matter as the electron donor (Xu et al., 2018). Therefore, the effect of organic substrates on the denitrification process in the MnO₂-containing reactor needs to be further investigated.

References

- Cao, G., Zhang, Y., Chen, L., Liu, J., Mao, K., Li, K., Zhou, J., 2015. Production of a biofloculant from methanol wastewater and its application in arsenite removal. *Chemosphere* 141, 274–281. <https://doi.org/10.1016/j.chemosphere.2015.08.009>
- Ferreira, C.M.H., Pinto, I.S.S., Soares, E. V., Soares, H.M.V.M., 2015. (Un)suitability of the use of pH buffers in biological, biochemical and environmental studies and their interaction with metal ions-a review. *RSC Adv.* 5, 30989–31003. <https://doi.org/10.1039/c4ra15453c>
- Furgal, K.M., Meyer, R.L., Bester, K., 2014. Removing selected steroid hormones, biocides and pharmaceuticals from water by means of biogenic manganese oxide nanoparticles in situ at ppb levels. *Chemosphere* 136, 321–326. <https://doi.org/10.1016/j.chemosphere.2014.11.059>
- Jiang, S., Kim, D.-G., Kim, J.-H., Ko, S.-O., 2010. Characterization of the biogenic manganese oxides produced by *Pseudomonas putida* strain MnB1. *Environ. Eng. Res.* 15, 183–190. <https://doi.org/10.4491/eer.2010.15.4.183>
- Meyer, T., Edwards, E.A., 2014. Anaerobic digestion of pulp and paper mill wastewater and sludge. *Water Res.* 65, 321–349. <https://doi.org/10.1016/j.watres.2014.07.022>
- Pacini, V.A., Ingallinella, A.M., Sanguinetti, G., 2005. Removal of iron and manganese using biological roughing up flow filtration technology. *Water Res.* 39, 4463–4475. <https://doi.org/10.1016/j.watres.2005.08.027>
- Punzi, M., Nilsson, F., Anbalagan, A., Svensson, B.M., Jönsson, K., Mattiasson, B., Jonstrup, M., 2015a. Combined anaerobic-ozonation process for treatment of textile wastewater: Removal of acute toxicity and mutagenicity. *J. Hazard. Mater.* 292, 52–60. <https://doi.org/10.1016/j.jhazmat.2015.03.018>
- Punzi, M., Anbalagan, A., Aragão Börner, R., Svensson, B.M., Jonstrup, M., Mattiasson, B., 2015b. Degradation of a textile azo dye using biological treatment followed by photo-Fenton oxidation: Evaluation of toxicity and microbial community structure. *Chem. Eng. J.* 270, 290–299. <https://doi.org/10.1016/j.cej.2015.02.042>
- Tran, T.N., Kim, D.G., Ko, S.O., 2018. Synergistic effects of biogenic manganese oxide and Mn(II)-oxidizing bacterium *Pseudomonas putida* strain MnB1 on the degradation of 17 α -ethinylestradiol. *J. Hazard. Mater.* 344, 350–359. <https://doi.org/10.1016/j.jhazmat.2017.10.045>

- Zhao, X., Wang, X., Liu, B., Xie, G., Xing, D., 2018. Characterization of manganese oxidation by *Brevibacillus* at different ecological conditions. *Chemosphere* 205, 553–558. <https://doi.org/10.1016/j.chemosphere.2018.04.130>
- Xu, Z., Dai, X., Chai, X., 2018. Effect of different carbon sources on denitrification performance, microbial community structure and denitrification genes. *Sci. Total Environ.* 634, 195–204. <https://doi.org/10.1016/j.scitotenv.2018.03.348>

This page is intentionally left blank

Appendix A. Publications arising from this thesis

A1. Publication list

Peer-reviewed journals

1. “*Multiple organic substrates support Mn(II) removal with enrichment of Mn(II)-oxidizing bacteria*”, **Ahmad Shoiful**, Taiki Ohta, Hiromi Kambara, Shuji Matsushita, Tomonori Kindaichi, Noriatsu Ozaki, Yoshiteru Aoi, Hiroyuki Imachi and Akiyoshi Ohashi*. *Journal of Environmental Management* xxx xxxx, accepted on 23 October 2019 (Elsevier, IF = 4.865).
2. “*Mn(II) oxidation and manganese-oxide reduction on the decolorization of an azo dye*”, **Ahmad Shoiful**, Hiromi Kambara, Linh Thi Thuy Cao, Shuji Matsushita, Tomonori Kindaichi, Yoshiteru Aoi, Noriatsu Ozaki, and Akiyoshi Ohashi*. *International Biodeterioration & Biodegradation* 146, 104820, accepted on 14 October 2019 (Elsevier, IF=3.824).

Conferences

1. **Ahmad Shoiful**, Tomonori Kindaichi, Yoshiteru Aoi, Noriatsu Ozaki, Akiyoshi Ohashi. (2019). Effects of Mn-oxides on biological decolorization of azo dye under aerobic and anaerobic conditions. The 16th IWA World conference on Anaerobic Digestion (AD16). Delft, The Netherlands, June 23-27, 2019. (Poster presentation).
2. Taiki Ohta, **Ahmad Shoiful**, Tomonori Kindaichi, Yoshiteru Aoi, Noriatsu Ozaki, Akiyoshi Ohashi. Mn oxidation performance of bioreactors enriched on different organic substrates. The 32nd JSME Annual Meeting & 10th ASME. Okinawa, Japan, July 11-13, 2018. (Poster presentation).
3. **Ahmad Shoiful**, Tomonori Kindaichi, Noriatsu Ozaki, Akiyoshi Ohashi. Development of down-flow hanging sponge (DHS) reactor for decolorization of azo dye. The 52nd Annual Conference of Japan Society on Water Environment. Sapporo, Japan, March 15-17, 2018. (Oral presentation).

A2. Accepted papers

1. “*Multiple organic substrates support Mn(II) removal with enrichment of Mn(II)-oxidizing bacteria*”, **Ahmad Shoiful**, Taiki Ohta, Hiromi Kambara, Shuji Matsushita, Tomonori Kindaichi, Noriatsu Ozaki, Yoshiteru Aoi, Hiroyuki Imachi and Akiyoshi Ohashi*. *Journal of Environmental Management* xxx xxxx, accepted on 23 October 2019 (Elsevier, IF = 4.865).
2. “*Mn(II) oxidation and manganese-oxide reduction on the decolorization of an azo dye*”, **Ahmad Shoiful**, Hiromi Kambara, Linh Thi Thuy Cao, Shuji Matsushita, Tomonori Kindaichi, Yoshiteru Aoi, Noriatsu Ozaki, and Akiyoshi Ohashi*. *International Biodeterioration & Biodegradation* 146, 104820, accepted on 14 October 2019 (Elsevier, IF=3.824).